ESTIMATION OF CATCHMENT RESPONSE TIME IN MEDIUM TO LARGE CATCHMENTS IN SOUTH AFRICA

by

OCKERT JACOBUS GERICKE

Submitted in fulfilment of the academic requirements for the degree of

Doctor of Philosophy

Bioresources Engineering

School of Engineering

College of Agriculture, Engineering and Science

University of KwaZulu-Natal

Pietermaritzburg

South Africa

December 2015

PREFACE

The research contained in this thesis was completed by the candidate while based in the Discipline of Bioresources Engineering, School of Engineering, College of Agriculture, Engineering and Science, University of KwaZulu-Natal, Pietermaritzburg, South Africa. The research was financially supported by the Central University of Technology, Free State, University of KwaZulu-Natal and the National Research Foundation.

The contents of this work have not been submitted in any form to another university and, except where the work of others is acknowledged in the text, the results reported are due to investigations by the candidate.

_____

Signed: Professor JC Smithers

Date: 1 December 2015

DECLARATION 1: PLAGIARISM

I, Ockert, Jacobus Gericke declare that:

(a) The research reported in this thesis, except where otherwise indicated or acknowledged, is my original work.

(b) This thesis has not been submitted in full or in part for any degree or examination to any other university.

(c) This thesis does not contain other persons' data, pictures, graphs or other information, unless specifically acknowledged as being sourced from other persons.

(d) This thesis does not contain other persons' writing, unless specifically acknowledged as being sourced from other researchers. Where other written sources have been quoted, then:

  (i) Their words have been re-written but the general information attributed to them has been referenced.

  (ii) Where their exact words have been used, their writing has been placed inside quotation marks, and referenced.

(e) Where I have used material for which publications followed, I have indicated in detail my role in the work.

(f) This thesis is primarily a collection of material, prepared by myself, published as journal articles or presented as oral presentations at conferences. In some cases, additional material has been included.

(g) This thesis does not contain text, graphics or tables copied and pasted from the Internet, unless specifically acknowledged, and the source being detailed in the thesis and in the References sections.

Signed: OJ Gericke

Date: 1 December 2015

DECLARATION 2: PUBLICATIONS

My role in each paper is indicated. The * indicates the corresponding author.

Chapter 2

Gericke, OJ* and Smithers, JC. 2014. Review of methods used to estimate catchment response time for the purpose of peak discharge estimation. *Hydrological Sciences Journal* 59 (11): 1935–1971. DOI: 10.1080/02626667.2013.866712.

This paper is based on a literature review I conducted. I reviewed, summarised and synthesised the literature and wrote the paper. My co-author, Prof Jeff Smithers, provided guidance and reviewed the paper prior to submission for publication. The paper, based on Chapter 2, was selected as the 'featured article' in Issue 59 (11) of the *Hydrological Sciences Journal* and considered for the Tison Award.

Chapter 3

Gericke, OJ* and Smithers, JC. 2015. An improved and consistent approach to estimate catchment response time: Case study in the C5 drainage region, South Africa. *Journal of Flood Risk Management.* DOI: 10.1111/jfr3.12206.

The research in this paper is based on primary streamflow data I obtained from the Department of Water and Sanitation. I extracted the individual flood hydrographs from the primary streamflow data sets, analysed all the flood hydrographs and investigated the relationship, similarity and proportionality ratios between various hydrograph shape parameters. I developed the Hydrograph Analysis Tool to analyse the large number of extracted flood hydrographs and to separate the volume of direct runoff and baseflow. I generated and analysed the results and wrote the paper. My co-author, Prof Jeff Smithers, provided guidance and reviewed the paper prior to submission for publication.

Chapter 4

Gericke, OJ* and Smithers, JC. 2016. Are estimates of catchment response time inconsistent as used in current flood hydrology practice in South Africa? *Journal of the South African Institution of Civil Engineering* 58 (1): 2–15. DOI: 10.17159/2309-8775/2016/v58n1a1.

In this paper, I highlighted the inherent variability and inconsistencies associated with the direct and indirect estimation of time parameters in three case studies. I identified the case study areas, designed the desk-top studies, analysed the data and wrote the paper. My co-author, Prof Jeff Smithers, provided guidance and reviewed the paper prior to submission for publication.

Chapter 5

Gericke, OJ* and Smithers, JC. 2015a. Direct estimation of catchment response time parameters in medium to large catchments using observed streamflow data. *Hydrological Processes* **[Submitted and under review]**.

In this paper, I developed a novel approach to estimate time parameters directly from observed streamflow data without the need for any rainfall data. I identified the four climatologically different study regions, designed the desk-top studies, analysed the data, generated the results and wrote the paper. My co-author, Prof Jeff Smithers, provided guidance and reviewed the paper prior to submission for publication.

Chapter 6

Gericke, OJ* and Smithers, JC. 2015b. Derivation and verification of empirical catchment response time equations for medium to large catchments in South Africa. *Hydrological Processes* **[Submitted and under review]**.

In this paper, I conducted multiple regression analyses to establish unique relationships between observed time parameters and key climatological and geomorphological catchment predictor variables. In addition to the regression analyses and assessment of results, I also wrote the paper. My co-author, Prof Jeff Smithers, provided guidance and reviewed the paper prior to submission for publication.

Signed: OJ Gericke

Date: 1 December 2015

ABSTRACT

As much as 75 % of the total error in estimates of peak discharge at catchment scales could be ascribed to errors in the estimation of time parameters. The time of concentration (T_C), lag time (T_L) and time to peak (T_P) are the time parameters commonly used to express the catchment response time. The primary objective of this research is to develop a new and consistent approach to estimate catchment response times in medium to large catchments (20 km² to 35 000 km²), expressed as the time to peak (T_{Px}), and derived using only observed streamflow data. The approximation of $T_C \approx T_P$ forms the basis for this new approach and the research focuses on the investigation of the relationship between time parameters and the relevance of conceptualised triangular-shaped direct runoff hydrograph approximations and linear catchment response functions in four climatologically different regions of South Africa. The estimation of observed T_{Px} values is followed by the derivation and verification of empirical equations to enable the estimation of representative catchment T_P values at a medium to large catchment scale in the four identified regions. The results showed that for design hydrology and for the calibration of empirical equations, the catchment T_{Px} should be estimated from both the use of an average catchment T_{Px} value computed using either the duration of total net rise of a multi-peaked hydrograph, or a triangular-shaped direct runoff hydrograph approximation, combined with a linear catchment response function. The use of the different methods in combination is not only practical, but also proved to be objective and with consistent results. The empirical equation(s) derived to estimate T_P also meet the requirement of consistency and ease of application. Independent verification tests confirmed the consistency, while the statistically significant independent variables included in the regressions provide a good indication of catchment response times and are also easy to determine by different practitioners when required for future applications in ungauged catchments. It is envisaged that the implementation of the results from this research will contribute fundamentally to both improved time parameter and peak discharge estimation at a medium to large catchment scale in South Africa. It is also recommended that the methodology used in this research should be expanded to other catchments in South Africa to enable the development of a regional approach to improve the accuracy of the estimation of catchment response time parameters, whilst warranting the combination and transfer of information within the identified homogeneous hydrological regions, *i.e.* increase the confidence in using the suggested methodology and equation(s) anywhere in South Africa.

EXTENDED ABSTRACT

Catchment response time parameters are one of the primary inputs required when design floods, especially in ungauged catchments, need to be estimated. The time parameters most frequently used to express catchment response time are the time of concentration (T_C), lag time (T_L) and time to peak (T_P). Time parameters are normally estimated using either hydraulic or empirical methods, but almost 95 % of all the time parameter estimation methods developed internationally are empirically-based. The two T_C methods recommended for general use in South Africa were both developed and calibrated in the United States of America for catchment areas ≤ 45 ha, while only the T_L methods as proposed by Pullen (1969) and Schmidt and Schulze (1984) were developed locally in South Africa. The methodologies of Schmidt and Schulze (1984) and Pullen (1969) are also limited to small (≤ 30 km²) and medium ($\leq 5\,000$ km²) catchments respectively. Hence, the focus of this research is on the contribution to new knowledge for reliably and consistently estimating catchment response times for design flood estimation in medium to large catchments in South Africa.

Chapter 2 presents a review of the time parameter estimation methods used nationally and internationally, with selected comparisons in medium to large catchments in the C5 secondary drainage region in South Africa. The comparison of different time parameter estimation methods with the currently 'recommended methods' used in South Africa confirmed that the application of empirical methods, with no local correction factors and beyond their original regions of development, must be avoided. The T_C was recognised as the most frequently used time parameter, followed by T_L. In acknowledging this, as well as the basic assumptions of the approximations $T_L = 0.6T_C$ and $T_C \approx T_P$, in conjunction with the similarity between the definitions of the T_P and the conceptual T_C, it was evident that the latter two time parameters should be further investigated to develop an alternative approach to estimate representative catchment response times that result in improved estimates of peak discharge at medium to large catchment scales in South Africa.

In acknowledging the findings and recommendations from Chapter 2, as well as the basic assumptions of the approximations $T_L = 0.6T_C$ and $T_C \approx T_P$, Chapter 3 contains details of a pilot study on the development and evaluation of an alternative, improved and consistent

approach to estimate observed and predicted T_P values which reflect the catchment response times in the C5 secondary drainage region in South Africa. The relationship, similarity and proportionality ratios between the various time parameters are also investigated in Chapter 3. It was concluded that the large errors in estimates of peak discharge in South Africa can be largely ascribed to significant errors in the estimation of the catchment response time, mainly as a consequence of the use of inappropriate time variables, the inadequate use of a simplified convolution process between rainfall and runoff time variables, and the lack of locally developed empirical methods to estimate catchment response time.

Chapter 4 provides a critical synthesis and reflection of the proposed methodology as recommended in Chapter 3. The latter proposed methodology and findings, in conjunction with the theoretical basis as established in Chapter 2, are applied in three sets of catchments in climatologically different regions in South Africa to highlight the inherent variability and inconsistencies associated with the direct and indirect estimation of T_C. In Chapter 4, the approximation of $T_C \approx T_P$ is also investigated, while a conceptual paradigm shift from T_P to T_C estimates is purposely implemented, since T_C was identified in Chapter 2 as the most frequently used and required time parameter in flood hydrology practice. The three case studies demonstrated that estimates of T_C, using different equations, may differ from each other by up to 800 %. As a consequence of this high variability, it was recommended that for design hydrology and calibration purposes, T_C values obtained directly from observed streamflow data (T_{Cx}) should be estimated using an average catchment T_{Cx} value, which is based on both the mean of the event T_{Cxi} values and a linear catchment response function.

Chapters 5 and 6 are a culmination of the findings and recommendations as contained in Chapters 2 to 4 and include the proposal for a new methodology to estimate catchment response time at medium to large catchment scales in four climatologically different regions of South Africa. In Chapter 5, the inadequacy of the simplified convolution process between observed rainfall and runoff time variables, as established in Chapter 3, is further investigated. Similarly, the use of such simplification was regarded as neither practical nor applicable in medium to large heterogeneous catchments where antecedent moisture from antecedent rainfall events and spatially non-uniform rainfall hyetographs can result in

multi-peaked hydrographs. Taking the latter into consideration, as well the proposed use of an average catchment response value in Chapter 4, the catchment T_{Px} values were estimated using three different methods: (i) duration of total net rise of a multi-peaked hydrograph, (ii) triangular-shaped direct runoff hydrograph approximations, and (iii) linear catchment response functions. The results showed that for design hydrology and for the calibration of empirical equations to estimate catchment response times, the catchment T_{Px} should be estimated from both the use of an average catchment T_{Px} value computed using either Methods (i) or (ii) and a linear catchment response function as used in Method (iii). The use of the different methods in combination is not only practical, but also proved to be objective and with consistent results.

In Chapter 6, the primary objective is to derive (calibrate) empirical equations to estimate T_P by using multiple regression analysis, *i.e.* to establish unique relationships between observed T_{Px} values (Chapter 5) and key climatological and geomorphological catchment predictor variables in order to estimate representative catchment T_P values at ungauged catchments. The results showed that the derived empirical T_P equation(s) meet the requirement of consistency and ease of application. Independent verification tests confirmed the consistency, while the statistically significant independent variables included in the regressions provide a good indication of catchment response times and are easy to determine by different practitioners when required for future applications in ungauged catchments.

It is envisaged that the implementation of the results from this research will contribute fundamentally to both improved time parameter and peak discharge estimations at a medium to large catchment scale in South Africa. In addition, the methodology used in this research could also be adopted internationally to enhance the estimation of catchment response time parameters to provide more reliable peak discharge and volume estimates as, to date, this remains a constant challenge in flood hydrology. It is also recommended that the methodology used in this research should be expanded to other catchments in South Africa to enable the development of a regional approach to improve the accuracy of the estimation of catchment response time parameters, whilst warranting the combination and transfer of information within the identified homogeneous hydrological regions, *i.e.* increase the confidence in using the suggested methodology and equation(s) anywhere in South Africa.

ACKNOWLEDGEMENTS

A number of special acknowledgements deserve specific mention:

(a) The Rectorate and relevant functionaries from the Central University of Technology, Free State, for the opportunity of completing this research;
(b) The various agencies for funding and in particular the Central University of Technology, Free State, University of KwaZulu-Natal and National Research Foundation;
(c) Prof JC Smithers, my supervisor, for guidance and support given;
(d) Mr D van der Spuy from the Department of Water and Sanitation (Directorate Hydrological Services: Flood Studies) for expert and technical assistance in flood hydrology and all relevant hydrological data;
(e) Mr F Sokolic (GIS Solutions) for technical assistance in compiling all the relevant Geographical Information System data;
(f) Department of Water and Sanitation for providing the observed streamflow data;
(g) The anonymous reviewers for their constructive review comments, which have helped to significantly improve the published papers (Chapters 2 to 6);
(h) My family and colleagues, for their patience and understanding throughout this research; and
(i) My wife, Berdine, and our three little girls for their love and support.

Acknowledgement above all to my Heavenly Father for setting my feet on a rock and making my steps secure (Ps. 40).

TABLE OF CONTENTS

Page

LIST OF TABLES

Page

LIST OF FIGURES

Page

LIST OF ABBREVIATIONS

ADNRW	Australian Department of Natural Resources and Water
BFI	Baseflow index
CCP	California Culvert Practice
CI	Central Interior
CN	Curve Number
CSIR	Council for Scientific and Industrial Research
CUHP	Colorado Urban Hydrograph Procedure
DAWS	Department of Agriculture and Water Supply
DEM	Digital Elevation Model
DWAF	Department of Water Affairs and Forestry
DWS	Department of Water and Sanitation
ESC	Eastern Summer Coastal
ESRI	Environmental Systems Research Institute
EX-HYD	Flood Hydrograph Extraction Software
FAA	Federal Aviation Agency
GIS	Geographical Information System
GOF	Goodness-of-Fit
HAT	Hydrograph Analysis Tool
HRU	Hydrological Research Unit
HYMO	Problem-oriented computer language for Hydrological Modelling
IEA	Institution of Engineers, Australia
JPV	Joint Peak-Volume
MAP	Mean Annual Precipitation
NERC	Natural Environment Research Council
NFSP	National Flood Studies Programme
NI	Northern Interior
NRCS	Natural Resources Conservation Service
NSCM	National Soil Conservation Manual
PDS	Partial Duration Series
RLMA	Regional Linear Moment Algorithm
RSA	Republic of South Africa

SANCOLD	South African National Committee on Large Dams
SANRAL	South African National Roads Agency Limited
SAWS	South African Weather Service
SCS	Soil Conservation Service
SDF	Standard Design Flood
SRTM	Shuttle Radar Topography Mission
SUH	Synthetic Unit Hydrograph
SWC	Southern Winter Coastal
T_C	Time of concentration
T_L	Lag time
T_P	Time to peak
TR	Technical Report
UDFCD	Urban Drainage and Flood Control District
UH	Unit Hydrograph
UK	United Kingdom
UK FSR	United Kingdom Flood Studies Report
USA	United States of America
USACE	United States Army Corps of Engineers
USBR	United States Bureau of Reclamation
USDA	United States Department of Agriculture
USGS	United States Geological Survey
WRC	Water Research Commission

1. INTRODUCTION

This chapter provides some background on the estimation of catchment response time parameters and the influence of catchment response times on the estimation of peak discharge and includes the rationale, justification and objectives of the research.

1.1 Rationale

The estimation of design flood events, *i.e.* floods characterised by a specific magnitude-frequency relationship, at a particular site in a specific region is necessary for the planning, design and operation of hydraulic structures (Pegram and Parak, 2004). Both the spatial and temporal distribution of runoff, as well as the critical duration of flood producing rainfall, are influenced by the catchment response time. However, the large variability in the runoff response of catchments to storm rainfall, which is innately variable in its own right, frequently results in failures of hydraulic structures in South Africa (Alexander, 2002). A given runoff volume may or may not represent a flood hazard or result in possible failure of a hydraulic structure, since hazard is dependent on the temporal distribution of runoff (McCuen, 2005). Consequently, most hydrological analyses of rainfall and runoff to determine hazard or risk, especially in ungauged catchments, require the estimation of catchment response time parameters as primary input.

Universally, three basic approaches to design flood estimation are available in South Africa, namely the probabilistic, deterministic and empirical methods (Alexander, 2001; Van der Spuy and Rademeyer, 2010). In using event-based deterministic design flood estimation methods in ungauged catchments, time parameters such as the time of concentration (T_C), lag time (T_L) and time to peak (T_P) are commonly used to express the catchment response time. T_C is not only the most frequently used and required time parameter in event-based methods (SANRAL, 2013; Gericke and Smithers, 2014), but also continues to find application in continuous simulation hydrological models (USACE, 2001; Neitsch *et al.*, 2005; Smithers *et al.*, 2013). More specifically, T_C is primarily used to estimate the critical storm duration of a specific design rainfall event used as input to deterministic methods, *i.e.* the Rational and Standard Design Flood (SDF) methods, while T_L is used as input to the deterministic Soil Conservation Services (SCS) and Synthetic

Unit Hydrograph (SUH) methods. The T_P is normally expressed as a function of the critical storm duration and T_L (Mockus, 1957).

Time parameters such as T_C, T_L and T_P serve as indicators of both the catchment storage and the effect thereof on the temporal distribution of runoff. The catchment response time is also directly related to, and influenced by, climatological variables (*e.g.* meteorology and hydrology), catchment geomorphology, catchment variables (*e.g.* land cover, soils and storage), and channel geomorphology (Schmidt and Schulze, 1984; Royappen *et al.*, 2002; McCuen, 2005). In medium to large catchments where channel flow in main watercourses generally dominates catchment response time, the estimation of T_C in South Africa is currently based on the length of the longest main watercourse (L_{CH}) and average main watercourse slope (S_{CH}) as primary catchment descriptors. Typically, catchment descriptors such as the hydraulic length (L_H), centroid distance (L_C), average catchment slope (S), runoff curve numbers (CN) and S_{CH} are used as input to estimate T_L. McCuen (2009) highlighted that, due to differences in the roughness and slope of catchments (overland flow) and main watercourses (channel flow), T_C estimates, based on only the main watercourse characteristics (L_{CH} and S_{CH}), are underestimated on average by 50 %. Consequently, the resulting peak discharges will be overestimated by between 30 % and 50 % (McCuen, 2009).

Despite the widespread use of all these time parameters, unique working definitions for each of the parameters are not currently available. Frequently, there is no distinction between these time parameters in the hydrological literature, hence the question whether they are true hydraulic or hydrograph time parameters, remains unrequited, while some methods as a consequence, are presented in a disparate form. However, the use of several conceptual and computational time parameter definitions are proposed in the literature, as summarised by McCuen (2009) and Gericke and Smithers (2014), some of which are adopted in practice.

Various researchers (*e.g.* Bondelid *et al.*, 1982; McCuen *et al.*, 1984; McCuen, 2009) demonstrated that as much as 75 % of the total error in estimates of peak discharge could be ascribed to errors in the estimation of time parameters. Gericke and Smithers (2014) showed that the underestimation of time parameters by 80 % or more could result in the

overestimation of peak discharges of up to 200 %, while the overestimation of time parameters beyond 800 % could result in maximum peak discharge underestimations of up to 100 %. Such errors in the estimation of time parameters could result in either the over- or under-design of hydraulic structures, but are also linked to several socio-economic implications and could result in infeasible projects. In medium to large catchments, Smithers *et al.* (2013) also concluded that the large errors in estimates of peak discharge can be largely ascribed to significant errors in the estimation of the catchment response time. Consequently, catchment response time parameters are regarded as one of the primary inputs required when design floods need to be estimated in ungauged catchments.

1.2 Justification

In considering observed rainfall and runoff data in gauged catchments, time parameters are normally defined by the difference between two interrelated observed time variables (McCuen, 2009), which represent individual events on either a hyetograph or hydrograph as illustrated in Figure 1.1. In small catchment areas (A) up to 20 km², the difference between two interrelated observed time variables is estimated using a simplified convolution process between a single rainfall hyetograph and resulting single-peaked hydrograph as shown in Figure 1.1. In medium to large heterogeneous catchment areas, typically ranging from 20 km² to 35 000 km², a similar convolution process is required where the temporal relationship between a catchment hyetograph, which may be derived from numerous rainfall stations, and the resulting outflow hydrograph, is established (Gericke and Smithers, 2014).

However, several problems are associated with such a simplified convolution procedure at medium to large catchment scales. Conceptually, such a procedure normally assumes that the volume of direct runoff is equal to the volume of effective rainfall, and that all rainfall prior to the start of direct runoff is regarded as initial abstraction, after which the loss rate is assumed to be constant (McCuen, 2005). Therefore, a uniform response to rainfall within a catchment is assumed, while the spatially non-uniform antecedent soil moisture conditions within the catchment, which are a consequence of both the spatially non-uniform rainfall and the heterogeneous nature of soils and land cover in the catchment, are ignored. Consequently, in contrast to small catchments with single-peaked hydrographs,

the variability evident in medium to large catchments typically results in multi-peaked hydrographs.

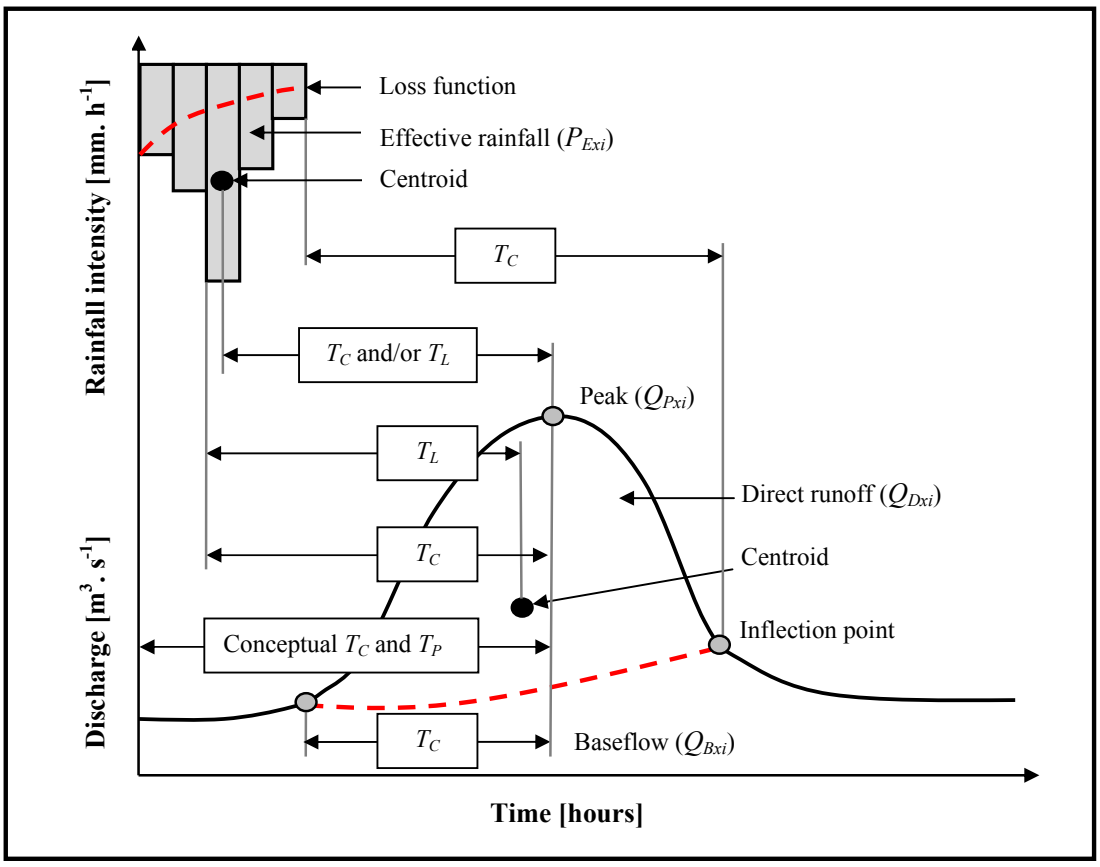

Figure 1.1 Schematic illustrative of the different time parameter relationships (after Gericke and Smithers, 2014)

Furthermore, the use of rainfall data to estimate catchment hyetographs at a medium to large catchment scale, also poses several additional problems as a consequence of the following (Schmidt and Schulze, 1984; Gericke and Smithers, 2014): (i) paucity of rainfall data at sub-daily timescales, both in the number of rainfall gauges and length of the recorded series, (ii) poor time synchronisation between point rainfall data sets from different gauges, (iii) difficulties in measuring time parameters for individual events directly from digitised autographic records owing to difficulties in determining the start time, end time and temporal and spatial distribution of effective rainfall over the catchment, and (iv) poor time synchronised rainfall and streamflow recorders.

In addition to the above-mentioned problems related to a simplified convolution process at medium to large catchment scales, the number of hydrometeorological monitoring stations, especially rainfall stations in South Africa and around the world, has declined steadily over the last few decades. According to Lorenz and Kunstmann (2012), the number of rainfall stations across Europe, declined by nearly 50 % between 1989 and 2006, *i.e.* from 10 000 to less than 6 000 stations, whilst a far more rapid decline occurred in South America, *i.e.* the nearly 4 300 rainfall stations has reduced to 400. Internationally, the United States of America (USA) has witnessed one of the slowest declines, while large parts of Africa and Asia remain without a single rainfall station (Lorenz and Kunstmann, 2012). South Africa is no exception and the rainfall monitoring network has declined over recent years with the number of stations reducing from more than 2 000 in the 1970s to the current situation where the network is no better than it was as far back as 1920 with less than a 1 000 useful stations open in a specific year (Pitman, 2011). Balme *et al.* (2006) also showed that a decline in the density of a rainfall monitoring network produces a significant increase in the errors of spatial estimation of rainfall at annual scales and even larger errors at event scales for large catchments. In contrast to rainfall data, streamflow data are generally less readily available internationally, but the data quantity and quality enable it to be used directly to estimate catchment response times at medium to large catchment scales. In South Africa for example, there are 708 flow-gauging station sites with more than 20 years of record available (Smithers *et al.*, 2014).

In ungauged catchments, catchment response time parameters are estimated using either empirically or hydraulically-based methods, although analytical or semi-analytical methods are also sometimes used (McCuen *et al.*, 1984; McCuen, 2009). Empirical methods are the most frequently used by practitioners to estimate the catchment response time and almost 95 % of all the methods developed internationally are empirically-based (Gericke and Smithers, 2014). However, the majority of these methods are applicable to and calibrated for small catchments, with only the research of Thomas *et al.* (2000) applicable to medium catchment areas of up to 1 280 km² and the research of Johnstone and Cross (1949), Pullen (1969), Mimikou (1984), Watt and Chow (1985), and Sabol (2008) focusing on larger catchments of up to 5 000 km².

In South Africa, unfortunately, none of the empirical T_C estimation methods recommended for general use were developed and verified using local data. In small, flat catchments with overland flow being dominant, the use of the Kerby equation (Kerby, 1959) is recommended, while the empirical United States Bureau of Reclamation (USBR) equation (USBR, 1973) is used to estimate T_C as channel flow in a defined watercourse (SANRAL, 2013). Both the Kerby and USBR equations were developed and calibrated in the USA for catchment areas less than 4 ha and 45 ha respectively (McCuen *et al.*, 1984). Consequently, practitioners in South Africa commonly apply these 'recommended methods' outside their bounds, both in terms of areal extent and their original developmental regions, without using any local correction factors.

The empirical estimates of T_L used in South Africa are limited to the family of equations developed by the Hydrological Research Unit, HRU (Pullen, 1969); the United States Department of Agriculture Natural Resource Conservation Service (USDA NRCS), formerly known as the USDA Soil Conservation Service, SCS (USDA SCS, 1985) and SCS-SA (Schmidt and Schulze, 1984) equations. Both the HRU and Schmidt-Schulze T_L equations were locally developed and verified. However, the use of the HRU methodology is recommended for catchment areas less than 5 000 km², while the Schmidt-Schulze (SCS-SA) methodology is limited to small catchments (up to 20 km²).

The simultaneous use of different time parameter definitions as proposed in literature and the inherent procedural limitations of the traditional simplified convolution process when applied in medium to large catchments, combined with the lack of both continuously recorded rainfall data and available direct measurements of rainfall and runoff relationships at these catchment scales, has not only curtailed the establishment of unbiased time parameter estimation procedures in South Africa, but also has had a direct impact on design flood estimation.

Therefore, the focus of this research is on the problems associated with the accurate estimation of the spatial and temporal distribution of runoff in medium to large catchment scales, by developing suitable time parameters to accurately reflect the catchment response time.

1.3 Objectives of Research

The primary objective of this research is to develop a new and consistent approach to estimate catchment response times in medium to large catchments (20 km² to 35 000 km²), expressed as the time to peak (T_{Px}), and derived using only observed streamflow data. The approximation of $T_C \approx T_P$ as proposed by Gericke and Smithers (2014) forms the basis for the new approach developed in this research to estimate T_{Px} and is based on the definition that the volume of effective rainfall equals the volume of direct runoff when a hydrograph is separated into direct runoff and baseflow. The separation point on the hydrograph is regarded as the start of direct runoff which coincides with the onset of effective rainfall. In other words, the required extensive convolution process normally required to estimate T_P is eliminated, since T_{Px} is estimated directly from the observed streamflow data without the need for rainfall data.

This research contributes new knowledge for estimating catchment response times, required for design flood estimation, in medium to large catchments in South Africa by solving the 'observed rainfall data problem' and synchronisation of rainfall and runoff data. To date, most of the empirical time parameter estimation methods developed internationally are applicable to small catchments, and are based on a simplified convolution process between observed rainfall and runoff data. Both the studies conducted by Pullen (1969) and Schmidt and Schulze (1984) in South Africa are also based on the measured time differences between rainfall and runoff responses and are limited to small and/or medium sized catchments. Therefore, this novel $T_C \approx T_P$ approach does not only overcome the procedural limitations associated with the traditional simplified convolution process at these catchment scales, but catchment response times, as a consequence of both the spatially non-uniform rainfall and the heterogeneous nature of soils and land cover in a catchment, are recognised. In the context of the overarching $T_C \approx T_P$ approach, the focus is primarily on the investigation of the relationship between the time parameters and the relevance of both conceptualised triangular-shaped direct runoff hydrograph approximations and linear catchment response functions in four climatologically different regions of South Africa.

The secondary objective of this research is to derive and independently verify empirical equations to reliably and consistently estimate T_P at a medium to large catchment

scale in four climatologically different regions of South Africa. The focus is on the use of multiple regression analysis to establish the unique relationships between the T_{Px} values estimated directly from observed streamflow data and key climatological and geomorphological catchment predictor variables. The derivation of empirical equation(s) was regarded as the secondary objective, since the new methodology used to estimate T_{Px} values from observed streamflow data is required for the calibration and verification of new empirical equations. Taking the recommendations for future research (Chapter 7) into consideration, *i.e.* regionalisation, it would be logical to accept that, after the application of the methodology based on the primary study objective at a national scale in South Africa, that new empirical equations will be derived for each of the identified hydrological homogeneous regions.

It is envisaged that the implementation of the primary and secondary research objectives, will contribute fundamentally to the improved estimation of both time parameters and peak discharges at a medium to large catchment scale in South Africa. The methodology developed could also be adopted internationally to improve the estimation of catchment response time parameters to provide more reliable peak discharge and volume estimates as, according to Cameron *et al.* (1999), this remains a constant challenge in flood hydrology.

1.4 Outline of Thesis Structure

Each chapter is mostly self-contained, containing a short literature review, materials and methods, results and discussion, and conclusions. The estimation of catchment response time parameters and the influence thereof on estimates of peak discharge are central to all chapters.

Chapter 2 is based on a paper published during 2014 in the *Hydrological Sciences Journal* and presents a review of the time parameter estimation methods used internationally, with selected comparisons in medium to large catchments in the C5 secondary drainage region in South Africa.

In acknowledging the findings and recommendations from Chapter 2, as well as the basic assumptions of the approximations $T_L = 0.6T_C$ and $T_C \approx T_P$, Chapter 3 contains details of a pilot study on the development and evaluation of an alternative, improved and consistent

approach to estimate observed and predicted T_P values which reflect the catchment response times in the C5 secondary drainage region in South Africa. The relationship, similarity and proportionality ratios between the various time parameters are also investigated. The content of Chapter 3 is based on a paper published during 2015 in the *Journal of Flood Risk Management*.

Chapter 4 contains a paper as accepted for publication in 2016 in the *Journal of the South African Institution of Civil Engineering*. This chapter provides a critical synthesis and reflection of the proposed methodology as recommended in Chapter 3. In essence, the proposed methodology, in conjunction with the theoretical basis as established in Chapter 2, are applied in three sets of catchments in climatologically different regions to highlight the inherent variability and inconsistencies associated with the direct and indirect estimation of T_C. In Chapter 4 the approximation of $T_C \approx T_P$ is also investigated, while a conceptual paradigm shift from the use of T_P to T_C estimates is purposely implemented, since T_C is regarded as the most frequently used and required time parameter in flood hydrology practice.

Chapters 5 and 6 are a culmination of the findings and recommendations as contained in Chapters 2 to 4 and include the development and assessment of a new methodology to estimate catchment response time at medium to large catchment scales in four climatologically different regions of South Africa. Chapter 5 presents the development of a new and consistent approach to estimate catchment response times (observed T_{Px} values) directly from streamflow data. The relationship between time parameters and the use of conceptualised triangular hydrograph approximations and linear catchment response functions is also investigated. In Chapter 6, the primary objective is to derive (calibrate) empirical T_P equations by using multiple regression analysis to establish unique relationships between observed T_{Px} values (Chapter 5) and key climatological and geomorphological catchment predictor variables to enable the estimation of consistent T_P values at a medium to large catchment scale. The content of both Chapters 5 and 6 is based on two papers submitted during 2015 for publication.

Chapter 7 presents a synthesis of all the information as discussed in Chapters 1 to 6, as well as some final conclusions and recommendations for future research.

2. REVIEW OF METHODS USED TO ESTIMATE CATCHMENT RESPONSE TIME FOR PEAK DISCHARGE ESTIMATION

This chapter is based on the following paper:

Gericke, OJ and Smithers, JC. 2014. Review of methods used to estimate catchment response time for the purpose of peak discharge estimation. *Hydrological Sciences Journal* 59 (11): 1935–1971. DOI: 10.1080/02626667.2013.866712.

2.1 Abstract

Large errors in peak discharge estimates at catchment scales can be attributed to errors in the estimation of catchment response time. The time parameters most frequently used to express catchment response time are the time of concentration (T_C), lag time (T_L) and time to peak (T_P). This chapter presents a review of the time parameter estimation methods used internationally, with selected comparisons in medium to large catchments in the C5 secondary drainage region in South Africa. The comparison of different time parameter estimation methods with recommended methods used in South Africa confirmed that the application of empirical methods, with no local correction factors, beyond their original developmental regions, must be avoided. The T_C is recognised as the most frequently used time parameter, followed by T_L. In acknowledging this, as well as the basic assumptions of the approximations $T_L = 0.6T_C$ and $T_C \approx T_P$, in conjunction with the similarity between the definitions of the T_P and the conceptual T_C, it was evident that the latter two time parameters should be further investigated to develop an alternative approach to estimate representative response times that result in improved estimates of peak discharge at these catchment scales.

Keywords: *catchment response time; floods; lag time; peak discharge; runoff; South Africa; time of concentration; time parameters; time to peak; time variables*

2.2 Introduction

This chapter presents a review of the time parameters as introduced in Chapter 1, with selected comparisons between international methods used to estimate the catchment response time in medium to large catchments in the C5 secondary drainage region in South Africa. The objectives of the research reported in this chapter are discussed in the next section, followed by an overview of the location and characteristics of the pilot study

area. Thereafter, the methods used to estimate catchment response time are reviewed. The methodologies involved in meeting the objectives are then expanded on in detail, followed by the results, discussion and conclusions.

2.3 Objectives and Assumptions

The objectives of this chapter are: (i) to review the catchment response time estimation methods currently used nationally and internationally, with emphasis on the inconsistencies introduced by the use of different time parameter definitions when catchment response times and design floods are estimated, (ii) to compare a selection of overland flow T_C methods using different slope-distance classes and roughness parameter categories, (iii) to compare time parameter estimation methods in medium to large catchment areas in the C5 secondary drainage region in South Africa in order to provide preliminary insight into the consistency between methods, and (iv) to translate the time parameter estimation results into design peak discharges in order to highlight the impact of these over- or underestimations on prospective hydraulic designs, while attempting to identify the influence of possible source(s) that might contribute to the differences in the estimation results.

Taking into consideration that this comparative research, in the absence of observed time parameters at this stage, would primarily only highlight biases and inconsistencies in the methods, the identification of the most suitable time parameters derived from observed data for improved estimation of catchment response time and peak discharge, would not be possible at this stage. However, when translating these identified inconsistent time parameter estimation results into design peak discharges, the significance thereof would be at least appreciated. Therefore, this is not regarded as a major deficit at this stage, since such important comparisons between the existing and/or newly derived empirical methods and observed data are to be addressed in the following chapters of this research.

In this chapter it was firstly assumed that the equations used to estimate catchment response time in South Africa have a significant influence on the resulting hydrograph shape and peak discharge as estimated with different design flood estimation methods. Secondly, it was assumed that the most appropriate and best performing time variables and catchment storage effects are not currently incorporated into the methods generally used in the C5 secondary drainage region in South Africa.

2.4 Study Area

South Africa is demarcated into 22 primary drainage regions, which are further delineated into 148 secondary drainage regions. The pilot study area is situated in primary drainage region C and comprises of the C5 secondary drainage region (Midgley *et al.*, 1994). As shown in Figure 2.1, the pilot study area covers 34 795 km^2 and is located between 28°25' and 30°17' S and 23°49' and 27°00' E and is characterised by 99.1 % rural areas, 0.7 % urbanisation and 0.2 % water bodies (DWAF, 1995). The natural vegetation is dominated by Grassland of the Interior Plateau, False Karoo and Karoo. Cultivated land is the largest human-induced land cover alteration in the rural areas, while residential and suburban areas dominate the urban areas (CSIR, 2001).

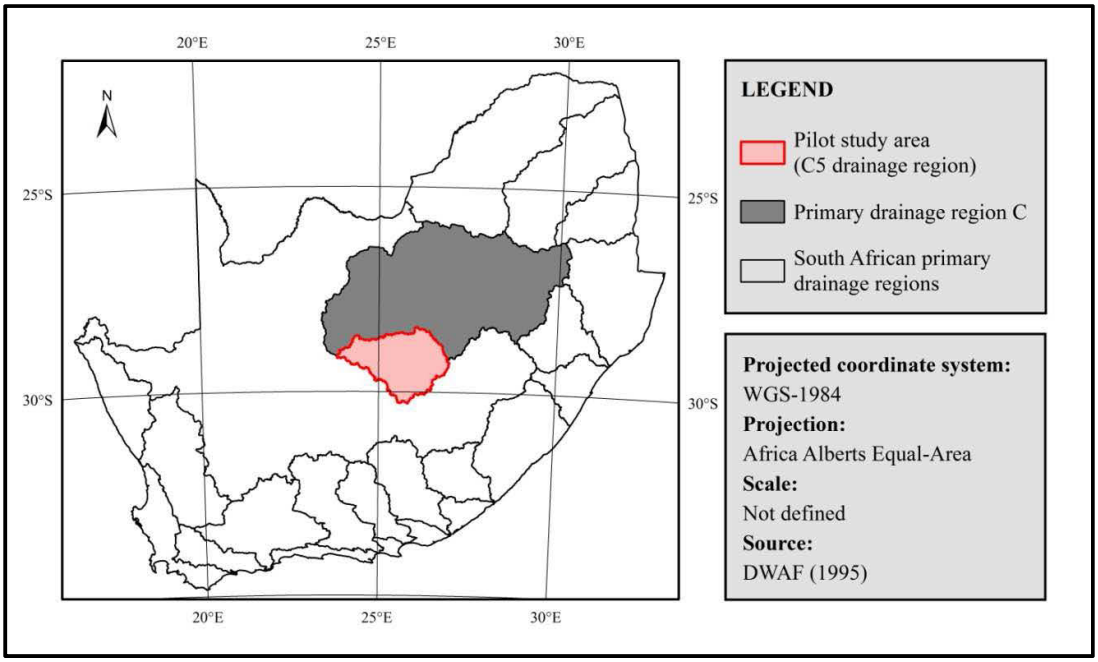

Figure 2.1 Location of the pilot study area (C5 secondary drainage region)

The topography is gentle with slopes between 2.4 % and 5.5 % (USGS, 2002), while water tends to pond easily, thus influencing the attenuation and translation of floods. According to Schulze (1995), the attenuation and translation of floods depend on (i) the volume of flow relative to the volume of storage through which the flow passes, and (ii) the physical characteristics of storage, *e.g.* length, slope, shape and hydraulic resistance of a river reach. The average Mean Annual Precipitation (*MAP*) for the C5 secondary drainage region is 424 mm, ranging from 275 mm in the west to 685 mm in the east (Lynch, 2004) and rainfall is characterised as highly variable and unpredictable. The rainy season starts in

early September and ends in mid-April with a dry winter. The Modder and Riet Rivers are the main river reaches and discharge into the Orange-Vaal River drainage system (Midgley *et al.*, 1994).

2.5 Review of Catchment Response Time Estimation Methods

It is necessary to distinguish between the various definitions for time variables and time parameters (T_C, T_L and T_P) before attempting to review the various time parameter estimation methods available.

2.5.1 Time variables

Time variables can be estimated from the spatial and temporal distributions of rainfall hyetographs and total runoff hydrographs. In order to estimate these time variables, hydrograph analyses based on the separation of: (i) total runoff hydrographs into direct runoff and baseflow, (ii) rainfall hyetographs into initial abstraction, losses and effective rainfall, and (iii) the identification of the rainfall-runoff transfer function, are required. A convolution process is used to transform the effective rainfall into direct runoff through a synthetic transfer function based on the principle of linear super-positioning, *i.e.* multiplication, translation and addition (Chow *et al.*, 1988; McCuen, 2005). In this thesis, 'convolution' refers to the process used to obtain observed time variables from hyetographs and hydrographs respectively, *i.e.* the transformation of effective rainfall into direct runoff through multiplication, translation and addition, where the volume of effective rainfall equals the volume of direct runoff. Consequently, time parameters are then based on the difference between two related time variables.

Effective rainfall hyetographs can be estimated from rainfall hyetographs in one of two different ways, depending on whether observed data are available or not. In cases where both observed rainfall and streamflow data are available, index methods such as the: (i) Phi-index method, where the index equals the average rainfall intensity above which the effective rainfall volume equals the direct runoff volume, and (ii) constant-percentage method, where losses are proportional to the rainfall intensity and the effective rainfall volume equals the direct runoff volume, can be used (McCuen, 2005). However, in ungauged catchments, the separation of rainfall losses must be based on empirical infiltration methods, which account for infiltration and other losses separately.

The percentage of direct runoff is normally fixed and based on factors such as soil and land-use, with some possible adjustments based on the antecedent soil moisture conditions and rainfall depth (IH, 1999; Kjeldsen, 2007). The SCS runoff curve number method (*CN* values associated with specific soils and land-use categories) is internationally the most widely used (Chow *et al.*, 1988).

In general, time variables obtained from hyetographs include the peak rainfall intensity, the centroid of effective rainfall and the end time of the rainfall event. Hydrograph-based time variables generally include peak discharges of observed surface runoff, the centroid of direct runoff and the inflection point on the recession limb of a hydrograph (McCuen, 2009).

2.5.2 Time parameters

Most design flood estimation methods require at least one time parameter (T_C, T_L or T_P) as input. In the previous sub-section it was highlighted that time parameters are based on the difference between two time variables, each obtained from a hyetograph and/or hydrograph. In practice, time parameters have multiple conceptual and/or computational definitions, and T_L is sometimes expressed in terms of T_C. Various researchers (*e.g.* McCuen *et al.*, 1984; Schmidt and Schulze, 1984; Simas, 1996; McCuen, 2005; Jena and Tiwari, 2006; Hood *et al.*, 2007; Fang *et al.*, 2008; McCuen, 2009) have used the differences between the corresponding values of time variables to define two distinctive time parameters: T_C and T_L. Apart from these two time parameters, other time parameters such as T_P and the hydrograph time base (T_B) are also frequently used.

In the following sub-sections the conceptual and computational definitions of T_C, T_L and T_P are detailed, and the various hydraulic and empirical estimation methods currently in use and their interdependency are reviewed. A total of three hydraulic and 44 empirical time parameter (T_C, T_L and T_P) estimation methods were found in the literature and evaluated. As far as possible, an effort was made to present all the equations in Système International d'Unités (SI Units). Alternatively, the format and units of the equations are retained as published by the original authors.

2.5.3 Time of concentration

Multiple definitions are used in the literature to define T_C. The most commonly used conceptual, physically-based definition of T_C is defined as the time required for runoff, as a result of effective rainfall with a uniform spatial and temporal distribution over a catchment, to contribute to the peak discharge at the catchment outlet or, in other words, the time required for a 'water particle' to travel from the catchment boundary along the longest watercourse to the catchment outlet (Kirpich, 1940; McCuen *et al*., 1984; McCuen, 2005; USDA NRCS, 2010; SANRAL, 2013).

Larson (1965) adopted the concept of time to virtual equilibrium (T_{VE}), *i.e.* the time when response equals 97 % of the runoff supply, which is also regarded as a practical measure of the actual equilibrium time. The actual equilibrium time is difficult to determine due to the gradual response rate to the input rate. Consequently, T_C defined according to the 'water particle' concept would be equivalent to T_{VE}. However, runoff supply is normally of finite duration, while stream response usually peaks before equilibrium is reached and at a rate lower than the runoff supply rate. Pullen (1969) argued that this 'water particle' concept, which underlies the conceptual definition of T_C is unrealistic, since streamflow responds as an amorphous mass rather than as a collection of drops.

In using such conceptual definition, the computational definition of T_C is thus the distance travelled along the principal flow path, which is divided into segments of reasonably uniform hydraulic characteristics, divided by the mean flow velocity in each of the segments (McCuen, 2009). The current common practice is to divide the principal flow path into segments of overland flow (sheet and/or shallow concentrated flow) and main watercourse or channel flow, after which, the travel times in the various segments are computed separately and totalled. Flow length criteria, *i.e.* overland flow distances (L_O) associated with specific overland slopes (S_O), are normally used as a limiting variable to quantify overland flow conditions, but flow retardance factors (i_p), Manning's overland roughness parameters (n) and overland conveyance factors (ϕ) are also used (Viessman and Lewis, 1996; Seybert, 2006; USDA NRCS, 2010). Seven typical overland slope-distance classes (based on above-mentioned flow length criteria) and as contained in the National Soil Conservation Manual (NSCM; DAWS, 1986) are listed in Table 2.1.

The NSCM criteria are based on the assumption that the steeper the overland slope, the shorter the length of actual overland flow before it transitions into shallow concentrated flow followed by channel flow. McCuen and Spiess (1995) highlighted that the use of such criteria could lead to less accurate designs, and proposed that the maximum allowable overland flow path length criteria must rather be estimated as $30.48S_O^{0.5}n^{-1}$. This criterion is based on the assumption that overland flow dominates where the flow depths are of the same order of magnitude as the surface resistance, *i.e.* roughness parameters in different slope classes.

Table 2.1 Overland flow distances associated with different slope classes (DAWS, 1986)

Slope class [S_O, %]	**Distance [L_O, m]**
0–3	110
3.1–5	95
5.1–10	80
10.1–15	65
15.1–20	50
20.1–25	35
25.1–30	20

The commencement of channel flow is typically defined at a point where a regular, well-defined channel exists with either perennial or intermittent flow, while conveyance factors (default value of 1.3 for natural channels) are also used to provide subjective measures of the hydraulic efficiency, taking both the channel vegetation and degree of channel improvement into consideration (Heggen, 2003; Seybert, 2006).

The second conceptual definition of T_C relates to the temporal distribution of rainfall and runoff, where T_C is defined as the time between the start of effective rainfall and the resulting peak discharge. The specific computations used to represent T_C based on time variables from hyetographs and hydrographs are discussed in the next paragraph to establish how the different interpretations of observed rainfall: runoff distribution definitions agree with the conceptual T_C definitions in this section (*cf.* Section 2.5.3).

Numerous computational definitions have been proposed for estimating T_C from observed rainfall and runoff data. The following definitions as illustrated in Figure 2.2 are occasionally used to estimate T_C from observed hyetographs and hydrographs (McCuen, 2009):

(a) The time from the end of effective rainfall to the inflection point on the recession limb of the total runoff hydrograph, *i.e.* the end of direct runoff. However, this is also the definition used by Clark (1945) to define T_L;

(b) The time from the centroid of effective rainfall to the peak discharge of total runoff. However, this is also the definition used by Snyder (1938) to define T_L;

(c) The time from the maximum rainfall intensity to the peak discharge; or

(d) The time from the start of total runoff (rising limb of hydrograph) to the peak discharge of total runoff.

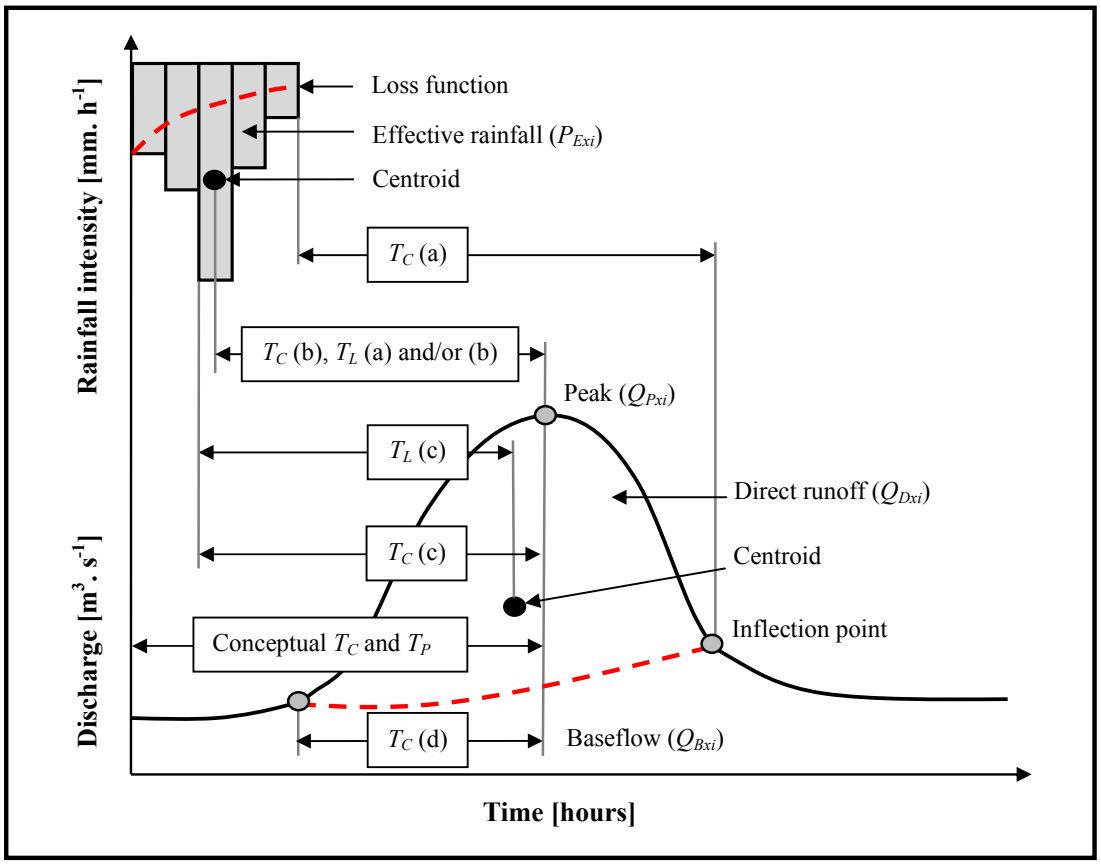

Figure 2.2 Schematic illustrative of the different time parameter definitions and relationships (after Heggen, 2003; McCuen, 2009)

In South Africa, the South African National Roads Agency Limited (SANRAL) recommends the use of T_C definition (d) (SANRAL, 2013), but in essence all these definitions are dependent on the conceptual definition of T_C. It is also important to note that all these definitions listed in (a) to (d) are based on time variables with an associated degree of uncertainty. The 'centroid values' denote 'average values' and are therefore

considered to be more stable time variables representative of the catchment response, especially in larger catchments or where flood volumes are central to the design (McCuen, 2009). In contrast to large catchments, the time variables related to peak rainfall intensities and peak discharges are considered to provide the best estimate of the catchment response in smaller catchments where the exact occurrence of the maximum peak discharge is of more importance. McCuen (2009) analysed 41 hyetograph-hydrograph storm event data sets from 20 catchment areas ranging from 1 to 60 ha in the USA. The results from floods estimated using the Rational and/or NRCS TR-55 methods indicated that the T_C based on the conceptual definition and principal flow path characteristics significantly underestimated the temporal distribution of runoff and T_C needed to be increased by 56 % in order to correctly reflect the timing of runoff from the entire catchment, while the T_C based on T_C definition (b) proved to be the most accurate and was therefore recommended.

The hydraulically-based T_C estimation methods are limited to overland flow, which is derived from uniform flow theory and basic wave mechanics, *e.g.* the kinematic wave (Henderson and Wooding, 1964; Morgali and Linsley, 1965; Woolhiser and Liggett, 1967), dynamic wave (Su and Fang, 2004) and kinematic Darcy-Weisbach (Wong and Chen, 1997) approximations. The empirically-based T_C estimation methods are derived from observed meteorological and hydrological data and usually consider the whole catchment, not the sum of sequentially computed reach/segment behaviours. Stepwise multiple regression analyses are generally used to analyse the relationship between the response time and geomorphological, hydrological and meteorological parameters of a catchment. The hydraulic and/or empirical methods commonly used in South Africa to estimate the T_C are discussed in the following paragraphs:

(a) **Kerby's method:** This empirical method [Eq. (2.1)] is commonly used to estimate the T_C both as mixed sheet and/or shallow concentrated overland flow in the upper reaches of small, flat catchments. It was developed by Kerby (1959; cited by Seybert, 2006) and is based on the drainage design charts developed by Hathaway (1945; cited by Seybert, 2006). Therefore, it is sometimes referred to as the Kerby-Hathaway method. The South African Drainage Manual (SANRAL, 2013) also recommends the use of Eq. (2.1) for overland flow in

South Africa. McCuen *et al.* (1984) highlighted that this method was developed and calibrated for catchments in the USA with areas less than 4 ha, average slopes of less than 1 % and Manning's roughness parameters (n) varying between 0.02 and 0.8. In addition, the length of the flow path is a straight-line distance from the most distant point on the catchment boundary to the start of a fingertip tributary (well-defined watercourse) and is measured parallel to the slope. The flow path length must also be limited to ± 100 m.

$$T_{C1} = 1.4394\left(\frac{nL_O}{\sqrt{S_O}}\right)^{0.467} \quad (2.1)$$

where T_{C1} = overland time of concentration [minutes],

L_O = length of overland flow path [m], limited to 100 m,

n = Manning's roughness parameter for overland flow, and

S_O = average overland slope [$m.m^{-1}$].

(b) **SCS method:** This empirical method [Eq. (2.2)] is commonly used to estimate the T_C as mixed sheet and/or concentrated overland flow in the upper reaches of a catchment. The USDA SCS (later NRCS) developed this method in 1962 for homogeneous, agricultural catchment areas up to 8 km² with mixed overland flow conditions dominating (Reich, 1962). The calibration of Eq. (2.2) was based on T_C definition (c) (*cf.* Section 2.5.3) and a T_C: T_L proportionality ratio of 1.417 (McCuen, 2009). However, McCuen *et al*. (1984) showed that Eq. (2.2) provides accurate T_C estimates for catchment areas up to 16 km².

$$T_{C2} = \frac{L_O^{0.8}\left[\frac{25400}{CN} - 228.6\right]^{0.7}}{706.9S^{0.5}} \quad (2.2)$$

where T_{C2} = overland time of concentration [minutes],

CN = runoff curve number,

L_O = length of overland flow path [m], and

S = average catchment slope [$m.m^{-1}$].

(c) **NRCS velocity method:** This hydraulic method is commonly used to estimate T_C both as shallow concentrated overland and/or channel flow (Seybert, 2006). Either Eqs. (2.3a) or (2.3b) can be used to express the T_C for concentrated overland or channel flow. In the case of main watercourse/channel flow, this method is referred to as the NRCS segmental method, which divides the flow path into segments of reasonably uniform hydraulic characteristics. Separate travel time calculations are performed for each segment based on either Eqs. (2.3a) or (2.3b), while the total T_C is computed using Eq. (2.3c) (USDA NRCS, 2010):

$$T_{C3i} = 0.0167\left(\frac{nL_{O,CH}}{R^{0.667}\sqrt{S_{O,CH}}}\right) \quad (2.3a)$$

$$T_{C3i} = 0.0167\left(\frac{L_{O,CH}}{18\log\left(\frac{12R}{k_s}\right)\sqrt{RS_{O,CH}}}\right) \quad (2.3b)$$

$$T_{C3} = \sum_{i=1}^{N} T_{Ci} \quad (2.3c)$$

where T_{C3} = overland/channel flow time of concentration computed using the NRCS method [minutes],

T_{C3i} = overland/channel flow time of concentration of segment i [minutes],

k_s = Chézy's roughness parameter [m],

$L_{O,\,CH}$ = length of flow path, either overland or channel flow [m],

n = Manning's roughness parameter,

R = hydraulic radius which equals the flow depth [m], and

$S_{O,\,CH}$ = average overland or channel slope [$m.m^{-1}$].

(d) **USBR method:** Equation (2.4) was proposed by the USBR (1973) to be used as a standard empirical method to estimate the T_C in hydrological designs, especially culvert designs based on the California Culvert Practice (CPP, 1955; cited by Li and Chibber, 2008). However, Eq. (2.4) is essentially a modified version of the Kirpich method (Kirpich, 1940) and is recommended by SANRAL (2013) for use in South Africa for defined, natural watercourses/channels. It is also used in conjunction with Eq. (2.1) which estimates overland flow time, to estimate the total

travel time (overland plus channel flow) for deterministic design flood estimation methods in South Africa. Van der Spuy and Rademeyer (2010) highlighted that Eq. (2.4) tends to result in estimates that are either too high or too low and recommend the use of a correction factor (τ) as shown in Eq. (2.4a) and listed in Table 2.2.

$$T_{C4} = \left(\frac{0.87 L_{CH}^{\ 2}}{1000 S_{CH}} \right)^{0.385} \tag{2.4}$$

$$T_{C4a} = \tau \left(\frac{0.87 L_{CH}^{\ 2}}{1000 S_{CH}} \right)^{0.385} \tag{2.4a}$$

where $T_{C4,4a}$ = channel flow time of concentration [hours],

L_{CH} = length of longest watercourse [km],

S_{CH} = average main watercourse slope [m.m^{-1}], and

τ = correction factor.

Table 2.2 Correction factors (τ) for T_C (Van der Spuy and Rademeyer, 2010)

Area [A, km²]	**Correction factor [τ]**
< 1	2
1 –100	2-0.5log$A$
100 –5 000	1
5 000 –100 000	2.42-0.385log$A$
> 100 000	0.5

In addition to the above-listed methods used in South Africa, Table 2.A1 in Appendix 2.A contains a detailed description of a selection of other T_C estimation methods used internationally. It is important to note that most of the T_C methods discussed and listed in Table 2.A1 are based on an empirical relationship between physiographic parameters and a characteristic response time, usually T_P, which is then interpreted as T_C.

2.5.4 Lag time

Conceptually, T_L is generally defined as the time between the centroid of effective rainfall and the peak discharge of the resultant direct runoff hydrograph, which is the same as T_C definition (b) as shown in Figure 2.2. Computationally, T_L can be estimated as a weighted T_C value when, for a given storm, the catchment is divided into sub-areas and the travel times from the centroid of each sub-area to the catchment outlet are established by

the relationship expressed in Eq. (2.5). This relationship is also illustrated in Figure 2.3 (USDA NRCS, 2010).

$$T_L = \frac{\sum(A_i Q_i T_{Ti})}{\sum(A_i Q_i)} \qquad (2.5)$$

where T_L = lag time [hours],

A_i = incremental catchment area/sub-area [km²],

Q_i = incremental runoff from A_i [mm], and

T_{Ti} = travel time from the centroid of A_i to catchment outlet [hours].

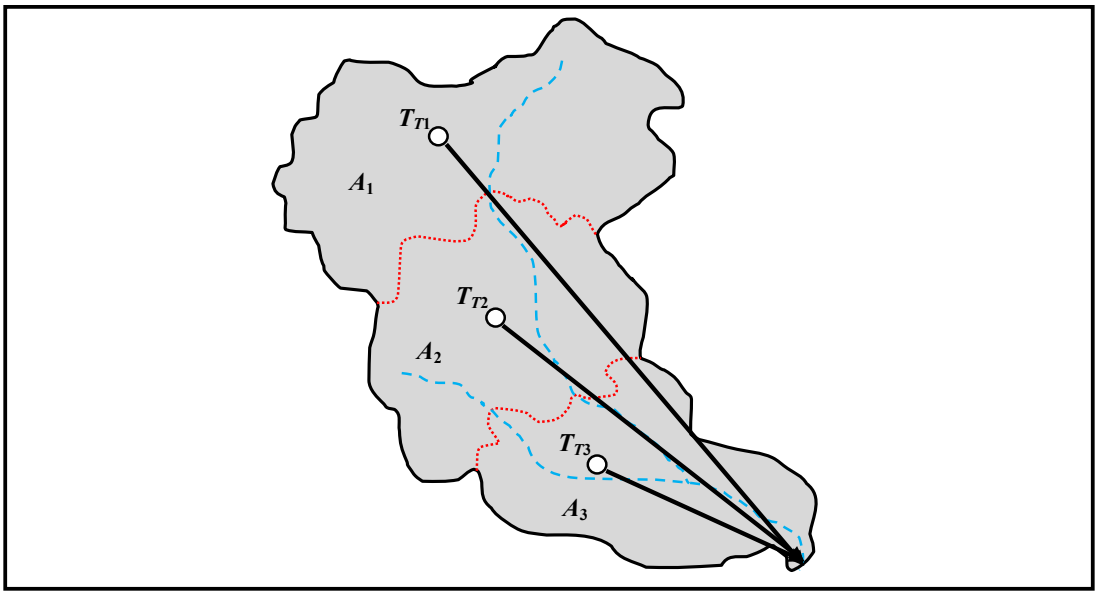

Figure 2.3 Conceptual travel time from the centroid of each sub-area to the catchment outlet (USDA NRCS, 2010)

In flood hydrology, T_L is normally not estimated using Eq. (2.5). Instead, either empirical or analytical methods are normally used to analyse the relationship between the response time and meteorological and geomorphological parameters of a catchment. In the following paragraph, the hydrological parameters, as defined by different interpretations of observed rainfall: runoff distribution definitions are explored.

Scientific literature often fails to clearly define and distinguish between the T_C and T_L, especially when observed data (hyetographs and hydrographs) are used to estimate these time parameters. The differences between time variables from various points on hyetographs to various points on the resultant hydrographs are sometimes misinterpreted as

T_C. The following definitions as illustrated in Figure 2.2 are occasionally used to estimate T_L as a time parameter from observed hyetographs and hydrographs (Heggen, 2003):

(a) The time from the centroid of effective rainfall to the time of the peak discharge of direct runoff;

(b) The time from the centroid of effective rainfall to the time of the peak discharge of total runoff; or

(c) The time from the centroid of effective rainfall to the centroid of direct runoff.

As in the case of the T_C, T_L is also based on uncertain, inconsistently defined time variables. However, T_L definitions (a) to (c) use 'centroid values' and are therefore considered likely to be more stable time variables which are representative of the catchment response in medium to large catchments. Pullen (1969) also highlighted that T_L is preferred as a measure of catchment response time, especially due to the incorporation of storm duration in these definitions. Definitions (a) to (c) are generally used or defined as T_L (Simas, 1996; Hood *et al.*, 2007; Folmar and Miller, 2008; Pavlovic and Moglen, 2008), although T_L definition (b) is also sometimes used to define T_C. Dingman (2002; cited by Hood *et al.*, 2007) recommended the use of Eq. (2.6) to estimate the centroid values of hyetographs or hydrographs respectively.

$$C_{P,Q} = \frac{\sum_{i=1}^{N} X_i t_i}{\sum_{i=1}^{N} X_i} \tag{2.6}$$

where $C_{P,Q}$ = centroid value of rainfall or runoff [mm or $m^3.s^{-1}$],

t_i = time for period i [hour],

N = sample size, and

X_i = rainfall or runoff for period i [mm or $m^3.s^{-1}$].

Owing to the difficulty in estimating the centroid of hyetographs and hydrographs, other T_L estimation techniques have been proposed. Instead of using T_L as an input for design flood estimation methods, it is rather used as input to the computation of T_C. In using T_L definition (c), T_C and T_L are normally related by $T_C = 1.417T_L$ (McCuen, 2009). In T_L definitions (a) and (b), the proportionality ratio increases to 1.667 (McCuen, 2009). However, Schultz (1964) established that for small catchments in Lesotho and South Africa, $T_L \approx T_C$, which conflicts with these proposed proportionality ratios.

The empirical methods commonly used in South Africa to estimate T_L are discussed in the following paragraphs:

(a) **HRU method:** This method was developed by the HRU (Pullen, 1969) in conjunction with the development of Synthetic Unit Hydrographs (SUHs) for South Africa (HRU, 1972). The lack of continuously recorded rainfall data for medium to large catchments in South Africa, forced Pullen (1969) to develop an indirect method to estimate T_L using only observed streamflow data from 96 catchment areas ranging from 21 km² to 22 163 km². Pullen (1969) assumed that the onset of effective rainfall coincides with start of direct runoff, and, that the T_P could be used to describe the time lapse between this mutual starting point and the resulting peak discharge. In essence, it was acknowledged that direct runoff is unable to recede before the end of effective rainfall; therefore the T_P was regarded as the upper limit storm duration during the implementation of the unit hydrograph theory using the *S*-curve technique. In other words, a hydrograph of 25 mm of direct runoff was initially assumed to be a T_P-hour unit hydrograph. However, due to non-uniform temporal and spatial runoff distributions, possible inaccuracies in streamflow measurements and non-linearities in catchment response characteristics, the *S*-curves fluctuated about the equilibrium discharge of amplitude. Therefore, the analysis was repeated using descending time intervals of 1-hour until the fluctuations of the *S*-curve ceiling value diminished to within a prescribed 5 % range. After the verification of the effective rainfall durations, all the hydrographs of 25 mm of direct runoff were converted to unit hydrographs of relevant duration. In order to facilitate the comparison of these unit hydrographs derived from different events in a given catchment, all the unit hydrographs for a given record were then converted by the *S*-curve technique to unit hydrographs of standard duration (Pullen, 1969).

Thereafter, the centroid of each unit hydrograph was determined by simple numerical integration of the unit hydrograph from time zero. The T_L values were then simply estimated as the time lapse between the centroid of effective rainfall and the centroid of a unit hydrograph (Pullen, 1969). The catchment-index ($L_C L_H S_{CH}^{-0.5}$), as proposed by the United States Army Corps of Engineers,

USACE (Linsley *et al.*, 1988) was used to estimate the delay of runoff from the catchments. The T_L values (dependent variables) were plotted against the catchment indices (independent variables) on logarithmic scales. Least-square regression analyses were then used to derive a family of T_L equations applicable to each of the nine homogeneous veld-type regions with representative SUHs in South Africa, as expressed by Eq. (2.7). The regionalisation scheme of the veld-type regions took into consideration catchment characteristics, *e.g.* topography, soil types, vegetation and rainfall, which are most likely to influence catchment storage and therefore T_L.

$$T_{L1} = C_{T1}\left(\frac{L_H L_C}{\sqrt{S_{CH}}}\right)^{0.36} \qquad (2.7)$$

where T_{L1} = lag time [hours],

C_{T1} = regional storage coefficient as listed in Table 2.3,

L_C = centroid distance [km],

L_H = hydraulic length of catchment [km], and

S_{CH} = average main watercourse slope [$m.m^{-1}$].

Table 2.3 Generalised regional storage coefficients (HRU, 1972)

Veld region	Veld-type description	C_{T1}
1	Coastal tropical forest	0.99
2	Schlerophyllous bush	0.62
3	Mountain sourveld	0.35
4	Grassland of interior plateau	0.32
5	Highland sourveld and Dohne sourveld	0.21
5A	Zone 5, soils weakly developed	0.53
6	Karoo	0.19
7	False Karoo	0.19
8	Bushveld	0.19
9	Tall sourveld	0.13

(b) **SCS lag method:** In sub-section 2.5.3 it was highlighted that this method was developed by the USDA SCS in 1962 (Reich, 1962) to estimate T_C where mixed overland flow conditions in catchment areas up to 8 km² exists. However, using the relationship of $T_L = 0.6T_C$, Eq. (2.8) can also be used to estimate T_L in catchment areas up to 16 km² (McCuen, 2005).

$$T_{L2} = \frac{L_H^{0.8}\left[\frac{25\,400}{CN} - 228.6\right]^{0.7}}{168.862\,S^{0.5}} \quad (2.8)$$

where T_{L2} = lag time [hours],

CN = runoff curve number,

L_H = hydraulic length of catchment [km], and

S = average catchment slope [m.m^{-1}].

(c) **Schmidt-Schulze (SCS-SA) method:** Schmidt and Schulze (1984) estimated T_L from observed rainfall and streamflow data in 12 agricultural catchments in South Africa and the USA with catchment areas smaller than 3.5 km² by using three different methods to develop Eq. (2.9). This equation is used in preference to the original SCS lag method [Eq. (2.8)] in South Africa, especially when stormflow response includes both surface and subsurface runoff as frequently encountered in areas of high *MAP* or on natural catchments with good land cover (Schulze *et al.*, 1992).

$$T_{L3} = \frac{A^{0.35} MAP^{1.10}}{41.67\,S^{0.3} i_{30}^{\ 0.87}} \quad (2.9)$$

where T_{L3} = lag time [hours],

A = catchment area [km²],

i_{30} = 2-year return period 30-minute rainfall intensity [mm.h^{-1}],

MAP = Mean Annual Precipitation [mm], and

S = average catchment slope [%].

The three different methods used to develop Eq. (2.9) are based on the following approaches (Schmidt and Schulze, 1984):

Initially, the relationship between peak discharge and volume was investigated by regressing linear peak discharge distributions (single triangular hydrographs) against the corresponding runoff volume obtained from observed runoff events to determine the magnitude and intra-catchment variability of T_L. Thereafter, the incremental triangular hydrographs were convoluted with observed effective rainfall to form compound hydrographs representative of the peak discharge and temporal runoff distribution of observed hydrographs. Lastly, the average time

response between effective rainfall and direct runoff was measured in each catchment to determine an index of catchment lag time. It was concluded that intra-catchment T_L estimates in unguaged catchments can be improved by incorporating indices of climate and regional rainfall characteristics into an empirical lag equation. The 2-year return period 30-minute rainfall intensity proved to be the dominant rainfall parameter that influences intra-catchment variations in T_L estimates (Schmidt and Schulze, 1984).

In addition to the above-listed methods used in South Africa, Table 2.A2 in Appendix 2.A contains a detailed description of a selection of other T_L estimation methods used internationally.

2.5.5 Time to peak

T_P, which is used in many hydrological applications, can be defined as the time from the start of effective rainfall to the peak discharge in a single-peaked hydrograph (McCuen *et al.*, 1984; USDA SCS, 1985; Linsley *et al.,* 1988; Seybert, 2006). However, this is also the conceptual definition used for T_C (*cf.* Figure 2.2). T_P is also sometimes defined as the time interval between the centroid of effective rainfall and the peak discharge of direct runoff (Heggen, 2003); however, this is also one of the definitions used to quantify T_C and T_L using T_C definition (b) and T_L definition (c) respectively. According to Ramser (1927), T_P is regarded to be synonymous with the T_C and that both these time parameters, are reasonably constant for a specific catchment. In contrast, Bell and Kar (1969) concluded that these time parameters are far from being constant; in fact, they may deviate between 40 % and 200 % from the median value.

The **SCS-Mockus method** [Eq. (2.10)] is the only empirical method occasionally used in South Africa to estimate T_P based on the SUH research conducted by Snyder (1938), while Mockus (1957; cited by Viessman *et al.*, 1989) developed the SCS SUHs from dimensionless unit hydrographs as obtained from a large number of natural hydrographs in various catchments with variable sizes and geographical locations. Only the T_P and Q_P values are required to approximate the associated SUHs, while the T_P is expressed as a

function of the storm duration and T_L. Equation (2.10) is based on T_L definition (b), while it also assumes that the effective rainfall is constant with the centroid at $\frac{P_D}{2}$

$$T_{P1} = \frac{P_D}{2} + T_L \quad (2.10)$$

where T_{P1} = time to peak [hours],

P_D = storm duration [hours], and

T_L = lag time based on Eq. (2.7) [hours].

Table 2.A3 in Appendix 2.A contains a detailed description of a selection of other T_P estimation methods used internationally.

2.6 Methodology

To evaluate and compare the consistency of a selection of time parameter estimation methods in the pilot study area, the following steps were initially followed: (i) estimation of climatological variables (driving mechanisms), and (ii) estimation of catchment variables and parameters (which act as buffers and/or responses to the drivers). The steps involved in (i) and (ii) are discussed first, followed by the evaluation and comparison of the catchment response time estimation methods.

It is acknowledged that the empirical methods selected for comparison purposes, are applied outside their bounds, both in terms of areal extent and their original developmental regions. This is purposely done for comparison purposes, as well as to reflect the engineering practitioners' dilemma in doing so, especially due to the absence of locally developed and verified methods at these catchment scales in South Africa.

2.6.1 Climatological variables

The average 2-year 24-hour design rainfall depths, as required by the NRCS kinematic wave method, Eq. (A2), of each catchment under consideration were obtained from Gericke and Du Plessis (2011) who applied the isohyetal method at a 25 mm interval using the *Interpolation and Reclass* toolset of the *Spatial Analyst Tools* toolbox in ArcGIS™ 9.3 in conjunction with the design point rainfall depths as contained in the Regional Linear Moment Algorithm SAWS *n*-day design point rainfall database (RLMA-SAWS)

(after Smithers and Schulze, 2000b). The critical storm durations as required to estimate T_P were obtained from Gericke (2010) and Gericke and Du Plessis (2013) who applied the SUH method in all the catchments under consideration. In each case, user-defined critical storm durations based on a trial-and-error approach were used to establish the critical storm duration which results in the highest peak discharge.

2.6.2 Catchment geomorphology

All the relevant Geographical Information System (GIS) and catchment related data were obtained from the Department of Water and Sanitation (DWS, Directorate: Spatial and Land Information Management), which is responsible for the acquisition, processing and digitising of the data. The specific GIS data feature classes (lines, points and polygons) applicable to the pilot study area and individual sub-catchments were extracted and created from the original GIS data sets. The data extraction was followed by data projection and transformation, editing of attribute tables and recalculation of catchment geometry (areas, perimeters, widths and hydraulic lengths). These geographical input data sets were transformed to a projected coordinate system using the Africa Albers Equal-Area projected coordinate system with modification (ESRI, 2006a).

The average slope of each catchment under consideration was based on a projected and transformed version of the Shuttle Radar Topography Mission (SRTM) Digital Elevation Model (DEM) data for Southern Africa at 90-metre resolution (USGS, 2002). The catchment centroid's were determined by making use of the *Mean Center* tool in the *Measuring Geographic Distributions* toolset contained in the *Spatial Statistics Tools* toolbox of ArcGIS^{TM} 9.3. Thereafter, all the above-mentioned catchment information was used to estimate the catchment shape parameters, circularity and elongation ratios, all of which may have an influence on the catchment response time.

2.6.3 Catchment variables

Both the weighted runoff curve numbers (*CN*), as required by Eqs. (2.2), (2.8) and (A32) and weighted runoff coefficients as required by Eq. (A4) were obtained from the analyses performed by Gericke and Du Plessis (2013). The catchment storage coefficients as applicable to the HRU T_L estimation method, Eq. (2.7), were obtained from Gericke (2010), while the catchment storage coefficients applicable to the T_L estimation

methods of Snyder (1938), Eq. (A16), USACE (1958), Eq. (A18) and Bell and Kar (1969), Eq. (A21), were all based on the default values as proposed by the original authors.

2.6.4 Channel geomorphology

The main watercourses in each catchment were firstly manually identified in ArcMap. Thereafter, a new shapefile containing polyline feature classes representative of the identified main watercourse was created by making use of the *Trace* tool in the *Editor* Toolbar using the polyline feature classes of the 20 m interval contour shapefile as the specified offset or point of intersection, to result in chainage distances between two consecutive contours. The average slope of each main watercourse was estimated using the 10-85 method (Alexander, 2001; SANRAL, 2013). The channel conveyance factors, as required by the Espey-Altman T_P estimation method, Eq. (A37), were based on the default values proposed by Heggen (2003) for natural channels. However, in practice, detailed surveys and mapping are required to establish these conveyance factors more accurately.

2.6.5 Estimation of catchment response time

The current common practice to divide the principal flow path into segments of overland flow and main watercourse or channel flow to estimate the total travel time, was acknowledged. However, since this research focuses on medium to large catchments in which main watercourse, *i.e.* channel flow generally dominates, the overland flow T_C estimation methods were not evaluated for specific catchments, but were estimated for the seven different NSCM slope-distance classes (DAWS, 1986) as listed in Table 2.1.

Six overland flow T_C estimation methods, Eqs. (2.1), (2.2) and (A2) – (A4), (A6) from Table 2.A1, with similar input variables were evaluated by taking cognisance of the maximum allowable overland flow path length criteria as proposed by McCuen and Spiess (1995). In addition, five different categories defined by specific, interrelated overland flow retardance (i_p), Manning's roughness (n) and overland conveyance (ϕ) factors were also considered. The five different categories (i_p, n and ϕ) were based on the work done by Viessman and Lewis (1996) who plotted the ϕ values as a function of Manning's n value and the i_p values. Typical ϕ values ranged from 0.6 (n = 0.02; i_p = 80 %), 0.8 (n = 0.06; i_p = 50 %), 1.0 (n = 0.09; i_p = 30 %), 1.2 (n = 0.13;

i_p = 20 %) to 1.3 (n = 0.15; i_p = 10 %). By considering all these factors, it was argued that both the consistency and sensitivity of the methods under consideration in this flow regime could be evaluated.

A selection of seven T_C [Eqs. (2.4), (2.4a) and Eqs. (A8 – A10, A13, A15b) from Table 2.A1], 15 T_L (Eqs. (2.7), (2.8) and Eqs. (A16 – A18, A21, A23 – A25, A27 – A29, A31 – A33) from Table 2.A2] and five T_P [Eq. (2.10) and Eqs. (A34 – 35, A37 – A38) from Table 2.A3] estimation methods were also applied to each sub-catchment under consideration using an automated spreadsheet developed in Microsoft Excel 2007. The selection of the methods was based on the similarity of catchment input variables required, *e.g.* A, CN, C_T, i_p, L_C, L_{CH}, L_H, S, S_{CH} and/or ϕ_{CH} (*cf.* Table 2.4).

2.6.6 Comparison of catchment response time estimation results

Taking into consideration that this chapter only attempts to provide preliminary insight into the consistency of the various time parameter estimation methods in South Africa, as well as to provide recommendations for improving catchment response time estimation in medium to large catchments, the comparison of the methods is intended to highlight only biases and inconsistencies in the methods. Therefore, in the absence of observed time parameters at this stage of the research, the selected methods were compared to the generally 'recommended methods' currently used in South Africa, *e.g.* overland flow T_C [Kerby's method, Eq. (2.1)], channel flow T_C [USBR method, Eq. (2.4)], T_L [HRU method, Eq. (2.7)] and T_P [SCS-Mockus method, Eq. (2.10)]. The mean error (difference in the average of the 'recommended value' and estimated values in different classes/categories/sub-catchments) was used as a measure of actual bias. However, a method's mean error could be dominated by errors in the large time parameter values; consequently a standardised bias statistic [Eq. (2.11); McCuen *et al.*, 1984] was also introduced. The standard error of the estimate was also used to provide another measure of consistency.

$$B_S = 100\left[\frac{1}{N}\sum_{i=1}^{N}\frac{\left|T_{yi}-T_{xi}\right|}{T_{xi}}\right] \tag{2.11}$$

where B_S = standardised bias statistic [%],

T_{xi} = time parameter estimate based on the 'recommended methods' [minutes or hours],

T_{yi} = time parameter estimate using other selected methods [minutes or hours], and

N = number of slope-distance categories (overland flow regime) or sub-catchments (channel flow regime).

In order to appreciate the significance of the inconsistencies introduced by using the various time parameter estimation methods, the results were translated into design peak discharges. In order to do so, the 100-year design rainfall depths associated with the critical storm duration in each of the 12 sub-catchments (Gericke and Du Plessis, 2011), in conjunction with the catchment areas and regional runoff coefficients (Table 2.4), were substituted into the Standard Design Flood (SDF) method to estimate design peak discharges. The SDF method [Eq. (2.12)] is a regionally calibrated version of the Rational method and is deterministic-probabilistic of nature and applicable to catchment areas up to 40 000 km² (Alexander, 2002; Gericke and Du Plessis, 2012; SANRAL, 2013).

$$Q_{PT} = 0.278\left[\frac{C_2}{100} + \left(\frac{Y_T}{2.33}\right)\left(\frac{C_{100}}{100} - \frac{C_2}{100}\right)\right] I_T A \qquad (2.12)$$

where Q_{PT} = design peak discharge [$m^3.s^{-1}$],

A = catchment area [km²],

C_2 = 2-year return period runoff coefficient [15 %; pilot study area],

C_{100} = 100-year return period runoff coefficient [60 %; pilot study area],

I_T = average design rainfall intensity [$mm.h^{-1}$], and

Y_T = Log-normal standard variate [return period factor].

2.7 Results

The results from the application of the methodology are presented in the next sub-sections.

2.7.1 Review of catchment response time estimation methods

The use of time parameters based on either hydraulic or empirical estimation methods was evident from the literature review conducted. It was confirmed that none of these hydraulic and empirical methods are highly accurate or consistent to provide the true value of these

time parameters, especially when applied outside their original developmental regions. In addition, many of these methods/equations proved to be in a disparate form and are presented without explicit unit specifications and suggested values for constants. For example, with the migration between dimensional systems and what seems to be a Manning's roughness parameter (n) value, is in fact a special-case roughness parameter. Heggen (2003), who summarised more than 80 T_C, T_L and T_P estimation methods from the literature, confirmed these findings.

2.7.2 General catchment information

The general catchment information (*e.g.* climatological variables, catchment geomorphology, catchment variables and channel geomorphology) applicable to each of the 12 sub-catchments in the pilot study area, are listed in Table 2.4. The influence of each variable or parameter listed in Table 2.4 will be highlighted where applicable in the subsequent sections which focus on the time parameter estimation results.

2.7.3 Comparison of catchment response time estimation results

The results from the application of the time parameter estimation methods applicable to the overland flow and predominant channel flow regimes, as well as a possible combination thereof, are listed and discussed in the subsequent sections.

2.7.3.1 Catchment time of concentration

The five methods used to estimate the T_C in the overland flow regime, relative to the T_C estimated using the Kerby method, Eq. (2.1), showed different biases when compared to this 'recommended method' in each of the five different flow retardance categories and associated slope-distance classes. As expected, all the T_C estimates decreased with an increase in the average overland slope, while T_C gradually increases with an increase in the flow retardance factors (i_p, n and ϕ). The SCS method [Eq. (2.2)] constantly underestimated T_C, while the Miller [Eq. (A3)] and Espey-Winslow [Eq. (A6)] methods overestimated T_C in all cases when compared to the estimates based on the Kerby method [Eq. (2.1)].

Table 2.4 General catchment information

Catchment descriptors	C5R001	C5R002	C5R003	C5R004	C5R005	C5H003	C5H012	C5H015	C5H016	C5H018	C5H022	C5H054
Climatological variables												
2-year return period 24-hour rainfall depth [P_2, mm]	50	48	54	54	54	54	48	54	50	52	54	54
Unit hydrograph critical storm duration [P_D, hours]	12	20	10	18	3	10	12	18	48	36	2	9
Catchment geomorphology												
Area [A, km²]	922	10 260	937	6 331	116	1 641	2 366	5 939	33 278	17 360	39	687
Circle-area perimeter = catchment perimeter [A_C, km²]	2 063	22 269	1 743	13 377	168	3 057	4 210	11 734	77 208	42 407	134	1 696
Perimeter [P, km]	161	529	148	410	46	196	230	384	985	730	41	146
Width [W, km]	17	98	23	66	10	32	47	66	125	64	11	12
Centroid distance [L_C, km]	53	97	31	113	8	41	45	81	230	174	3	33
Hydraulic length of catchment [L_H, km]	86	202	54	187	16	71	87	160	378	375	8	67
Max. length parallel to principle drainage line [L_M, km]	55	136	42	141	14	54	60	125	301	272	7	55
Max. straight-line catchment length [L_S, km]	49	132	43	118	14	54	59	118	250	225	7	51
Average catchment slope [S, m.m^{-1}]	0.03054	0.04369	0.05044	0.04186	0.05500	0.03900	0.03279	0.02765	0.02087	0.01725	0.10287	0.02070
Shape parameter [$F_S = L_S^2/A$]	2.6	1.7	2.0	2.2	1.7	1.8	1.5	2.3	1.9	2.9	1.3	3.8
Circularity ratio [$R_C = P/(4\pi A)^{0.5}$]	1.5	1.5	1.4	1.5	1.2	1.4	1.3	1.4	1.5	1.6	1.9	1.6
Elongation ratio [$R_E = 2/L_M(A/\pi)^{0.5}$]	0.6	0.8	0.8	0.6	0.9	0.8	0.9	0.7	0.7	0.5	1.0	0.5
Catchment variables												
Imperviousness/urbanisation factor [i_p, %]	5	8	5	5	8	5	10	5	5	5	8	5
Weighted runoff curve number [CN]	78	77.6	76.3	74.4	76.2	76.3	78.3	74.4	69.8	69.8	76.2	77.6
Weighted rational runoff coefficient [C, T = 2-year]	0.368	0.365	0.358	0.319	0.491	0.358	0.417	0.319	0.283	0.283	0.491	0.283
Regional SDF runoff coefficient [C_{SDF}, T = 100-year]	0.600	0.600	0.600	0.600	0.600	0.600	0.600	0.600	0.600	0.600	0.600	0.600
HRU regional storage coefficient [C_{T1}]	0.268	0.221	0.320	0.317	0.320	0.320	0.194	0.317	0.246	0.246	0.320	0.291
Snyder's storage coefficient [C_{T2}]	1.350	1.350	1.500	1.600	1.500	1.500	1.350	1.600	1.600	1.600	1.500	1.500
USACE storage coefficient [C_{T3}]	0.249	0.268	0.278	0.266	0.327	0.278	0.273	0.266	0.254	0.254	0.327	0.259
Bell-Kar storage coefficient [C_{T4}]	0.050	0.050	0.050	0.050	0.050	0.050	0.050	0.050	0.050	0.050	0.050	0.050
Channel geomorphology												
Length of channel flow path [L_{CH}, km]	86	202	54	187	16	71	87	160	378	375	8	67
Average slope of channel flow path [S_{CH}, m.m^{-1}]	0.00229	0.00133	0.00273	0.00131	0.00895	0.00255	0.00271	0.00144	0.00102	0.00079	0.01702	0.00260
Channel conveyance factor [ϕ_{CH}]	1.3	1.3	1.3	1.3	1.3	1.3	1.3	1.3	1.3	1.3	1.3	1.3
USBR channel flow correction factor [τ]	1	0.876	1	0.956	1	1	1	0.967	0.679	0.788	1.204	1

The NRCS kinematic wave method [Eq. (A2)] underestimated T_C in relation to Eq. (2.1) in Category 1, while other T_C underestimations were witnessed in Categories 2 ($S_O \geq 0.10$ m.m^{-1}), 3 ($S_O \geq 0.15$ m.m^{-1}), and 4 to 5 ($S_O \geq 0.20$ m.m^{-1}). The poorest results in relation to the Kerby method [Eq. (2.1)] were obtained using the Espey-Winslow method [Eq. (A6)] and could be ascribed to the use of default conveyance (ϕ) factors which might not be representative, since this is the only method using ϕ as a primary input parameter.

In considering the overall average consistency measures compared to the Kerby method [Eq. (2.1)] as listed in Table 2.5, the NRCS kinematic wave method [Eq. (A2)] provided relatively the smallest bias (< 10 %), with a mean error ≤ 1 minute. Both the standardised bias (469.2 %) and mean error (26 minutes) of the Espey-Winslow method [Eq. (A6)] were large compared to the other methods. The SCS method [Eq. (2.2)] resulted in the smallest maximum absolute error of 3.3 minutes, while the Espey-Winslow method had a maximum absolute error of 82 minutes. The standard deviation of the errors provides another measure of correlation, with standard errors < 1 minute [Eqs. (2.2), (A2) and (A4)].

Table 2.5 Consistency measures for the test of overland flow T_C estimation methods compared to the 'recommended method', Eq. (2.1)

Methods	Consistency measures					
	Mean recommended T_C [min.]	**Mean estimated T_C [min.]**	**Standard bias statistic [%]**	**Mean error [min.]**	**Maximum error [min.]**	**Standard error [min.]**
SCS, Eq. (2.2)	5.3	3.4	-44.6	-1.9	-3.3	0.8
NRCS, Eq. (A2)	5.3	6.0	-6.2	0.6	8.9	0.5
Miller, Eq. (A3)	5.3	23.8	327.3	18.5	49.5	1.1
FAA, Eq. (A4)	5.3	6.6	20.3	1.3	4.2	0.4
Espey-Winslow, Eq. (A6)	5.3	31.1	469.2	25.8	81.5	1.8

Table 2.6 contains the NSCM flow length criteria (*cf.* Table 2.1; DAWS, 1986) and the maximum allowable overland flow path length results based on the McCuen and Spiess (1995) criteria. The results differed significantly and could be ascribed to the fact that McCuen and Spiess (1995) associated the occurrence of overland flow with flow depths that are of the same order of magnitude as the surface resistance, while the NSCM criteria are based on the assumption that the steeper the overland slope, the shorter the length of actual overland flow before it transitions to shallow concentrated flow followed by channel flow.

Table 2.6 Comparison of maximum overland flow length criteria

Average overland slope class [S_O, m.m^{-1}]		0.03	0.05	0.10	0.15	0.20	0.25	0.30
NSCM flow length criteria [L_O, m]		110	95	80	65	50	35	20
Roughness parameters	***n*-value**	**McCuen-Spiess flow length criteria [L_O, m]**						
	0.02	264	341	482	590	682	762	835
	0.06	88	114	161	197	227	254	278
	0.09	59	76	107	131	151	169	185
	0.13	41	52	74	91	105	117	128
	0.15	35	45	64	79	91	102	111

In applying the McCuen-Spiess criteria, the shorter overland flow path lengths were associated with flatter slopes and higher roughness parameter values. Although, the latter association with higher roughness parameter values seems to be logical in such a case, the proposed relationship of $30.48S_O^{0.5}n^{-1}$ occasionally resulted in overland lengths of up to 835 m. It is important to note that most of the overland flow equations are assumed to be applicable up to ± 100 m (USDA SCS, 1985), which almost coincides with the maximum overland flow length of 110 m as proposed by the DAWS (1986).

The six methods used to estimate T_C, under predominant channel flow conditions, relative to the T_C estimated using the USBR equation [Eq. (2.4)], showed different biases when compared to this 'recommended method' in each of the 12 sub-catchments of the pilot study area as illustrated in Figure 2.4. As expected, all the T_C estimates increased with an increase in catchment size, although in the areal range between 922 km² (C5R001) and 937 km² (C5R003), the T_C estimates decreased despite the increase in area. This is most likely due to the steeper average catchment slope and shorter channel flow path characterising the larger catchment area. Table 2.7 contains the overall average consistency measures based on the comparisons depicted in Figure 2.4. The Kirpich method [Eq. (A9)] showed the smallest bias and mean error of zero respectively; this was expected since Eq. (2.4) is essentially a modified version of the Kirpich method. The USBR [Eq. (2.4a)] and Johnstone-Cross [Eq. (A10)] methods also provided relatively small negative biases (< -50 %), but their associated negative mean errors were 5 hours and 20.4 hours respectively. Both the standardised biases (156 % and 544 %) and mean errors (38 hours and 168 hours) of the Colorado-Sabol [Eq. (A15b)] and Sheridan [Eq. (A13)] methods respectively were much larger when compared to the other methods.

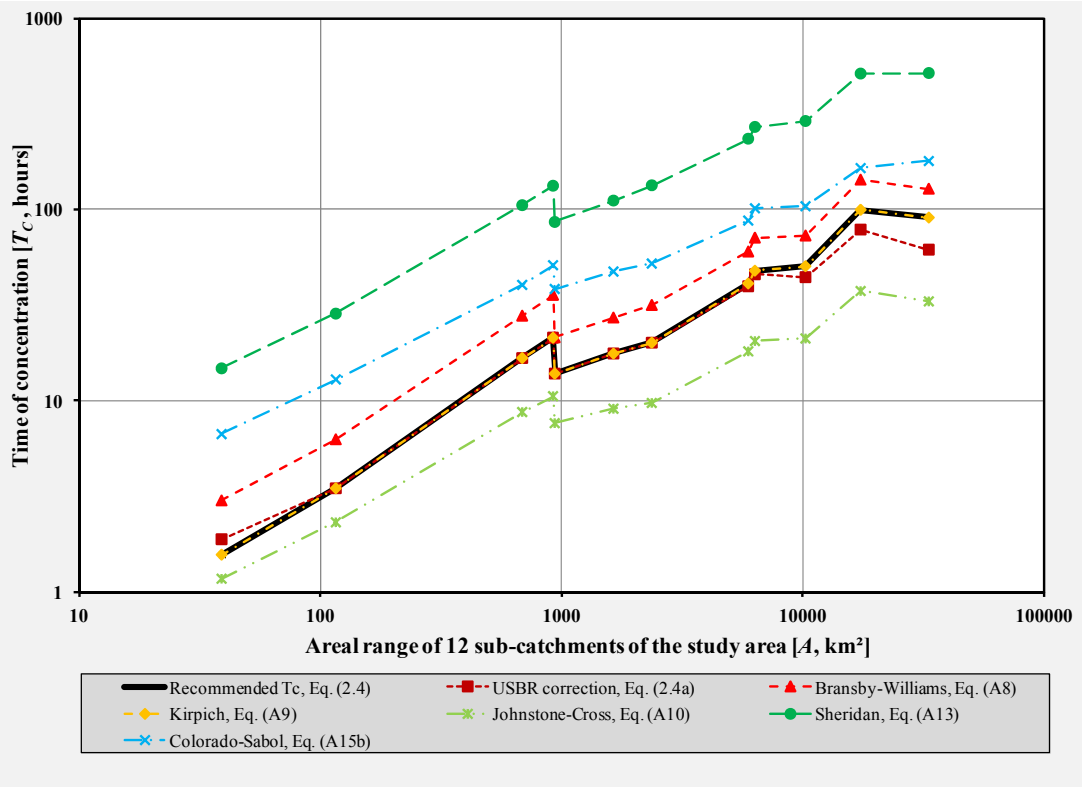

Figure 2.4 T_C estimation results

Table 2.7 Consistency measures for the test of channel flow T_C estimation methods compared to the 'recommended method', Eq. (2.4)

Methods	Consistency measures					
	Mean recommended T_C [h]	Mean estimated T_C [h]	Standard bias statistic [%]	Mean error [h]	Maximum error [h]	Standard error [h]
USBR corrected, Eq. (2.4a)	35.4	30.4	-4.4	-5.0	-29.1	5.9
Bransby-Williams, Eq. (A8)	35.4	52.4	58.1	17.0	43.5	1.1
Kirpich, Eq. (A9)	35.4	35.4	0.0	0.0	-0.1	0.0
Johnstone-Cross, Eq. (A10)	35.4	14.9	-50.0	-20.4	-62.2	3.0
Sheridan, Eq. (A13)	35.4	203.3	544.1	167.9	426.5	2.4
Colorado-Sabol, Eq. (A15b)	35.4	73.8	156.4	38.4	88.5	4.9

Most of the methods showed inconsistency in at least one of the 12 sub-catchments. The Kirpich method [Eq. (A9)] resulted in the smallest maximum absolute error of -0.1 hours in three sub-catchments, while Sheridan's method had maximum absolute errors of 427 hours in catchment C5H016. Typically, the high errors associated with Sheridan's method could be ascribed to the fact that only one independent variable (*e.g.* main watercourse length) was used in attempt to accurately reflect the catchment response time, *i.e.* the dependent variable.

In translating these mean errors of between -15 % and 462 % at a catchment level into design peak discharges using the SDF method, the significance thereof is truly appreciated. The underestimation of T_C is associated with the overestimation of peak discharges or vice versa, *viz.* the overestimation of T_C results in underestimated peak discharges. Typically, the T_C underestimations ranged between 20 % and 65 % and resulted in peak discharge overestimations of between 30 % and 175 %, while T_C overestimations of up to 800 % resulted in maximum peak discharge underestimations of > 90 %.

2.7.3.2 Catchment lag time

Figure 2.5 illustrates the results of the 14 methods used to estimate T_L relative to the T_L estimated using the HRU equation [Eq. (2.7)] in each of the 12 sub-catchments of the pilot study area.

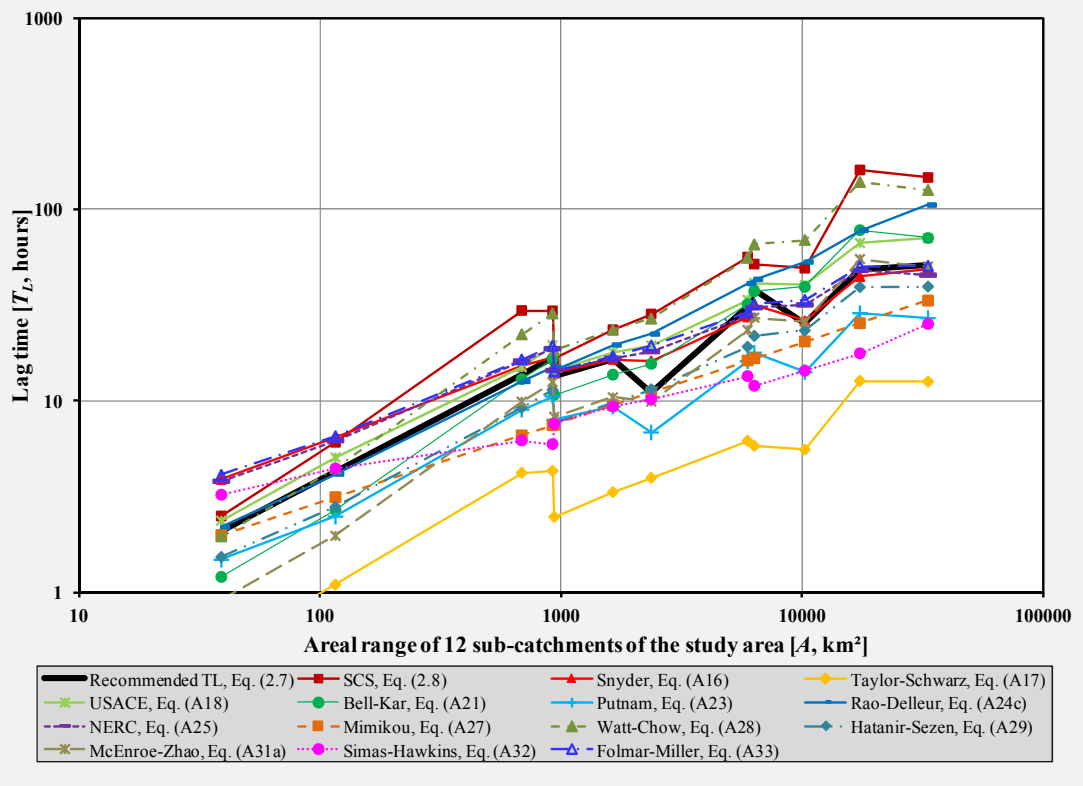

Figure 2.5 T_L estimation results

It is interesting to note that, as in the case of the T_C estimates, most of the methods based on $(L_{CH}.S_{CH}^{-1})^X$ ratios as primary input, resulted in T_L estimates that decreased despite the increase in area. This was quite evident in catchments with a decreasing channel flow path length (L_{CH}) and increasing average channel slope (S_{CH}) associated with an increase in catchment size. In addition, these lower L_{CH} values contributed to shape parameter (F_S, Table 2.4) differences of more than 0.5. This also confirms that catchment geomorphology and catchment variables play a key role in catchment response times.

Table 2.8 contains the overall average consistency measures based on the comparisons depicted in Figure 2.5.

Table 2.8 Consistency measures for the test of T_L estimation methods compared to the 'recommended method', Eq. (2.7)

Methods	Consistency measures					
	Mean recommended T_L [h]	**Mean estimated T_L [h]**	**Standard bias statistic [%]**	**Mean error [h]**	**Maximum error [h]**	**Standard error [h]**
SCS, Eq. (2.8)	22.6	50.1	92.6	27.5	112.4	6.5
Snyder, Eq. (A16)	22.6	22.3	13.3	-0.3	-6.0	2.3
Taylor-Schwarz, Eq. (A17)	22.6	5.2	-76.0	-17.4	-38.4	5.4
USACE, Eq. (A18)	22.6	28.9	25.2	6.3	19.8	3.6
Bell-Kar , Eq. (A21)	22.6	27.6	6.3	5.0	29.7	4.7
Putnam, Eq. (A23)	22.6	12.6	-41.5	-10.0	-24.0	2.6
Rao-Delleur, Eq. (A24c)	22.6	34.2	36.1	11.6	54.4	5.7
NERC, Eq. (A25)	22.6	23.1	17.8	0.5	-7.0	4.0
Mimikou, Eq. (A27)	22.6	13.3	-35.8	-9.3	-22.7	5.7
Watt-Chow, Eq. (A28)	22.6	48.5	84.4	25.8	90.7	4.8
Haktanir-Sezen, Eq. (A29)	22.6	16.4	-28.0	-6.2	-15.9	4.2
McEnroe-Zhao, Eq. (A31a)	22.6	19.6	-23.9	-3.0	-10.5	4.2
Simas-Hawkins, Eq. (A32)	22.6	10.8	-36.4	-11.8	-30.5	6.8
Folmar-Miller, Eq. (A33)	22.6	24.4	23.7	1.8	8.4	4.0

The 14 T_L estimation methods (Table 2.8) proved to be less biased than the T_C estimation methods when compared to the 'recommended method' [HRU, Eq. (2.7)], with standardised biases ranging from -76 % to 92.6 %. Five methods (*e.g.* Snyder, Bell-Kar, NERC, McEnroe-Zhao and Folmar-Miller) with similar independent variables (*e.g.* L_H and S_{CH}) as used in the 'recommended method' showed the smallest biases (< 25 %) and mean errors (≤ 5 hours). The USACE method [Eq. (A18)], which is essentially identical to the 'recommended method', apart from the different regional storage coefficients, proved to be less satisfactorily with mean errors up to 7 hours. The latter results once again emphasise that these empirical coefficients represent regional effects. Hence, the use of these methods outside their region of original development without any adjustments is regarded as

inappropriate. In addition, it was also interesting to note that by comparing the 'mean recommended T_C' (Table 2.7) estimates with the 'mean recommended T_L' (Table 2.8) estimates, it resulted in a proportionality ratio of 0.64, which is in close agreement with the literature, *i.e.* $T_L = 0.6T_C$.

2.7.3.3 Catchment time to peak

The individual T_P estimation results (Figure 2.6) and overall average consistency measures (Table 2.9) showed different biases when compared to the 'recommended method' [SCS-Mockus, Eq. (2.10)], with maximum absolute errors ranging from ± 60 to 80 hours. These errors might be ascribed to the fact that all these methods had only one independent variable (L_H) in common with the 'recommended method', while the inclusion of independent variables such as catchment area and conveyance factors [Eqs. (A34) and (A37)] proved to be most inappropriate in this case.

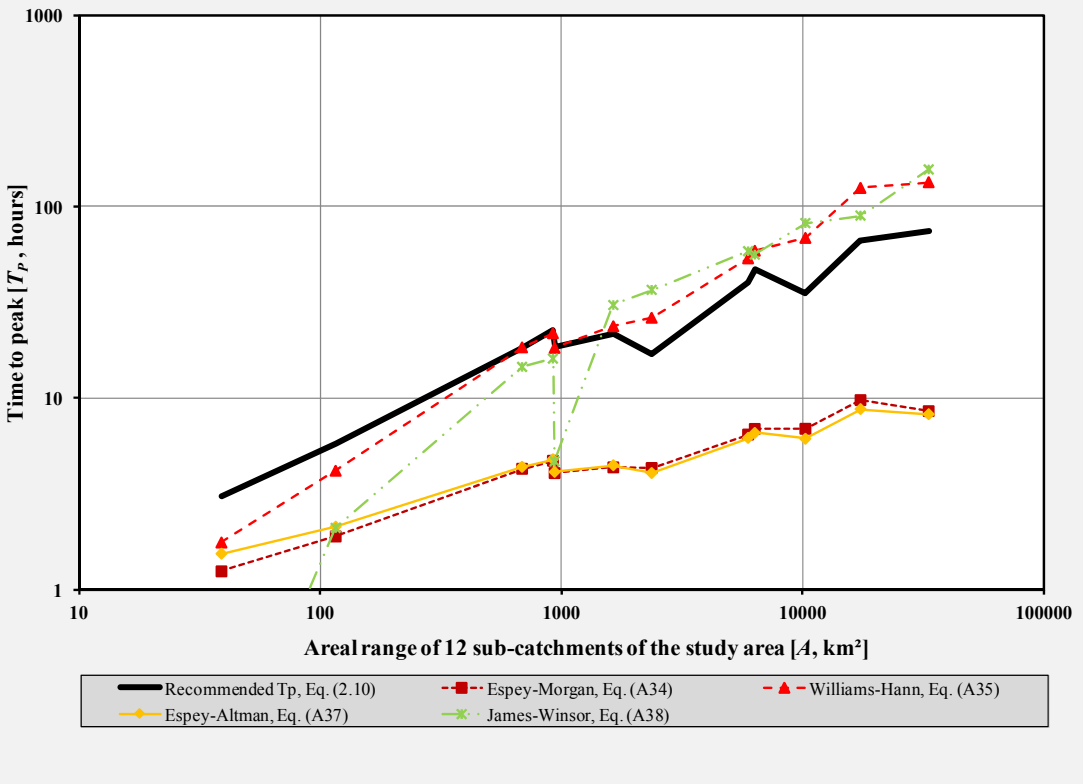

Figure 2.6 T_P estimation results

Table 2.9 Consistency measures for the test of T_P estimation methods compared to the 'recommended method', Eq. (2.10)

Methods	Consistency measures					
	Mean recommended T_P [h]	**Mean estimated T_P [h]**	**Standard bias statistic [%]**	**Mean error [h]**	**Maximum error [h]**	**Standard error [h]**
Espey-Morgan, Eq. (A34)	30.9	5.3	-78.2	-25.6	-66.4	7.0
Williams-Hann, Eq. (A35)	30.9	46.2	25.8	15.4	59.0	5.2
Espey-Altman, Eq. (A37)	30.9	5.1	-77.5	-25.7	-66.8	6.1
James-Winsor, Eq. (A38)	30.9	45.6	17.8	14.8	81.4	8.9

Taking cognisance of the proportionality ratio between the T_C and T_L as discussed in Section 2.7.3.2, it is also important to take note of the relationship between T_C, T_L and T_P by revisiting Eq. (2.10). In recognition of $T_L = 0.6T_C$ and assuming that T_C represents the critical storm duration of which the effective rainfall is constant, while the centroid being at $\frac{P_D}{2}$, then Eq. (2.10) becomes:

$$\begin{aligned} T_P &= \frac{T_C}{2} + 0.6T_C \\ &= 1.1T_C \end{aligned} \qquad (2.13)$$

where T_P = time to peak [hours], and

T_C = time of concentration [hours].

By comparing the 'mean recommended T_C' (Table 2.7) estimates with the 'mean recommended T_P' (Table 2.9) estimates, it resulted in a proportionality ratio of 0.87, which is in essence almost the reciprocal of the proportionality ratio in Eq. (2.13). However, such a ratio difference, especially at a medium to large catchment scale, might imply and confirm that stream responses would most likely peak before equilibrium is reached and at a lower runoff supply rate. Consequently, this close agreement (ratio difference of 0.1) with Larson's (1965) concept of virtual equilibrium, *i.e.* $T_{VE} \approx 0.97T_P$ is presumably not by coincidence. Therefore, the approximation of $T_C \approx T_P$ at this scale could be regarded as sufficiently accurate.

On the other hand, this relationship is based on the assumption that effective rainfall remains constant, while the critical storm duration under consideration being regarded as short; which is not the case in medium to large catchments. It is also important to note that T_P is normally defined as the time interval between the start of effective rainfall and the

peak discharge of a single-peaked hydrograph, but this definition is also regarded as the conceptual definition of T_C (McCuen *et al.*, 1984; USDA SCS, 1985; Linsley *et al.*, 1988; Seybert, 2006).

However, single-peaked hydrographs are more likely to occur in small catchments, while Du Plessis (1984) emphasised that T_P in medium to large catchments, could rather be expressed as the duration of the total net rise (excluding the recession limbs in-between) of a multiple-peaked hydrograph, *e.g.* $T_P = t_1 + t_2 + t_3$, if three discernible peaks are evident.

2.8 Discussion

It was quite evident from the literature review that catchment characteristics, such as climatological variables, catchment geomorphology, catchment variables, and channel geomorphology are highly variable and have a significant influence on the catchment response time. Many researchers have identified the catchment area as the single most important geomorphological variable as it demonstrates a strong correlation with many flood indices affecting the catchment response time. Apart from the catchment area, other catchment variables such as hydraulic and main watercourse lengths, centroid distance, average catchment and main watercourse slopes, have been shown to be equally important and worthwhile to be considered as independent variables to estimate T_C, T_L and/or T_P at a medium to large catchment scale.

In addition to these geomorphological catchment variables, the importance and influence of climatological and catchment variables on the catchment response time were also evident. Owing to the high variability of catchment variables at a large catchment level, the use of weighted *CN* values as representative independent variables to estimate time parameters as opposed to site-specific values could be considered. Simas (1996) and Simas and Hawkins (2002), proved that *CN* values can be successfully incorporated to estimate lag times in medium sized catchments (*cf.* Table 2.A2). However, weighted *CN* values are representative of a linear catchment response and therefore, the use of *MAP* values as a surrogate for these values could be considered in order to present the non-linear catchment responses better.

The inclusion of climatological (rainfall) variables as suitable predictors of catchment response time in South Africa has, to date, been limited to the research conducted by Schmidt and Schulze (1984), which used the two-year return period 30-minute rainfall intensity variable in the SCS-SA method [Eq. (2.9)]. Rainfall intensity-related variables such as this might be worthwhile to be considered as catchment response time independent variables in small catchments. However, in medium to large catchments, the antecedent soil moisture status and the quantity and distribution of rainfall relative to the attenuation of the resulting flood hydrograph as it moves towards the catchment outlet are probably of more importance than the relationship between rainfall intensity and the infiltration rate of the soil. Furthermore, the design accuracy of time parameters obtained from observed hyetographs and hydrographs depends on the computational accuracy of the corresponding observed input variables. The rainfall data in South Africa are generally only widely available at more aggregated levels, such as daily and this reflects a paucity of rainfall data at sub-daily timescales, both in the number of rainfall gauges and length of the recorded series. Under natural conditions, especially in medium to large catchments, uniform effective rainfall seldom occurs, since both spatial and temporal variations affect the resulting runoff. In addition, the paucity of rainfall data and non-uniform distribution, time parameters for an individual event cannot always be measured directly from autographic records owing to the difficulties in determining the start time, end time and temporal and spatial distribution of effective rainfall. Problems are further compounded by poorly synchronised rainfall and runoff recorders which contribute to inaccurate time parameter estimates.

Apart from the afore-mentioned variables, the use of multiple definitions to define time parameters is regarded as also having a large influence on the inconsistency between different methods. The definitions of T_C introduced, highlighted that T_C is a hydraulic time parameter, and not a true hydrograph time parameter. Hydrological literature, unfortunately, often fails to make this distinction. Time intervals from various points during a storm extracted from a hyetograph to various points on the resultant hydrograph are often misinterpreted as T_C. Therefore, these points derived from hyetographs and hydrographs should be designated as T_L or T_P. Some T_L estimates are interpreted as the time interval between the centroid of a hyetograph and hydrograph, while in other definitions the time starts at the centroid of effective rainfall, and not the total rainfall. It can also be argued that the accuracy of T_L estimation is, in general, so poor that differences

in T_L starting and ending points are insignificant. The use of these multiple time parameter definitions, in conjunction with the fact that no 'standard method' could be used to estimate time parameters from observed hyetographs and hydrographs, emphasise why the proportionality ratio of T_L: T_C could typically vary between 0.5 and 2 for the same catchment.

The comparison of the consistency of time parameter estimation methods in medium to large catchment areas in the C5 secondary drainage region in South Africa highlighted that, irrespective of whether an empirical time parameter estimation method (*e.g.* T_C, T_L or T_P) is relatively unbiased with insignificant variations compared to the 'recommended methods' used in South Africa, the latter 'recommended methods', would most likely also show significant variation from the observed catchment response times characterising South African catchments. These significant variations could be ascribed to the fact that these methods have been developed and calibrated for values of the input variables (*e.g.* storage coefficients, channel slope, main watercourse length and/or centroid distances) that differ significantly from the pilot study area and with the values summarised in Table 2.4. Consequently, the use of these empirical methods must be limited to their original developmental regions, especially if no local correction factors are used, otherwise these estimates could be subjected to considerable errors. In such a case, the presence of potential observation, spatial and temporal errors/variations in geomorphological and meteorological data cannot be ignored.

In contrary, in South Africa at this stage and catchment level, practitioners have no choice but to apply these empirical methods outside their bounds, since apart from the HRU [Eq. (2.7)] and Schmidt-Schulze [Eq. (2.9)] T_L estimation methods, none of the other methods have been verified using local hyetograph-hydrograph data. Unfortunately, not only the empirical time parameter estimation methods are used outside their bounds, but practitioners frequently also apply some of the deterministic flood estimation methods, *e.g.* Rational method, beyond their intended field of application. Consequently, such practice might contribute to even larger errors in peak discharge estimation.

The in- or exclusion of independent variables to establish calibrated time parameters representative of the physiographical catchment-indices influencing the temporal runoff

distribution in a catchment should always be based on stepwise multiple regression analyses using the minimisation of total variation and testing of statistical significance. In doing so, the temporal runoff distribution would not be condensed as a linear catchment response. Apart from the minimisation of total variation and testing of statistical significance, is it also of paramount importance to take cognisance of which time parameters are actually required to improve estimates in medium to large catchments in South Africa. However, apart from statistical significance, the independent catchment variables to be included in a regression model must also make sense from a hydrological perspective, *i.e.* the conceptual phases of input, transfer and output must be clearly defined to express the overall catchment process. It was quite evident from the literature review that many researchers identified catchment area and catchment shape as the most important 'transfer functions' which affect the catchment response time. Catchment area influences both the time parameters describing the catchment response and total volume of runoff as a result of catchment-wide rainfall. Catchment shape reflects the way in which runoff will be distributed, both in time and space. In wide, fan-shaped catchments the response time will be shorter with higher associated peak runoff rates as opposed to in long, narrow catchments. In circular catchments with a homogeneous slope distribution, the runoff from various parts of the catchment would reach the outlet simultaneously, while an elliptical catchment equal in size with its outlet at one end of the major axis, would cause the runoff to be distributed over time, thus resulting in smaller peak runoff rates compared to that of a circular catchment. Many researchers also regarded distance (*e.g.* L_{CH}, L_H and L_C) and slope (*e.g.* S_{CH} and S) as equally important 'transfer functions'. The combined use of distance and slope variables is regarded as both conceptually and physically necessary to provide a good indication of catchment storage effects.

The estimation of either T_C or T_L from observed hyetograph-hydrograph data at a large catchment scale normally requires a convolution process based on the temporal relationship between averaged compounded hyetographs (due to numerous rainfall stations) and hydrographs. Conceptually, such a procedure would assume that the volume of direct runoff is equal to the volume of effective rainfall, that all rainfall prior to the start of direct runoff is initial abstraction, after which, the loss rate is assumed to be constant. However, this simplification might ignore the antecedent moisture conditions in a catchment as a result of previous rainfall events. According to the Institute of Hydrology

(IH, 1999), the latter effect of these antecedent moisture conditions could be incorporated by considering an antecedent precipitation index based on rainfall observed within 5 days prior to a specific event. These compounded hyetographs also require that the degree of synchronisation between point rainfall data sets be established first, after which, the conversion to averaged compounded rainfall hyetographs could take place. These inherent procedural shortcomings, in conjunction with the difficulty in estimating catchment rainfall for medium to large catchments due to the lack of continuously recorded rainfall data, as well as the problems encountered with the estimation of hyetograph and/or hydrograph centroid values at this catchment scale, emphasise that an alternative approach should be developed.

The approximation of $T_C \approx T_P$ could be used as basis for such an alternative approach, while the use thereof could be justified by acknowledging that, by definition, the volume of effective rainfall is equal to the volume of direct runoff. Therefore, when separating a hydrograph into direct runoff and baseflow, the separation point could be regarded as the start of direct runoff which coincides with the onset of effective rainfall. In using such approach, the required extensive convolution process is eliminated, since T_P is directly obtained from observed streamflow data. However, it is envisaged that, T_P derived from a range of flood events, would vary over a wide range. Consequently, factors such as antecedent moisture conditions and non-uniformities in the temporal and spatial distribution of storm rainfall have to be accounted for when flood events are extracted from the observed streamflow data sets. Upper limit T_P values and associated maximum runoff volumes would most probably be observed when the entire catchment receives rainfall for the critical storm duration. Lower limit T_P values would most likely be observed when effective rainfall of high average intensity does not cover the entire catchment, especially when a storm is centered near the outlet of a catchment.

2.9 Conclusions

The use of different conceptual definitions in the literature to define the relationship between two time variables to estimate time parameters, not only creates confusion, but also results in significantly different estimates in most cases. Evidence of such conceptual/computational misinterpretations also highlights the uncertainty involved in the process of time parameter estimation.

T_C is the most frequently used and required time parameter in flood hydrology practice, followed by T_L. In acknowledging this, as well as the basic assumptions of the approximations $T_L = 0.6T_C$ and $T_C \approx T_P$, in conjunction with the similarity between the definitions of T_P and the conceptual T_C, it is evident that the latter two time parameters should be further investigated to develop an alternative approach to estimate representative catchment response times using the most appropriate and best performing time variables and catchment storage effects.

Given the sensitivity of design peak discharges to estimated time parameter values, the use of inappropriate time variables resulting in over- or underestimated time parameters in South African flood hydrology practice highlights that considerable effort is required to ensure that time parameters are representative and consistently estimated. Such over- or underestimations in the catchment response time must also be clearly understood in the context of the actual travel time associated with the size of a particular catchment, as the impact of a 10 % difference in estimates might be critical in a small catchment, while being less significant in a larger catchment. However, in general terms, such under- or overestimations of the peak discharge may result in the over- or under-design of hydraulic structures, with associated socio-economic implications, which might render some projects as infeasible.

The next chapter presents the development and evaluation of an alternative, improved and consistent approach to estimate observed and predicted T_P values to reflect the catchment response time in the C5 secondary drainage region as a pilot study area in South Africa.

2.10 Appendix 2.A: Summary of International Catchment Response Time Estimation Methods

Table 2.A1 Summary of T_C estimation methods used internationally

Approach (Flow regime)	Method	Mathematical relationship	Comments
Hydraulic (Sheet overland flow)	**Kinematic wave method** (Morgali and Linsley, 1965)	$T_{C5} = \frac{6.978}{i^{0.4}}\left(\frac{nL_O}{\sqrt{S_O}}\right)^{0.6}$ (A1) where T_{C5} = time of concentration [minutes], i = critical rainfall intensity of duration T_C [mm.h^{-1}], L_O = length of overland flow path [m], n = Manning's roughness parameter (between 0.01 and 0.8), and S_O = average overland slope [m.m^{-1}].	• This method is based on a combination of Manning's equation and a kinematic wave approximation • Assumes that the hydraulic radius of the flow path is equal to the product of travel time and rainfall intensity • The iterative use of this method is limited to paved areas
Hydraulic (Sheet overland flow)	**NRCS kinematic wave method** (Welle and Woodward, 1986)	$T_{C6} = \frac{5.476}{P_2^{0.5}}\left(\frac{nL_O}{\sqrt{S_O}}\right)^{0.8}$ (A2) where T_{C6} = time of concentration [minutes], L_O = length of overland flow path [m], n = Manning's roughness parameter for sheet flow, P_2 = two-year return period 24 hour design rainfall depth [mm], and S_O = average overland slope [m.m^{-1}].	• This method was originally developed to avoid the iteratively use of the original Kinematic wave method [Eq. (A1)] • It is based on a power-law relationship between design rainfall intensity and duration

Table 2.A1 (continued)

Approach (Flow regime)	Method	Mathematical relationship	Comments
Empirical/Semi-analytical (Sheet overland flow)	**Miller's method** (Miller, 1951; ADNRW, 2007)	$T_{C7} = 107\left[\frac{nL_O^{0.333}}{(100S_O)^{0.2}}\right]$ (A3) where T_{C7} = time of concentration [minutes], L_O = length of overland flow path [m], n = Manning's roughness parameter for overland flow, and S_O = average overland slope [m.m^{-1}].	• This method is based on a nomograph for shallow sheet overland flow as published by the Institution of Engineers, Australia (IEA, 1977)
Empirical/Semi-analytical (Mixed sheet/concentrated overland flow)	**Federal Aviation Agency (FAA) method** (FAA, 1970; McCuen *et al*., 1984)	$T_{C8} = \frac{1.8(1.344 - C)L_O^{0.5}}{(100S_O)^{0.333}}$ (A4) where T_{C8} = time of concentration [minutes], L_O = length of overland flow path [m], C = Rational method runoff coefficient, and S_O = average overland slope [m.m^{-1}].	• Commonly used in urban overland flow estimations, since the Rational method's runoff coefficient (C) is included
Empirical/Semi-analytical (Concentrated overland/ channel flow)	**Eagleson's method** (Eagleson, 1962; McCuen *et al.*, 1984)	$T_{C9} = 0.0165\left(\frac{nL_{O,CH}}{R^{0.667}\sqrt{S_{O,CH}}}\right)$ (A5) where T_{C9} = time of concentration [minutes], $L_{O,\,CH}$ = length of flow path, either overland or channel flow [m], n = Manning's roughness parameter, R = hydraulic radius which equals the flow depth [m], and $S_{O,\,CH}$ = average overland or channel slope [m.m^{-1}].	• This method provides an estimation of T_L, *i.e.* the time between the centroid of effective rainfall and the peak discharge of a direct runoff hydrograph • A conversion factor of 1.667 was introduced to estimate T_C in catchment areas smaller than ± 20 km² • The variables that were used during the development and calibration were based on the characteristics of a sewer system

Table 2.A1 (continued)

Approach (Flow regime)	Method	Mathematical relationship	Comments
Empirical/Semi-analytical (Concentrated overland/ channel flow)	**Espey-Winslow method** (Espey and Winslow, 1968)	$T_{C10} = 44.1\left[\frac{\phi L_{O,CH}^{0.29}}{S_{O,CH}^{0.145} i_p^{0.6}}\right]$ (A6) where T_{C10} = time of concentration [minutes], i_p = imperviousness factor [%], $L_{O,CH}$ = length of flow path, either overland or channel flow [m], ϕ = conveyance factor, and $S_{O,CH}$ = average overland or channel slope [m.m^{-1}].	• According to Schultz and Lopez (1974; cited by Fang *et al.*, 2005), this method was developed by Espey and Winslow (1968) for 17 catchments in Houston, USA • The catchment areas varied between 2.6 km² and 90.7 km², while 35 % of the catchments were predominantly rural • Imperviousness (i_p) and conveyance (ϕ) factors were introduced • The imperviousness factor (i_p) represents overland flow retardance, while the conveyance factor (ϕ) measures subjectively the hydraulic efficiency of a watercourse/channel, taking both the condition of channel vegetation and degree of channel improvement into consideration • Typical ϕ values vary between 0.8 (concrete lined channels) to 1.3 (natural channels) (Heggen, 2003)
Empirical/Semi-analytical (Concentrated overland/ channel flow)	**Kadoya-Fukushima method** (Kadoya and Fukushima, 1979; Su, 1995)	$T_{C11} = C_T\left(\frac{A^{0.22}}{i_E^{0.35}}\right)$ (A7) where T_{C11} = time of concentration [hours], A = catchment area [km²], C_T = catchment storage coefficient (typically between 190 and 290), and i_E = effective rainfall intensity [mm.h^{-1}].	• This method is based on the kinematic wave theory and geomorphological characteristics of the slope-channel network in catchment areas between 0.5 km² and 143 km² • It is physically-based with the catchment area and effective rainfall intensity incorporated to estimate T_C
Empirical (Channel flow)	**Bransby-Williams method** (Williams, 1922; Li and Chibber, 2008)	$T_{C12} = 0.2426\left(\frac{L_{CH}}{A^{0.1} S_{CH}^{0.2}}\right)$ (A8) where T_{C12} = time of concentration [hours], A = catchment area [km²], L_{CH} = length of main watercourse/channel [km], and S_{CH} = average main watercourse slope [m.m^{-1}].	• The use of this method is limited to rural catchment areas less than ± 130 km² (Fang *et al.*, 2005; Li and Chibber, 2008) • The Australian Department of Natural Resources and Water (ADNRW, 2007) highlighted that the initial overland flow travel time is already incorporated; therefore an overland flow or standard inlet time should not be added

Table 2.A1 (continued)

Approach (Flow regime)	Method	Mathematical relationship	Comments
Empirical (Channel flow)	**Kirpich method** (Kirpich, 1940)	$T_{C13} = 0.0663\left(\frac{L_{CH}^{\ 2}}{S_{CH}}\right)^{0.385}$ (A9) where T_{C13} = time of concentration [hours], L_{CH} = length of longest watercourse [km], and S_{CH} = average main watercourse slope [$m.m^{-1}$].	• Kirpich (1940) calibrated two empirical equations to estimate T_C in small, agricultural catchments in Pennsylvania and Tennessee, USA • The catchment areas ranged from 0.4 to 45.3 ha, with average catchment slopes between 3 % and 10 % • The estimated T_C values should be multiplied by 0.4 (overland flow) and 0.2 (channel flow) respectively where the flow paths in a catchment are lined with concrete/asphalt • Although this method is proposed to estimate T_C in main watercourses as channel flow, McCuen *et al.* (1984) highlighted that the coefficients used probably reflect significant portions of overland flow travel time, especially if the relatively small catchment areas used during the calibration are taken into consideration • The empirically-based coefficients represent regional effects, therefore the use thereof outside the calibration catchments must be limited • McCuen *et al.* (1984) also showed that this method had a tendency to underestimate T_C values in 75 % of the urbanised catchment areas < 8 km², while in 25 % of the catchments (8 km² < A ≤ 16 km²) with substantial channel flow, it had the smallest bias • Pilgrim and Cordery (1993) also confirmed that the latter was also evident from studies conducted in Australia
Empirical (Channel flow)	**Johnstone-Cross method** (Johnstone and Cross, 1949; Fang *et al.* , 2008)	$T_{C14} = 0.0543\left(\frac{L_{CH}}{S_{CH}}\right)^{0.5}$ (A10) where T_{C14} = time of concentration [hours], L_{CH} = length of longest watercourse [km], and S_{CH} = average main watercourse slope [$m.m^{-1}$].	• This method was developed to estimate T_C in the Scioto and Sandusky River catchments (Ohio Basin) • The catchment areas ranged from 65 km² to 4 206 km² • It is primarily a function of the main watercourse length and average main watercourse slope

Table 2.A1 (continued)

Approach (Flow regime)	Method	Mathematical relationship	Comments
Empirical/Semi-analytical (Channel flow)	**McCuen-Wong method** (McCuen *et al.* , 1984)	$T_{C15} = 2.254\left[\frac{L_{CH}^{0.5552}}{i_2^{0.7164} S_{CH}^{0.2070}}\right]$ (A11a) $T_{C15} = 2.572\left[\frac{L_{CH}^{0.4450} \phi^{0.5517}}{i_2^{0.7231} S_{CH}^{0.2260}}\right]$ (A11b) where T_{C15} = time of concentration [hours], i_2 = 2-year critical rainfall intensity of duration T_C [mm.h^{-1}], L_{CH} = length of longest watercourse [km], ϕ = conveyance factor, and S_{CH} = average main watercourse slope [m.m^{-1}].	• Two empirical equations were developed to estimate T_C in 48 urban catchment areas < 16 km² • Stepwise multiple regression analyses were used to select the independent variables • There was not a substantial difference in the Goodness-of-Fit (GOF) statics of these equations • Equation (A11a) is preferred to estimate T_C, except when the hydraulic characteristics of a main watercourse/channel differ substantially from reach to reach • In such cases, the conveyance factor (ϕ) should be estimated and used as input to Eq. (A11b)
Empirical/Semi-analytical (Channel flow)	**Papadakis-Kazan method** (Papadakis and Kazan, 1987; USDA NRCS, 2010)	$T_{C16} = 2.154\left[\frac{n^{0.52} L_{CH}^{0.5}}{i^{0.38} S_{CH}^{0.31}}\right]$ (A12) where T_{C16} = time of concentration [hours], i = critical rainfall intensity of duration T_C [mm.h^{-1}], L_{CH} = length of longest watercourse [km], n = Manning's roughness parameter, and S_{CH} = average main watercourse slope [m.m^{-1}].	• Data from 84 rural catchment areas < 12.4 km², as well as experimental data from the United States Army Corps of Engineers (USACE), Colorado State University and the University of Illinois, USA were analysed • Stepwise multiple regression analyses were used to select the independent variables from a total of 375 data points to estimate T_C

Table 2.A1 (continued)

Approach (Flow regime)	Method	Mathematical relationship	Comments
Empirical (Channel flow)	**Sheridan's method** (Sheridan, 1994; USDA NRCS, 2010)	$T_{C17} = 2.2 L_{CH}^{0.92}$ (A13) where T_{C17} = time of concentration [hours], and L_{CH} = length of longest watercourse [km].	• Sheridan (1994) performed research on nine catchment areas between 2.6 km² and 334.4 km² in Georgia and Florida, USA • Multiple regression analyses were performed using geomorphological catchment parameters to estimate T_C • The main watercourse/channel length proved to be the overwhelming characteristic that correlated with T_C • On average, the coefficient of determination (r^2) equalled 0.96
Empirical (Channel flow)	**Thomas-Monde method** (Thomas *et al.*, 2000)	$T_{C18} = 0.133 \left[\frac{L_{CH}^{0.475} (101 - i_p)^{0.861} (W_B + 1)^{0.154} (10^{0.194 A_P}) (10^{0.366 C_P})}{S_{CH}^{0.187} (101 - F_R)^{0.144}} \right]$ (A14) where T_{C18} = time of concentration [hours], A_P = (1) if the catchment is in the Appalachian Plateau, otherwise (0), C_P = (1) if the catchment is in the Coastal Plain, otherwise (0), F_R = forest areas [%], i_p = imperviousness factor [%], L_{CH} = length of longest watercourse [km], S_{CH} = average main watercourse slope [m.km^{-1}], and W_B = waterbodies (lakes and ponds) [%].	• Thomas *et al.* (2000) estimated average T_C values for 78 rural and urban catchment areas between 4 km² and 1 280 km² in three distinctive climatic regions (Appalachian Plateau, Coastal Plain and Piedmont) of Maryland, USA • This method was developed by using stepwise multiple regression analyses, *i.e.* transforming T_C and the catchment characteristics (area, main watercourse length and average slope, %-distribution of land use and vegetation, water bodies and impervious areas) to logarithms and fitting a linear regression model to the transformed data • This method was compared with the catchment lag times observed by the USGS and estimated with the SCS and Kirpich methods. It overestimated the USGS values by 5 %, while the two other methods were consistently lower

Table 2.A1 (continued)

Approach (Flow regime)	Method	Mathematical relationship	Comments
Empirical (Channel flow)	**Colorado-Sabol method** (Sabol, 2008)	Rocky Mountain/Great Plains/Colorado Plateau: $T_{C19} = 0.310\left[\frac{A^{0.1}(L_{CH}L_C)^{0.25}}{S_{CH}^{0.2}}\right]$ (A15a) Rural: $T_{C19} = 0.929\left[\frac{A^{0.1}(L_{CH}L_C)^{0.25}}{S_{CH}^{0.2}}\right]$ (A15b) Urban: $T_{C19} = 0.691\left[\frac{A^{0.1}(L_{CH}L_C)^{0.25}}{i_p^{0.36}S_{CH}^{0.14}}\right]$ (A15c) where T_{C19} = time of concentration [hours], A = catchment area [km²], i_p = imperviousness factor [%], L_C = centroid distance [km], L_{CH} = length of longest watercourse [km], and S_{CH} = average main watercourse slope [$m.m^{-1}$].	• Sabol (2008) proposed three different empirical T_C methods to be used in drainage regions with distinctive geomorphological and land-use characteristics in the State of Colorado, USA • Stepwise multiple regression analyses were used to select the independent variables based on the catchment geomorphology and developmental variables • Thereafter, the catchments were grouped as: (i) Rocky Mountain, Great Plains and Colorado Plateau, (ii) rural, and (iii) urban

Table 2.A2 Summary of T_L estimation methods used internationally

Approach	Method	Mathematical relationship	Comments
Empirical/Semi-analytical	**Snyder's method** (Snyder, 1938)	$T_{L4} = C_{T2}(L_H L_C)^{0.3}$ (A16) where T_{L4} = lag time [hours], C_{T2} = catchment storage coefficient (typically between 1.35 and 1.65), L_C = centroid distance [km], and L_H = hydraulic length [km].	• Snyder (1938; cited by Viessman *et al*., 1989) developed a SUH method derived from the relationships between standard unit hydrographs and geomorphological catchment descriptors • The catchment areas evaluated varied between 25 km² and 25 000 km² and are located in the Appalachian Highlands, USA • The catchment storage coefficient's (C_T) were established regionally and include the effects of slope and storage • T_L is defined as the time between the centroid of effective rainfall and the time of peak discharge
Empirical	**Taylor-Schwarz method** (Taylor and Schwarz, 1952)	$T_{L5} = \frac{0.6}{\sqrt{S}}(L_H L_C)^{0.3}$ (A17) where T_{L5} = lag time [hours], L_C = centroid distance [km], L_H = hydraulic length of catchment [km], and S = average catchment slope [%].	• Taylor and Schwarz (1952; cited by Chow, 1964) proved that the catchment storage coefficient (C_T) as used in Snyder's method (1938) is primarily influenced by the average catchment slope • Consequently, a revised version of Snyder's method was proposed • A total of 20 catchments in the North and Middle Atlantic States, USA were evaluated
Empirical/Semi-analytical	**USACE method** (Linsley *et al.*, 1988)	$T_{L6} = C_{T3}\left(\frac{L_H L_C}{\sqrt{S_{CH}}}\right)^{0.38}$ (A18) where T_{L6} = lag time [hours], C_{T3} = catchment storage coefficient, L_C = centroid distance [km], L_H = hydraulic length of catchment [km], and S_{CH} = average main watercourse slope [$m.m^{-1}$].	• According to Linsley *et al.* (1988), the United States Army Corps of Engineers (USACE) developed a general expression for T_L in 1958 based on the Snyder (1938) and Taylor-Schwarz (1952) methods • In this method, the average catchment slope (S, %) was replaced with the average main watercourse slope (S_{CH}, $m.m^{-1}$) • Typical C_T values proposed were: 0.24 (valleys; 0 – 10 % slopes), 0.50 (foothills; 10 – 30 % slopes) and 0.83 (mountains; > 30 % slopes)

Table 2.A2 (continued)

Approach	Method	Mathematical relationship	Comments
Empirical	**Hickok-Keppel method** (Hickok *et al.*, 1959)	$T_{L7} = 2.297\left[\left(\frac{\sqrt{L_{CSA}+W_{SA}}}{S_{SA}\sqrt{D}}\right)^{0.65}\right]$ (A19) where T_{L7} = lag time [hours], D = drainage density of entire catchment [km^{-1}], L_{CSA} = centroid distance of source area [km], S_{SA} = average slope of source area [%], and W_{SA} = average width of source area [km].	• Rainfall and runoff records for 14 catchment areas between 27 ha and 1 952 ha in Arizona, New Mexico and Colorado, USA were analysed • The runoff represented by unit hydrographs is related to the spatial distribution of effective rainfall and consequently controlled the runoff source area, *i.e.* sub-divided catchments • It was also found that the slope of the runoff source areas could be useful in T_L estimations, while a runoff source area was defined as that portion of the catchment with the highest average slope • The T_L estimates are significant in relating the influences of catchment variables to the hydrograph shape, with the average catchment slope more correlated than the average watercourse slope • The drainage density parameter reflects the proportion of channel versus overland flow, thus providing a measure of the hydraulic efficiency
Empirical	**Kennedy-Watt method** (Kennedy and Watt, 1967; Heggen, 2003)	$T_{L8} = 0.280\left[\frac{\left(\frac{L_H}{\sqrt{S_{CH}}}\right)^{0.667}}{\left(1+20\frac{A_W}{A}\right)^{1.21}}\right]$ (A20) where T_{L8} = lag time [hours], A = catchment area [km^2], A_W = area of waterbodies in the upper two-thirds of the catchment [km^2], L_H = hydraulic length of catchment [km], and S_{CH} = average main watercourse slope [$m.m^{-1}$].	• This method takes into consideration the distribution and extent of waterbodies (lakes, marshes and ponds) in a catchment • Multiple regression analyses were used to establish the independent variables from the catchment geomorphology and distribution of waterbodies in the upper two-thirds of the catchments

Table 2.A2 (continued)

Approach	Method	Mathematical relationship	Comments
Empirical/Semi-analytical	**Bell-Kar method** (Bell and Kar, 1969)	$T_{L9} = C_{T4}\left[\frac{L_H^{0.77}}{S_{CH}^{0.39}}\right]$ (A21) where T_{L9} = lag time [hours], C_{T4} = catchment storage coefficient (typically between 1 and $3.4*10^{-4}$), L_H = hydraulic length of catchment [km], and S_{CH} = average main watercourse slope [$m.m^{-1}$].	• T_L is primarily dependent on the geomorphological catchment characteristics • Critical T_L values, which are arguably suitable representatives of the critical storm duration of design rainfall, were used • This method is a modified version of the Kirpich method
Empirical/Semi-analytical	**Askew's method** (Askew, 1970)	$T_{L10} = 2.12\left[\frac{A^{0.57}}{Q_{WM}^{0.23}}\right]$ (A22) where T_{L10} = lag time [hours], A = catchment area [km^2], and Q_{WM} = weighted mean runoff rate [$m^3.s^{-1}$].	• The variable temporal rainfall distributions had little effect on T_L, while T_L can only be correlated with the weighted mean runoff rate in a catchment • The weighted mean runoff rate was defined as the mean ratio of the total runoff rate divided by the time of occurrence of direct runoff, weighted in proportion to the direct runoff discharge rate • A constant exponent was used as a fixed regression coefficient to develop a means of predicting the constant term in this method, which reflects a measure of a linear model's estimation of T_L • A high degree of association existed between the regression constant and the catchment area
Empirical	**Putnam's method** (Putnam, 1972)	$T_{L11} = \frac{0.045}{i_p^{0.57}}\left(\frac{L_{CH}}{\sqrt{S_{CH}}}\right)^{0.5}$ (A23) where T_{L11} = lag time [hours], i_p = imperviousness factor [fraction], L_{CH} = main watercourse length [km], and S_{CH} = average main watercourse slope [$m.m^{-1}$].	• According to Haan *et al*. (1994), this method was developed by Putnam (1972) for 34 catchments in North Carolina, USA • Multiple regression analyses were used to establish the independent variables from the catchment geomorphology and degree of urbanisation • T_L is defined as the time from the centroid of effective rainfall to the centroid of direct runoff

Table 2.A2 (continued)

Approach	Method	Mathematical relationship	Comments
Empirical/Semi-analytical	**Rao-Delleur method** (Rao and Delleur, 1974; Heggen, 2003; Fang *et al.*, 2005; ADNRW, 2007)	$T_{L12} = 0.248\left(\frac{A^{0.496} L_{CH}^{0.073}}{S_{CH}^{0.075}(1+i_p)^{1.289}}\right)$ (A24a) $T_{L12} = 0.253\left(\frac{A^{0.542}}{S_{CH}^{0.081}(1+i_p)^{1.210}}\right)$ (A24b) $T_{L12} = 0.493\left(\frac{A^{0.512}}{(1+i_p)^{1.433}}\right)$ (A24c) $T_{L12} = 1.274\left(\frac{A^{0.458} D_{PE}^{0.371}}{P_E^{0.267}(1+i_p)^{1.662}}\right)$ (A24d) where T_{L12} = lag time [hours], A = catchment area [km²], D_{PE} = duration of effective rainfall [hours], i_p = imperviousness factor [fraction], L_{CH} = main watercourse length [km], P_E = effective rainfall [mm], and S_{CH} = average watercourse slope [m.m^{-1}].	• It was established that average T_L values (based on the time lapse between the centroid's of effective rainfall and direct runoff) could not be used alone for runoff estimation, since it's dependent on various geomorphological and meteorological characteristics • Three equations based on stepwise multiple regression analyses were developed with the independent variables only related to catchment geomorphology and developmental variables • It was established that Eq. (A24c), which included only the catchment area and imperviousness factor (i_p), is as effective as Eqs. (A24a & A24b), which include both the main watercourse length and average catchment slope • An additional equation, Eq. (A24d) was developed to take meteorological parameters (effective rainfall and duration) also into consideration • T_L is not only a unique catchment characteristic, but varies from storm to storm
Empirical	**NERC method** (NERC, 1975)	$T_{L13} = 2.8\left(\frac{L_{CH}}{\sqrt{S_{CH}}}\right)^{0.47}$ (A25) where T_{L13} = lag time [hours], L_{CH} = main watercourse length [km], and S_{CH} = average main watercourse slope [m.km^{-1}].	• The United Kingdom Flood Studies Report (UK FSR) (NERC, 1975) proposed the use of this method to estimate T_L in ungauged UK catchments • T_L is primarily dependent on the geomorphological catchment characteristics, *e.g.* main watercourse length and average slope

Table 2.A2 (continued)

Approach	Method	Mathematical relationship	Comments
Empirical/Semi-analytical	**CUHP method** [Urban Drainage and Flood Control District (UDFCD), 1984; cited by Heggen, 2003]	$T_{L14} = C_T \left(\frac{L_H L_C}{\sqrt{S_{CH}}} \right)^{0.48}$ (A26) where T_{L14} = lag time [hours], C_T = $ai_p^2+bi_p+c$, imperviousness storage coefficients, i_p = imperviousness factor [%], L_C = centroid distance [km], L_H = hydraulic length of catchment [km], and S_{CH} = average main watercourse slope [$m.m^{-1}$].	• This method (Colorado Urban Hydrograph Procedure) is a modified version of Snyder's method as used in urban catchment areas between 40 ha and 80 ha in the State of Colorado, USA • This method is also commonly used to derive unit hydrographs for both urban and rural catchment areas ranging from 0.36 km² to 13 km² • In catchment areas larger than 13 km², it is recommended that the catchment be subdivided into sub-catchments of 13 km^2 or less
Empirical	**Mimikou's method** (Mimikou, 1984)	$T_{L15} = 0.430A^{0.418}$ (A27) where T_{L15} = lag time [hours], and A = catchment area [km²].	• This method was developed for catchment areas between 202 km² and 5 005 km² in the western and north-western regions of Greece • T_L and unit hydrograph peaks (Q_P) were estimated at the catchment outlets from unit hydrographs produced by 10 mm effective rainfall and 6-hour storm durations • Storm durations of 6-hours were used in all the catchments in order to avoid the effect of variable storm durations on the variation of T_L and Q_P values from catchment to catchment. In other words, complex areal storms of various durations were delineated in 6-hour intervals according to the well known multi-period technique described in the literature (Linsley *et al.*, 1988) • It was established that T_L and Q_P associated with specific storm durations, are increasing power functions of the catchment size • Mimikou (1984) also emphasised that the developed regional T_L relationship is only applicable to the study area

Table 2.A2 (continued)

Approach	Method	Mathematical relationship	Comments
Empirical	**Watt-Chow method** (Watt and Chow, 1985)	$T_{L16} = 0.000326\left(\frac{1000L_{CH}}{\sqrt{S_{CH}}}\right)^{0.79}$ (A28) where T_{L16} = lag time [hours], L_{CH} = main watercourse length [km], and S_{CH} = average main watercourse slope [m.m^{-1}].	• This method is based on geomorphological data from 44 catchment areas between 0.01 km² and 5 840 km² across the USA and Canada • The main watercourse slopes ranged between 0.00121 m.m^{-1} and 0.0978 m.m^{-1}
Empirical	**Haktanir-Sezen method** (Haktanir and Sezen, 1990; cited by Fang *et al.*, 2005)	$T_{L17} = 0.2685L_{CH}^{0.841}$ (A29) where T_{L17} = lag time [hours], and L_{CH} = main watercourse length [km].	• SUHs based on two-parameter Gamma and three-parameter Beta distributions for 10 catchments in Anatolia were developed • Regression analyses were used to establish the relationships between T_L and the main watercourse length
Analytical	**Loukas-Quick method** (Loukas and Quick, 1996)	$T_{L18} = 0.072\left(\frac{B^{0.6}}{k^{0.4}\left(i_E K_{Avg} S_{CH}\right)^{0.2}}\right)$ (A30) where T_{L18} = lag time [hours], B = catchment shape factor as a $f(k, L_{CH}$ and regressed catchment parameters), i_E = effective rainfall intensity [mm.h^{-1}], K_{Avg} = average saturated hydraulic conductivity of soil [mm.h^{-1}], k = main watercourse shape factor, as a f(channel side slopes and bed width), and S_{CH} = average main watercourse slope [m.m^{-1}].	• This method estimates T_L in forested mountainous catchments, where most of the flow is generated through subsurface pathways • The data acquired from field experiments were combined with the kinematic wave equation to describe the flow generation from steep, forested hillslopes • The hillslope runoff was used as input to the main watercourses, where the runoff movement in the channels was described by roughness parameters and slopes that vary from point to point along the main watercourse • The resulting equations were integrated to obtain this method, which relate the geomorphological characteristics, effective rainfall intensity and average saturated hydraulic conductivity of a catchment to its response time through an analytical mathematical procedure • This method provides reliable T_L estimates, however, compared to existing empirical methods (Snyder, 1938; NERC, 1975 and Watt-Chow, 1985), it underestimated T_L significantly in catchment areas ranging from 3 km² to 9.5 km² in Coastal British Columbia, Canada

Table 2.A2 (continued)

Approach	Method	Mathematical relationship	Comments
Empirical	**McEnroe-Zhao method** (McEnroe and Zhao, 2001)	$T_{L19} = 0.058\left(\frac{L_{CH}}{\sqrt{S_{CH}}}\right)^{0.74} e^{-3.5 i_p}$ (A31a) $T_{L19} = 0.106\left(\frac{L_{CH}}{\sqrt{S_{CH}}}\right)^{0.63} e^{-0.1 R_D}$ (A31b) where T_{L19} = lag time [hours], i_p = imperviousness factor [fraction], L_{CH} = main watercourse length [km], R_D = road density [km^{-1}], and S_{CH} = average main watercourse slope [m.m^{-1}].	• T_L was estimated utilising geomorphological catchment characteristics • Individual and average T_L values were estimated in gauged catchments from 85 observed rainfall and runoff events at 14 different sites in Johnson County, Kansas, USA • Two regression equations were developed through multiple regression analyses to estimate T_L in urban and developing catchments • The catchment and channel geomorphology were obtained from DEMs and manipulated in an ArcGIS™ environment • It was established that urbanisation has a major impact on T_L; in fully developed catchments, T_L can be as much as 50 % less than in a natural catchment • In small urban catchments with curb-and-gutter streets and storm sewers, the T_L values can even be shorter
Empirical/Semi-analytical	**Simas-Hawkins method** (Simas, 1996; Simas and Hawkins, 2002)	$T_{L20} = 0.22653\left(\frac{\left(\frac{A}{L_H}\right)^{0.5937}\left(\frac{25\,400}{CN} - 254\right)^{0.3131}}{S^{0.1505}}\right)$ (A32) where T_{L20} = lag time [hours], A = catchment area [km²], CN = runoff curve number, L_H = hydraulic length of catchment [km], and S = average catchment slope [m.m^{-1}].	• T_L is defined as the time difference between the centroid of effective rainfall and direct runoff and was estimated from over 50 000 rainfall: runoff events in 168 catchment areas between 0.1 ha and 1 412.4 ha in the USA • The catchments were grouped into different geographical, catchment management practice, land-use and hydrological behaviour regions to explain the variation of T_L between catchments • Multiple regression analyses were performed to establish the most representative T_L relationship

Table 2.A2 (continued)

Approach	Method	Mathematical relationship	Comments
Empirical	**Folmar-Miller method** (Folmar and Miller, 2008)	$T_{L21} = \frac{(1\,000 L_H)^{0.65}}{83.4}$ (A33) where T_{L21} = lag time [hours], and L_H = hydraulic length of catchment [km].	• Multiple regression analyses were performed on T_L values obtained from 10 000 direct runoff events in 52 gauged catchment areas between 1 ha and 4 991 ha in eight different states throughout the USA • It was established that T_L correlates strongly ($r^2 = 0.89$; $N = 52$) with the catchment hydraulic length (L_H) and therefore only this parameter was used to develop this method • The inclusion of any other geomorphological catchment characteristics in the method did not improve its ability to predict T_L • This method, as well as the NRCS methods were used to estimate T_L in all the catchments, after which, the results were compared with the T_L values obtained from observed hyetographs and hydrographs • Overall, this method and the NRCS methods underestimated the T_L values by 65 % and 62 % respectively

Table 2.A3 Summary of T_P estimation methods used internationally

Approach	Method	Mathematical relationship	Comments
Empirical	**Espey-Morgan method** (Espey *et al.*, 1966; cited by Fang *et al.*, 2005)	$T_{P2} = 0.1167\left(\frac{L_{CH}^{0.12}}{S_{CH}^{0.52}}\right)$ (A34) where T_{P2} = time to peak [hours], L_{CH} = main watercourse length [km], and S_{CH} = average main watercourse slope [m.m^{-1}].	• Multiple regression analyses were used to establish T_P for 11 rural and 24 urban catchments in Texas, New Mexico and Oklahoma, USA • This method is only applicable to the large, rural catchments used during this research
Empirical	**Williams-Hann method** (Williams and Hann, 1973; cited by Viessman *et al*., 1989)	$T_{P3} = 0.0601\left[\left(\frac{A^{0.422}}{S_{CH}^{0.460}}\right)\left(\frac{L_H}{W}\right)^{0.133}\right]$ (A35) where T_{P3} = time to peak [hours], A = catchment area [km²], L_H = hydraulic length of catchment [km], S_{CH} = average main watercourse slope [m.m^{-1}], and W = width of catchment [km].	• This method is incorporated in the problem-oriented computer language for hydrological modelling (HYMO) to simulate surface runoff from catchments • Regional regression analyses were used to establish T_P for 34 catchment areas between 1.3 km² and 65 km² in Texas, Oklahoma, Arkansas, Louisiana, Mississippi and Tennessee, USA
Empirical/Semi-analytical	**NERC method** (NERC, 1975)	$T_{P4} = 46.6\left(\frac{L_{CH}^{0.14}}{S_{CH}^{0.38}(1+i_p)^{1.99}C_i^{0.4}}\right)$ (A36) where T_{P4} = time to peak [hours], C_i = climatic index of the flood runoff potential, i_p = imperviousness factor [%], L_{CH} = main watercourse length [km], and S_{CH} = average main watercourse slope [m.km^{-1}].	• T_P was related to the climate, catchment and channel geomorphology and developmental variables by using stepwise multiple regression analyses • The average main watercourse slope and degree of imperviousness were identified as the most important variables explaining the variance of T_P • The main watercourse length was surprisingly less critical than the degree of imperviousness due to the significant inverse correlation of main watercourse length with average slope, while the degree of imperviousness had a direct influence on the efficiency of drainage networks, flow velocities and the proportion of total runoff

Table 2.A3 (continued)

Approach	Method	Mathematical relationship	Comments
Empirical/Semi-analytical	**Espey-Altman method** (Espey and Altman, 1978)	$T_{P5} = 0.3326\left(\frac{L_H^{0.23}\phi^{1.57}}{S_{CH}^{0.25} i_p^{0.18}}\right)$ (A37) where T_{P5} = time to peak [hours], i_p = imperviousness factor [%], L_H = hydraulic length of catchment [km], ϕ = conveyance factor, and S_{CH} = average main watercourse slope [$m.m^{-1}$].	• A set of regional regression equations to represent 10-minute SUHs from a series of effective rainfall events were developed • Forty-one catchment areas between 4 ha and 3 885 ha were analysed • This method is based on the concept of Snyder's UHs (1938)
Empirical	**James-Winsor method** (James *et al.*, 1987; cited by Fang *et al.*, 2005)	<u>Mild slope (< 5 %):</u> $T_{P6} = 0.85\left(\frac{A^{0.9}}{H_T^{0.1} L_{CH}^{0.6}}\right)$ (A38a) <u>Medium slope (5 to 10 %):</u> $T_{P6} = 0.92\left(\frac{A^{0.5}}{H_T^{0.2} L_{CH}^{0.2}}\right)$ (A38b) <u>Steep slope (> 10 %):</u> $T_{P6} = 0.91\left(\frac{A^{0.2}}{H_T^{0.3} L_{CH}^{0.8}}\right)$ (A38c) where T_{P6} = time to peak [hours], A = catchment area [km²], L_{CH} = main watercourse length [km], and H_T = height difference between the catchment outlet and water divide along the longest flow path [m].	• 283 Rainfall events were analysed in catchment areas between 0.7 km² and 62 km² in 13 states in the USA • The climate and geomorphology in these catchments were highly variable • Only 48 catchments (31 calibration catchments and 17 verification catchments) were used in the multiple regression analyses to relate the physical catchment characteristics to T_P • Three empirical equations were developed for three distinctive slope classes: mild, medium and steep

Table 2.A3 (continued)

Approach	Method	Mathematical relationship	Comments
Empirical	**Jena-Tiwari method** (Jena and Tiwari, 2006)	1-hour SUH: $T_{P7} = 1.688 L_M^{0.270} L_C^{0.280}$ (A39a) 2-hour SUH: $T_{P7} = 2.099 L_C^{0.546}$ (A39b) where T_{P7} = time to peak [hours], L_C = centroid distance [km], and L_M = maximum catchment length parallel to the principle drainage line [km].	• 1-hour and 2-hour SUHs were developed for two catchments (158 km² and 69 km²) in India based on SUH parameters such as T_P, Q_P and T_B, which are all related to the catchment and channel geomorphology • A correlation matrix between the SUH parameters and geomorphological parameters was generated to identify the most suitable geomorphological parameters • The best single predictor for T_P was found to be the catchment hydraulic length, followed by the main watercourse length and centroid distance • Regression equations were developed between the individual SUH parameters and the selected geomorphological parameters

3. CASE STUDY OF AN ALTERNATIVE APPROACH TO ESTIMATE CATCHMENT RESPONSE TIME

This chapter is based on the following paper:

Gericke, OJ and Smithers, JC. 2015. An improved and consistent approach to estimate catchment response time: Case study in the C5 drainage region, South Africa. *Journal of Flood Risk Management.* DOI: 10.1111/jfr3.12206.

3.1 Abstract

Large errors in estimates of peak discharge in medium to large catchments in South Africa can be largely ascribed to significant errors in the estimation of the catchment response time, mainly as a consequence of the use of inappropriate time variables, the inadequate use of a simplified convolution process between observed rainfall and runoff time variables, and the lack of locally developed empirical methods to estimate catchment response time parameters. Furthermore, the use of a typical convolution process between a single hyetograph and hydrograph to estimate observed time parameters at large catchment scales is regarded as not practical, as such simplification is not applicable in real, large heterogeneous catchments where antecedent moisture from previous rainfall events and spatially non-uniform rainfall hyetographs can result in multi-peaked hydrographs. This chapter presents the development and evaluation of an alternative, improved and consistent approach to estimate catchment response time expressed as the time to peak (T_P) in the C5 secondary drainage region in South Africa, while the relationship, similarity and proportionality ratios between T_P and the conceptual time of concentration (T_C) and lag time (T_L) are also investigated.

Keywords: *baseflow; direct runoff; lag time; time of concentration; time to peak*

3.2 Introduction

In acknowledging the findings and recommendations from Chapter 2, as well as the basic assumptions of the approximations $T_L = 0.6T_C$ and $T_C \approx T_P$, this chapter presents the development and evaluation of an alternative, improved and consistent approach to estimate observed and predicted T_P values to reflect the catchment response time in the C5 secondary drainage region as a pilot study area in South Africa.

In this chapter, subscripts 'x' and 'y' are used to distinguish between estimates from observed data (x) and estimated values (y) using either the developed empirical time parameter equation (this chapter) or applying the 'recommended methods' as commonly used in South Africa. The estimation of T_{Cx} or T_{Lx} from observed hyetograph-hydrograph data at a medium to large catchment scale normally requires a convolution process based on the temporal relationship between averaged hyetographs from numerous rainfall stations to estimate catchment rainfall and the resulting hydrograph. In Chapter 2, the inherent procedural limitations of such a convolution process and the difficulty in estimating catchment rainfall for medium to large catchments were discussed, which highlighted the need for the development of an alternative approach (Gericke and Smithers, 2014).

In Chapter 2 (Gericke and Smithers, 2014) it was demonstrated that the approximation of $T_C \approx T_P$ could be used as basis for such an alternative approach at medium to large catchment scales, while the use of this approximation could be justified by acknowledging that, by definition, the volume of effective rainfall is equal to the volume of direct runoff. Therefore, when separating a hydrograph into direct runoff and baseflow, the separation point could be regarded as the start of direct runoff which coincides with the onset of effective rainfall. In addition, rainfall prior to the start of direct runoff, could also contribute to the antecedent soil moisture status of a catchment, which mainly affects the percentage of direct runoff. In using such an approach, the required extensive convolution process is eliminated, since T_{Px} is obtained directly from observed streamflow data without the need for rainfall data.

The objectives of the research reported in this chapter are discussed in the next section, followed by a graphical overview of the pilot study area. Thereafter, the methodologies involved in meeting the objectives are detailed, followed by the results, discussion, and conclusions.

3.3 Objectives and Assumptions

The overall objective of this chapter is to improve estimates of peak discharge at a medium to large catchment scale (*e.g.* 20 km² to 35 000 km²) in the C5 secondary drainage region in South Africa by developing an empirical equation to estimate the catchment response

time, which has a significant influence on the resulting hydrograph shape and peak discharge. The focus is on using an alternative and consistent approach to estimate catchment response time, *i.e.* adopt the approximation of $T_C \approx T_P$ as recommended in Chapter 2 (Gericke and Smithers, 2014), with T_{Px} estimated directly from the observed streamflow data.

The specific objectives are: (i) to extract the flood event characteristics (*e.g.* peak, volume and duration) using primary streamflow data from 16 flow-gauging stations located in the pilot study area, (ii) to separate the extracted hydrographs into direct runoff and baseflow using different recursive filtering methods, (iii) to estimate the direct runoff/effective rainfall volumes, (iv) to investigate and analyse the relationship between different hydrograph shape parameters (T_P, T_C, T_L) and key climatological and geomorphological catchment variables in order to verify the developed regionalised empirically-based time parameter equation, and (v) to compare the observed time parameters with both the derived relationship and 'recommended methods' currently used in South Africa in order to highlight the impact of inconsistent results when translated into estimates of peak discharge.

It is important to note that this chapter will primarily highlight biases and inconsistencies in the 'recommended methods' currently used when compared to the calibrated regional time parameter equation and observed time parameters. However, when translating the time parameter estimation results into design peak discharges, the significance of the results is evident.

This chapter is based on the following assumptions:

(a) **The conceptual T_C equals the time of virtual equilibrium (T_{VE}):** The conceptual T_C is defined as the time required for runoff, as a result of effective rainfall with a uniform spatial and temporal distribution over a catchment, to contribute to the peak discharge at the catchment outlet, or, in other words, the time required for a 'water particle' to travel from the catchment boundary along the longest watercourse to the catchment outlet (Kirpich, 1940; McCuen *et al.,* 1984; McCuen, 2005; USDA NRCS, 2010; SANRAL, 2013). T_{VE} is the time when

response equals 97 % of the total surface runoff, which is also regarded as a practical measure of the actual equilibrium time (Larson, 1965). The actual equilibrium time is difficult to determine due to the gradual response rate to the input rate. Consequently, T_C defined according to the 'water particle' concept would be equivalent to T_{VE}. Gericke and Smithers (2014) also obtained results in close agreement with Larson's (1965) concept of virtual equilibrium, *i.e.* $T_{VE} \approx 0.97T_C$.

(b) **The conceptual T_C equals T_P:** The T_P is normally defined as the time interval between the start of effective rainfall and the peak discharge of a single-peaked hydrograph, but this definition is also regarded as the conceptual definition of T_C (McCuen *et al.,* 1984; USDA SCS, 1985; Linsley *et al*., 1988; Seybert, 2006). However, in medium to large catchments, T_{Pxi} could be defined as the duration of the total net rise of a multiple-peaked hydrograph (Du Plessis, 1984) as shown in Figure 3.1 and expressed in Eq. (3.1).

$$T_{Pxi} = \sum_{j=1}^{N} t_j \qquad (3.1)$$

where T_{Pxi} = observed time to peak which equals the conceptual T_C for individual flood events [hours],

t_j = duration of the total net rise (excluding the in-between recession limbs) of a multiple-peaked hydrograph [hours], and

N = sample size.

(c) **T_C-T_L proportionality ratio:** The catchment T_{Lx}, defined as the time from the centroid of effective rainfall to the time of the peak discharge of total or direct runoff (Figure 3.1), is related to the conceptual T_C by $T_{Lx} = 0.6T_C$ (McCuen, 2009).

In acknowledging the similarity between the definitions of the conceptual T_C, T_{VE} and T_P, Gericke and Smithers (2014) argued that the approximation of $T_C \approx T_P$ in medium to large catchments could be regarded as sufficiently accurate. However, it is expected that, T_{Pxi} derived from a number of flood events, will vary over a wide range of values. Thus, factors such as antecedent moisture conditions and non-uniformity in the temporal and spatial distribution of storm rainfall have to be accounted for when flood hydrographs are extracted from the observed streamflow data sets.

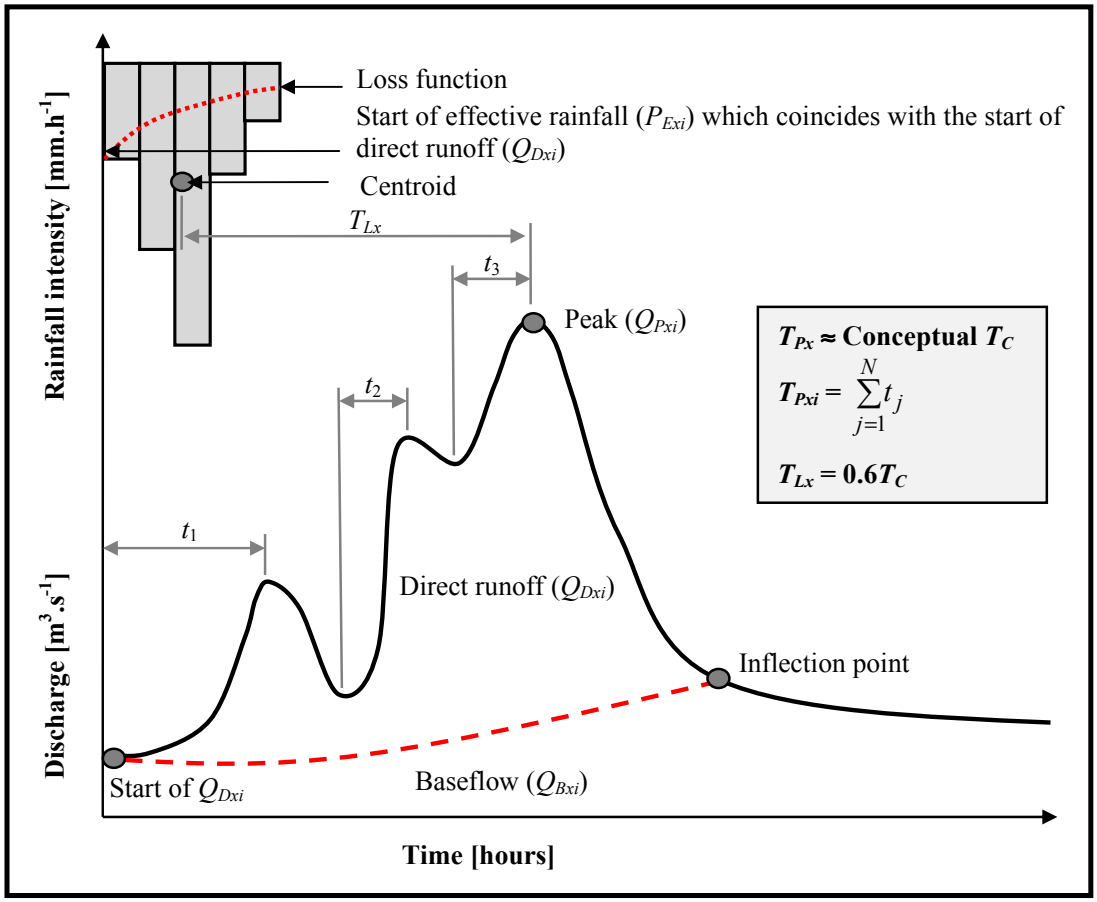

Figure 3.1 Schematic illustrative of the relationships between the different catchment response time parameters (conceptual T_C, T_{Px} and T_{Lx}) for multi-peaked hydrographs

3.4 Study Area

South Africa, which is located on the most southern tip of Africa (Figure 3.2), is demarcated into 22 primary drainage regions, which are further delineated into 148 secondary drainage regions. The pilot study area is situated in primary drainage region C and comprises of the C5 secondary drainage region (Midgley *et al.,* 1994).

Please refer to Chapter 2 (*cf.* Section 2.4) for an overview of the location and characteristics of the pilot study area. The layout of each catchment, river networks and locality of individual calibration and verification flow-gauging stations are shown in Figure 3.2.

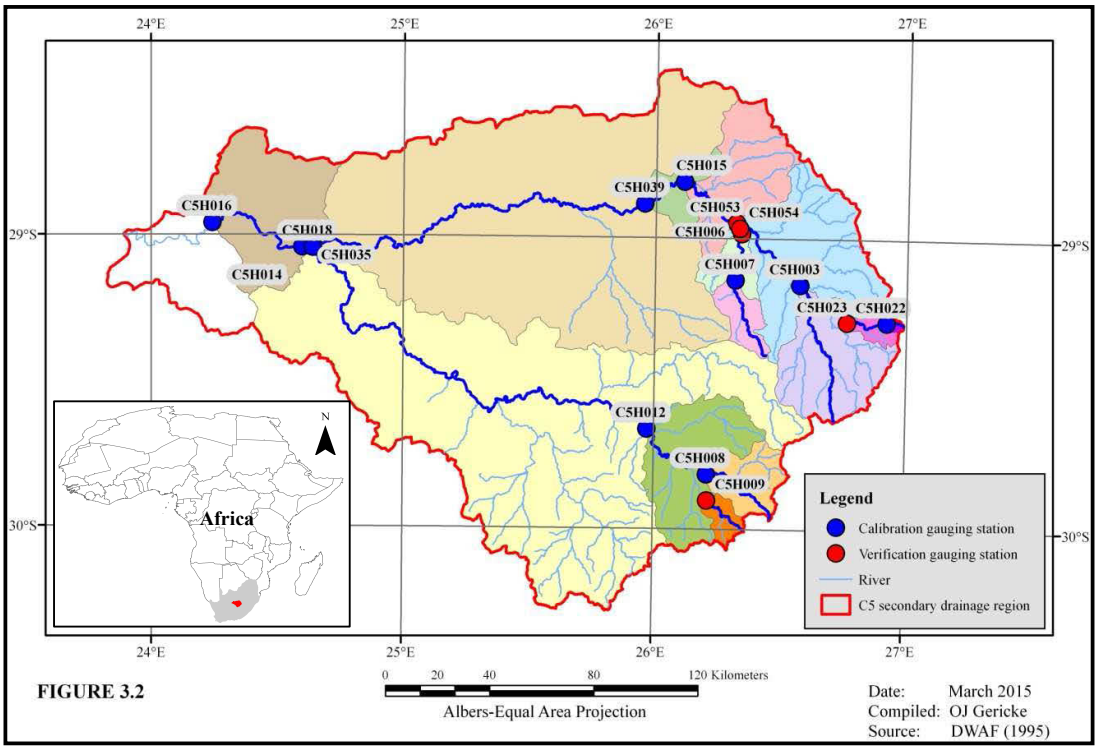

Figure 3.2 Location of the pilot study area (C5 secondary drainage region)

3.5 Methodology

In this section, a flow diagram (Figure 3.3) is used to provide a general overview of the methodology followed in this chapter.

In addition, for sections denoted with ** in Figure 3.3, a detailed discussion is included in the next sub-sections to provide further details and clarification on the methodology contained in Figure 3.3.

3.5.1 Analyses of flood hydrographs

As summarised in Figure 3.3, it is important to note that Smakhtin and Watkins (1997) adopted the methodology as proposed by Nathan and McMahon (1990) with some modifications for a national-scale study in South Africa. Consequently, based on these recommendations, as well as the need for consistency and reproducibility, the above-mentioned three methods were considered in this chapter.

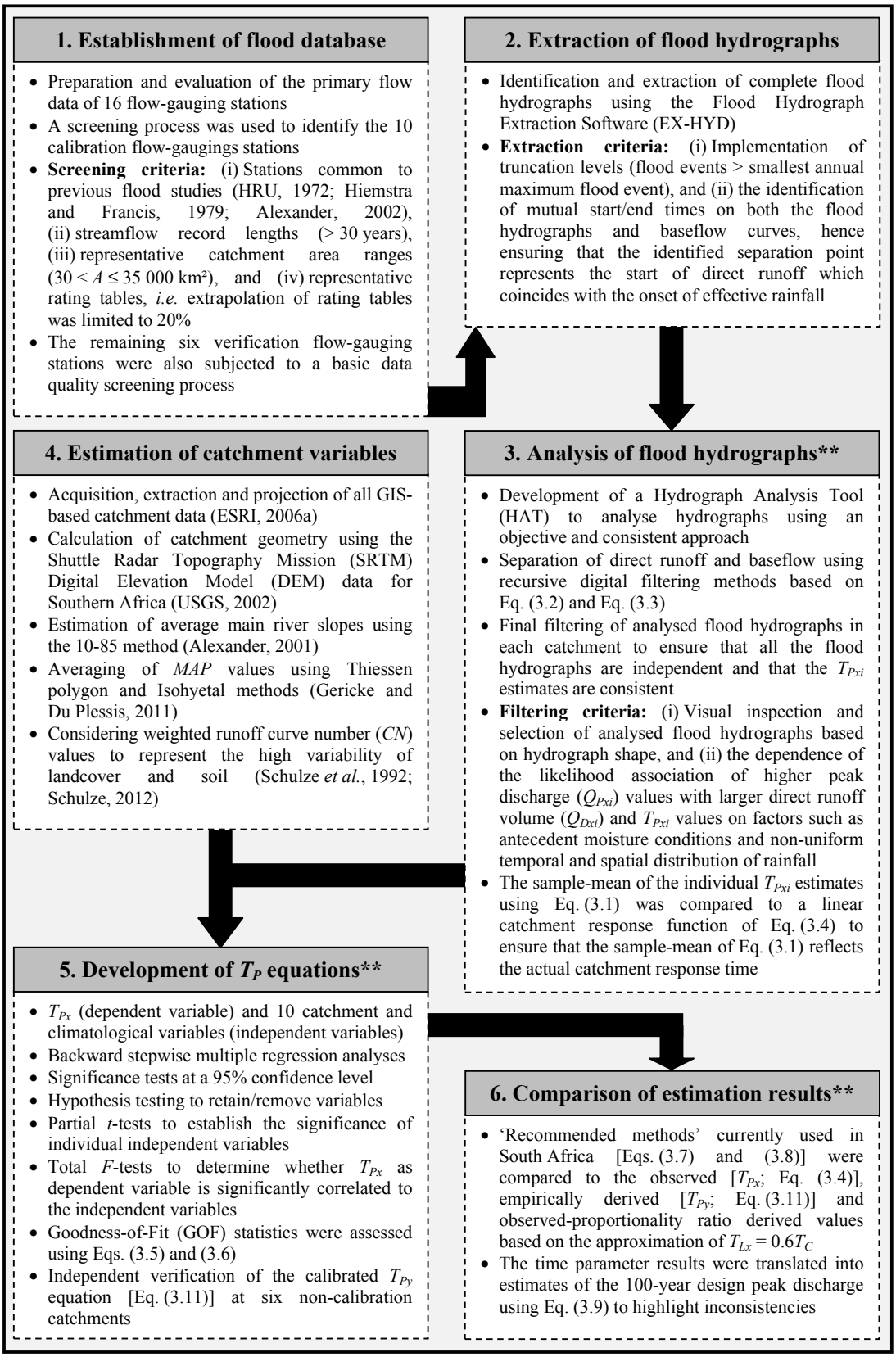

Figure 3.3 Schematic flow diagram illustrative of the implemented methodology

The equations as proposed by Nathan and McMahon [1990; Eq. (3.2)] and Chapman [1999; Eq. (3.3)] are given by:

$$Q_{Dxi} = \alpha Q_{Dx(i-1)} + \beta(1+\alpha)\left(Q_{Txi} - Q_{Tx(i-1)}\right) \quad (3.2)$$

$$Q_{Dxi} = \left(\frac{(3\alpha-1)}{(3-\alpha)}\right) Q_{Dx(i-1)} + \frac{2}{(3-\alpha)}\left(Q_{Txi} - Q_{Tx(i-1)}\right) \quad (3.3)$$

where Q_{Dxi} = filtered direct runoff at time step i, which is subject to $Q_{Dx} \geq 0$ for time i [$m^3.s^{-1}$],

α,β = filter parameters, and

Q_{Txi} = total streamflow (*i.e.* direct runoff plus baseflow) at time step i [$m^3.s^{-1}$].

In using Eq. (3.2) in their national-scale study in South Africa, Smakhtin and Watkins (1997) established that a fixed α-parameter value of 0.995 is suitable to most catchments in South Africa, although in some catchments, α-parameter values of 0.997 proved to be more appropriate. Hughes *et al.* (2003) also highlighted that a fixed β-parameter value of 0.5 could be used with daily time-step data, since there is more than enough flexibility in the setting of the α-parameter value to achieve an acceptable result. Consequently, a fixed α-parameter value of 0.995 was used in all the catchments under consideration. However, in some of the catchments with data sets having sub-daily data with time intervals as short as 12 minutes (especially after the year 2000), the α-parameter value of 0.995 resulted in a too high proportion of baseflow relative to total flow. In such cases, the average baseflow index (BFI) of the pre-2000 data years was used to adjust the baseflow volumes accordingly. Comparable/similar results were obtained by increasing the α-parameter value to 0.997.

In addition to the filtering criteria listed in Figure 3.3, the relationship between the observed peak discharge (Q_{Pxi}) and volume of direct runoff (Q_{Dxi}) was also investigated. The slope of the linear regression between corresponding Q_{Pxi} and Q_{Dxi} values was computed using Eq. (3.4) for each catchment to provide an estimate of the observed catchment response time. In other words, the slope of the assumed linear catchment response function in Eq. (3.4) depicts the rate of change between corresponding Q_{Pxi} and Q_{Dxi} values along the linear regression and equals the average catchment response time by considering all the individual Q_{Pxi} and Q_{Dxi} values in a particular catchment.

The derivation of the linear catchment response function [Eq. (3.4)] is included in Section 5.8, Chapter 5. Although, Eq. (3.4) assumes a linear catchment response function, it is very useful as a 'representative value' to ensure that the average of individual responses [using Eq. (3.1)] provides a good indication of the catchment conditions and sample-mean. The need for and applicability of such an investigation was also highlighted by Schmidt and Schulze (1984). Schmidt and Schulze (1984) also regarded the averaging of observed time responses between effective rainfall and direct runoff for individual events to provide an index of catchment response, as impractical for peak discharge estimation. This also provides some justification for the use of this alternative approach, as initially suggested by Gericke and Smithers (2014).

$$T_{Avg} = \frac{1}{3600x}\left[\frac{\sum_{i=1}^{N}\left(Q_{Pxi}-\overline{Q_{Px}}\right)\left(Q_{Dxi}-\overline{Q_{Dx}}\right)}{\sum_{i=1}^{N}\left(Q_{Pxi}-\overline{Q_{Px}}\right)^2}\right] \quad (3.4)$$

where T_{Avg} = 'average' observed catchment response time [T_{Px}, T_{Cx} or T_{Lx}; hours],

Q_{Dxi} = volume of direct runoff for individual flood events [m^3],

$\overline{Q_{Dx}}$ = mean of Q_{Dxi} [m^3],

Q_{Pxi} = observed peak discharge for individual flood events [$m^3.s^{-1}$],

$\overline{Q_{Px}}$ = mean of Q_{Pxi} [$m^3.s^{-1}$],

N = sample size, and

x = variable proportionality ratio which depends on the catchment response time parameter under consideration, *i.e.* T_{Px} ($x = 1$), T_{Cx} ($x = 1$) and/or T_{Lx} ($x = 1.667$).

The variable proportionality ratio (x) is included in Eq. (3.4) to increase the flexibility and use of this equation, *i.e.* with $x = 1$, either T_{Px} or T_{Cx} could be estimated by acknowledging the approximation of $T_C \approx T_P$ (Gericke and Smithers, 2014) and with $x = 1.667$, T_L could be estimated by assuming that $T_L = 0.6T_C$, which is the time from the centroid of effective rainfall to the time of peak discharge (McCuen, 2009).

3.5.2 Development of T_P equations

The 10 independent geomorphological catchment and climatological variables, as referred to in Figure 3.3 and considered as potential predictor variables to estimate T_{Px} are: (i) area

[A, km²], (ii) perimeter [P, km], (iii) hydraulic length [L_H, km], (iv) main watercourse length [L_{CH}, km], (v) centroid distance [L_C, km], (vi) average catchment slope [S, %], (vii) average main watercourse slope [S_{CH}, %], (viii) drainage density [D_D, km.km^{-2}], (ix) *MAP* [mm], and (x) weighted *CN* values (representative of land-use and cover, and hydrological soil characteristics). The details of the coefficient of multiple-correlation and the standard error of estimate as used to assess the GOF statistics are shown by Eqs. (3.5) and (3.6) respectively (McCuen, 2005).

$$R_i^2 = \frac{\sum_{i=1}^{N}\left(y_i - \bar{x}\right)^2}{\sum_{i=1}^{N}\left(x_i - \bar{x}\right)^2} \tag{3.5}$$

$$S_E = \left[\frac{1}{v}\sum_{i=1}^{N}\left(y_i - x_i\right)^2\right]^{0.5} \tag{3.6}$$

where R_i = multiple-correlation coefficient for an equation with i independent variables,

S_E = standard error of estimate,

x_i = observed value (dependent variable),

$\bar{x}$ = mean of observed values (dependent variables),

y_i = estimated value of dependent variable (x_i),

i = number of independent variables,

N = number of observations (sample size), and

v = degrees of freedom (N- i; with y-intercept = 0).

3.5.3 Comparison of estimation results

The 'recommended methods' referred to in Figure 3.3, are shown in Eq. (3.7) (USBR, 1973) and Eq. (3.8) (HRU, 1972) respectively.

$$T_{Cy} = \left(\frac{0.87{L_H}^2}{10S_{CH}}\right)^{0.385} \tag{3.7}$$

$$T_{Ly1} = C_T\left(\frac{L_H L_C}{\sqrt{\frac{S_{CH}}{100}}}\right)^{0.36} \tag{3.8}$$

where T_{Cy} = estimated channel flow time of concentration [hours],

T_{Ly1} = estimated lag time [hours],

C_T = regional storage coefficient (ranging from 0.19 to 0.32 in the C5 secondary drainage region),

L_C = centroid distance [km],

L_H = hydraulic length of catchment [km], and

S_{CH} = average main watercourse slope [%].

The details of the Standard Design Flood (SDF) method [Eq. (3.9); Alexander, 2002] as referred to in Figure 3.3, are as follows:

$$Q_{PT} = 0.278\left[\frac{C_2}{100} + \left(\frac{Y_T}{2.33}\right)\left(\frac{C_{100}}{100} - \frac{C_2}{100}\right)\right] I_T A \qquad (3.9)$$

where Q_{PT} = design peak discharge [$m^3.s^{-1}$],

A = catchment area [km^2],

C_2 = 2-year return period runoff coefficient [15 %; pilot study area],

C_{100} = 100-year return period runoff coefficient [60 %; pilot study area],

I_T = average design rainfall intensity [$mm.h^{-1}$], and

Y_T = 100-year return period factor [2.33].

3.6 Results and Discussion

The results from the application of the methodology are presented in the next sections. The station numbers of the DWS flow-gauging stations located at the outlet of each catchment are used as catchment descriptors for easy reference in all the tables and figures. Subscripts '*x*' and '*y*' are used to distinguish between estimates from observed data (*x*) and estimated values (*y*) using either the developed empirical time parameter equation (this research) or applying the 'recommended methods' as commonly used in South Africa.

3.6.1 Estimation of catchment variables

The general catchment attributes (*e.g.* climatological variables, catchment geomorphology, catchment variables and channel geomorphology) for each catchment in the pilot study area, are listed in Table 3.1. The influences of each variable or parameter listed in Table 3.1 are highlighted where applicable in the subsequent sections.

Table 3.1 General catchment information

Catchment descriptors	C5H003	C5H006	C5H007	C5H008	C5H009	C5H012	C5H014	C5H015	C5H016	C5H018	C5H022	C5H023	C5H035	C5H039	C5H053	C5H054
Climatological variables																
MAP [Thiessen polygon, mm]	559	524	508	462	477	449	435	522	430	461	675	648	461	519	531	524
MAP [Isohyetal, mm]	552	515	495	451	464	440	433	519	428	459	654	611	459	516	529	515
Catchment geomorphology																
Area [A, km²]	1 641	676	346	598	189	2 366	31 283	5 939	33 278	17 361	39	185	17 359	6 331	4 569	687
Perimeter [P, km]	196	145	100	122	71	230	927	384	980	730	28	65	730	411	329	146
Hydraulic length [L_H, km]	71	64	41	41	24	87	326	160	378	375	8	29	373	187	120	68
Centroid distance [L_C, km]	41	29	17	22	14	45	207	81	230	174	3	17	173	103	56	33
Average catchment slope [S, %]	3.90	2.02	1.75	4.83	3.66	3.28	2.13	2.77	2.09	1.73	10.29	7.09	1.73	2.66	3.08	2.07
Catchment variables																
Urban areas/imperviousness [%]	2.18	12.54	1.19	0.00	0.00	0.07	0.70	2.72	0.66	1.18	0.00	0.02	1.18	2.55	3.42	12.34
Rural areas/perviousness [%]	95.09	85.91	97.57	99.11	98.83	98.78	95.93	95.17	96.04	94.64	98.22	97.08	94.64	94.94	94.59	86.06
Water bodies/DWS dams [%]	2.72	1.55	1.24	0.89	1.17	1.15	3.37	2.11	3.30	4.18	1.78	2.90	4.18	2.51	1.99	1.60
Weighted *CN* value	68.0	73.6	73.4	67.3	67.1	67.3	68.8	69.8	69.0	70.1	67.8	67.9	70.1	69.8	69.8	73.6
SDF runoff coefficient [T = 100-yr]	0.60	0.60	0.60	0.60	0.60	0.60	0.60	0.60	0.60	0.60	0.60	0.60	0.60	0.60	0.60	0.60
HRU storage coefficient [C_T]	0.32	0.32	0.32	0.25	0.19	0.21	0.23	0.32	0.23	0.25	0.32	0.32	0.25	0.32	0.32	0.32
Channel geomorphology																
Main watercourse length [L_{CH}, km]	71	64	40	41	24	87	326	160	378	375	8	29	373	187	119	67
Total length of all the rivers [L, km]	380	123	66	104	37	431	3 320	1196	3 372	1 617	8	37	1 629	1 236	937	127
Avg. main river slope [S_{CH}, %]	0.26	0.27	0.34	0.49	0.60	0.27	0.10	0.14	0.10	0.08	1.70	0.58	0.08	0.13	0.18	0.26
Strahler catchment order	4	3	2	3	2	4	5	4	5	4	1	2	4	4	4	3
Shreve stream network magnitude	14	7	3	5	2	18	102	42	102	47	1	4	47	42	34	7
Drainage density [D_D, km.km^{-2}]	0.2	0.2	0.2	0.2	0.2	0.2	0.1	0.2	0.1	0.1	0.2	0.2	0.1	0.2	0.2	0.2

3.6.2 Establishment of flood database

The details of the 16 flow-gauging stations used during the establishment of the flood database are listed in Table 3.2. The average data record length in the pilot study area is 46 years.

Table 3.2 Information of catchments as included in the flood database

Catchment descriptor	Area [km²]	HRU (1972)	Hiemstra and Francis (1979)	Alexander (2002)	Record length		
					Start	End	Years
C5H003*	1 641	X			1918	2013	95
C5H006	676				1922	1926	4
C5H007*	346	X	X	X	1923	2013	90
C5H008*	598			X	1931	1986	55
C5H009	189				1931	1986	55
C5H012*	2 366	X	X	X	1936	2013	77
C5H014*	31 283				1938	2013	75
C5H015*	5 939		X	X	1949	1983	34
C5H016*	33 278				1953	1999	46
C5H018*	17 361				1960	1999	39
C5H022*	39				1980	2013	33
C5H023	185				1983	2008	25
C5H035	17 359				1989	2013	24
C5H039*	6 331				1970	2013	43
C5H053	4 569				1999	2013	14
C5H054	687				1995	2013	18

* = Flow-gauging stations used for the calibration of Eq. (3.11)
X = Flow-gauging stations used in previous flood studies

3.6.3 Extraction of flood hydrographs

A total of 1 134 complete flood hydrographs were extracted from the primary flow data sets, with between 13 and 117 individual flood hydrographs per flow-gauging station/catchment. An example of a typical flood hydrograph is illustrated in Figure 3.4.

3.6.4 Analyses of flood hydrographs

Due to the nature of flood hydrographs, it is important to note that the Hydrograph Analysis Tool (HAT) developed as part of this study, could not cater for all variations in flood hydrographs; hence a measure of user intervention was required, especially when T_{Pxi} was determined for multi-peaked hydrographs. Input to HAT is the extracted flood hydrographs obtained using the Flood Hydrograph Extraction Software (EX-HYD) developed by Görgens *et al.*, 2007, while the output includes the following: (i) start/end date/time of flood hydrograph, (ii) observed peak discharge [Q_{Pxi}, $m^3.s^{-1}$],

(iii) total volume of runoff [Q_{Txi}, m^3], (iv) volume of direct runoff [Q_{Dxi}, m^3], (v) volume of baseflow [Q_{Bxi}, m^3], (vi) BFI, (vii) depth of effective rainfall [P_{Exi}, mm]; based on the assumption that the volume of direct runoff equals the volume of effective rainfall and that the total catchment area is contributing to runoff, (viii) time to peak [T_{Pxi}, hours], and (ix) summary of results in different T_P ranges (both at a catchment and regional level).

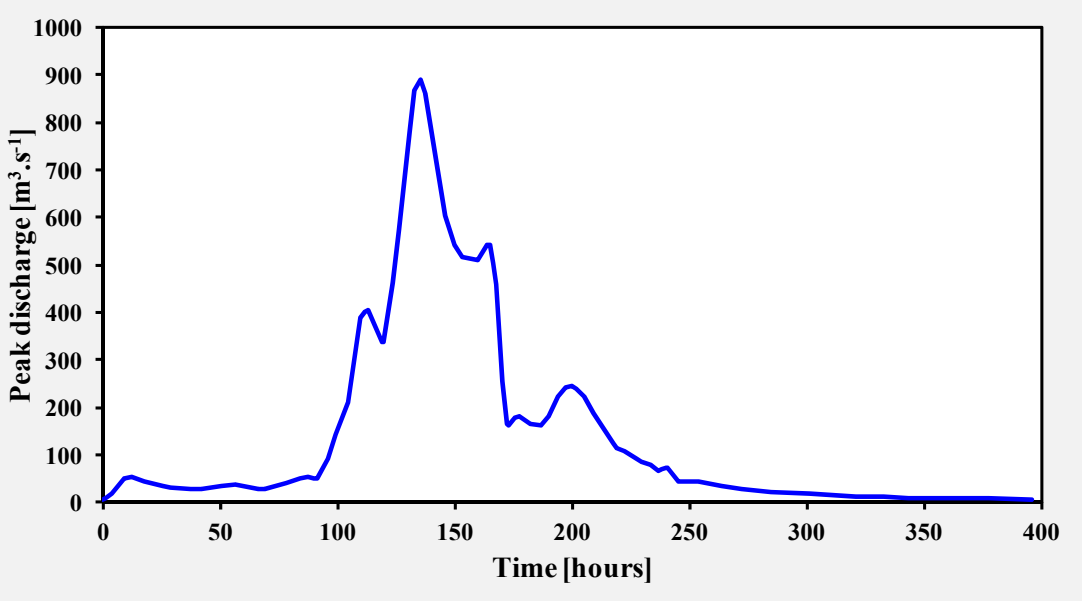

Figure 3.4 Example of extracted flood hydrograph at C5H015

Typical baseflow separation results using the three recursive filtering methods are illustrated in Figure 3.5. The data series plots of Nathan and McMahon (1990) and Chapman (1999) are based on a fixed α-parameter value of 0.995, while the data series plot of Smakhtin and Watkins (1997) is based on a fixed α-parameter value of 0.997. This was specifically done to illustrate the flexibility in setting the α-parameter values, while the equations of Nathan and McMahon (1990) and Smakhtin and Watkins (1997) are identical. By considering both the recommendations made by Smakhtin and Watkins (1997) and Hughes *et al.* (2003), Eq. (3.2) was used to separate the direct runoff and baseflow in this chapter.

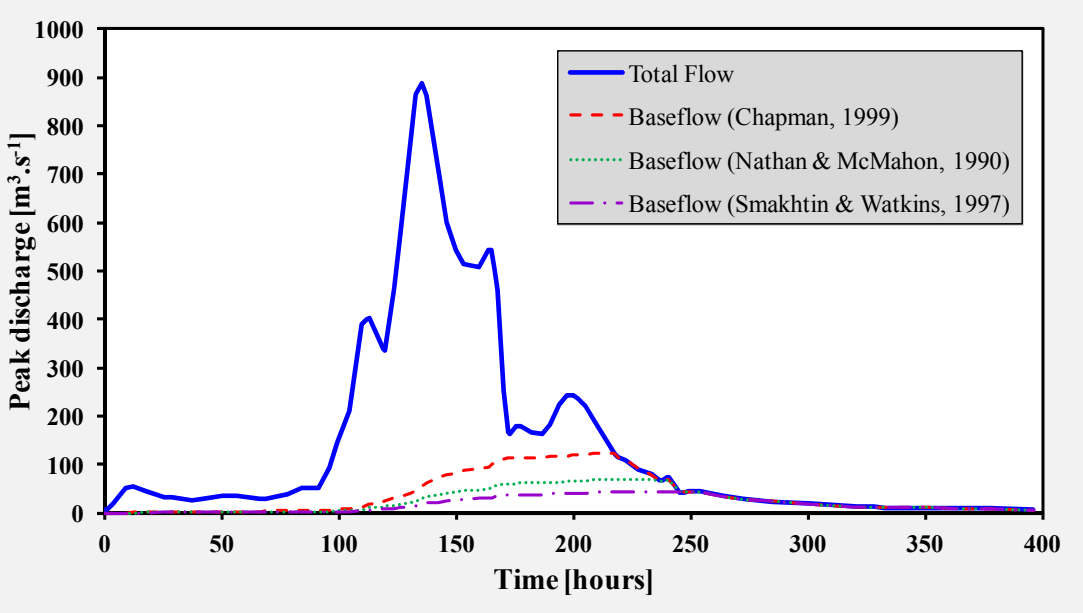

Figure 3.5 Example of the baseflow separation results at C5H015

The initial number (1 134) of extracted flood hydrographs was reduced to 935 following the final filtering process, as detailed in the Methodology summarised in this section and in Figure 3.3. Table 3.3 contains a summary of typical results as obtained using the HAT software (*cf.* Figure 3.3) at a catchment level (C5H015), after the individual filtering of all flood hydrographs.

Table 3.3 Typical summary of hydrograph analysis results using the HAT software at C5H015

Catchment information	T_P range [h]	Number of events	Averages associated with each T_P range					
			Q_{Tx} [10^6 m^3]	Q_{Dx} [10^6 m^3]	Q_{Px} [m^3.s^{-1}]	T_{Px} [Eq. (3.1), h]	P_{Ex} [mm]	BFI
C5H015	0 ≤ 5	5	13.6	12.1	113.5	4.1	2.0	0.1
	6 ≤ 10	14	10.0	9.1	113.3	7.8	1.5	0.1
	11 ≤ 15	6	17.1	15.0	142.7	13.4	2.5	0.1
Area: 5 939 km²	16 ≤ 20	9	15.3	13.5	130.6	17.9	2.3	0.1
	21 ≤ 30	21	15.1	13.4	121.0	25.6	2.3	0.1
Data period: 1949/01/01– 1983/11/22	31 ≤ 40	14	21.7	18.9	200.2	33.8	3.2	0.1
	41 ≤ 50	13	38.3	35.6	337.9	43.3	6.0	0.1
	51 ≤ 75	8	66.1	60.4	544.3	57.4	10.2	0.1
Averages/totals		**90**	**23.3**	**21.0**	**203.1**	**26.7**	**3.5**	**0.1**

It is evident from Table 3.3 that, as expected, the largest average T_{Px} values are associated with the maximum direct runoff volumes. Taking the bigger average P_{Ex} values in the T_P ranges into consideration, the likelihood of the entire catchment receiving rainfall for

the critical storm duration becomes a more realistic assumption. Consequently, the lower limit T_{Pxi} values could be expected when effective rainfall of high average intensity does not cover the entire catchment, especially when a storm is centered near the outlet of a catchment. Figure 3.6 shows the scatter plot of corresponding Q_{Pxi} and T_{Pxi} [using Eq. (3.1)] values at catchment C5H015.

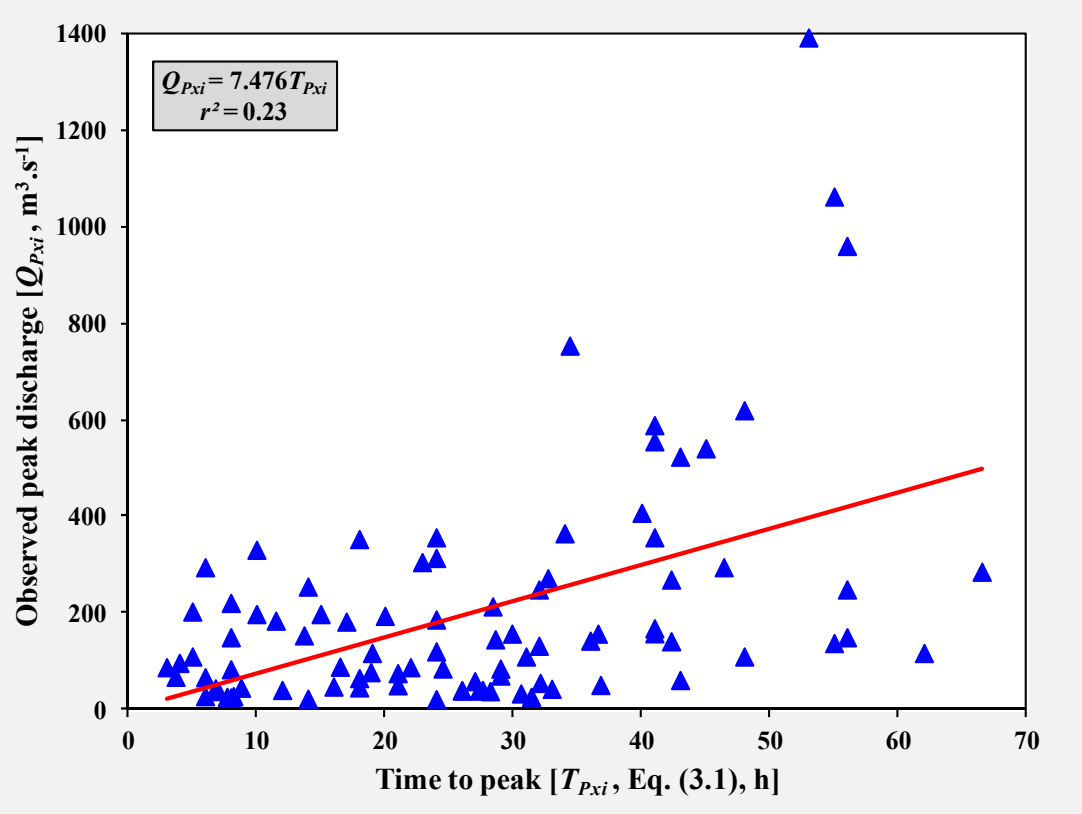

Figure 3.6 Scatter plot of Q_{Pxi} versus T_{Pxi} [Eq. (3.1)] values at C5H015

However, from the results in Figure 3.6, similar trends are evident, but the variability between individual catchment responses and corresponding peak discharge values become more obvious and also highlight that the use of averages could be misleading and not always representative of the actual catchment responses. For example, small T_{Pxi} values occurring more frequently will incorrectly have a larger influence on the average value which will result in an underestimated catchment T_{Px} value. 'High outliers' occurring less frequently are not as problematic, because at medium to large catchment scales, the contribution of the whole catchment to peak discharge seldom occurs due to the spatial and temporal distribution of rainfall. In principal, these events are actually required to adhere to

the conceptual definition of T_C ($\approx T_P$), which assumes that T_C is the time required for runoff, generated from effective rainfall with a uniform spatial and temporal distribution over the whole catchment, to contribute to the peak discharge at the catchment outlet. Similar results as contained in Table 3.3 and Figure 3.6 were also evident in all the other 15 catchments under consideration and support the use of Eq. (3.4) as a catchment 'representative value', which is discussed in the next paragraph and shown in Figure 3.7.

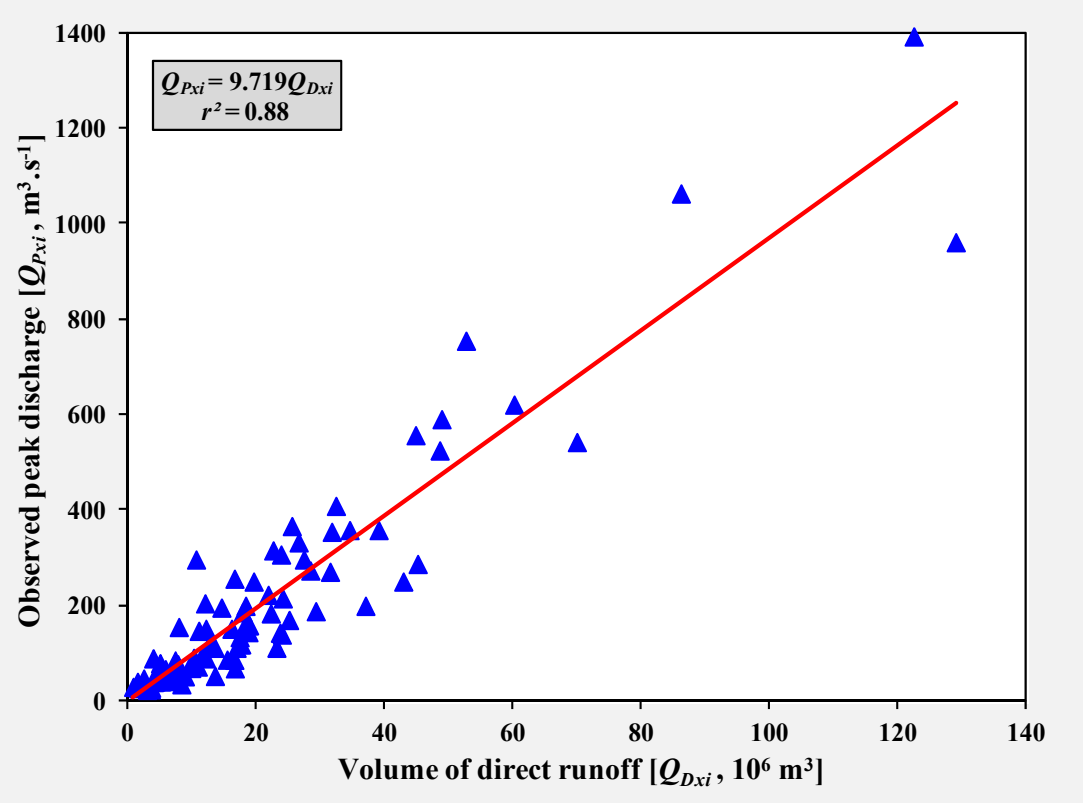

Figure 3.7 Scatter plot of Q_{Pxi} versus Q_{Dxi} values at C5H015

Figure 3.7 shows a typical scatter plot of corresponding Q_{Pxi} and Q_{Dxi} and values at catchment C5H015. The slope of the linear trend-line equals T_{Px} and is computed using Eq. (3.4) with a proportionality ratio $x = 1$. In using Eq. (3.4) at a catchment level, and as illustrated in Figure 3.7, a moderate to acceptable degree of association (r^2 values ranging from 0.50 to 0.98) was obtained between the corresponding Q_{Pxi} and Q_{Dxi} values in all the other 15 catchments under consideration. A scatter plot of the T_{Px} pair values based on the use of Eq. (3.4) and the average of Eq. (3.1) respectively and associated with all the catchments under consideration is shown in Figure 3.8.

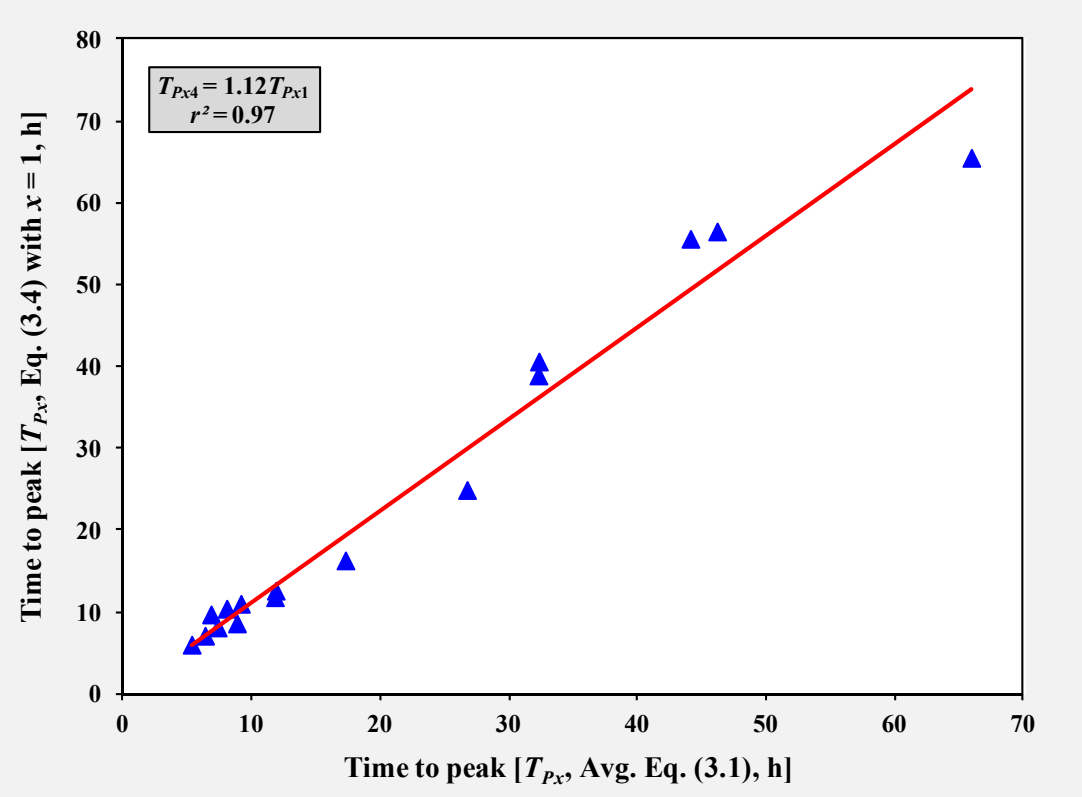

Figure 3.8 Scatter plot of T_{Px} [Eq. (3.4) with x = 1] versus average T_{Px} [Eq. (3.1)] values in all the catchments

The results illustrated in Figure 3.8 indicate a high degree of association, with an average T_{Px4}/T_{Px1} ratio of 1.12 and r^2 value = 0.97. The T_{Px4} values [Eq. (3.4) with x = 1] are generally larger than the T_{Px1} values [Avg. of Eq. (3.1)], with only 25 % of the catchments characterised by T_{Px4}/T_{Px1} ratios of ≤ 1. The differences in estimated catchment response time must be viewed in the context of the actual travel time associated with the size of a particular catchment, as the impact of a 10 % difference in estimates might be critical in a small catchment, while being less significant in a larger catchment. It is evident that these percentage differences are not correlated to the catchment area. The average slope descriptors (S and S_{CH}) in the different catchments are very similar, hence their insignificant potential influence on the results. Other catchment shape parameters, such as the circularity ratio, expressed as $P/\sqrt{4\pi A}$ and the ratio of L_C: L_H, also proved to have an insignificant influence on the results. However, the catchments characterised by T_{Px4}/T_{Px1} ratios ≤ 1 also had L_C: L_H ratios < 0.5, hence the association between the shorter centroid distances and lower T_{Px4} values.

A summary of the average catchment conditions based on the individual analysis in each catchment is listed in Table 3.4.

Table 3.4 Summary of average catchment results in the C5 secondary drainage region

Catchment descriptor	Data period	Number of events	Average catchment values						
			Q_{Tx} [10^6 m^3]	Q_{Dx} [10^6 m^3]	Q_{Px} [m^3.s^{-1}]	T_{Px} [Eq. (3.1), h]	T_{Px} [Eq. (3.4), h]	P_{Ex} [mm]	BFI
C5H003	1918/07/01 to 2013/06/26	101	2.1	1.7	32.8	9.1	11.1	1.0	0.2
C5H006	1922/11/13 to 1926/12/31	14	1.4	1.3	36.0	7.3	8.2	1.9	0.1
C5H007	1923/10/01 to 2013/08/06	91	1.2	1.0	28.0	6.4	7.2	2.9	0.1
C5H008	1931/04/01 to 1986/04/01	112	2.2	2.0	44.7	8.0	10.5	3.3	0.1
C5H009	1931/03/01 to 1986/05/11	13	1.0	0.8	14.3	11.8	12.7	4.5	0.1
C5H012	1936/04/01 to 2013/02/13	68	3.3	2.3	41.5	11.8	11.9	1.0	0.3
C5H014	1938/10/17 to 2013/07/25	28	46.7	36.5	168.3	46.2	56.6	1.2	0.2
C5H015	1949/01/01 to 1983/11/22	90	23.3	21.0	203.1	26.7	25	3.5	0.1
C5H016	1953/02/01 to 1999/03/10	40	31.0	27.0	105.6	65.9	65.6	0.8	0.1
C5H018	1960/02/23 to 1999/03/15	50	22.8	19.7	105.0	32.3	39.0	1.1	0.1
C5H022	1980/10/14 to 2013/10/24	69	0.4	0.3	11.5	5.3	6.1	8.0	0.2
C5H023	1983/06/04 to 2008/03/22	58	0.8	0.6	15.6	6.8	9.8	3.3	0.2
C5H035	1989/08/03 to 2013/07/23	20	10.8	9.1	58.9	32.3	40.7	0.5	0.2
C5H039	1970/11/24 to 2013/08/08	56	34.0	29.2	136.2	44.1	55.7	4.6	0.1
C5H053	1999/11/29 to 2013/08/08	65	8.3	5.7	93.1	17.3	16.4	1.3	0.3
C5H054	1995/10/18 to 2013/08/08	60	1.3	0.8	21.3	8.8	8.7	1.2	0.4

3.6.5 Development of T_P equations

The backward stepwise multiple linear regression analyses using untransformed data showed promising results, however, some predictions in both the calibration and verification catchments resulted in negative values. In the case of transformed data, power-transformed independent variables, *e.g.* $y = ax^b$, resulted in the highest degree of association when individually plotted against the dependent variables, although when included as part of the multiple regression analyses, the transformed independent variables performed less satisfactorily. Backward stepwise multiple Log-linear regression analyses with deletion resulted in the best prediction model for T_{Px}. The following independent predictor variables were retained and included in the calibrated equation: (i) *MAP*, (ii) area, (iii) centroid distance, (iv) hydraulic length, and (v) average catchment slope.

The derived T_{Py} regression is shown in Eqs. (3.10) and (3.11):

$$\ln(T_{Py}) = \ln(x_1)MAP + \ln(x_2)A + \ln(x_3)L_C + \ln(x_4)L_H + \ln(x_5)S \qquad (3.10)$$

In applying some simplification, the final T_{Py} regression is shown in Eq. (3.11):

$$T_{Py} = x_1^{MAP} x_2^{A} x_3^{L_C} x_4^{L_H} x_5^{S} \qquad (3.11)$$

where T_{Py} = estimated time to peak [hours],

A = catchment area [km²],

L_C = centroid distance [km],

L_H = hydraulic length [km],

MAP = Mean Annual Precipitation [mm],

S = average catchment slope [%]; and

x_1 to x_5 = calibration coefficients [Table 3.5].

The GOF statistics, correlation matrix and hypothesis testing results are listed in Tables 3.5 and 3.6.

Table 3.5 Summary of GOF statistics and correlation matrix

Criterion	**Independent predictor variables**				
	MAP	***A***	***L_C***	***L_H***	***S***
Calibration coefficient (x_i)	1.00312	0.99984	1.05965	0.98663	0.98219
Standard error of x_i coefficients	0.00080	0.00005	0.01429	0.00485	0.05944
t-Statistic of independent variables (t)	3.902	3.434	4.054	2.778	0.302
Critical *t*-statistic value (t_α)	2.571	2.571	2.571	2.571	2.571
Correlation matrix					
Independent predictor variables	*MAP*	*A*	L_C	L_H	*S*
MAP [mm]	**1.000**	0.315	0.345	0.328	0.608
A [km²]	0.315	**1.000**	0.935	0.832	0.203
L_C [km]	0.345	0.935	**1.000**	0.963	0.313
L_H [km]	0.328	0.832	0.963	**1.000**	0.342
S [%]	0.608	0.203	0.313	0.342	**1.000**

At a confidence level of 95 %, the independent variables listed in Table 3.5 contributed significantly towards the prediction accuracy, however, the average catchment slope (S) proved to be less significant with $t < t_\alpha$. Despite of being statistically less significant, the correlation (r^2 values) between S and the other independent predictor variables was less than 0.6. A high degree of correlation is evident between some of the statistically significant variables, *e.g.* A, L_C and L_H, with r^2 values ranging between 0.83 and 0.96. The latter issue of colliniarity could have an influence on the stability of the prediction model.

However, the inclusion of the five independent variables in Eq. (3.11) resulted in the best estimation results, *i.e.* reduced prediction errors were evident in all the catchments under consideration. Furthermore, from a hydrological perspective at this stage, the inclusion of S is regarded as both conceptually and physically necessary to ensure that the other retained independent variables, *i.e.* the size (A) and distance (L_C and L_H) predictors provide a good indication of catchment storage effects, while the MAP incorporates the rainfall variability. In addition, the distance (L_C and L_H) predictors are also regarded as necessary to describe the shape of a catchment when considered in combination with the catchment area.

The five independent variables included in the prediction model are also regarded as consistent and easy to apply should practitioners need to determine the variables in ungauged catchments. However, Eq. (3.11) also has potential limitations, especially in terms of its application in ungauged catchments beyond the boundaries of the pilot study area. Therefore, the methodology followed in this research should be expanded to other South African study areas in climatologically different regions, followed by regionalisation. The regionalisation will improve the accuracy of the time parameter estimates, whilst warranting the combination and transfer of information within the identified homogeneous hydrological regions. Typically, a clustering method (Hosking and Wallis, 1997) could be used, which utilises the geomorphological catchment characteristics and flood statistics to establish the regions and to test the homogeneity respectively. The problems associated with the identified colliniarity could then also be addressed by lowering the significance levels for the in- and/or exclusion of independent predictor variables. However, this will be considered when the proposed regionalisation (*cf.* Section 7.7, Chapter 7) is completed, followed by the derivation of new empirical equations in each hydrological homogeneous region.

Table 3.6 Summary of GOF statistics and hypothesis testing results

Criterion	**T_{Pv} [Eq. (3.11)] results**
Confidence level [(1- α), %]	95
Coefficient of multiple-correlation [Eq. (3.5)]	0.98
Standard error of T_{Pv} estimate [Eq. (3.6), h]	4.34
F-Observed value (F-statistic)	283.70
Critical F-statistic (F_α)	5.05

The estimations based on Eq. (3.11) as listed in Table 3.6 showed a high degree of association with the observed values (both for calibration and independent verification), with the standard error of the T_{Py} estimate = 4.34 hours and an associated coefficient of multiple-correlation = 0.98. The rejection of the null hypothesis ($F > F_{\alpha}$, with $F_{\alpha} = 5.1$) confirmed that T_{Py} ($F = 284$) as a dependent variable is related significantly to the independent variables as included in the regression model.

It is also important to compare the results obtained with the generally accepted time parameter definitions and proportionality ratios for small catchments as documented in the literature, since both have a large influence on the inconsistency between different methods. In using T_{Lx} defined as the time from the centroid of effective rainfall to the centroid of direct runoff, T_{Lx} and the conceptual T_C ($\approx T_{Px}$) can be related by $T_L = 0.705T_C$ (McCuen, 2009). In using T_{Lx} defined as the time from the centroid of effective rainfall to the time of the peak discharge of total or direct runoff, the proportionality ratio decreases to 0.6 (McCuen, 2009) as illustrated in Figure 3.1. In acknowledging that $T_C \approx T_P$ and $T_L = 0.6T_C$, the latter proportionality ratio of 0.6 could also be applied to Eqs. (3.4) and (3.11) to provide an indication of the observed T_{Lx} and estimated T_{Ly2} values respectively as listed in Table 3.7.

Table 3.7 Calibration and verification T_L results based on a 0.6 proportionality ratio

Catchment descriptor	T_{Lx} observed [Eq. (3.4), $x = 1.667$, h]	T_{Ly1} estimated [Eq. (3.8), h]	T_{Ly2} estimated [0.6*Eq. (3.11), h]	T_{Ly1}/T_{Lx} ratio	T_{Ly2}/T_{Lx} ratio
Calibration					
C5H003	6.7	16.6	10.3	2.49	1.54
C5H007	4.3	9.5	4.2	2.19	0.98
C5H008	6.3	7.6	4.4	1.21	0.69
C5H012	7.1	11.8	6.7	1.65	0.94
C5H014	34.0	43.2	31.2	1.27	0.92
C5H015	15.0	31.4	14.7	2.10	0.98
C5H016	39.4	46.9	42.4	1.19	1.08
C5H018	23.4	49.3	25.0	2.11	1.07
C5H022	3.7	2.0	4.0	0.55	1.09
C5H039	33.4	37.0	33.9	1.11	1.01
Verification					
C5H006	4.9	14.0	6.2	2.86	1.26
C5H009	7.6	3.9	3.8	0.51	0.50
C5H023	5.9	7.6	6.5	1.30	1.10
C5H035	24.4	49.0	23.2	2.01	0.95
C5H053	9.8	23.8	7.5	2.42	0.76
C5H054	5.2	14.9	7.1	2.86	1.36

In comparing the results based on Eq. (3.8) to the T_{Lx} values in both the calibration and verification catchments, the T_{Ly1} values were overestimated in 90 % of the catchments and overestimations of up to +186 % were evident. Underestimations were limited to -49 %. However, the above-mentioned T_{Lx} definition with an associated proportionality ratio of 0.6, is also used in literature (McCuen, 2009; Gericke and Smithers, 2014) to define T_{Cx}, thus by implication, $T_C \approx T_L$. In agreement with the latter implication, but in contradiction to other literature, Schultz (1964) also established that for catchments in Lesotho and South Africa, $T_C \approx T_L$. Taking cognisance of this, the proportionality ratio of 0.6 then increases to unity. Thus, by comparing the results based on Eq. (3.8) to the T_{Px} (instead of T_{Lx}) values in both the calibration and verification catchments, the overestimation of T_{Ly1} are reduced to 72 %, while the underestimations are slightly increased to -69 %. These improved results also suggest and support the approximation of $T_C \approx T_L$ at these catchment scales. Furthermore, Eq. (3.8) was locally developed by the HRU (1972) for application in catchment areas ranging from 20 to 5 000 km² which is within the areal range classified as medium in this chapter.

These results, as well as Schultz's (1964) results support the argument that the suggested proportionality ratios are all based on research conducted in a limited number of small catchments. In small catchments, the exact occurrence of the maximum peak discharge is of more importance as opposed to larger catchments where flood volumes are central to the design. In addition, the simplifications used in small catchments are not applicable in real, large heterogeneous catchments where antecedent moisture from previous rainfall events and spatially non-uniform runoff producing rainfall hyetographs can result in multi-peaked hydrographs. Furthermore, Gericke and Smithers (2014) also argued that the accuracy of T_L estimation is, in general, so poor that differences in the T_L and T_C starting and ending points are insignificant. The use of these multiple time parameter definitions, combined with the fact that no 'standard method' could be used to estimate time parameters from observed hyetographs and hydrographs, emphasise why the proportionality ratio of T_L: T_C could typically vary between 0.5 and 2 for the same catchment. The verification of the derived regression [Eq. (3.11)] to estimate T_{Py} and a comparison with values estimated using the 'recommended methods', are discussed in the following section.

3.6.6 Comparison of estimation results

The average observed T_{Px} values estimated from the extracted flood hydrographs using Eq. (3.4) with x = 1, the estimated T_{Py} values using Eq. (3.11) and T_C ($\approx T_P$) based on Eq. (3.7) and denoted as T_{Cy}, are all listed in Table 3.8. The 100-year design peak discharges computed using Eq. (3.9) are also included in Table 3.8 to reflect the engineers' dilemma when time parameters obtained from empirical time parameter estimation methods are translated to design peak discharges using event-based deterministic methods in ungauged catchments. Both the calibration and verification results are shown. The relationship between the estimated (y) and observed (x) time parameters (T_Y/T_X) ratios and resulting peak discharge (Q_Y/Q_X) ratios are shown in Figures 3.9 (calibration) and 3.10 (verification) respectively.

Table 3.8 Calibration and verification time parameter and peak discharge results

Catchment descriptor	T_{Px} observed [Eq. (3.4), x = 1, h]	T_{Cy} estimated [Eq. (3.7), h]	T_{Py} estimated [Eq. (3.11), h]	Q_{TPx} [$m^3.s^{-1}$]	Q_{TCy} [$m^3.s^{-1}$]	Q_{TPy} [$m^3.s^{-1}$]
Calibration						
C5H003	11.1	17.6	17.1	3 005	1 894	1 946
C5H007	7.2	10.3	7.0	901	631	922
C5H008	10.5	9.0	7.3	973	1 133	1 409
C5H012	11.9	20.1	11.2	3 967	2 350	4 203
C5H014	56.6	81.3	52.1	15 147	10 542	16 468
C5H015	25.0	41.1	24.5	5 606	3 414	5 731
C5H016	65.6	90.8	70.6	13 742	9 931	12 764
C5H018	39	99.4	41.6	12 934	5 076	12 130
C5H022	6.1	1.6	6.6	84	323	77
C5H039	55.7	48.5	56.4	2 668	3 061	2 633
Verification						
C5H006	8.2	16.0	10.4	1 932	989	1 529
C5H009	12.7	5.5	6.4	261	600	518
C5H023	9.8	6.5	10.8	228	344	207
C5H035	40.7	98.9	38.6	12 393	5 098	13 053
C5H053	16.4	30.1	12.5	5 619	3 059	7 358
C5H054	8.7	16.8	11.9	1 551	801	1 136

The results contained in Table 3.8 and illustrated in Figures 3.9 and 3.10 are characterised by several trends. In applying Eq. (3.7) in both the calibration and verification catchments, the T_{Cy} values were under- and overestimated with between -74 % and +155 % in comparison to the T_{Px} values, while the degree of association (r^2 value) was 0.75.

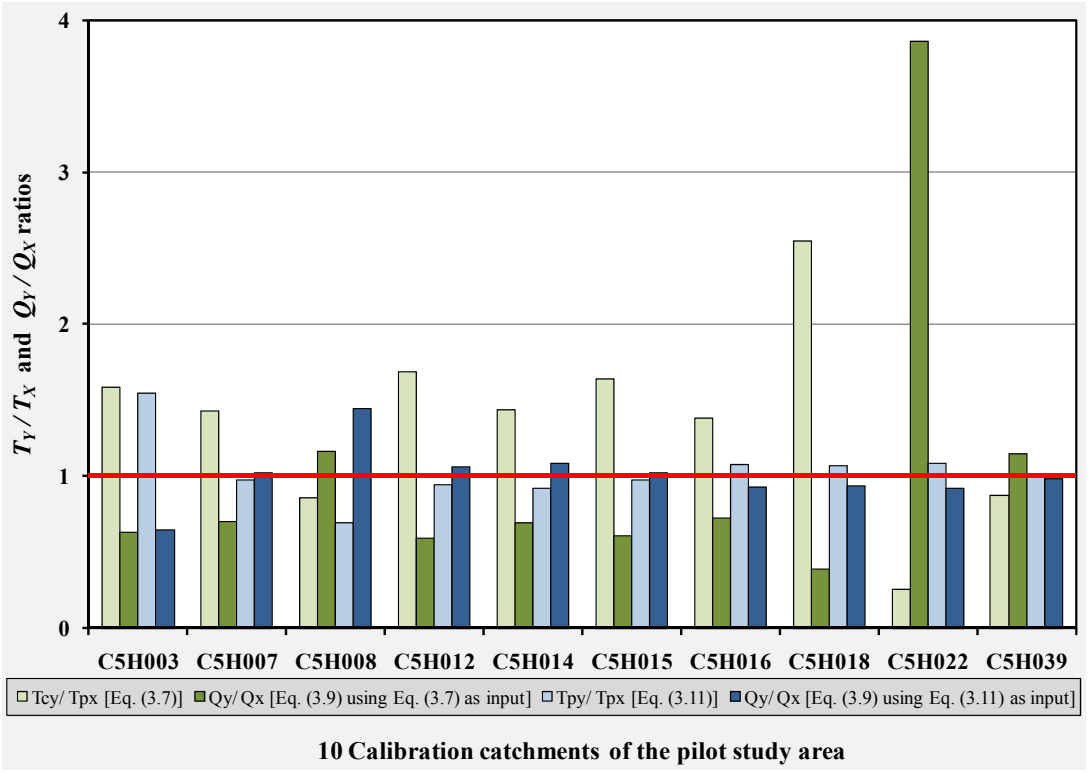

Figure 3.9 Calibration: Time parameter (T_Y/T_X) and peak discharge (Q_Y/Q_X) ratios

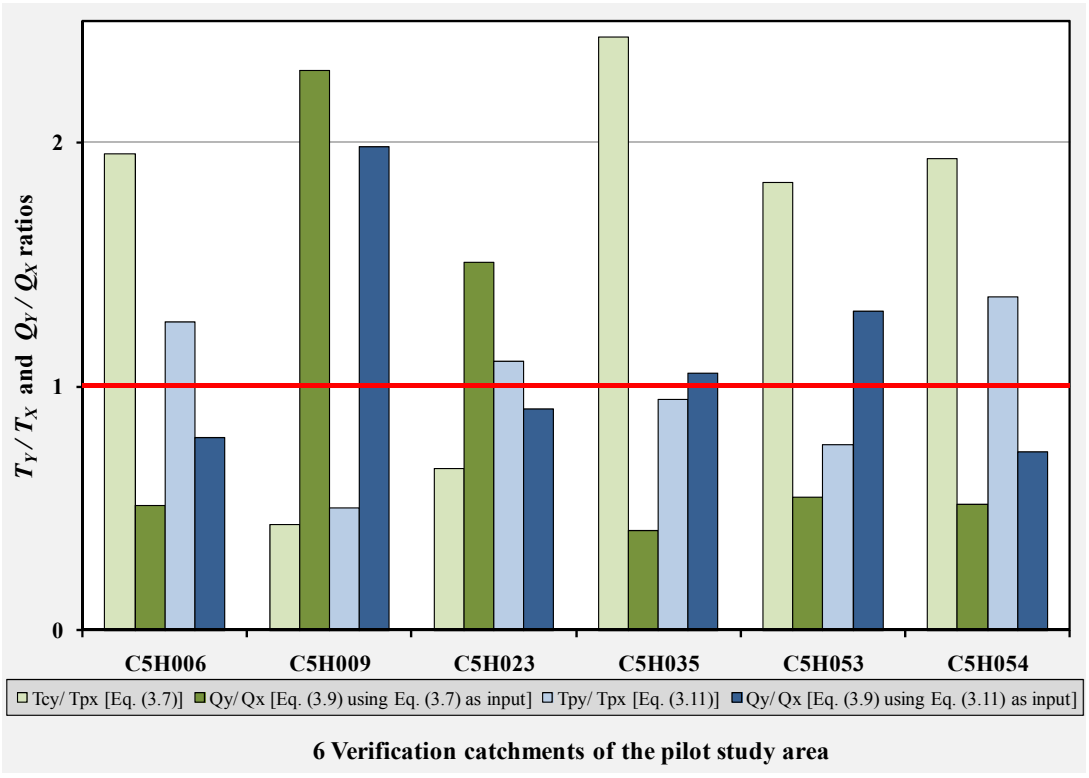

Figure 3.10 Verification: Time parameter (T_Y/T_X) and peak discharge (Q_Y/Q_X) ratios

The T_{Py} estimations based on Eq. (3.11) showed a high degree of association with the observed T_{Px} values during the calibration and verification process, with r^2 values ranging from 0.98 (calibration) to 0.91 (verification) and estimates of between -50 % and +54 % (Figures 3.9 and 3.10). The fact that Eq. (3.11) provided similar results during the verification phase, confirms the reliability of time parameters estimated using Eq. (3.11).

In translating the corresponding time parameter estimation 'errors' into design peak discharges using the SDF method [Eq. (3.9)], the significance is evident. The underestimation of T_P (conceptual T_C) is associated with the overestimation of peak discharges and vice versa, *viz.* the overestimation of T_P results in underestimated peak discharges. It is clearly evident from Figures 3.9 and 3.10 that the time parameter underestimations ranging from -2 % to -74 % are likely to result in peak discharge overestimations of between +2 % and +286 %, while time parameter overestimations of up to +155% could result in peak discharge underestimations of -61 %.

3.7 Conclusions

The developed empirical equation to estimate the catchment response time at a medium to large catchment scale in the C5 secondary drainage region in South Africa meets the requirement of consistency and ease of application. Independent verification tests confirmed the consistency, while the statistically significant independent variables retained, provide a good indication of catchment response times. These independent variables are also easy to determine by practitioners when required for future applications in ungauged catchments. The developed empirical equation also highlighted the inherent limitations and inconsistencies introduced when the 'recommended' empirical methods are applied outside their bounds. However, the developed empirical equation also has potential limitations, especially in terms of its application in ungauged catchments beyond the boundaries of the pilot study area. Therefore, the methodology followed in this chapter should be expanded to other climatologically different regions in South Africa, followed by regionalisation. Adopting the approximation of $T_C \approx T_P$ using only observed streamflow data, confirmed that the design accuracy of any time parameter obtained from observed hyetographs or hydrographs, depends on the computational accuracy of the corresponding input variables. The proposed T_{Px} estimation procedure based on a linear catchment response function [Eq. (3.4) with $x = 1$] and which is reliant on only observed streamflow

variables, not only demonstrated a high degree of association with the sample-means of T_{Pxi} [Eq. (3.1)], but such a procedure is also less influenced by the paucity of rainfall data and non-uniform spatial and temporal rainfall distribution in medium to large catchments. Furthermore, the similarity in the conceptual T_C, T_P and T_L estimates also questions the proposed use of the multiple time parameter definitions found in literature. The use of such multiple time parameter definitions, combined with the absence of a 'standard method' to estimate time parameters from observed data, emphasise why the proportionality ratio of T_L: T_C could typically vary between 0.5 and 2 for the same catchment/region.

Given the sensitivity of design peak discharges to estimated time parameter values, the use of inappropriate time variables results in over- or underestimated time parameters in South African flood hydrology practice and highlights that considerable effort is required to ensure that time parameter estimations are representative and consistently estimated. In general terms, such under- or overestimations of the peak discharge may result in the over- or under-design of hydraulic structures, with associated socio-economic implications, which might render some projects as infeasible.

Building upon the critical assessment of available definitions, estimation procedures and the results from this pilot study, the current approaches used for the estimation of time parameters in medium to large catchments in South Africa could be modernised by implementing the identified research values. For instance, the results suggest that the methodology, based on the approximation of $T_P \approx T_C$, should be expanded to other study areas in climatologically different regions in South Africa, followed by a clustered regionalisation scheme.

Chapter 5 is the direct logic outflow from this chapter (Chapter 3). However, in order to test the proposed methodology first at a smaller scale than opposed to the 74 catchments in the other climatologically different regions in South Africa (as included in Chapter 5), Chapter 4 needs to follow first. Therefore, Chapter 4 provides a critical synthesis and reflection of the proposed methodology as recommended in this chapter by considering 12 catchments in two climatologically different regions. The inherent variability and inconsistencies associated with the direct and indirect estimation of time parameters are also further investigated.

4. THE INCONSISTENCY OF TIME PARAMETER ESTIMATES

This chapter is based on the following paper:

Gericke, OJ and Smithers, JC. 2016. Are estimates of catchment response time inconsistent as used in current flood hydrology practice in South Africa? *Journal of the South African Institution of Civil Engineering* 58 (1): 2–15. DOI: 10.17159/2309-8775/2016/v58n1a1.

4.1 Abstract

Catchment response time parameters are one of the primary inputs required when design floods, especially in ungauged catchments, need to be estimated. The time of concentration (T_C) is the most frequently used time parameter in flood hydrology practice and continues to find application in both event-based methods and continuous hydrological models. Despite the widespread use of the T_C, a unique working definition and equation(s) are currently lacking in South Africa. This chapter presents the results of the direct and indirect T_C estimation for three sets of catchments, which highlights their inherent variability and inconsistencies. These case studies demonstrate that estimates of T_C, using different equations, may differ from each other by up to 800 %. As a consequence of this high variability and uncertainty, it is recommended that for design hydrology and calibration purposes, observed T_C values should be estimated using both the average catchment T_C value, which is based on the event means, and a linear catchment response function. This approach is not only practical, but also proved to be objective and consistent in the study areas investigated in this chapter.

Keywords: *catchment response time; lag time; peak discharge; time of concentration; time to peak*

4.2 Introduction

This chapter provides a critical synthesis and reflection of the proposed methodology as recommended in Chapter 3. In summary, the methodology and findings from Chapter 3, in conjunction with the theoretical basis as established in Chapter 2, are applied in three sets of catchments in climatologically different regions to investigate the inherent variability and inconsistencies associated with the direct (Chapter 3 methodology) and indirect (empirical methods, Chapter 2) estimation of time parameters.

Acknowledging that the 'traditional' convolution process, as introduced in Chapter 2, is not only impractical, but also not applicable in real, large heterogeneous catchments (where antecedent moisture from previous rainfall events and spatially non-uniform rainfall hyetographs can result in multi-peaked hydrographs), the conceptual and practical value of using such alternative approach (*cf.* Chapter 3) is recognised and warrants further investigation.

The objectives of the research reported in this chapter are discussed in the next section, followed by a description of the case studies. Thereafter, the methodologies involved in meeting the objectives are detailed, followed by the results, discussion, and conclusions.

4.3 Objectives

In this chapter, selected definitions and associated estimation procedures are utilised for the analysis of three case studies with the two-fold objective of critically investigating the similarity between T_C and T_P at a medium to large catchment scale and comparing different estimation methods. The latter comparison focuses on the use of direct estimation (from observed streamflow data in medium to large catchments) and indirect estimation (empirical equations) methodologies. The specific objectives are: (i) to compare a selection of overland flow T_C equations using different slope-distance classes and roughness parameter categories to highlight any inherent limitations and inconsistencies, (ii) to explicate the variability of T_C estimations resulting from the $T_C \approx T_P$ approach implemented on observed streamflow data at a medium to large catchment scale, and (iii) to ascertain the inherent limitations and inconsistency of the empirical channel flow T_C equations when compared to the direct estimation of T_C from observed streamflow data.

The three case studies are presented in the next section.

4.4 Case Studies

Three case studies were selected to benchmark the different equations commonly used internationally to estimate T_C in practice at different catchment scales and to investigate their similarities, differences and limitations. The selected case studies are:

(a) **Conceptual urban catchment:** Urban catchments are normally characterised by highly variable and complex flow paths, although, it could equally be argued that flow paths in urban catchments are simpler and more well-defined (impervious

surfaces and pipe flow) than in natural catchments dominated by heterogeneous soil matrices. Therefore, instead of using actual urban catchments, a conceptualised urban catchment setup with overland flow being dominant was selected by considering the combination of different variables such as flow length criteria (*i.e.* overland flow distances associated with specific slopes), overland conveyance factors (ϕ), flow retardance/imperviousness factors (i_p), Manning's overland roughness parameters (n) and runoff curve numbers (CN). The flow length criteria are based on the recommendations made in the National Soil Conservation Manual (NSCM; DAWS, 1986). The NSCM criteria (Table 4.1) are based on the assumption that the steeper the overland slope, the shorter the length of actual overland flow before it transitions into shallow concentrated flow followed by channel flow. A total of five categories defined by different ϕ, i_p, n and CN values in seven slope-distances classes are considered.

Table 4.1 Overland flow distances associated with different slope classes (DAWS, 1986)

Slope class [S_O, %]	**Distance [L_O, m]**
0–3	110
3.1–5	95
5.1–10	80
10.1–15	65
15.1–20	50
20.1–25	35
25.1–30	20

(b) **Central Interior (CI):** Six catchment areas, ranging from 39 km² to 33 278 km² situated in the C5 secondary drainage region (Midgley *et al.,* 1994), were selected as case study areas in this climatological region predominantly characterised by convective rainfall during the summer months. The Mean Annual Precipitation (*MAP*) ranges from 428 mm to 654 mm (Lynch, 2004). The topography is gentle with elevations varying from 1 021 m to 2 120 m and with average catchment slopes between 1.7 % and 10.3 % (USGS, 2002). A total of 450 observed flood events from 1931 to 2013 are included in the analysis.

(c) **Southern Winter Coastal (SWC) region:** Six catchment areas, ranging from 47 km² to 2 878 km² situated in the G1, H1, H4 and H6 secondary drainage regions (Midgley *et al.,* 1994), were selected as case study areas in this climatological region predominantly characterised by winter rainfall. The *MAP* ranges from 450 mm to 915 mm (Lynch, 2004) and rainfall is classified as either orographic and/or frontal rainfall. The topography is very steep with elevations varying from 86 m to 2 240 m and with average catchment slopes ranging between 25.6 % and 41.6 % (USGS, 2002). A total of 460 observed flood events from 1932 to 2013 are included in the analysis.

The location of the case study areas as listed in (b) and (c) is shown in Figure 4.1.

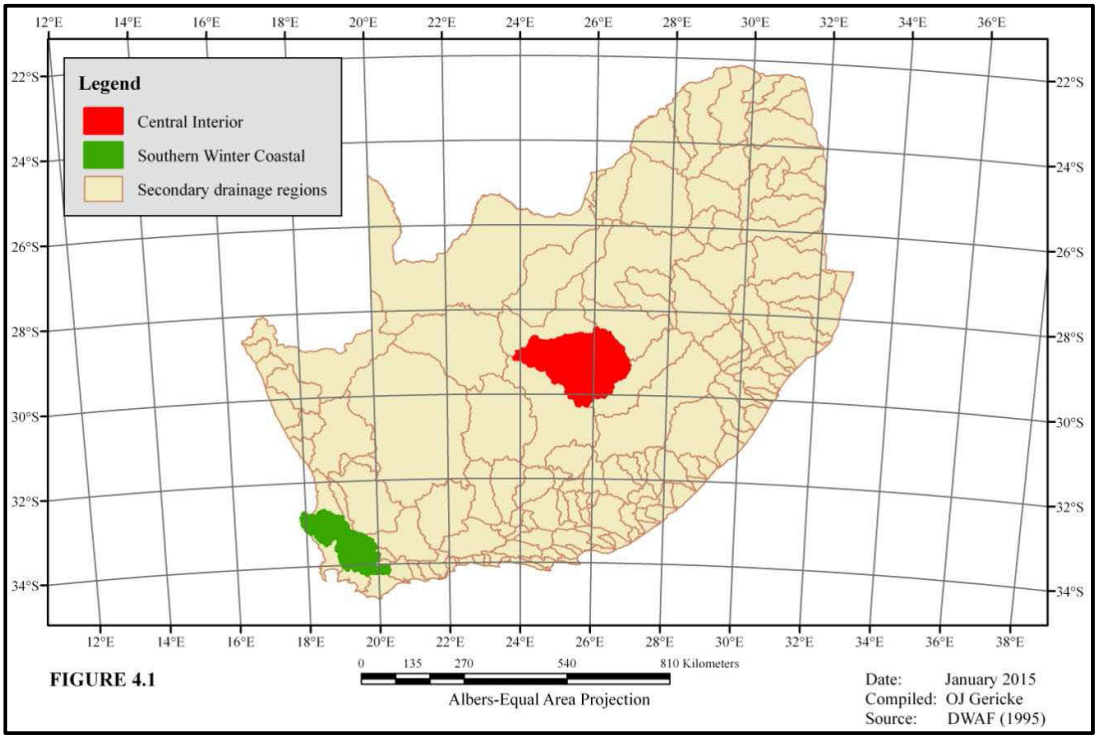

Figure 4.1 Location of case study areas (b) and (c)

Table 4.2 contains a summary of the main morphometric properties for each catchment under consideration. The influences of each variable or parameter listed in Table 4.2 are highlighted where applicable in the subsequent sections.

Table 4.2 Main morphometric properties of catchments in the Central Interior and SWC region

Central Interior						
Catchment descriptor	**C5H008**	**C5H012**	**C5H015**	**C5H016**	**C5H022**	**C5H035**
Area [A, km²]	598	2 366	5 939	33 278	39	17 359
Minimum elevation [m]	1 397	1 322	1 254	1 021	1 531	1 104
Maximum elevation [m]	1 740	1 780	2 120	2 120	2 060	2 120
Average catchment slope [S, m.m^{-1}]	0.0483	0.0328	0.0277	0.0209	0.1029	0.0173
Hydraulic length [L_H, km]	41.0	86.9	160.5	378.1	8.0	373.3
Centroid distance [L_C, km]	22.4	45.3	81.0	230.2	2.7	172.7
Main river/ watercourse length [L_{CH}, km]	40.9	86.7	160.2	377.9	7.9	373.0
Average main river slope [S_{CH}, m.m^{-1}]	0.0049	0.0027	0.0014	0.0010	0.0170	0.0008
Southern Winter Coastal						
Catchment descriptor	**G1H003**	**G1H007**	**H1H007**	**H1H018**	**H4H006**	**H6H003**
Area [A, km²]	47	724	80	109	2 878	500
Minimum elevation [m]	199	86	273	375	185	297
Maximum elevation [m]	1 400	1 780	1 700	1 960	2 240	1 660
Average catchment slope [S, m.m^{-1}]	0.2889	0.2621	0.4069	0.4161	0.2921	0.2556
Hydraulic length [L_H, km]	9.7	55.5	19.0	22.8	109.9	38.6
Centroid distance [L_C, km]	5.0	29.0	9.5	9.3	26.9	13.6
Main river/ watercourse length [L_{CH}, km]	9.2	55.3	18.9	22.8	101.5	38.2
Average main river slope [S_{CH}, m.m^{-1}]	0.0177	0.0046	0.0333	0.0320	0.0047	0.0098

The next section includes the detailed methodology followed during this research which focuses on the indirect estimation (empirical equations) and direct estimation (from observed streamflow data) of T_C.

4.5 Methodology: Time of Concentration Estimation Procedures

In order to evaluate and compare the consistency of a selection of time parameter estimation methods in case study areas (a) to (c), the following steps were followed: (i) application and comparison of six overland flow T_C equations to the Kerby equation [Eq. (4.2)] in different slope-distance classes and roughness parameter categories, (ii) direct estimation of T_C from observed streamflow data based on the $T_C \approx T_P$ approach, and (iii) application of six channel flow T_C equations in 12 medium to large catchments in order to compare their results with the results as obtained in (ii).

The details of the empirical equations as used in (i) and (iii) are listed and discussed first, followed by a description of the procedures followed in (ii).

4.5.1 Indirect estimation using empirical equations

The empirical equations selected require a limited amount of information and similar input variables to estimate T_C in ungauged catchments, as proposed by Williams (1922),

Kirpich (1940), Johnstone and Cross (1949), Miller (1951), Kerby (1959), Reich (1962), Espey and Winslow (1968), FAA (1970), USBR (1973), Sheridan (1994), and Sabol (2008). The empirical equations are detailed in the next two sub-sections for overland flow and channel flow regimes. All the equations are presented in Système International d'Unités (SI Units).

4.5.1.1 Overland flow regime

The empirical overland flow T_C equations are applied within the 'Conceptual urban catchment' [case study (a)] by considering the seven different NSCM slope-distance classes and five categories with associated flow conveyance (ϕ), retardance (imperviousness, i_p), Manning's roughness (n) and runoff curve number (CN) variables. The five different ϕ categories are based on the work done by Viessman and Lewis (1996), with typical ϕ values ranging from 0.6 (i_p = 80 %; n = 0.02; CN = 95); 0.8 (i_p = 50 %; n = 0.06; CN = 85); 1.0 (i_p = 30 %; n = 0.09; CN = 75); 1.2 (i_p = 20 %; n = 0.13; CN = 72) to 1.3 (i_p = 10 %; n = 0.15; CN = 70).

The six overland flow T_C equations are summarised in Eqs. (4.1) to (4.6).

(a) **Miller (1951):** Equation (4.1) is based on a nomograph for shallow sheet overland flow as published by the Institution of Engineers, Australia (Miller, 1951; IEA, 1977; ADNRW, 2007).

$$T_{C1} = 107\left[\frac{nL_O^{0.333}}{(100S_O)^{0.2}}\right] \quad (4.1)$$

where T_{C1} = overland time of concentration [minutes],
L_O = length of overland flow path [m],
n = Manning's roughness parameter for overland flow, and
S_O = average overland slope [m.m^{-1}].

(b) **Kerby (1959):** Equation (4.2) is commonly used to estimate the T_C both as mixed sheet and/or shallow concentrated overland flow in the upper reaches of small, flat catchments. The Drainage Manual (SANRAL, 2013) also recommends the use thereof in South Africa. McCuen *et al.* (1984) highlighted that Eq. (4.2) was developed and calibrated for catchments in the United States of America (USA)

with areas less than 4 ha, with average slopes of less than 1 % and Manning's roughness parameters (n) varying between 0.02 and 0.8.

$$T_{C2} = 1.4394\left(\frac{nL_O}{\sqrt{S_O}}\right)^{0.467} \quad (4.2)$$

where T_{C2} = overland time of concentration [minutes],
L_O = length of overland flow path [m],
n = Manning's roughness parameter for overland flow, and
S_O = average overland slope [m.m^{-1}].

(c) **SCS (1962):** Equation (4.3) is commonly used to estimate the T_C as mixed sheet and/or concentrated overland flow in the upper reaches of a catchment. The USDA SCS developed this equation in 1962 (Reich, 1962) for homogeneous, agricultural catchment areas up to 8 km² with mixed overland flow conditions dominating (USDA SCS, 1985).

$$T_{C3} = \frac{L_O^{0.8}\left[\frac{25400}{CN} - 228.6\right]^{0.7}}{706.9\,S_O^{0.5}} \quad (4.3)$$

where T_{C3} = overland time of concentration [minutes],
CN = runoff curve number,
L_O = length of overland flow path [m], and
S_O = average overland slope [m.m^{-1}].

(d) **Espey-Winslow (1968):** Equation (4.4) was developed using data from 17 catchments in Houston, USA, with areas ranging from 2.6 km² to 90.7 km². The imperviousness factor (i_p) represents overland flow retardance, while the conveyance factor (ϕ) measures subjectively the hydraulic efficiency of a flow path, taking both the condition of the surface cover and degree of development into consideration (Espey and Winslow, 1968).

$$T_{C4} = 44.1\left[\frac{\phi L_O^{0.29}}{S_O^{0.145} i_p^{0.6}}\right] \quad (4.4)$$

where T_{C4} = overland time of concentration [minutes],

i_p = imperviousness factor [%],

ϕ = conveyance factor,

L_O = length of overland flow path [m], and

S_O = average overland slope [m.m^{-1}].

(e) **Federal Aviation Agency (FAA, 1970):** Equation (4.5) is commonly used in urban overland flow estimations, since the Rational method's runoff coefficient (C) is included (FAA, 1970; McCuen *et al*., 1984).

$$T_{C5} = \frac{1.8(1.344 - C)L_O^{0.5}}{(100S_O)^{0.333}} \quad (4.5)$$

where T_{C5} = overland time of concentration [minutes],

C = Rational method runoff coefficient (≈ default i_p fraction values),

L_O = length of overland flow path [m], and

S_O = average overland slope [m.m^{-1}].

(f) **NRCS kinematic wave (1986):** Equation (4.6) was originally developed by Welle and Woodward (1986) to avoid the iterative use of the original kinematic wave equation (Morgali and Linsley, 1965) and is based on a power-law relationship between design rainfall intensity and duration.

$$T_{C6} = \frac{5.476}{P_2^{0.5}}\left(\frac{nL_O}{\sqrt{S_O}}\right)^{0.8} \quad (4.6)$$

where T_{C6} = overland time of concentration [minutes],

L_O = length of overland flow path [m],

n = Manning's roughness parameter for overland flow,

P_2 = two-year return period 24 hour design rainfall depth [mm], and

S_O = average overland slope [m.m^{-1}].

4.5.1.2 Channel flow regime

In the medium to large catchments located in case study areas (b) and (c), channel flow in the main watercourses is assumed to dominate. Consequently, a selection of six channel flow T_C equations with similar input variables are applied and compared to the direct T_C

estimation results (referred to as T_{Cx} in this chapter) obtained from observed streamflow data using the assumption of the conceptual $T_C \approx T_P$.

The six channel flow T_C equations are summarised in Eqs. (4.7) to (4.12).

(g) **Bransby-Williams (1922):** The use of Equation (4.7) (Williams, 1922) is limited to rural catchment areas less than ± 130 km² (Fang *et al.*, 2005; Li and Chibber, 2008). The Australian Department of Natural Resources and Water (ADNRW, 2007) highlighted that the initial overland flow travel time is already incorporated; therefore an overland flow or standard inlet time should not be added.

$$T_{C7} = 0.2426\left(\frac{L_{CH}}{A^{0.1}S_{CH}^{0.2}}\right) \quad (4.7)$$

where T_{C7} = channel flow time of concentration [hours],

A = catchment area [km²],

L_{CH} = length of longest watercourse [km], and

S_{CH} = average main watercourse slope [$m.m^{-1}$; using the 10-85 method].

Note: In the 10-85 method, the average main watercourse slope is estimated by dividing the difference in elevation at 10 % and 85 % of the main watercourse length by 75 % of the total main watercourse length (SANRAL, 2013).

(h) **Kirpich (1940):** Equation (4.8) was calibrated in small, agricultural catchments (< 45 ha) located in the USA with average catchment slopes ranging between 3 % and 10 %. McCuen *et al.* (1984) showed that Eq. (4.8) had a tendency to underestimate T_C values in 75 % of urbanised catchments with areas smaller than 8 km², while in 25 % of the catchments (8 km² < $A \leq$ 16 km²) with substantial channel flow, it had the smallest bias when compared to the observed T_{Cx} values.

$$T_{C8} = 0.0663\left(\frac{L_{CH}^{2}}{S_{CH}}\right)^{0.385} \quad (4.8)$$

where T_{C8} = channel flow time of concentration [hours],

L_{CH} = length of longest watercourse [km], and

S_{CH} = average main watercourse slope [m.m^{-1}; using the 10-85 method].

(i) **Johnstone-Cross (1949):** Equation (4.9) was developed to estimate T_C in the Scioto and Sandusky River catchments (Ohio Basin) with areas ranging from 65 km² to 4 206 km² (Johnstone and Cross, 1949; Fang *et al.*, 2008).

$$T_{C9} = 0.0543\left(\frac{L_{CH}}{S_{CH}}\right)^{0.5} \quad (4.9)$$

where T_{C9} = channel flow time of concentration [hours],

L_{CH} = length of longest watercourse [km], and

S_{CH} = average main watercourse slope [m.m^{-1}; using the 10-85 method].

(j) **USBR (1973):** Equation (4.10) was proposed by the USBR (1973) to be used as a standard empirical equation to estimate the T_C in hydrological designs, especially culvert designs based on the California Culvert Practice, CCP (1955; cited by Li and Chibber, 2008). However, in essence it is a modified version of Eq. (4.8) as proposed by Kirpich (1940) and is recommended by SANRAL (2013) for general use in South Africa.

$$T_{C10} = \left(\frac{0.87{L_{CH}}^2}{1000S_{CH}}\right)^{0.385} \quad (4.10)$$

where T_{C10} = channel flow time of concentration [hours],

L_{CH} = length of longest watercourse [km], and

S_{CH} = average main watercourse slope [m.m^{-1}; using the 10-85 method].

(k) **Sheridan (1994):** Equation (4.11) was developed to estimate the T_C using data from nine catchments in Georgia and Florida, USA, with catchment areas ranging between 2.6 km² and 334.4 km² (Sheridan, 1994; USDA NRCS, 2010).

$$T_{C11} = 2.2{L_{CH}}^{0.92} \quad (4.11)$$

where T_{C11} = channel flow time of concentration [hours], and

L_{CH} = length of longest watercourse [km].

(l) **Colorado-Sabol (2008):** Sabol (2008) proposed three different empirical T_C equations to be used in catchments with distinctive geomorphological and land-use characteristics in the State of Colorado, USA. Equation (4.12) is the equation applicable to rural catchments.

$$T_{C12} = 0.9293\left[\frac{A^{0.1}\left(L_{CH}L_C\right)^{0.25}}{S_{CH}^{0.2}}\right] \quad (4.12)$$

where T_{C12} = channel flow time of concentration [hours],

A = catchment area [km²],

L_C = centroid distance [km],

L_{CH} = length of longest watercourse [km], and

S_{CH} = average main watercourse slope [$m.m^{-1}$; using the 10-85 method].

The direct estimation of T_{Cx} from observed streamflow data is discussed in the next section.

4.5.2 Direct estimation from observed streamflow data

The procedure as proposed by Gericke and Smithers (2014) and implemented by them (Gericke and Smithers, 2015) in Chapters 2 and 3 respectively is used to estimate T_{Cx} directly from observed streamflow data. In summary, the following steps were followed and also implemented in this chapter:

4.5.2.1 Establishment of flood database

Department of Water and Sanitation (DWS) primary flow data consisting of an up-to-date sample (2013) of the 12 continuous flow-gauging stations located at the outlet of each catchment in the CI and SWC region were prepared and evaluated using the screening process as proposed Gericke and Smithers (2015). The screening process accounts for: (i) streamflow record lengths (> 30 years), (ii) representative catchment area ranges ($20 < A \leq 35\,000$ km²), and (iii) representative rating tables, *i.e.* extrapolation of rating tables was limited to 20 % in cases where the observed river stage exceeded the maximum rated levels (H). Gericke and Smithers (2015) used third-order polynomial regression analyses to extrapolate the rating tables. Hydrograph shape (especially the peakedness as a result of a steep rising limb, in relation to the hydrograph base length) and the relationship between individual observed peak discharge (Q_{Pxi}) and direct runoff volume (Q_{Dxi}) pair

values were used as additional criteria to justify the individual stage extrapolations (H_E) up to a 20 % limit, *i.e.* $H_E \leq 1.2\,H$. Typically, in such an event, the additional volume of direct runoff (Q_{DE}) due to the extrapolation was limited to 5 %, *i.e.* $Q_{DE} \leq 0.05\,Q_{Dxi}$; hence the error made by using larger direct runoff volumes had little impact on the sample statistics of the total flood volume. This approach was justified in having samples of reasonable size (a total of 1 134 flood hydrographs in the C5 secondary drainage region), while the primary focus was on the time when the peak discharge occurs, not necessarily just the magnitude thereof. It is also important to note that Görgens (2007) also used a 20 % stage limit to extrapolate rating tables as used in the development of the Joint Peak-Volume (JPV) method.

4.5.2.2 Extraction of flood hydrographs

Complete flood hydrographs were extracted using the selection criteria as proposed by Gericke and Smithers (2015) and are based on: (i) the implementation of truncation levels (*i.e.* only flood events > smallest annual maximum flood event were extracted), and (ii) the identification of mutual start/end times on both the flood hydrographs and baseflow curves, hence ensuring that when a hydrograph is separated into direct runoff and baseflow, that the identified separation point represents the start of direct runoff which coincides with the onset of effective rainfall. The end of a flood event was also determined using a recursive filtering method (Nathan and McMahon, 1990).

4.5.2.3 Analyses of flood hydrographs

The direct runoff and baseflow were separated using the recursive digital filtering method [Eq. (4.13)] as initially proposed by Nathan and McMahon (1990) and adopted by Smakhtin and Watkins (1997) in a national-scale study in South Africa.

$$Q_{Dxi} = \alpha Q_{Dx(i-1)} + \beta(1+\alpha)\left(Q_{Txi} - Q_{Tx(i-1)}\right) \qquad (4.13)$$

where Q_{Dxi} = filtered direct runoff at time step i, which is subject to $Q_{Dx} \geq 0$ for time i [$m^3.s^{-1}$],

α, β = filter parameters, and

Q_{Txi} = total streamflow (*i.e.* direct runoff plus baseflow) at time step i [$m^3.s^{-1}$].

The application of Eq. (4.13) using a fixed α-parameter value of 0.995 (Smakhtin and Watkins, 1997) and a fixed β-parameter value of 0.5 (Hughes *et al.* 2003) resulted in the estimation of the following hydrograph parameters: (i) start/end date/time of flood hydrograph, (ii) observed peak discharge [Q_{Pxi}, $m^3.s^{-1}$], (iii) total volume of runoff [Q_{Txi}, m^3], (iv) volume of direct runoff [Q_{Dxi}, m^3], (v) volume of baseflow [Q_{Bxi}, m^3], (vi) baseflow index [BFI, which equals the ratio of Q_{Bxi}/Q_{Txi}], (vii) depth of effective rainfall [P_{Exi}, mm, based on the assumption that the volume of direct runoff equals the volume of effective rainfall and that the total catchment area is contributing to runoff], and (viii) time to peak [T_{Pxi}, hours, with $T_{Pxi} \approx T_{Cxi}$).

Lastly, the analysed flood hydrographs were subjected to a final filtering process (Gericke and Smithers, 2015) to ensure that all the flood hydrographs are independent and that the conceptual T_{Cxi} values are consistent, *i.e.* the likelihood of higher Q_{Pxi} values to be associated with larger Q_{Dxi} and T_{Cxi} values, while taking cognizance of their dependence on factors such as antecedent moisture conditions and non-uniformities in the temporal and spatial distribution of storm rainfall. Furthermore, the use of 'truncation levels', *i.e.* when only flood events larger than the smallest annual maximum flood event on record were extracted, ensured that all minor events were excluded, while all the flood events retained were characterised as multiple events being selected in a specific hydrological year. This approach resulted in a Partial Duration Series (PDS) of independent flood peaks above a certain level. It is important to note that Gericke and Smithers (2014; 2015) defined the T_{Cxi} values as shown in Eq. (4.14).

$$T_{Cxi} = \sum_{j=1}^{N} t_j \tag{4.14}$$

where T_{Cxi} = conceptual time of concentration which equals the observed T_{Pxi} values for individual flood events [hours],

t_j = duration of the total net rise (excluding the in-between recession limbs) of a multiple-peaked hydrograph [hours], and

N = sample size.

The mean of the individual flood events in each catchment calculated using Eq. (4.14) could be used as the actual catchment response time. However, Gericke and Smithers (2015) highlighted that the use of such averages could be misleading and might not be a good reflection of the actual catchment response time, since small T_{Pxi} values, which occurred more frequently, have a large influence on the average value of Eq. (4.14), and consequently result in an underestimated catchment T_{Px} value. Therefore, by considering the high variability between individual T_{Pxi} values estimated from different flood events for the same catchment, as well as taking cognisance of the procedure adopted by Gericke and Smithers (2015), the use of a 'representative average value' equal to the linear catchment response function of Eq. (4.15) (Gericke and Smithers, 2015) was used to confirm the validity and representativeness of the mean of the values calculated from each event.

$$T_{C\,linear} = \frac{1}{3600}\left[\frac{\sum_{i=1}^{N}\left(Q_{Pxi} - \overline{Q_{Px}}\right)\left(Q_{Dxi} - \overline{Q_{Dx}}\right)}{\sum_{i=1}^{N}\left(Q_{Pxi} - \overline{Q_{Px}}\right)^2}\right] \tag{4.15}$$

where $T_{C\,linear}$ = conceptual T_C assuming a linear catchment response [hours],

Q_{Dxi} = volume of direct runoff for individual flood events [m^3],

$\overline{Q_{Dx}}$ = mean of Q_{Dxi} [m^3],

Q_{Pxi} = observed peak discharge for individual flood events [$m^3.s^{-1}$],

$\overline{Q_{Px}}$ = mean of Q_{Pxi} [$m^3.s^{-1}$], and

N = sample size.

In each catchment, the results based on Eqs. (4.14) and (4.15) were compared to establish their degree of association. Despite the high degree of association evident, Eq. (4.15) was regarded as the most consistent procedure to estimate the most representative catchment T_{Cx} values. The preferential use of Eq. (4.15) is motivated by the fact that the Hydrograph Analysis Tool (HAT) developed by Gericke and Smithers (2015) could not always, due to the nature of flood hydrographs, cater for the different variations in flood hydrographs, especially when Eq. (4.14) was applied. Therefore, some user intervention is sometimes required and consequently it could be argued that some inherent inconsistencies could have possibly been introduced. Taking cognizance of the latter possibility, the use of Eq. (4.15) is therefore regarded as being more objective and with consistent results.

A standardised bias statistic [Eq. (4.16); McCuen *et al.*, 1984) was used with the mean error (difference in the average of the observed and estimated values in different classes/categories/catchments) as a measure of actual bias and to ensure that the T_C estimation results are not dominated by errors in the large T_C values. The standard error of the estimate was also used to provide another measure of consistency.

$$B_S = 100\left[\frac{1}{N}\sum_{i=1}^{N}\frac{\left|T_{Cyi} - T_{Cxi}\right|}{T_{Cxi}}\right] \tag{4.16}$$

where B_S = standardised bias statistic [%],

T_{Cxi} = observed time of concentration [minutes or hours],

T_{Cyi} = estimated time of concentration [minutes or hours], and

N = number of slope-distance categories (overland flow regime) or sub-catchments (channel flow regime).

4.6 Results and Discussion

The results from the application of the methodology using different T_C estimation procedures as applied in case study areas (a) to (c) are presented in this section. The station numbers of the DWS flow-gauging stations located at the outlet of each catchment are used as the catchment descriptors for easy reference in all the table(s) and figures.

4.6.1 Indirect T_C estimation results (overland flow)

The empirical overland flow T_C equations were applied within the 'Conceptual urban catchment' [Case study (a)] by considering the seven different NSCM slope-distance classes and five categories with associated flow conveyance (ϕ), retardance (imperviousness, i_p), Manning's roughness (n) and runoff curve number (CN) variables.

The results from the estimated overland flow T_C for the seven different NSCM slope-distance classes and five categories are shown in Figures 4.2 to 4.6. From the results contained in Figures 4.2 to 4.6, the five equations [Eqs. (4.1) and (4.3) to (4.6)] used to estimate the overland flow T_C in case study area (a), relative (not absolute) to the T_C estimated using the Kerby equation [Eq. (4.2)], showed different biases when compared in each of the five different flow retardance categories and associated slope-distance classes.

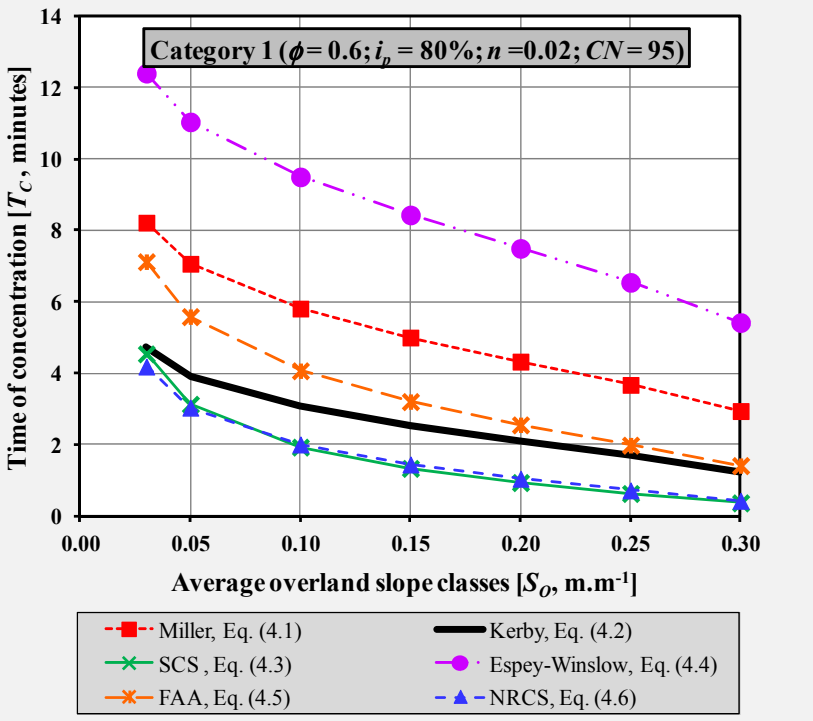

Figure 4.2 Category 1: Variation of overland flow T_C estimates in different average overland slope classes

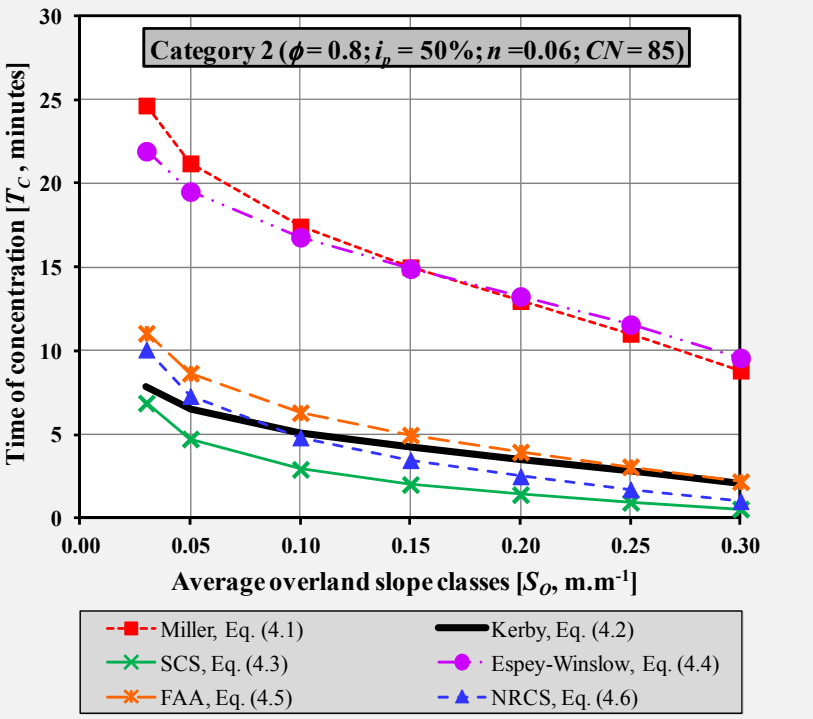

Figure 4.3 Category 2: Variation of overland flow T_C estimates in different average overland slope classes

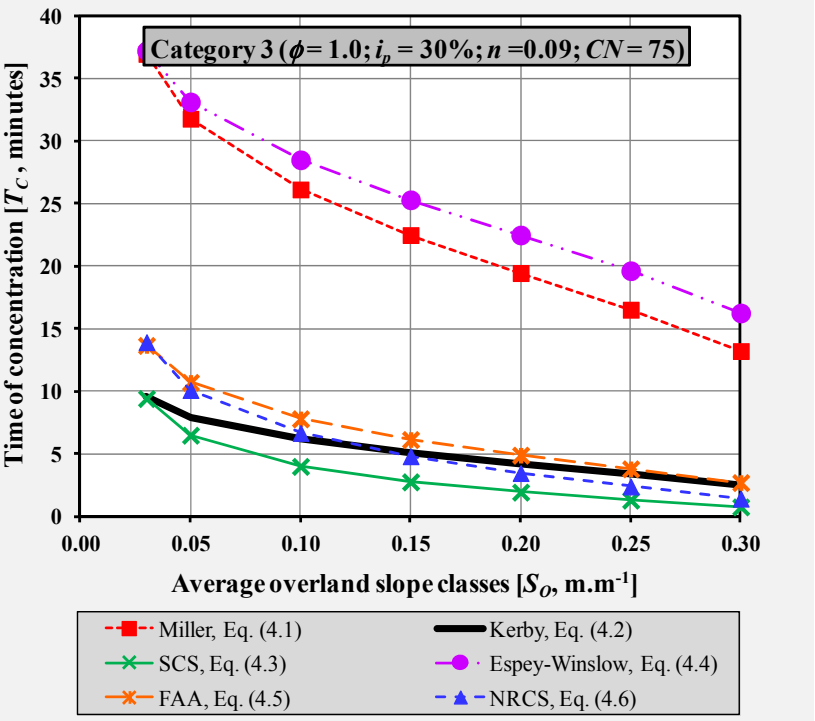

Figure 4.4 Category 3: Variation of overland flow T_C estimates in different average overland slope classes

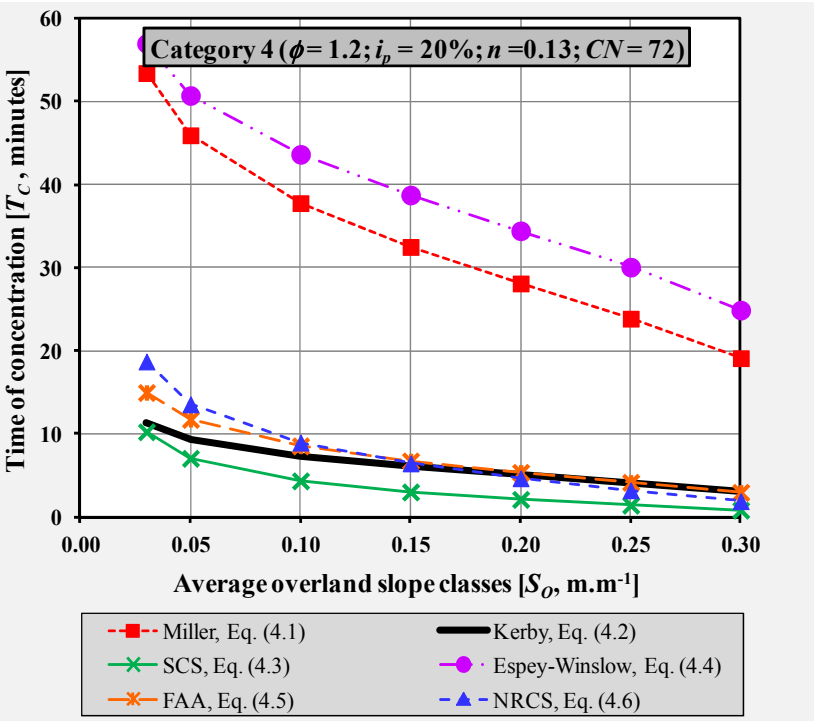

Figure 4.5 Category 4: Variation of overland flow T_C estimates in different average overland slope classes

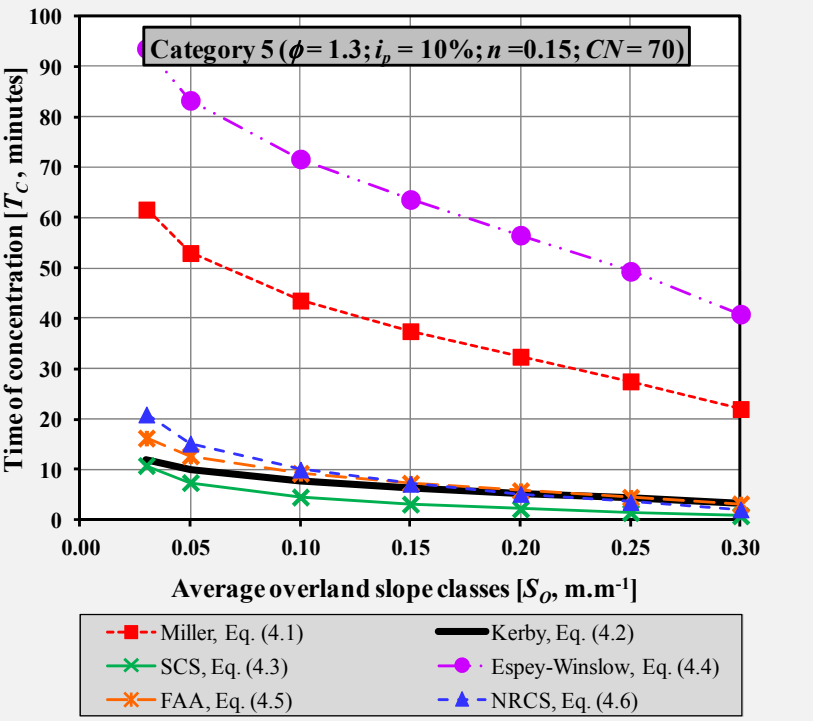

Figure 4.6 Category 5: Variation of overland flow T_C estimates in different average overland slope classes

As expected, all the T_C estimates decreased with an increase in the average overland slope, while T_C gradually increases with an increase in the surface roughness and permeability. The SCS equation [Eq. (4.3)] constantly underestimated T_C, while the Miller [Eq. (4.1)] and Espey-Winslow [Eq. (4.4)] equations overestimated T_C in all cases when compared to the estimates based on the Kerby equation [Eq. (4.2)]. The NRCS kinematic wave equation [Eq. (4.6)] underestimated T_C in relation to the Kerby equation [Eq. (4.2)] in Category 1, while other T_C underestimations were witnessed in Categories 2 ($S_O \geq 0.10$ m.m^{-1}), 3 ($S_O \geq 0.15$ m.m^{-1}), and 4 to 5 ($S_O \geq 0.20$ m.m^{-1}). The poorest results in relation to the Kerby equation [Eq. (4.2)] were obtained using the Espey-Winslow equation [Eq. (4.4)] and could be ascribed to the use of default conveyance (ϕ) factors which might not be representative, since this is the only equation using ϕ as a primary input parameter.

The overall average consistency measures compared to the Kerby equation [Eq. (4.2)] are listed in Table 4.3.

Table 4.3 Consistency measures for the test of overland flow T_C estimation equations compared to Eq. (4.2) (Kerby, 1959)

Equations	Consistency measures					
	Mean estimated T_C [Eq. (4.2), min.]	**Mean estimated T_C [min.]**	**Standard bias statistic [%]**	**Mean error [min.]**	**Maximum error [min.]**	**Standard error [min.]**
Miller [Eq. (4.1)]	5.3	23.8	327.3	18.5	49.5	1.1
SCS [Eq. (4.3)]	5.3	3.4	-44.6	-1.9	-3.3	0.8
Espey-Winslow [Eq. (4.4)]	5.3	31.1	469.2	25.8	81.5	1.8
FAA [Eq. (4.5)]	5.3	6.6	20.3	1.3	4.2	0.4
NRCS [Eq. (4.6)]	5.3	6.0	-6.2	0.6	8.9	0.5

In considering the overall average consistency measures compared to the Kerby equation [Eq. (4.2)] as listed in Table 4.3, the NRCS kinematic wave equation [Eq. (4.6)] provided relatively the smallest bias (< 10 %), with a mean error ≤ 1 minute. Both the standardised bias (469.2 %) and mean error (26 minutes) of the Espey-Winslow equation [Eq. (4.4)] were large compared to the other equations. The SCS equation [Eq. (4.3)] resulted in the smallest maximum absolute error of 3.3 minutes, while the Espey-Winslow equation [Eq. (4.4)] had a maximum absolute error of 82 minutes. The standard deviation of the errors provides another measure of correlation, with standard errors < 1 minute [Eqs. (4.3), (4.5) and (4.6)].

4.6.2 Direct T_C estimation results

Only 5.6 % and 6.9 % of the total number of flood hydrographs analysed in the CI and SWC region respectively were subjected to the extrapolation of stage values (H_E) above the maximum rated levels (H) within the range $H_E \leq 1.2\ H$ and $Q_{DE} \leq 0.05\ Q_{Dxi}$. Thus, the error made by using larger direct runoff volumes had little impact on the sample statistics of the total flood volume, especially if the total sample size of the analysed flood hydrographs is taken into consideration. It is important to note, as highlighted before, that the primary focus is on the time when the peak discharge occurs, not necessarily just the magnitude thereof.

The averaged hydrograph parameters computed using Eq. (4.13) with $\alpha = 0.995$ and $\beta = 0.5$ applied to the extracted observed hydrograph data are listed in Table 4.4. Figures 4.7 (CI) and 4.8 (SWC region) show the regional observed peak discharge (Q_{Pxi}) versus the conceptual T_{Cxi} ($\approx T_{Pxi}$) values for all the catchments under consideration.

Table 4.4 Summary of average hydrograph parameters for different catchments in the Central Interior and SWC region

Central Interior									
Catchment descriptor	Data period	Number of events	Average catchment values						
			Q_{Tx} [10^6 m^3]	Q_{Dx} [10^6 m^3]	Q_{Px} [m^3.s^{-1}]	T_{Cx} [Eq. (4.14), h]	$T_{C\ linear}$ [Eq. (4.15), h]	P_{Ex} [mm]	BFI
C5H008	1931/04/01 – 1986/04/01	112	2.2	2.0	44.7	8.0	10.5	3.3	0.1
C5H012	1936/04/01 – 2013/02/13	68	3.3	2.3	41.5	11.9	11.9	1.0	0.3
C5H015	1949/01/01 – 1983/11/22	90	23.3	21.0	203.1	26.7	25.0	3.5	0.1
C5H016	1953/02/01 – 1999/03/10	40	31.0	27.0	105.6	65.9	65.6	0.8	0.1
C5H022	1980/10/14 – 2013/10/24	70	0.37	0.31	11.5	5.3	6.1	8.0	0.2
C5H035	1989/08/03 – 2013/07/23	70	19.4	16.6	91.8	38.8	41.0	1.0	0.1
Southern Winter Coastal									
Catchment descriptor	Data period	Number of events	Average catchment values						
			Q_{Tx} [10^6 m^3]	Q_{Dx} [10^6 m^3]	Q_{Px} [m^3.s^{-1}]	T_{Cx} [Eq. (4.14), h]	$T_{C\ linear}$ [Eq. (4.15), h]	P_{Ex} [mm]	BFI
G1H003	1949/03/21 – 2013/08/27	75	1.6	1.2	20.6	8.3	9.2	24.4	0.2
G1H007	1951/04/02 – 1977/05/31	75	50.4	43.9	238.9	36.0	37.1	60.7	0.1
H1H007	1950/04/10 – 2013/07/25	98	10.5	7.6	196.8	10.3	10.3	95.0	0.3
H1H018	1969/02/26 – 2013/07/26	80	15.0	11.0	323.3	11.1	10.9	100.9	0.3
H4H006	1950/04/19 – 1990/08/06	80	105.7	78.9	453.5	43.9	44.8	27.4	0.2
H6H003	1932/10/01 – 1974/11/11	52	16.9	13.2	58.1	31.5	32.1	26.3	0.2

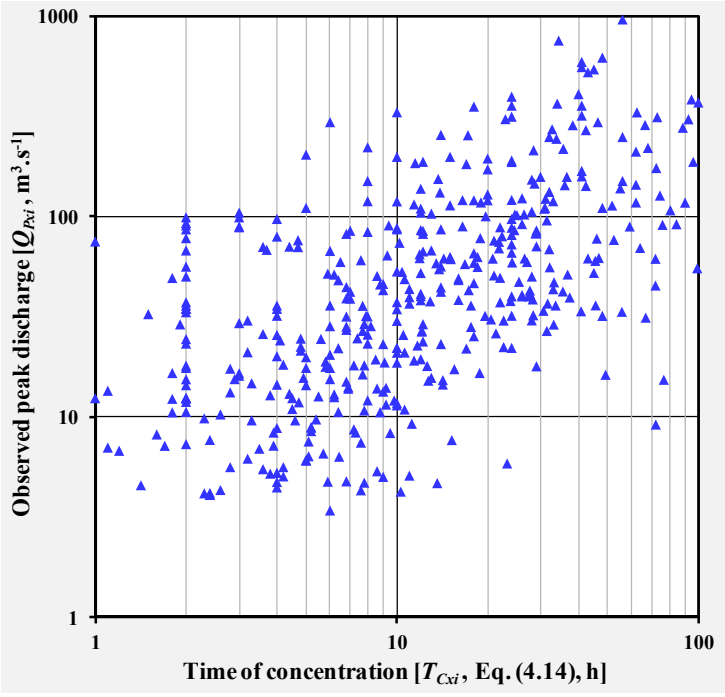

Figure 4.7 Regional Q_{Pxi} versus conceptual T_{Cxi} values (Central Interior)

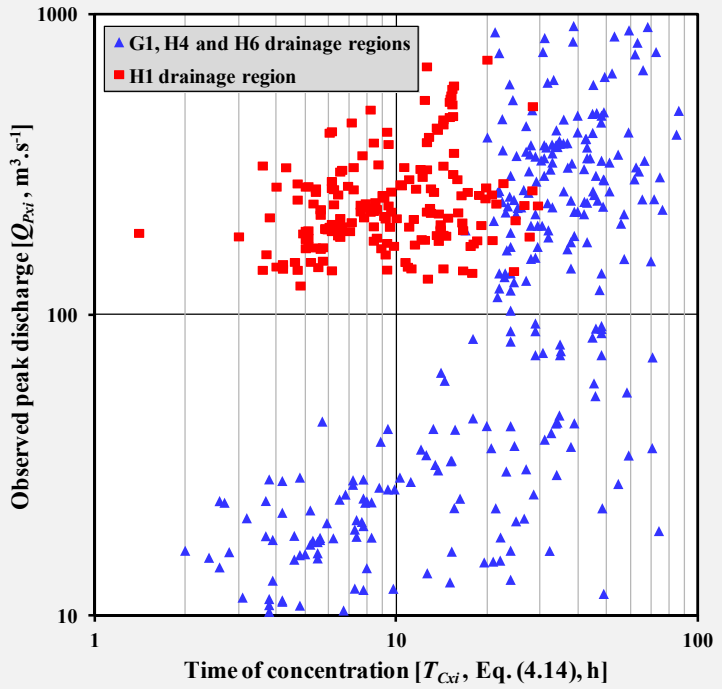

Figure 4.8 Regional Q_{Pxi} versus conceptual T_{Cxi} values (SWC region)

The data scatter in these figures demonstrates the inherent variability of Q_{Pxi} and T_{Cxi} in medium to large catchments at a regional level, *i.e.* the Q_{Pxi} and T_{Cxi} values representative of each individual flood event in all the catchments in a particular region. It is evident that the direct T_{Cxi} estimations from the observed streamflow data [Eq. (4.14)] could vary significantly, with the largest Q_{Pxi} and T_{Cxi} values associated with the likelihood of the entire catchment receiving rainfall for the critical storm duration. Smaller T_{Cxi} values could be expected when effective rainfall of high average intensity does not cover the entire catchment, especially when a storm is centered near the outlet of a catchment. The regional T_{Cxi} values in Figure 4.7 show a stronger linear correlation ($r^2 = 0.70$) when compared to the regional T_{Cxi} values ($r^2 = 0.40$) in Figure 4.8. The latter stronger linear correlation shown in Figure 4.7 confirms that more homogeneous catchment responses were obtained in the Central Interior than in SWC region (Figure 4.8).

However, in Figure 4.8 (SWC region), the T_{Cxi} values consist of two 'different populations', *i.e.* the T_{Cxi} in relation to Q_{Pxi} and the catchment area varies from catchment to catchment. This could be ascribed to differences in their morphometric properties, as well as to the spatial location of these catchments in different secondary drainage regions. The catchment responses in the H1 secondary drainage region differ from those catchments

situated in the G1, H4 and H6 secondary drainage regions, with the Q_{Pxi} values generally larger for corresponding or shorter T_{Cxi} values, while the catchment areas are also smaller. Apart from the smaller catchment areas, the average catchment slope (S) and average main river slope (S_{CH}) are also much steeper (*cf.* Table 4.2).

The linear regression plots of the paired Q_{Pxi} and Q_{Dxi} values applicable to the Central Interior and SWC region are shown in Figures 4.9 and 4.10 respectively.

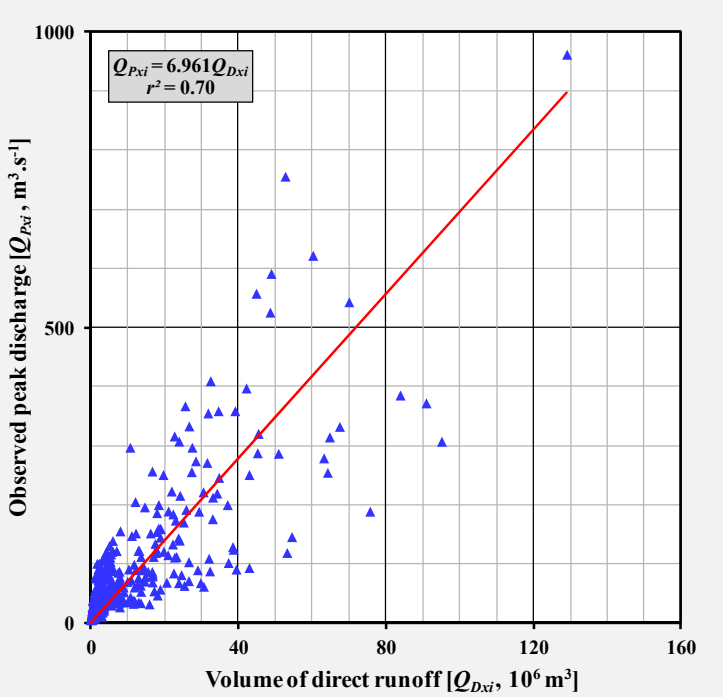

Figure 4.9 Direct estimation of T_{Cx} [Eq. (4.15)] from observed streamflow data (Central Interior)

At a regional level, the paired Q_{Pxi} and Q_{Dxi} values showed an acceptable degree of association with r^2 values between 0.4 and 0.7. The r^2 values deviated similarly or less from unity at a catchment level and such deviations could be ascribed to non-linear changes in the rainfall pattern and catchment conditions (*e.g.* soil moisture status) between individual flood events in a particular catchment. Consequently, Gericke and Smithers (2015a) proposed the use of correction factors (*cf.* Chapter 5) to provide individual catchment responses associated with a specific flood event. However, in this research, Eq. (4.15) is used to confirm the validity and representativeness of the sample-means using Eq. (4.14) and thus the correction factors were not applied.

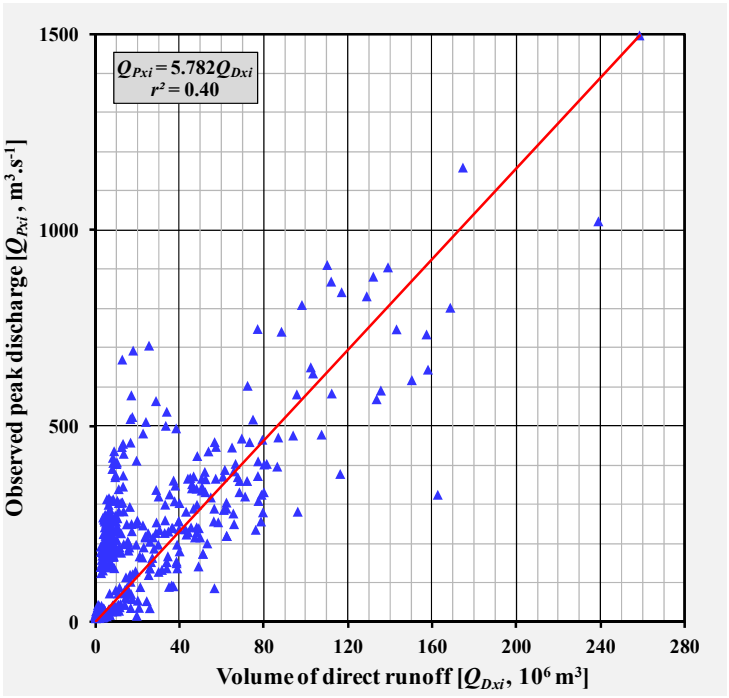

Figure 4.10 Direct estimation of T_{Cx} [Eq. (4.15)] from observed streamflow data (SWC region)

The high degree of association ($r^2 > 0.99$) between Eqs. (4.14) and (4.15) (*cf.* Table 4.4) also confirmed that the extracted flood events in each catchment do reflect the actual catchment processes, and despite the variability of individual catchment responses does not result in large differences in average catchment values.

4.6.3 Comparison of indirect and direct T_C estimation (channel flow)

In Figures 4.11 and 4.12 box plots are used to highlight the inherent variability of the T_{Cxi} values [Eq. (4.14)] estimated directly from the observed streamflow data. In these figures, the whiskers represent the minimum and maximum values, the boxes the 25th and 75th percentile values and the change in box colour represent the median value. The results of the six equations [Eqs. (4.7) to (4.12)] used to estimate T_C, under predominant channel flow conditions, are also super-imposed on Figures 4.11 and 4.12.

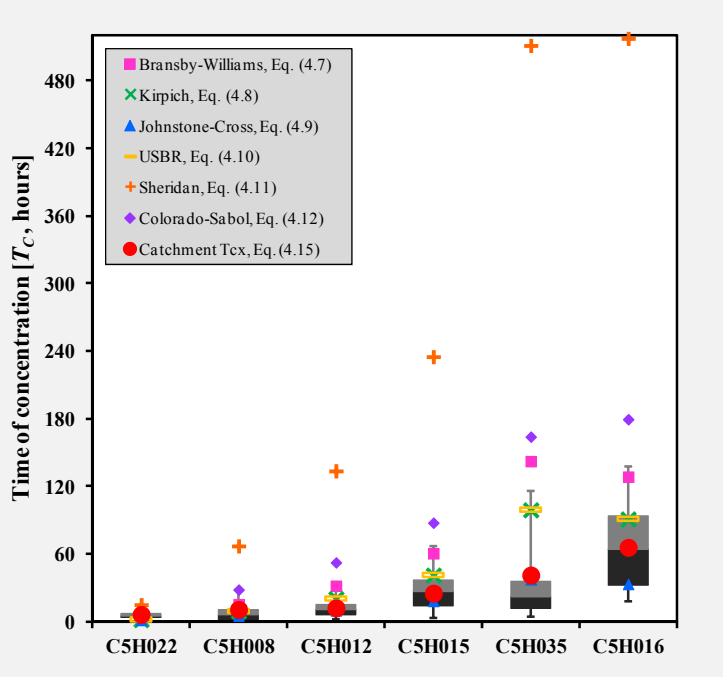

Figure 4.11 Box plots of T_{Cxi} values [Eq. (4.14)] and super-imposed data series values of the catchment T_{Cx} [Eq. (4.15)] and empirical T_C estimates for the six catchments of the Central Interior

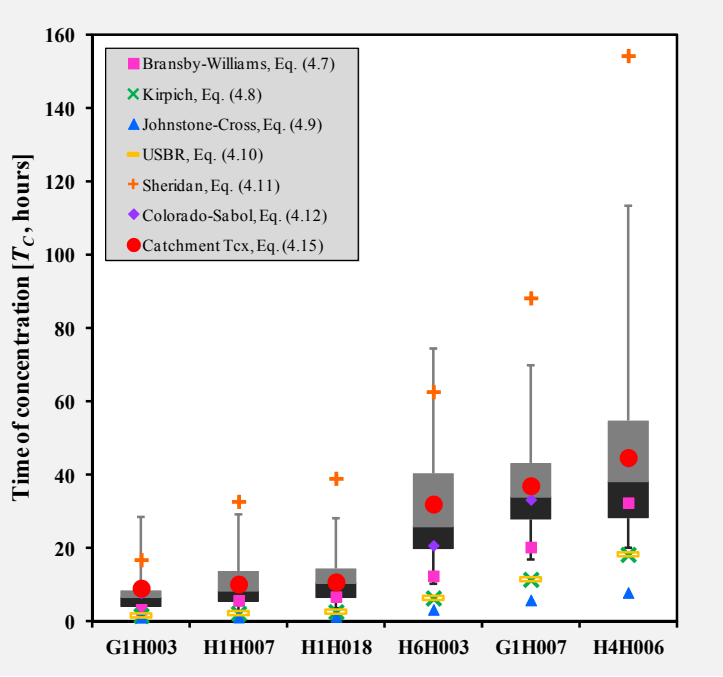

Figure 4.12 Box plots of T_{Cxi} values [Eq. (4.14)] and super-imposed data series values of the catchment T_{Cx} [Eq. (4.15)] and empirical T_C estimates for the six catchments of the SWC region

In practical terms, the high T_{Cxi} variability evident in these figures would not be easily incorporated into design hydrology. Consequently, a reasonable catchment T_{Cx} value for design purposes and for the calibration of empirical equations should be a convergence value based on the similarity of the results obtained when Eqs. (4.14) and (4.15) are used in combination. As mentioned before, the results based on these equations were compared in each catchment to establish their degree of association, but the results based on Eq. (4.15) were accepted as the most representative catchment T_{Cx} values (shown as red circle markers in Figures 4.11 and 4.12).

Furthermore, it is clearly evident from Figures 4.11 and 4.12 that the high variability in T_{Cxi} estimation is directly related and amplified by the catchment area, with variations up to ± 800 %. The Bransby-Williams [Eq. (4.7)] and Colorado-Sabol [Eq. (4.12)] equations are the only equations which includes the catchment area as an independent predictor variable; therefore it is not surprising that it demonstrated poorer results in the larger catchment area ranges (A > 5 000 km²) of the Central Interior as opposed to the medium catchment area ranges (50 < A ≤ 3 000 km²) of the SWC region. The latter catchment area ranges is outside the maximum catchment areas used in the calibration of these equations. It could also be argued that the differences are because the Bransby-Williams equation [Eq. (4.7)] was derived from Australian rural catchments which are decidedly different to South African catchments and with catchment areas used in the calibration limited to ± 130 km². However, the Colorado-Sabol equation [Eq. (4.12)] which was derived for catchment areas up to 5 150 km², demonstrated slightly poorer results when compared to Eq. (4.7) in the Central Interior with predominantly larger catchments areas. Therefore, the inclusion of the catchment area as an independent variable is not the obvious reason why results are poorer in this case, but it actually confirms that when different empirical equations are applied outside the bounds of their original developmental regions, that their calibration exponents are no longer valid. In addition, all the independent variables contained in Eqs. (4.7) to (4.12) are generally regarded as both conceptually and physically acceptable predictors, *i.e.* the shape (A), distance (L_C and L_{CH}) and slope (S_{CH}) predictors would arguably provide a good indication of catchment storage effects (attenuation and travel time). The latter re-emphasises that the poorer results obtained are not due to the use of inappropriate catchment response variables, but could be attributed to the use of empirical equations without local correction factors being applied.

The Goodness-of-Fit (GOF) statistics for the test of these equations in the 12 catchments are listed in Tables 4.5 and 4.6 respectively. In considering the overall average GOF statistics as listed in Tables 4.5 and 4.6, the six empirical equations showed different biases when compared to the 'direct measurement' of T_{Cx}.

Table 4.5 GOF statistics for the test of channel flow T_C estimation equations compared to the direct estimation of T_{Cx} from observed streamflow data in the Central Interior

Equations	GOF statistics					
	Mean observed T_{Cx} [h]	**Mean estimated T_C [h]**	**Standard bias statistic [Eq. (4.16), %]**	**Mean error [h]**	**Maximum error [h]**	**Standard error [h]**
Bransby-Williams [Eq. (4.7)]	26.7	63.4	107.0	36.7	101.1	10.6
Kirpich [Eq. (4.8)]	26.7	43.5	37.1	16.8	57.8	10.3
Johnstone-Cross [Eq. (4.9)]	26.7	17.4	-39.7	-9.3	-32.6	11.2
USBR [Eq. (4.10)]	26.7	43.5	37.2	16.9	57.9	10.3
Sheridan [Eq. (4.11)]	26.7	246.3	728.8	219.6	469.9	8.8
Colorado-Sabol [Eq. (4.12)]	26.7	86.2	205.9	59.5	122.7	7.7

In the Central Interior (Table 4.5) only the Johnstone-Cross equation [Eq. (4.9)] underestimated the T_{Cx} with a relatively low bias (-39.7 %) and mean error (-9.3 hours). The Kirpich [Eq. (4.8)] and USBR [Eq. (4.10)] equations, with almost identical results, provided the smallest positive biases (≈ 37.1 % each) and associated positive mean errors of ≈ 16.8 hours. The similarity of the latter results could be ascribed to the fact that Eq. (4.10) (USBR, 'recommended' for use in South Africa) is essentially a modified version of the Kirpich equation [Eq. (4.8)].

Table 4.6 GOF statistics for the test of channel flow T_C estimation equations compared to the direct estimation of T_{Cx} from observed streamflow data in the SWC region

Equations	GOF statistics					
	Mean observed T_{Cx} [h]	**Mean estimated T_C [h]**	**Standard bias statistic [Eq. (4.16), %]**	**Mean error [h]**	**Maximum error [h]**	**Standard error [h]**
Bransby-Williams [Eq. (4.7)]	24.1	13.6	-46.1	-10.5	-19.5	6.2
Kirpich [Eq. (4.8)]	24.1	7.2	-73.4	-16.8	-26.4	6.1
Johnstone-Cross [Eq. (4.9)]	24.1	3.6	-86.0	-20.5	-36.8	5.0
USBR [Eq. (4.10)]	24.1	7.2	-73.4	-16.8	-26.4	6.1
Sheridan [Eq. (4.11)]	24.1	65.7	173.4	41.6	109.5	7.0
Colorado-Sabol [Eq. (4.12)]	24.1	21.2	-9.4	-2.8	-11.2	4.8

In contradiction to the Central Interior results as contained in Table 4.5, the Bransby-Williams [Eq. (4.7)] and Colorado-Sabol [Eq. (4.12)] equations provide the best estimates

in the SWC region (Table 4.6), with biases of ≤ 46.1 % and associated mean errors of ≤ 10.5 hours. However, all the mean error results must be clearly understood in the context of the actual travel time associated with the size of a particular catchment, since in the latter region, some of the catchments have average T_{Cx} values < 10 hours.

On average, all the other empirical equations, except the Johnstone-Cross equation [Eq. (4.9)], overestimated the T_{Cx} in the Central Interior (Table 4.5) with maximum absolute errors up to 470 hours, while the opposite is evident from Table 4.6 (SWC region). In the latter region, T_{Cx} was underestimated in all cases, except for Eq. (4.11). However, the poorest results in both the Central Interior and SWC region are also demonstrated by Eq. (4.11), with maximum absolute errors of between 110 hours and 470 hours. Typically, the large errors associated with the Sheridan equation [Eq. (4.11)] could be ascribed to the inclusion of only one independent variable (*e.g.* main watercourse length) to accurately reflect the catchment T_{Cx}.

4.7 Conclusions

This chapter demonstrates the estimation of T_C using direct and indirect estimation procedures with observed streamflow data and empirical equations respectively. Empirical equations applicable to the overland flow regime were implemented on a conceptualised urban catchment, while both a direct estimation method and empirical equations applicable to channel flow were implemented on two other case study areas. The results clearly display the wide variability in T_C estimates using different equations. In the estimation of overland flow, the variability and inconsistencies demonstrated are most likely due to the fact that the characteristics of the five different flow retardance categories and associated slope-distance classes considered are decidedly different from those initially used to derive and calibrate the relevant equations. In general, the variability and inconsistencies witnessed in the channel flow regime can be ascribed to the equations being applied outside the bounds of their original developmental regions without the use of local correction factors. However, the fact that either improved or poorer results were obtained with a specific empirical equation in either the Central Interior or SWC region, also confirm that the results obtained are not due to the use of inappropriate independent predictor variables to estimate the catchment response time. The latter could rather be ascribed to the differences in catchment geomorphology. In addition, it could also be

argued that the wide variability and inconsistencies are further exacerbated by the discrepancies in the T_C definitions and estimation procedures found in the literature.

The direct estimation procedure considering both the use of an average catchment T_{Cx} value based on the event means of Eq. (4.14) and a linear catchment response function [Eq. (4.15)] proved to be an objective and consistent approach to estimate observed T_{Cx} values by using only streamflow data. In using the latter direct estimation procedure, the validity of the approximation $T_C \approx T_P$ was also confirmed to be sufficiently similar at a medium to large catchment scale. In order to accommodate the high variability and uncertainty involved in the estimation of T_C, it is recommended that for design hydrology and for the calibration of empirical equations, T_{Cx} should be estimated using the proposed direct estimation procedure. Ultimately, these observed T_{Cx} values can be used to develop and calibrate new, local empirical equations that meet the requirement of consistency and ease of application, *i.e.* including independent predictor variables (*e.g.* A, L_C, L_{CH} and S_{CH}) that are easy to determine by practitioners when required for future applications in ungauged catchments. In order to overcome the limitations of an empirical equation calibrated and verified in a specific region, the proposed methodology should also be expanded to other regions, followed by regionalisation.

In conclusion, the results from this chapter indicate that estimates of catchment response time are inconsistent and vary widely as applied in current flood hydrology practice in South Africa. Therefore, if practitioners continue to use these inappropriate time parameter estimation methods, this would limit possible improvements when both event-based design flood estimation methods and advanced stormwater models are used, despite the current availability of technologically advanced input parameters in these methods/models. In addition, not only will the accuracy of the above methods/models be limited, but it will also have an indirect impact on hydraulic designs, *i.e.* underestimated T_C values would result in over-designed hydraulic structures and the overestimation of T_C would result in under-designs.

In the next chapter, the use of a new approach to estimate catchment response parameters, as an alternative and improvement to the traditional simplified convolution process used between rainfall and runoff time variables, is further developed and assessed.

5. DIRECT ESTIMATION OF CATCHMENT RESPONSE TIME PARAMETERS IN MEDIUM TO LARGE CATCHMENTS USING OBSERVED STREAMFLOW DATA

This chapter is based on the following paper:

Gericke, OJ and Smithers, JC. 2015a. Direct estimation of catchment response time parameters in medium to large catchments using observed streamflow data. *Hydrological Processes* **[Manuscript submitted]**.

5.1 Abstract

In small catchments, a simplified convolution process between a single observed hyetograph and hydrograph is generally used to estimate time parameters such as the time to peak (T_P), time of concentration (T_C) and lag time (T_L). However, such simplification is neither practical nor applicable in medium to large heterogeneous catchments where antecedent moisture from previous rainfall events and spatially non-uniform rainfall hyetographs can result in multi-peaked hydrographs. In addition, the paucity of rainfall data at sub-daily timescales further limits the reliable estimation of catchment responses using observed hyetographs and hydrographs at a medium to large catchment scale. This chapter presents the development of a new and consistent approach to estimate catchment response times, expressed as the time to peak (T_{Px}) obtained directly from observed streamflow data. The relationships between catchment response time parameters and a conceptualised triangular-shaped hydrograph approximation and linear catchment response functions are investigated in four climatologically different regions of South Africa. Flood event characteristics using primary streamflow data from 74 flow-gauging stations were extracted and analysed to derive unique relationships between peak discharge, baseflow, direct runoff and catchment response time in terms of T_{Px}. The T_{Px} values are estimated from observed streamflow data using three different methods: (i) duration of total net rise of a multi-peaked hydrograph, (ii) triangular-shaped direct runoff hydrograph approximations, and (iii) linear catchment response functions. The results show that for design hydrology and for the derivation of empirical equations to estimate catchment response times, the catchment T_{Px} should be estimated from both the use of an average catchment T_{Px} value computed using either Methods (i) or (ii) and a linear catchment response function as used in Method (iii). The use of the different

methods in combination is not only practical, but is also objective and has consistent results.

Keywords: *baseflow; catchment response time; direct runoff; hydrograph; large catchments*

5.2 Introduction

The inherent procedural limitations associated with the traditional simplified convolution process used between rainfall and runoff time variables to estimate time parameters were discussed and highlighted in Chapters 1 to 4. In addition, the difficulty in estimating catchment rainfall for medium to large catchments, as well as the relatively few catchment response time studies conducted in medium to large catchments internationally, were also highlighted. All the above-mentioned problems emphasise the need for the development of an alternative approach to estimate response times for medium to large catchments using only observed streamflow data. In order to develop relationships to estimate catchment response times in ungauged catchments, it is necessary to estimate the catchment response times from gauged catchments. Typically, the observed time parameters obtained from this research could be used to derive empirical time parameter equations by using multiple regression analysis to establish the unique relationships between observed response times and key climatological and geomorphological catchment variables. This will enable the estimation of consistent catchment response times at a medium to large catchment scale.

The objective of this chapter is to develop a new and consistent approach to estimate catchment response times in medium to large catchments (20 km² to 35 000 km²), expressed as the time to peak (T_{Px}), using only observed streamflow data. This is done by investigating the relationship between time parameters and the relevance of conceptualised triangular-shaped direct runoff hydrograph approximations and linear catchment response functions in four climatologically different regions of South Africa. The assumptions used in the research are discussed in the next section. An overview of the location and characteristics of the study area is then presented, and this is followed by the methodology developed for the research. The results are then presented, followed by a discussion and conclusions.

5.3 Research Assumptions

This research is based on the following assumptions:

(a) **The conceptual T_C equals T_P:** The conceptual T_C is normally defined as the time required for the entire catchment to contribute runoff at the catchment outlet, *i.e.* the time taken to flow to the outlet from the furthest point in the catchment, while T_P is defined as the time interval between the start of effective rainfall and the peak discharge of a single-peaked hydrograph (Kirpich, 1940; McCuen *et al.*, 1984; McCuen, 2005; USDA NRCS, 2010; SANRAL, 2013). However, this definition of T_P is also regarded as the conceptual definition of T_C (McCuen *et al.*, 1984; USDA SCS, 1985; Linsley *et al.*,1988; Seybert, 2006) and Gericke and Smithers (2014) also showed that $T_C \approx T_P$.

(b) **T_P equals the total net rise of a multiple-peaked hydrograph:** At medium to large catchment scales, Du Plessis (1984) demonstrated that T_{Pxi} as shown in Figure 5.1 and expressed in Eq. (5.1) is equal to the duration of the total net rise of a multi-peaked hydrograph.

$$T_{Pxi} = \sum_{j=1}^{N} t_j \qquad (5.1)$$

where T_{Pxi} = observed time to peak which equals the conceptual T_C for individual flood events [hours],

t_j = duration of the total net rise (excluding the in-between recession limbs) of a multiple-peaked hydrograph [hours], and

N = sample size.

The approximation of $T_C \approx T_P$ as proposed by Gericke and Smithers (2014) forms the basis for the new approach developed in this chapter to estimate T_{Px} and is based on the definition that the volume of effective rainfall equals the volume of direct runoff when a hydrograph is separated into direct runoff and baseflow. The separation point on the hydrograph is regarded as the start of direct runoff which coincides with the onset of effective rainfall. In other words, the required extensive convolution process normally required to estimate T_P is eliminated, since T_{Px} is estimated directly from the observed streamflow data without the need for rainfall data.

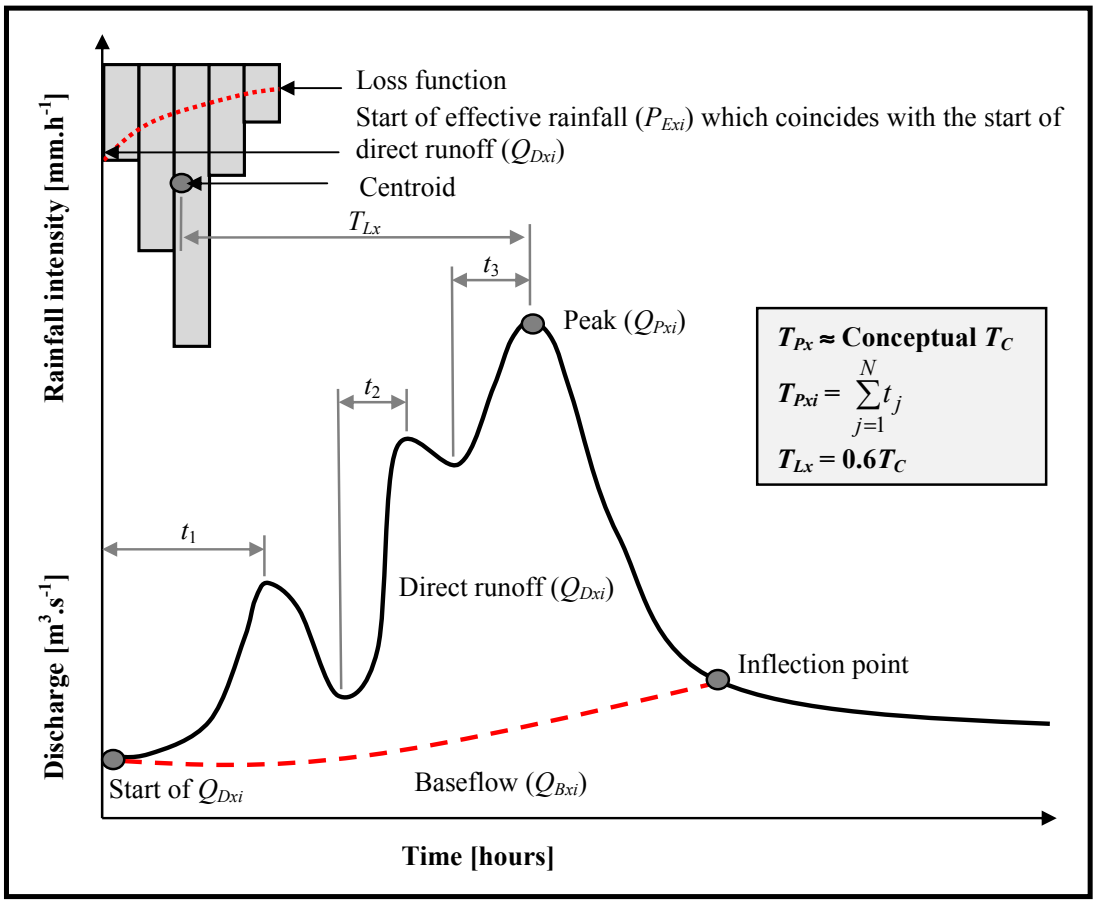

Figure 5.1 Schematic illustrative of the conceptual T_C and T_{Px} relationship for multi-peaked hydrographs (after Gericke and Smithers, 2015)

5.4 Study Area

South Africa, which is located on the most southern tip of Africa (Figure 5.2), is demarcated into 22 primary drainage regions (Midgley *et al.*, 1994), which are further delineated into 148 secondary drainage regions. In this research, 74 study catchments were selected in four climatologically different regions (Figure 5.2), summarised as follows:

(a) **Northern Interior (NI):** Seventeen catchments with areas ranging from 61 km² to 23 852 km² and located in the A2, A3, A5 to A7 and A9 secondary drainage regions (Midgley *et al.*, 1994), were selected in this climatological region which is predominantly characterised by summer rainfall. The Mean Annual Precipitation (*MAP*) ranges from 348 mm to 2 031 mm (Lynch, 2004) and rainfall is characterised as highly variable. The topography is moderately steep with elevations varying from 544 m to 1 763 m and with average catchment slopes

between 3.5 % and 21.6 % (USGS, 2002). A total of 823 observed flood events from 1904 to 2013 were extracted and included in the final analysis.

(b) **Central Interior (CI):** Sixteen catchments with areas ranging from 39 km² to 33 278 km² and extending across the C5 secondary drainage region (Midgley *et al.*, 1994) were selected in this climatological region which is predominantly characterised by convective rainfall during the summer months. The *MAP* ranges from 275 mm to 686 mm (Lynch, 2004). The topography is gentle with elevations varying from 1 021 m to 2 120 m and with average catchment slopes ranging between 1.7 % and 10.3 % (USGS, 2002). A total of 935 observed flood events from 1918 to 2013 were extracted and included in the final analysis.

(c) **Southern Winter Coastal (SWC):** Nineteen catchments with areas ranging from 22 km² to 2 878 km² and located in the G1, G2, G4, H1 to H4 and H6 to H7 secondary drainage regions (Midgley *et al.*, 1994) were selected in this climatological region. The *MAP* ranges from 192 mm to 1 834 mm (Lynch, 2004) and the winter rainfall is classified as either orographic and/or frontal rainfall. The topography is very steep with elevations varying from 86 m to 2 060 m and with average catchment slopes ranging between 2.8 % and 51.9 % (USGS, 2002). A total of 1 291 observed flood events from 1920 to 2013 were extracted and included in the final analysis.

(d) **Eastern Summer Coastal (ESC):** Twenty-two catchments with areas ranging from 129 km² to 28 893 km² and located in the T1, T3 to T5, U2, U4, V1 to V3 and V5 to V6 secondary drainage regions (Midgley *et al.*, 1994) were selected in this climatological region which is predominantly characterised by all year and/or summer rainfall. The *MAP* ranges from 616 mm to 1 564 mm (Lynch, 2004). The topography is very steep with elevations varying from 31 m to 3 149 m and with average catchment slopes ranging between 11 % and 41.4 % (USGS, 2002). A total of 1 090 observed flood events from 1927 to 2013 were extracted and included in the final analysis.

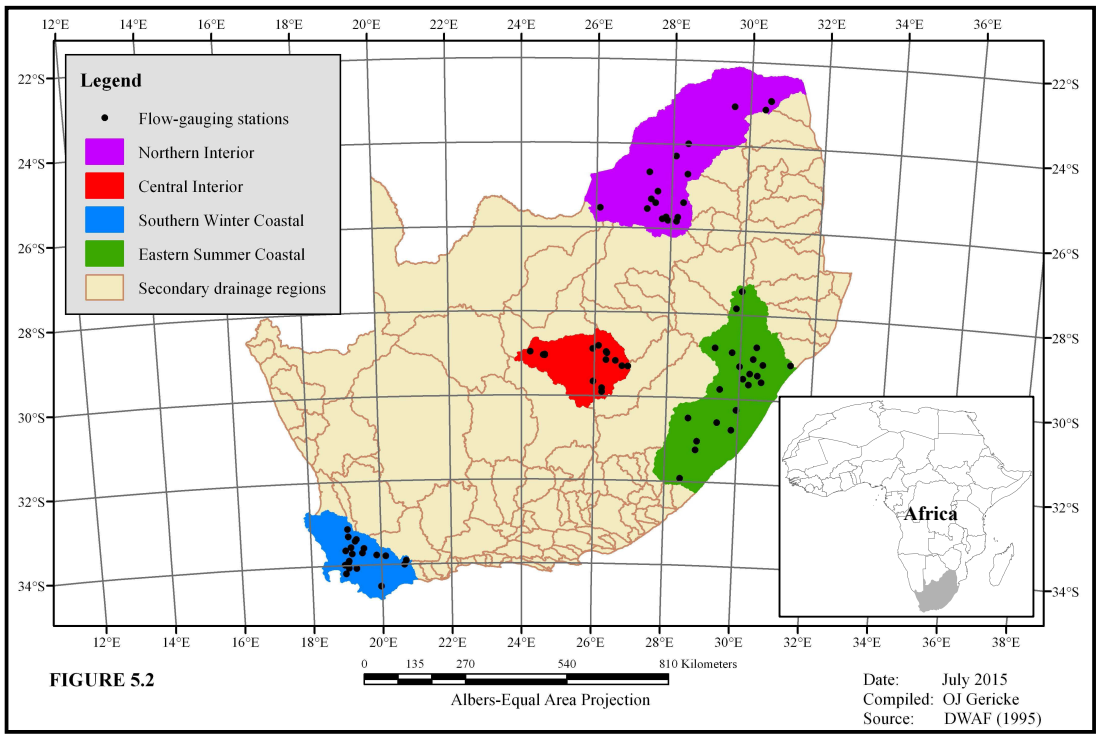

Figure 5.2 Location of the four regions

5.5 Methodology

This section provides the detailed methodology followed to estimate representative catchment T_{Px} values. The methods adopted in the four climatological regions are: (i) to establish a flood database using Department of Water and Sanitation (DWS) primary streamflow data up to 2013 from 74 flow-gauging stations, (ii) to extract the flood event characteristics (*e.g.* peak, volume and duration) of each hydrograph, (ii) to analyse the extracted hydrographs and separate the total hydrographs into direct runoff and baseflow using different recursive filtering methods, and (iii) to estimate direct runoff volumes and the proportion thereof under the rising limb of each hydrograph.

The methodology adopted in the four climatological regions enabled the investigation and analyses of: (i) the variability in individual time to peak (T_{Pxi}) values derived from individual flood events and the use of these to estimate representative catchment T_{Px} values, (ii) the use of triangular-shaped direct runoff hydrograph approximations to represent individual T_{Pxi} values by incorporating variable hydrograph shape parameters which reflect the actual percentage of direct runoff under the rising limb of each individual hydrograph, (iii) the relationship between paired individual observed peak discharge (Q_{Pxi})

and direct runoff volume (Q_{Dxi}) values by assuming a linear catchment response function to estimate the catchment T_{Px}, and (iv) the combined use of a linear catchment response function and triangular-shaped direct runoff hydrograph approximations of individual storms to compute representative estimates of event T_{Pxi} values.

The station numbers of the DWS flow-gauging stations located at the outlet of each catchment are used as the catchment descriptors for easy reference in all the tables and figures.

5.5.1 Establishment of flood database

A flood database was established by evaluating, preparing and extracting primary flow data for the period up to 2013 from the DWS flow database for 74 continuous flow-gauging stations present in the four regions. The screening criteria used to select the stations for analysis in this research include the following:

(a) **Stations common to previous flood studies:** All the flow-gaugings stations used by HRU (1972), Hiemstra and Francis (1979), Alexander (2002), Görgens (2007) and Görgens *et al.* (2007) were considered; resulting in 64 flow-gauging stations meeting this criteria.

(b) **Record length:** Only streamflow records of longer than 20 years were considered; as a result six of the 74 flow-gauging stations did not met the criteria. However, three of the latter six flow-gauging stations met the criteria as stipulated in (a) and (c); hence their inclusion for further analysis. The remaining three stations only met the criteria as stipulated in (c).

(c) **Catchment area:** In addition to above-listed criteria, the catchment areas of the selected flow-gauging stations should cover the range of catchment areas present in the different regions.

(d) **High flows and discharge rating table:** Ideally, the selected flow-gauging stations must be able to record all the flood events at the gauging site, while the rating table must extend to the full range of recorded flood levels. Overall, 92.7 % of the flood hydrographs analysed in the 74 catchments were based on standard DWS discharge

rating tables, *i.e.* no extrapolation procedure was required. However, in cases where the observed flood levels exceeded the maximum rated flood level (H), the rating table was extrapolated by up to 20 % using third-order polynomial regression analysis. The hydrograph shape, especially the peakedness as a result of a steep rising limb in relation to the hydrograph base length, and the relationship between individual Q_{Pxi} and Q_{Dxi} pair values, were used as additional criteria to justify the individual stage extrapolations (H_E) up to a 20 % limit, *i.e.* $H_E \leq 1.2\ H$. Typically, in such an event, the additional volume of direct runoff (Q_{DE}) due to the extrapolation was limited to 5 %, *i.e.* $Q_{DE} \leq 0.05\ Q_{Dxi}$; hence the error made by using larger direct runoff volumes will have little impact on the sample statistics of the total flood volume. This approach is justified in having samples of reasonable size, while the primary focus is on the time when the peak discharge occurs, and not just on the discharge value.

Figure 5.3 illustrates a typical example of an extrapolated rating curve at flow-gauging station H4H006 located in the SWC region. The rated flood levels shown have been extrapolated by up to 20 % [$H_E = 4.57$ m & $Q_P = 1\ 514\ m^3.s^{-1}$]. However, in this particular case, the $H_E \leq 1.2H$ and $Q_{DE} \leq 0.05\ Q_{Dxi}$ criteria were both implemented and resulted in H_E and Q_{DE} extrapolations limited to 12 % and 4 % respectively, with the results of the extrapolation shown in Figure 5.4.

Of the flood hydrographs analysed, only 1 % in NI, 6.4 % in CI, 13.1 % in SWC and 6 % in ESC regions had observed flood levels which exceeded the maximum rated levels. Typically, in using extrapolated discharge values within the range $H_E \leq 1.2\ H$ and $Q_{DE} \leq 0.05\ Q_{Dxi}$ at the 26 flow-gauging stations where the observed levels exceeded the maximum rated levels, the potential error made by using larger direct runoff volumes had little impact on the sample statistics of the total flood volume, especially if the total sample size of the analysed flood hydrographs is taken into consideration.

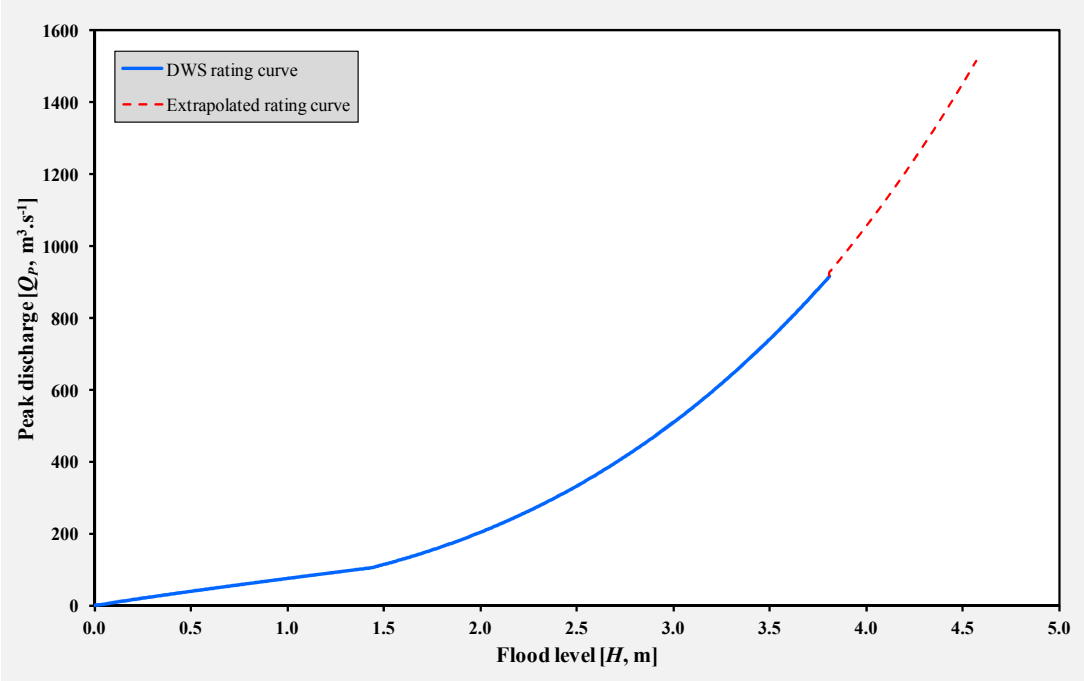

Figure 5.3 Example of an extrapolated rating curve at flow-gauging station H4H006

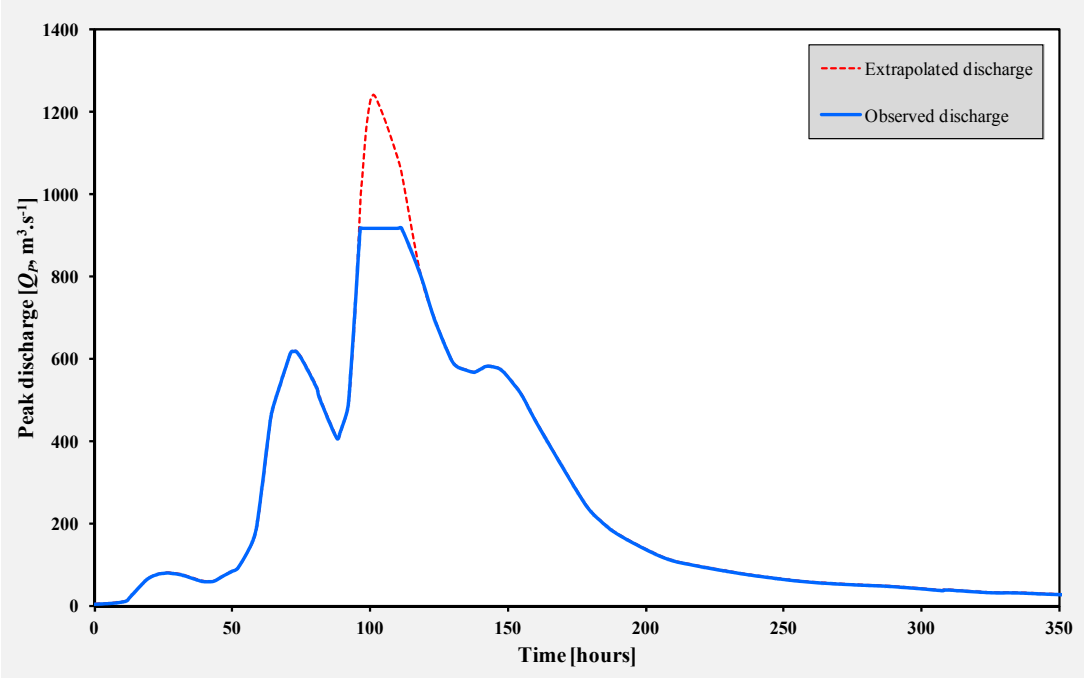

Figure 5.4 Extrapolated discharge at flow-gauging station H4H006 with $H_E \leq 1.12\,H$ and $Q_{DE} \leq 0.04\,Q_{Dxi}$

The details of the 74 flow-gauging stations selected for inclusion in the flood database are listed in Table 5.1. The average data record length of all the flow-gauging stations listed in Table 5.1 is 52 years. The above-listed screening criteria and location of each flow-gauging station in relation to other stations within a particular secondary drainage region were used to objectively select the calibration and verification flow-gauging stations respectively. A total of 47 calibration flow-gauging stations (denoted with * in Table 5.1) were used, whilst the remaining 27 flow-gauging stations were used for independent verification purposes of the empirical T_P equations derived (refer to Chapter 6) for each of the four regions.

Table 5.1 Information of the 74 flow-gauging stations as included in the flood database

Catchment descriptor	Area [km²]	HRU (1972)	Hiemstra and Francis (1979)	Alexander (2002)	Görgens (2007) and Görgens *et al.* (2007)	Record length		
						Start	End	Years
Northern Interior								
A2H005*	774			X		1904	1950	46
A2H006*	1 030	X		X	X	1905	2013	108
A2H007	145			X		1908	1951	43
A2H012	2 555		X	X	X	1922	2013	91
A2H013	1 161	X		X	X	1922	2013	91
A2H015*	23 852		X			1927	1941	14
A2H017*	1 082		X			1927	1937	10
A2H019	6 120				X	1951	2013	62
A2H020*	4 546	X				1951	1971	20
A2H021*	7 482				X	1955	2013	58
A3H001*	1 175	X	X	X		1906	1939	33
A5H004*	636			X	X	1955	2013	58
A6H006	180			X	X	1949	2013	64
A7H003*	6 700			X		1947	1995	48
A9H001	914	X				1912	2006	94
A9H002*	103	X				1931	2000	69
A9H003*	61	X				1931	2013	72
Central Interior								
C5H003*	1 641	X				1918	2013	95
C5H006	676					1922	1926	4
C5H007*	346	X	X	X		1923	2013	90
C5H008*	598			X		1931	1986	55
C5H009	189					1931	1986	55
C5H012*	2 366	X	X	X		1936	2013	77
C5H014*	31 283					1938	2013	75
C5H015*	5 939		X	X		1949	1983	34
C5H016*	33 278					1953	1999	46
C5H018*	17 361					1960	1999	39
C5H022*	39					1980	2013	33
C5H023	185					1983	2008	25
C5H035	17 359					1989	2013	24
C5H039*	6 331					1970	2013	43
C5H053	4 569					1999	2013	14
C5H054	687					1995	2013	18

Table 5.1 (continued)

Catchment descriptor	Area [km²]	HRU (1972)	Hiemstra and Francis (1979)	Alexander (2002)	Görgens (2007) and Görgens *et al.* (2007)	Record length		
						Start	End	Years
Southern Winter Coastal								
G1H002*	186	X	X			1920	1970	50
G1H003	47	X		X		1949	2013	64
G1H004*	69	X		X	X	1949	2007	58
G1H007*	724	X		X		1951	1977	26
G1H008	394	X		X	X	1954	2013	59
G2H008*	22	X		X		1947	1995	48
G4H005*	146			X	X	1957	2013	56
H1H003*	656	X		X		1923	2013	90
H1H006	753		X		X	1950	2013	63
H1H007*	80	X	X	X	X	1950	2013	63
H1H018*	109		X		X	1969	2013	44
H2H003	743	X		X	X	1950	1986	36
H3H001	594			X		1925	1948	23
H4H005*	29			X	X	1950	1981	31
H4H006*	2 878			X	X	1950	1990	40
H6H003*	500			X		1932	1974	42
H6H008	39			X		1964	1992	28
H7H003	458	X				1949	1992	43
H7H004*	28	X	X	X	X	1951	2013	62
Eastern Summer Coastal								
T1H004*	4 923			X	X	1956	2007	51
T3H002*	2 102	X	X	X		1949	2013	64
T3H004	1 026	X		X		1947	2013	66
T3H005	2 565	X			X	1951	2013	62
T3H006*	4 282				X	1951	2013	62
T4H001*	723	X		X	X	1951	2013	62
T5H001*	3 639	X		X		1931	1979	48
T5H004*	537	X		X		1949	2013	64
U2H005*	2 523			X	X	1950	2013	63
U2H006	338				X	1954	2013	59
U2H011*	176				X	1957	2013	56
U2H012	431	X			X	1960	2013	53
U2H013*	296	X				1960	2013	53
U4H002	317			X		1949	2013	64
V1H004*	446	X				1962	1975	13
V1H009*	195	X			X	1954	2013	59
V2H001*	1 951	X		X		1931	1976	45
V2H002	945	X		X	X	1950	2013	63
V3H005*	677			X	X	1947	1993	46
V3H007	128				X	1948	2013	65
V5H002	28 893			X	X	1956	2013	57
V6H002*	12 854			X		1927	2013	86

* = Flow-gauging stations used for the calibration of Eq. (6.8), Chapter 6

X = Flow-gauging stations used in previous flood studies

5.5.2 Extraction of flood hydrographs

The next stage involved the identification and extraction of complete flood hydrographs from the primary flow data sets. The Flood Hydrograph Extraction Software (EX-HYD) developed by Görgens *et al.* (2007) was used to assist in identifying and extracting complete flood hydrographs. A Hydrograph Analysis Tool (HAT) was also developed in Microsoft Excel to analyse the large number of extracted flood hydrographs. The use of HAT not only reduced the repetitive processing time of hydrograph analysis and baseflow separation, but it also ensured that an objective and consistent approach was implemented. The following flood hydrograph extraction criteria were used to extract the flood hydrographs:

(a) **Truncation levels:** Only flood events larger than the smallest annual maximum flood event on record were extracted. Consequently, all minor events were excluded, while all the flood events retained were characterised as multiple events being selected in a specific hydrological year. This approach resulted in a partial duration series (PDS) of independent flood peaks above a certain level.

(b) **Start/end time of flood hydrographs:** Flood peaks and flood volumes for the same event were obtained by extracting complete hydrographs. Initially, a large number of streamflow data points prior the start of a hydrograph, identified by physical inspection where the flow changes from nearly constant or declining values to rapidly increasing values, were included in order to identify the potential start of direct runoff. Thereafter, it was acknowledged that, by definition, the volume of effective rainfall is equal to the volume of direct runoff. Therefore, when separating a hydrograph into direct runoff and baseflow using a recursive filtering method, the separation point could be regarded as the start of direct runoff which coincides with the onset of effective rainfall. Similarly, the end of a flood event, which is when the direct runoff has subsided to only baseflow, which is not directly related to the causative rainfall for that event, was also determined by using recursive filtering methods. Two different baseflow separation/filtering methods were used and are detailed in the following section.

(c) **Extrapolation of rising and recession limbs to zero baseflow line:** In some cases, due to the nature of the data, the above-mentioned starting point indentified by physical inspection as the lowest recording, did not necessarily coincide with the

baseflow starting point as identified using the recursive filtering methods. In such cases, a similar approach as followed by Görgens *et al.* (2007) was adopted, where a straight vertical line extrapolation from the identified starting point to the zero baseflow line was applied to enable the estimation of direct runoff volumes. This additional volume of runoff introduced, was regarded as negligible, while the differences between flow rates at the 'different' starting points were limited to < 5 %.

A total of 5 625 complete flood hydrographs met the extraction criteria as detailed in Steps (a) to (c) and were considered for further analysis. Due to the nature of the extracted flood hydrographs, it is important to note that the HAT software tool could not automatically deal with all variations in flood hydrographs; hence a measure of user intervention was required, especially when T_{Pxi} was determined for multi-peaked hydrographs. Input to HAT are the extracted flood hydrographs obtained using the EX-HYD software (Görgens *et al.*, 2007), while the output includes the following: (i) start/end date/time of flood hydrograph, (ii) Q_{Pxi} [$m^3.s^{-1}$], (iii) total volume of runoff [Q_{Txi}, m^3], (iv) Q_{Dxi} [m^3], (v) volume of baseflow [Q_{Bxi}, m^3], (vi) baseflow index (BFI), (vii) depth of effective rainfall [P_{Exi}, mm] based on the assumption that the volume of direct runoff equals the volume of effective rainfall and that the total catchment area is contributing to runoff, (viii) T_{Pxi} [computed using Eq. (5.1), hours], and (ix) a summary of results.

The application of two baseflow separation methods to enable the hydrograph parameter analysis, are discussed in the following section.

5.5.3 Analyses of flood hydrographs

A number of methods (*e.g.* graphical, recursive digital filters, frequency-duration and recession analysis) have been proposed in the literature to separate direct runoff and baseflow (Nathan and McMahon, 1990; Arnold *et al.*, 1995; Smakhtin, 2001; McCuen, 2005). The selection or preference for any method will depend on the type and volume of observed data available versus the accuracy required and time constraints. Recursive digital filtering methods are the most frequently used approaches to separate direct runoff and baseflow, despite having no true physical or hydrological basis, but it is objective and reproducible for continuous baseflow separation (Arnold *et al.*, 1995).

According to Smakhtin (2001), the most well-known and widely used recursive filtering methods are those developed by Nathan and McMahon (1990) and Chapman (1999). Smakhtin and Watkins (1997) also adopted the methodology as proposed by Nathan and McMahon (1990) with some modifications in a national-scale study in South Africa.

Hence, based on these recommendations, as well as the need for consistency and reproducibility, the above-mentioned methods were considered in this research. Equation (5.2) as proposed by Nathan and McMahon (1990) was implemented by Smakhtin and Watkins (1997), while Chapman (1999) used Equation (5.3).

$$Q_{Dxi} = \alpha Q_{Dx(i-1)} + \beta(1+\alpha)\left(Q_{Txi} - Q_{Tx(i-1)}\right) \quad (5.2)$$

$$Q_{Dxi} = \left(\frac{(3\alpha-1)}{(3-\alpha)}\right)Q_{Dx(i-1)} + \frac{2}{(3-\alpha)}\left(Q_{Txi} - Q_{Tx(i-1)}\right) \quad (5.3)$$

where Q_{Dxi} = filtered direct runoff at time step i, which is subject to $Q_{Dx} \geq 0$ for time i [$m^3.s^{-1}$],

α,β = filter parameters, and

Q_{Txi} = total streamflow (*i.e.* direct runoff plus baseflow) at time step i [$m^3.s^{-1}$].

Smakhtin and Watkins (1997) established that a fixed α-parameter value of 0.995 is suitable for most catchments in South Africa, although in some catchments, α-parameter values of 0.997 proved to be more appropriate. Hughes *et al.* (2003) also highlighted that a fixed β-parameter value of 0.5 could be used with daily time-step data, since there is more than enough flexibility in the setting of the α-parameter value to achieve an acceptable result. Consequently, a fixed α-parameter value = 0.995 and β-parameter value = 0.5 was used in all the catchments in this chapter. However, in some of the catchments with data sets having sub-daily data with time intervals as short as 12 minutes (especially after the year 2000), the α-parameter value of 0.995 resulted in a too high a proportion of baseflow relative to total flow. In such cases, the average BFI of the pre-2000 data years was used to adjust the baseflow volumes accordingly. Comparable/similar results were obtained by increasing the α-parameter value to 0.997.

An example of typical baseflow separation results at flow-gauging station C5H012 located in the CI is illustrated in Figure 5.5. The data series based on Chapman (1999) uses a fixed α-parameter value of 0.995, while the two data series plots of Smakhtin and Watkins (1997) are based on fixed α-parameter values of 0.995 and 0.997 respectively. This example illustrates the flexibility in setting the α-parameter values, while using a fixed β-parameter value of 0.5. By considering both the recommendations made by Smakhtin and Watkins (1997) and Hughes *et al.* (2003), Eq. (5.2) was used to separate the direct runoff and baseflow.

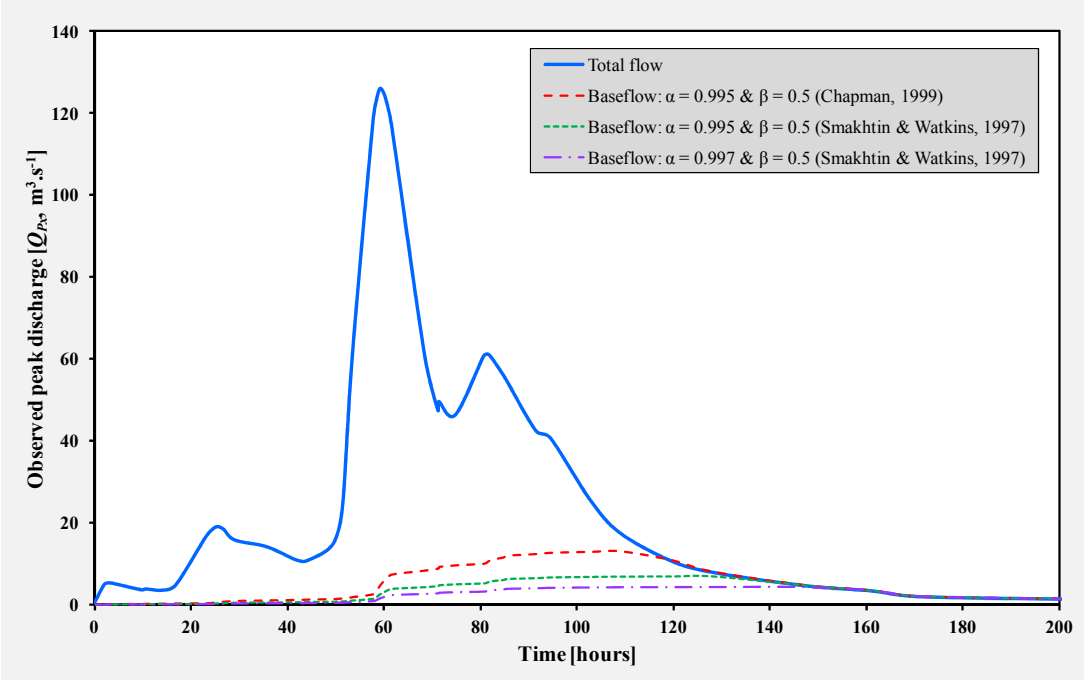

Figure 5.5 Example of the baseflow separation results at flow-gauging station C5H012

The number of flood hydrographs analysed in each catchment were then subjected to a final screening process to ensure that all the flood hydrographs are independent and that the T_{Pxi} estimates are consistent. The final screening process included the following:

(a) The analysed flood hydrographs were visually inspected and initially selected based on hydrograph shape, *e.g.* number and nature of multiple peaks and smoothness of recession limbs.

(b) The remaining flood hydrographs, as selected in Step (a), were then ranked in terms of Q_{Pxi} in a descending order of magnitude in order to check for inconsistencies between Q_{Pxi}, Q_{Dxi} and T_{Pxi} values. The 'inconsistencies' refer to the fact that the direct T_{Cxi} estimations from observed streamflow data could vary significantly and acknowledge that the largest Q_{Pxi} and T_{Cxi} values are associated with the likelihood of the entire catchment receiving rainfall, while smaller T_{Cxi} values could be expected when effective rainfall of high average intensity does not cover the entire catchment.

(c) Thereafter, a triangular approximation of each direct runoff hydrograph based on Eq. (5.4) and illustrated in Figure 5.6 was used to estimate individual T_{Pxi} values for the purpose of comparison with the values computed using Eq. (5.1). Equation (5.4) incorporates a variable hydrograph shape parameter *(K)* to present the actual direct runoff volumes under the rising limb *(Q_{DRi})* of each hydrograph as shown in Figure 5.6. The *K* values are estimated using Eq. (5.4a).

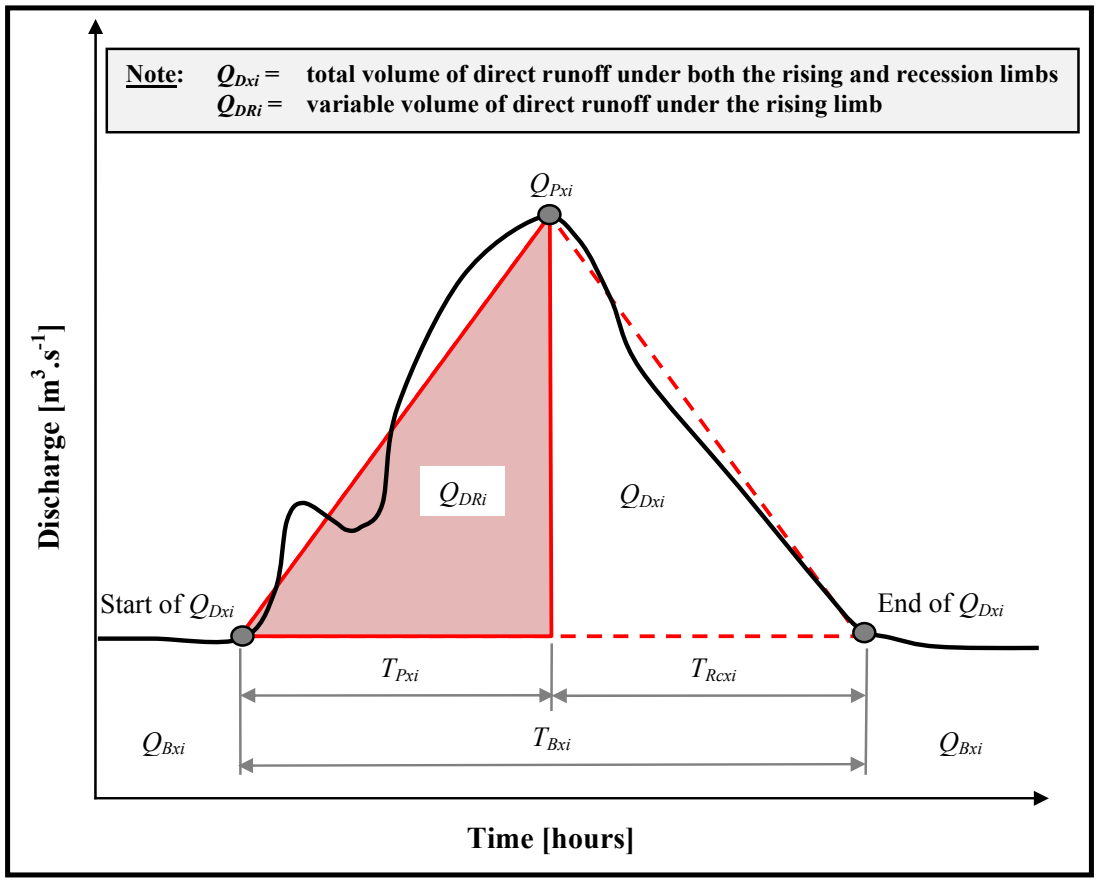

Figure 5.6 Schematic illustrative of the triangular-shaped direct runoff hydrograph approximation [Eq. (5.4)]

Solving for the base length of the triangle, if one unit of time T_{Pxi} equals the variable Q_{DRi} percent of volume (fraction), then the hydrograph base length equals $1/Q_{DRi}$ units of time. Therefore, the associated recession time (T_{Rcxi}) and triangular hydrograph base length (T_{Bxi}) could be estimated using Eqs. (5.4b) and (5.4c) respectively.

(d) The relationship between Q_{Pxi} and Q_{Dxi} was then investigated using the slope of the linear regression between corresponding Q_{Pxi} and Q_{Dxi} values of each flood event in individual catchments to provide an estimation of the catchment T_{Px} value using Eq. (5.5). In other words, the slope of the assumed linear catchment response function in Eq. (5.5) depicts the rate of change between corresponding Q_{Pxi} and Q_{Dxi} values along the linear regression and equals the average catchment T_{Px} value by considering all the individual Q_{Pxi} and Q_{Dxi} values in a particular catchment. As a result, the slope of the linear regression is also expressed in units of time [hours]. The derivation of the linear catchment response function [Eq. (5.5)] is included in Section 5.8.

(e) The final set of flood hydrographs in a specific catchment was regarded as acceptable and free of any outliers when the averages of the individual T_{Pxi} values using both Eqs. (5.1) and (5.4) were similar to the catchment T_{Px} value based on Eq. (5.5). Equation (5.5) is regarded as a very useful 'representative value' to ensure that the averages of individual T_{Pxi} values [using either Eqs. (5.1) and/or (5.4)] provide a good indication of the catchment conditions and sample-mean.

$$T_{Pxi} = K\left[\frac{Q_{Dxi}}{3600xQ_{Pxi}}\right] \tag{5.4}$$

$$K = 2\left[\frac{Q_{DRi}}{Q_{Dxi}}\right] \tag{5.4a}$$

$$T_{Rcxi} = T_{Pxi}\left[\left(\frac{Q_{Dxi}}{Q_{DRi}}\right)-1\right] \tag{5.4b}$$

$$T_{Bxi} = T_{Pxi} + T_{Rcxi} \tag{5.4c}$$

$$T_{Px} = \frac{1}{3600x}\left[\frac{\sum_{i=1}^{N}\left(Q_{Pxi}-\overline{Q_{Px}}\right)\left(Q_{Dxi}-\overline{Q_{Dx}}\right)}{\sum_{i=1}^{N}\left(Q_{Pxi}-\overline{Q_{Px}}\right)^2}\right] \quad (5.5)$$

where T_{Bxi} = triangular hydrograph base length for individual flood events [hours],

T_{Px} = 'average' catchment time to peak based on a linear catchment response function [hours],

T_{Pxi} = triangular approximated time to peak for individual flood events [hours],

T_{Rcxi} = recession time for individual flood events [hours],

Q_{Dxi} = volume of direct runoff for individual flood events [m^3],

Q_{DRi} = volume of direct runoff under the rising limb for individual events [m^3],

$\overline{Q_{Dx}}$ = mean of Q_{Dxi} [m^3],

Q_{Pxi} = observed peak discharge for individual flood events [$m^3.s^{-1}$],

$\overline{Q_{Px}}$ = mean of Q_{Pxi} [$m^3.s^{-1}$],

K = hydrograph shape parameter,

N = sample size, and

x = variable proportionality ratio (default $x = 1$), which depends on the catchment response time parameter under consideration.

The variable proportionality ratio (x) is included in Eqs. (5.4) and (5.5) to increase the flexibility and use of these equations, *i.e.* with $x = 1$, either T_{Px} or T_{Cx} could be estimated by acknowledging the approximation of $T_C \approx T_P$ (Gericke and Smithers, 2014) and with $x = 1.667$, T_L could be estimated by assuming that $T_L = 0.6T_C$, which is the time from the centroid of effective rainfall to the time of peak discharge (McCuen, 2009).

Tables 5.2 to 5.5 provide a summary of the average catchment conditions based on the individual analysis using above-mentioned procedures and the averages of Eqs. (5.1) and (5.4), as well as the catchment T_{Px} values computed using Eq. (5.5) in each catchment under consideration.

Table 5.2 Summary of average catchment results in the Northern Interior

Catchment	Data period	Number of events	Average catchment values							
			Q_{Tx} [10^6 m^3]	Q_{Dx} [10^6 m^3]	Q_{Px} [$m^3.s^{-1}$]	T_{Px} [Eq. (5.1)]	T_{Px} [Eq. (5.4)]	T_{Px} [Eq. (5.5)]	P_{Ex} [mm]	BFI
A2H005	1904/11/16 to 1950/10/01	60	2.1	1.7	14.7	12.8	14.8	14.3	2.2	0.2
A2H006	1905/03/01 to 2013/09/17	100	8.6	6.4	79.8	11.4	11.2	11.2	6.2	0.2
A2H007	1908/07/01 to 1951/08/01	60	0.8	0.7	40.2	4.0	2.4	4.1	4.6	0.2
A2H012	1922/10/01 to 2013/09/18	70	17.3	11.0	190.9	11.9	10.8	12.4	4.3	0.3
A2H013	1922/10/01 to 2013/09/18	60	6.0	3.9	80.3	8.1	7.6	8.0	3.4	0.3
A2H015	1927/10/01 to 1931/09/41	15	12.6	10.7	85.8	28.0	23.9	28.8	0.4	0.2
A2H017	1927/12/08 to 1937/01/31	18	1.4	1.2	29.6	5.9	5.5	6.2	1.1	0.1
A2H019	1951/02/15 to 2013/08/27	60	42.3	33.5	205.1	25.0	27.4	25.5	5.5	0.2
A2H020	1951/02/01 to 1970/11/23	40	28.3	22.8	250.0	21.5	21.1	24.4	5.0	0.2
A2H021	1955/09/01 to 2013/08/27	30	74.8	49.0	145.3	80.7	80.4	79.6	6.5	0.3
A3H001	1906/09/01 to 1939/09/30	50	1.0	0.8	34.0	3.3	3.1	3.3	0.7	0.1
A5H004	1955/12/01 to 2013/08/22	30	19.5	10.3	89.6	18.3	17.1	19.0	16.2	0.5
A6H006	1949/08/01 to 2013/08/22	65	1.9	1.5	21.5	12.7	12.6	12.4	8.3	0.2
A7H003	1947/10/01 to 1995/11/08	40	7.1	5.8	53.6	17.6	20.6	19.9	0.9	0.2
A9H001	1912/12/12 to 2006/04/27	60	15.8	10.8	58.8	32.5	30.7	30.2	11.8	0.3
A9H002	1931/09/20 to 2000/02/23	16	6.5	3.9	66.7	7.3	7.2	7.5	38.2	0.3
A9H003	1931/09/02 to 2013/08/14	49	3.4	1.7	49.3	3.5	3.3	4.3	28.3	0.4

Table 5.3 Summary of average catchment results in the Central Interior

Catchment	Data period	Number of events	Average catchment values							
			Q_{Tx} [10^6 m^3]	Q_{Dx} [10^6 m^3]	Q_{Px} [$m^3.s^{-1}$]	T_{Px} [Eq. (5.1)]	T_{Px} [Eq. (5.4)]	T_{Px} [Eq. (5.5)]	P_{Ex} [mm]	BFI
C5H003	1918/07/01 to 2013/06/26	101	2.1	1.7	32.8	9.1	11.0	11.1	1.0	0.2
C5H006	1922/11/13 to 1926/12/31	14	1.4	1.3	36.0	7.3	6.4	8.2	1.9	0.1
C5H007	1923/10/01 to 2013/08/06	91	1.2	1.0	28.0	6.4	7.3	7.2	2.9	0.1
C5H008	1931/04/01 to 1986/04/01	112	2.2	2.0	44.7	8.0	8.6	10.5	3.3	0.1
C5H009	1931/03/01 to 1986/05/11	13	1.0	0.8	14.3	11.8	13.0	12.7	4.5	0.1
C5H012	1936/04/01 to 2013/02/13	68	3.3	2.3	41.5	11.8	11.0	11.9	1.0	0.3
C5H014	1938/10/17 to 2013/07/25	28	46.7	36.5	168.3	46.2	57.0	56.6	1.2	0.2
C5H015	1949/01/01 to 1983/11/22	90	23.3	21.0	203.1	26.7	24.8	25.0	3.5	0.1
C5H016	1953/02/01 to 1999/03/10	40	31.0	27.0	105.6	65.9	54.7	65.6	0.8	0.1
C5H018	1960/02/23 to 1999/03/15	50	22.8	19.7	105.0	32.3	37.8	39.0	1.1	0.1
C5H022	1980/10/14 to 2013/10/24	69	0.4	0.3	11.5	5.3	5.5	6.1	8.0	0.2
C5H023	1983/06/04 to 2008/03/22	58	0.8	0.6	15.6	6.8	7.7	9.8	3.3	0.2

Table 5.3 (continued)

Catchment	Data period	Number of events	Average catchment values							
			Q_{Tx} [10^6 m^3]	Q_{Dx} [10^6 m^3]	Q_{Px} [$m^3.s^{-1}$]	T_{Px} [Eq. (5.1)]	T_{Px} [Eq. (5.4)]	T_{Px} [Eq. (5.5)]	P_{Ex} [mm]	BFI
C5H035	1989/08/03 to 2013/07/23	20	10.8	9.1	58.9	32.3	41.8	40.7	0.5	0.2
C5H039	1970/11/24 to 2013/08/08	56	34.0	29.2	136.2	44.1	54.7	55.7	4.6	0.1
C5H053	1999/11/29 to 2013/08/08	65	8.3	5.7	93.1	17.3	15.3	16.4	1.3	0.3
C5H054	1995/10/18 to 2013/08/08	60	1.3	0.8	21.3	8.8	8.2	8.7	1.2	0.4

Table 5.4 Summary of average catchment results in the SWC region

Catchment	Data period	Number of events	Average catchment values							
			Q_{Tx} [10^6 m^3]	Q_{Dx} [10^6 m^3]	Q_{Px} [$m^3.s^{-1}$]	T_{Px} [Eq. (5.1)]	T_{Px} [Eq. (5.4)]	T_{Px} [Eq. (5.5)]	P_{Ex} [mm]	BFI
G1H002	1920/12/01 to 1970/10/05	90	8.1	5.8	123.8	8.7	6.4	6.4	31.1	0.3
G1H003	1949/03/21 to 2013/08/27	75	1.6	1.2	20.6	8.3	9.1	9.2	24.4	0.2
G1H004	1949/04/01 to 2007/05/17	77	12.1	9.8	228.9	13.2	10.1	13.3	142.4	0.2
G1H007	1951/04/02 to 1977/05/31	75	50.4	43.9	238.9	36.0	35.0	37.1	60.7	0.1
G1H008	1954/05/01 to 2013/07/25	75	12.2	8.5	139.5	11.9	10.0	10.8	21.6	0.3
G2H008	1947/06/01 to 1995/04/07	106	1.7	1.3	23.7	8.4	8.9	8.9	60.6	0.2
G4H005	1957/03/11 to 2013/08/29	55	15.8	12.5	79.7	31.4	31.5	32.4	79.2	0.2
H1H003	1923/02/22 to 2013/07/15	72	15.1	11.6	115.0	21.2	21.0	21.2	17.7	0.2
H1H006	1950/04/16 to 2013/07/25	90	25.9	18.1	273.6	14.6	15.4	15.1	24.1	0.3
H1H007	1950/04/10 to 2013/07/25	98	10.5	7.6	196.8	10.3	10.2	10.3	95.0	0.3
H1H018	1969/02/26 to 2013/07/26	80	15.0	11.0	323.3	11.1	8.3	10.9	100.9	0.3
H2H003	1950/05/01 to 1986/05/05	45	7.6	5.3	67.9	11.2	12.6	12.8	7.1	0.3
H3H001	1925/11/01 to 1948/05/01	25	5.6	5.2	97.8	11.9	10.1	12.5	8.8	0.1
H4H005	1950/04/01 to 1981/12/21	30	0.8	0.6	12.1	8.7	8.6	8.6	20.5	0.2
H4H006	1950/04/19 to 1990/08/06	80	105.7	78.8	453.5	43.9	41.3	44.8	27.4	0.2
H6H003	1932/10/01 to 1974/11/11	52	16.9	13.1	58.1	31.5	32.1	32.1	26.3	0.2
H6H008	1964/04/18 to 1992/09/07	60	2.6	1.9	41.2	6.1	6.6	6.7	49.2	0.2
H7H003	1949/03/15 to 1992/10/01	70	8.3	7.3	74.7	16.0	16.4	16.5	15.9	0.1
H7H004	1951/05/02 to 2013/06/19	36	1.2	0.8	25.2	7.0	6.6	6.8	29.8	0.3

Table 5.5 Summary of average catchment results in the ESC region

Catchment	Data period	Number of events	Average catchment values							
			Q_{Tx} [10^6 m^3]	Q_{Dx} [10^6 m^3]	Q_{Px} [$m^3.s^{-1}$]	T_{Px} [Eq. (5.1)]	T_{Px} [Eq. (5.4)]	T_{Px} [Eq. (5.5)]	P_{Ex} [mm]	BFI
T1H004	1956/06/04 to 2007/04/04	80	42.9	30.7	271.7	30.8	26.6	30.8	6.2	0.4
T3H002	1949/08/01 to 2013/10/16	67	46.2	26.1	203.6	28.5	27.8	28.8	12.4	0.4
T3H004	1947/09/01 to 2013/10/17	38	18.5	10.1	48.2	35.4	36.7	37.2	9.9	0.4
T3H005	1951/09/20 to 2013/10/17	60	97.0	53.6	385.7	32.1	34.9	34.9	18.4	0.4
T3H006	1951/10/16 to 2013/10/17	75	155.8	92.5	552.0	34.1	39.7	39.6	19.7	0.4
T4H001	1951/09/05 to 2013/10/10	30	37.3	18.7	184.8	24.6	18.7	24.8	25.9	0.5
T5H001	1931/07/19 to 1979/05/07	42	255.3	187.4	444.6	58.5	57.2	57.7	51.5	0.3
T5H004	1949/07/01 to 2013/10/11	30	46.9	28.6	117.8	22.4	28.9	25.7	48.8	0.4
U2H005	1950/11/01 to 2013/06/07	36	68.3	39.7	151.3	30.3	33.4	32.2	15.7	0.4
U2H006	1954/01/04 to 2013/07/30	32	25.5	17.3	50.0	38.9	39.7	35.7	50.1	0.3
U2H011	1957/12/24 to 2013/07/16	40	6.2	3.5	95.6	7.3	6.4	8.8	20.0	0.4
U2H012	1960/08/11 to 2013/08/13	40	7.6	4.4	72.7	6.2	5.8	6.4	10.3	0.4
U2H013	1960/08/10 to 2013/05/07	52	11.9	7.1	58.2	9.6	10.3	9.9	23.3	0.4
U4H002	1949/08/12 to 2013/10/17	30	10.3	6.7	19.9	30.7	37.5	31.1	19.6	0.3
V1H004	1962/04/08 to 1975/12/10	38	19.0	12.6	119.8	8.6	8.6	8.9	28.3	0.3
V1H009	1954/01/15 to 2013/11/04	70	4.4	3.8	150.8	5.9	5.0	5.6	19.2	0.2
V2H001	1931/09/14 to 1976/02/08	62	77.1	60.8	191.5	47.1	45.0	47.1	31.2	0.2
V2H002	1950/06/12 to 2013/10/20	45	62.4	41.6	136.0	57.9	60.6	59.8	43.9	0.3
V3H005	1947/08/06 to 1993/03/31	60	27.2	19.5	72.6	36.7	38.2	37.2	28.8	0.3
V3H007	1948/07/01 to 2013/07/16	58	7.0	4.7	51.1	7.3	9.1	9.1	36.3	0.4
V5H002	1956/08/01 to 2013/09/29	75	635.1	385.8	1430.4	62.5	65.2	65.3	13.0	0.4
V6H002	1927/01/01 to 2013/09/13	30	704.7	456.5	1136.6	62.7	69.3	67.7	35.2	0.3

The T_{Pxi} values computed using the triangular-shaped approximation [Eq. (5.4)] could also be used to compute the estimated peak discharge (Q_{Pyi}) and/or estimated direct runoff volume (Q_{Dyi}) values as shown in Eqs. (5.6) and (5.7) respectively.

$$Q_{Pyi} = K\left[\frac{Q_{Dxi}}{3600xT_{Pxi}}\right] \tag{5.6}$$

$$Q_{Dyi} = 1800T_{Bxi}Q_{Pyi} \tag{5.7}$$

In order to illustrate the use of Eqs. (5.4) to (5.7) at a catchment level, typical results obtained at flow-gauging station A9H002 in the NI are included in Table 5.6.

Table 5.6 Example of triangular direct runoff hydrograph approximations at flow-gauging station A9H002 in the Northern Interior

Q_{Pxi} [$m^3.s^{-1}$]	Q_{Dxi} [10^6 m^3]	Q_{DRi} [10^6 m^3]	T_{Pxi} [Eq. (5.4)]	K [Eq. (5.4a)]	T_{Rxi} [Eq. (5.4b)]	T_{Bxi} [Eq. (5.4c)]	T_{Px} [Eq. (5.5)]	Q_{Pyi} [Eq. (5.6)]	Q_{Dyi} [Eq. (5.7)]
60.1	0.265	0.090	0.8	0.675	1.6	2.5	7.5	60.1	0.265
26.7	5.359	0.422	8.8	0.157	102.7	111.4	7.5	26.7	5.359
54.8	0.827	0.251	2.5	0.607	5.8	8.4	7.5	54.8	0.827
22.0	5.941	0.143	3.6	0.048	146.7	150.3	7.5	22.0	5.941
24.7	2.692	1.308	29.4	0.972	31.1	60.6	7.5	24.7	2.692
278.8	4.336	0.735	1.5	0.339	7.2	8.6	7.5	278.8	4.336
183.4	13.344	1.902	5.8	0.285	34.7	40.4	7.5	183.4	13.344
40.8	4.500	1.856	25.3	0.825	36.0	61.2	7.5	40.8	4.500
26.9	0.576	0.116	2.4	0.402	9.5	11.9	7.5	26.9	0.576
33.0	2.476	0.260	4.4	0.210	37.4	41.7	7.5	33.0	2.476
29.8	5.034	0.581	10.8	0.231	83.0	93.8	7.5	29.8	5.034
21.9	0.316	0.096	2.4	0.610	5.6	8.0	7.5	21.9	0.316
35.0	0.893	0.150	2.4	0.336	11.8	14.2	7.5	35.0	0.893
73.8	1.563	1.034	7.8	1.323	4.0	11.8	7.5	73.8	1.563
49.6	0.483	0.067	0.8	0.279	4.6	5.4	7.5	49.6	0.483
106.3	14.366	1.255	6.6	0.175	68.5	75.1	7.5	106.3	14.366
Avg.	-	-	**7.2**	**0.467**	-	-	**7.5**	-	-

It is evident from Table 5.6 that the triangular hydrograph approximations based on variable shape parameters resulted in $Q_{Pxi} \approx Q_{Pyi}$ and $Q_{Dxi} \approx Q_{Dyi}$ for all the individual flood events under consideration; hence confirming the usefulness of such an approach. On average, the shape parameter (K) equals 0.47 which is equivalent to 23.4 % volume of direct runoff under the rising limb in this particular case.

Furthermore, it is also important to note that the use of Eq. (5.5) provides only a single averaged catchment T_{Px} value as used for design flood estimation. However, corrections factors would be required when individual T_{Pxi} values associated with specific flood events are computed using Eq. (5.5) as an independent approach. Owing to the need for the latter correction factors, in conjunction with the inverse relationship between Q_{Pxi} and catchment response time, the non-linear deviations of observed Q_{Pxi} values from the estimated peak discharge (Q_{Pyi}) values based on a single catchment T_{Px} value must be equated with deviations of the response times from the linearly estimated catchment T_{Px} values in Eq. (5.5). Therefore, in using the T_{Px} values estimated with Eq. (5.5), the Q_{Pyi} values could be computed using Eq. (5.8), while the catchment response deviations are equated in Eq. (5.9):

$$Q_{Pyi} = K\left[\frac{Q_{Dxi}}{3600xT_{Px}}\right] \quad (5.8)$$

$$\frac{T_{Pxi(corrected)}}{T_{Px}} = \frac{Q_{Pyi}}{Q_{Pxi}} \quad (5.9)$$

By substituting Eq. (5.5) into Eq. (5.9), $T_{Pxi\ (corrected)}$ can be computed using Eq. (5.10):

$$T_{Pxi\ (corrected)} = \frac{1}{3600x}\left[\frac{\sum_{i=1}^{N}\left(Q_{Pxi}-\overline{Q_{Px}}\right)\left(Q_{Dxi}-\overline{Q_{Dx}}\right)}{\sum_{i=1}^{N}\left(Q_{Pxi}-\overline{Q_{Px}}\right)^2}\right]\left[\frac{Q_{Pyi}}{Q_{Pxi}}\right] \quad (5.10)$$

Therefore, in acknowledging the use of an assumed linear catchment response function combined with individual storm characteristics, Eq. (5.10) provides estimates of individual T_{Pxi} values. An example of typical results obtained at flow-gauging station A9H002 in the NI is included in Table 5.7 to illustrate the combination and use of Eqs. (5.5) and (5.8) to (5.10) at a catchment level.

Table 5.7 Example of the combination of a linear catchment response function and individual storm characteristics at flow-gauging station A9H002 in the Northern Interior

Q_{Pxi} [$m^3.s^{-1}$]	T_{Pxi} [Eq. (5.4)]	T_{Px} [Eq. (5.5)]	Q_{Pyi} [Eq. (5.8)]	Q_{Pyi} / Q_{Pxi} [Eq. (5.9)]	$T_{Pxi\ (corrected)}$ [Eq. (5.10)]
60.1	0.8	7.5	6.6	0.111	0.8
26.7	8.8	7.5	31.3	1.171	8.8
54.8	2.5	7.5	18.6	0.340	2.5
22.0	3.6	7.5	10.6	0.481	3.6
24.7	29.4	7.5	97.0	3.927	29.4
278.8	1.5	7.5	54.5	0.196	1.5
183.4	5.8	7.5	141.0	0.769	5.8
40.8	25.3	7.5	137.6	3.370	25.3
26.9	2.4	7.5	8.6	0.319	2.4
33.0	4.4	7.5	19.2	0.584	4.4
29.8	10.8	7.5	43.1	1.444	10.8
21.9	2.4	7.5	7.2	0.327	2.4
35.0	2.4	7.5	11.1	0.318	2.4
73.8	7.8	7.5	76.6	1.038	7.8
49.6	0.8	7.5	5.0	0.101	0.8
106.3	6.6	7.5	93.0	0.875	6.6
Avg.	**7.2**	**7.5**	**-**	**-**	**7.2**

The single catchment T_{Px} value [Eq. (5.5)] = 7.5 hours at flow-gauging station A9H002. In Table 5.7 the non-linear peak discharge deviations (Q_{Pyi}/Q_{Pxi}) are applied to Eq. (5.5), as

shown in Eq. (5.9), to result in Eq. (5.10). The big differences between the Q_{Pyi} [Eq. (5.8)] and the observed Q_{Pxi} values are due to the fact that the assumed linear catchment response function [Eq. (5.5)] does not accurately reflect the individual storm characteristics; hence the need for Eq. (5.10) to provide event-specific T_{Pxi} estimates. It is evident that Eqs. (5.4) and (5.10) provide similar T_{Pxi} results when applied at individual flood events, while their average (T_{Px} = 7.2 hours) is in close agreement with the 7.5 hours estimated using Eq. (5.5).

5.6 Results

The flood hydrograph analysis results are presented in the next sub-section.

5.6.1 Analyses of flood hydrographs

The 5 625 analysed flood hydrographs were characterised by a high variability between individual T_{Pxi} responses [Eq. (5.1)] and corresponding Q_{Pxi} values. In general, the largest Q_{Pxi} and T_{Pxi} values are associated with the likelihood of the entire catchment receiving rainfall for the critical storm duration, while smaller T_{Pxi} values could be expected to occur when the effective rainfall does not cover the entire catchment, especially when a storm is centered near the outlet of a catchment. In considering the specific data sets, the smaller T_{Pxi} values which occurred more frequently, have a large influence on the average value and consequently result in an underestimated catchment T_{Px} value. On the other hand, the 'high outliers' with a lower frequency of occurrence, were regarded as acceptable because at medium to large catchment scales the contribution of the whole catchment to peak discharge seldom occurs due to the spatial and temporal distribution of rainfall. In principal, these events are actually required to adhere to the conceptual definition of T_C ($\approx T_P$), which assumes that T_C is the time required for runoff, generated from effective rainfall with a uniform spatial and temporal distribution over the whole catchment, to contribute to the peak discharge at the catchment outlet. The results highlight the high variability of event-based catchment responses which could result in misleading average catchment values which are not representative of the true catchment processes, and confirmed the need for the final screening process, as detailed in the Methodology. Consequently, the analysed flood hydrographs were reduced to 4 139 after the final screening. Figure 5.7 shows the regional observed Q_{Pxi} values versus the T_{Pxi} values derived using Eq. (5.1) for all the catchments in each of the four regions.

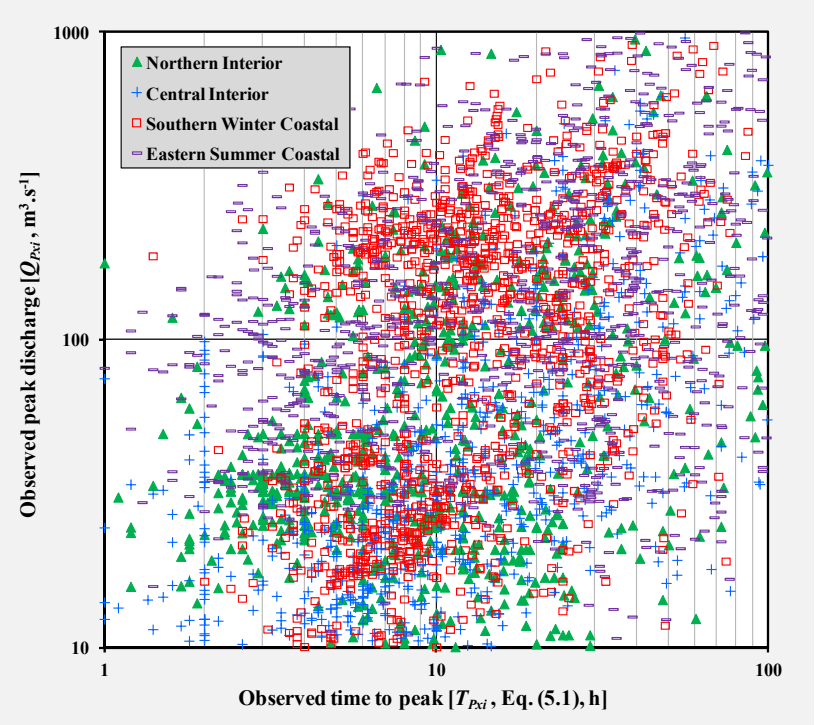

Figure 5.7 Regional Q_{Pxi} versus T_{Pxi} values in the four regions

Despite following the final screening process, the scatter of data in Figure 5.7 still demonstrates the inherent variability of T_{Pxi} at a regional level. It is also evident that the catchments in each region are characterised by a unique Q_{Pxi}-T_{Pxi} relationship which could be ascribed to the differences in their catchment geomorphology and spatial location. This is especially the case in the ESC region, with the Q_{Pxi} values generally larger for corresponding or shorter T_{Pxi} values, while in some cases, the catchment areas (*cf.* Table 5.1) are also smaller.

In using Eq. (5.4) to estimate individual T_{Pxi} values by incorporating a triangular approximated hydrograph shape parameter, the variability of Q_{DRi} under the rising limb of individual hydrographs is evident. In Figure 5.8, a frequency distribution histogram of the Q_{DRi} values expressed as a percentage of the total direct runoff volume (Q_{Dxi}) is shown. The Q_{DRi} values are plotted on the ordinate at 10 % intervals, while the corresponding relative frequencies for each 10 % range are plotted on the abscissa.

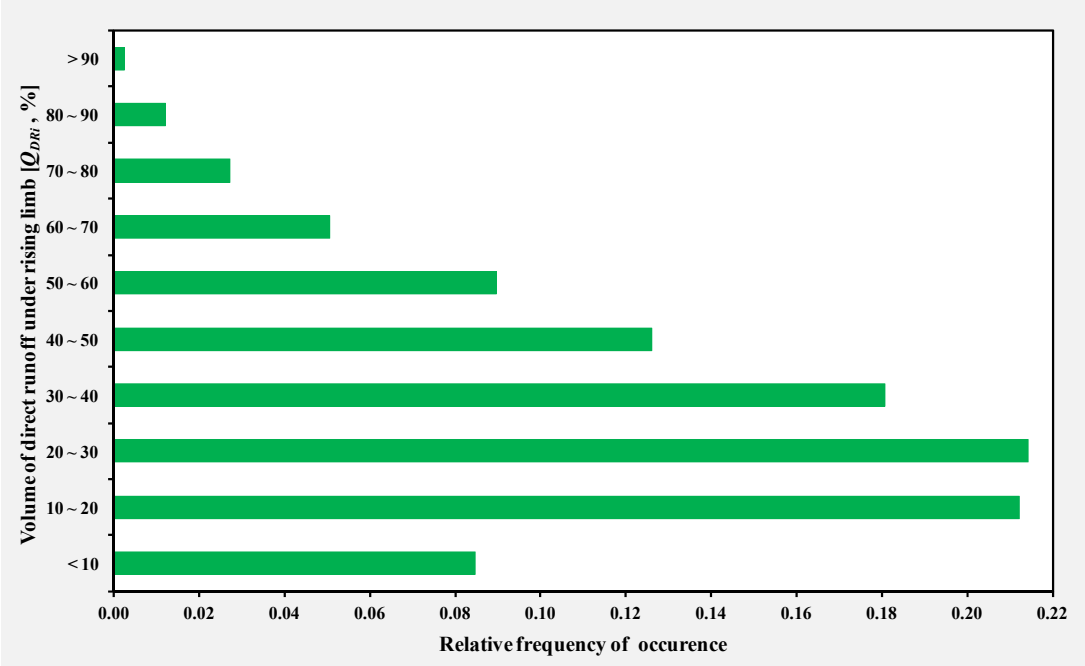

Figure 5.8 Frequency distribution histogram of the Q_{DRi} values (%) based on the 4 139 analysed flood hydrographs

Typically, the Q_{DRi} values varied between 0.4 % and 98.1 % for individual flood hydrographs in the four regions. Taking into consideration that 5 625 individual flood hydrographs were analysed, a few flood events could be characterised by either low (0.4 %) or high (98.1 %) Q_{DRi} values. However, more than 60 % of the Q_{DRi} values are within the 20 ~ 40 % range. At a catchment level, the values of Q_{DRi} ranged on average from 29.3 % to 36.3 % in the four regions. The latter Q_{DRi} percentages are in close agreement with the 37.5 % of the volume under the rising limb generally associated with the conceptual curvilinear unit hydrograph theory (USDA NRCS, 2010).

A scatter plot of the T_{Pxi} values computed using of Eqs. (5.1) and (5.4) respectively for all the catchments under consideration is shown in Figure 5.9, which indicates a relatively high degree of association between the T_{Pxi} values estimated using Eqs. (5.1) and (5.4). In comparing Eqs. (5.1) and (5.4) at a catchment level in the four regions, the r^2 value of 0.69 (based on the 4 139 flood hydrographs) not only confirmed their degree of association, but also the usefulness of Eq. (5.4). The similarity between the results based on Eqs. (5.4) and (5.9) also supports the use of Eq. (5.4) to estimate individual T_{Pxi} values (*cf.* Table 5.7). The regional linear regression plots of the paired Q_{Pxi} and Q_{Dxi} values applicable to the four regions are shown in Figures 5.10 to 5.13.

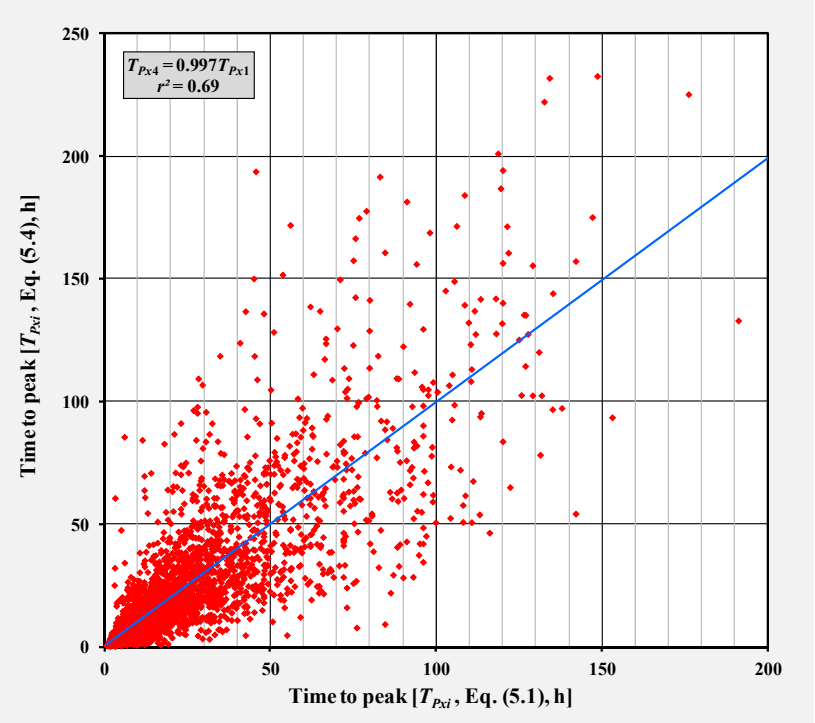

Figure 5.9 Scatter plot of the T_{Pxi} pair values based on the use of Eq. (5.1) and Eq. (5.4)

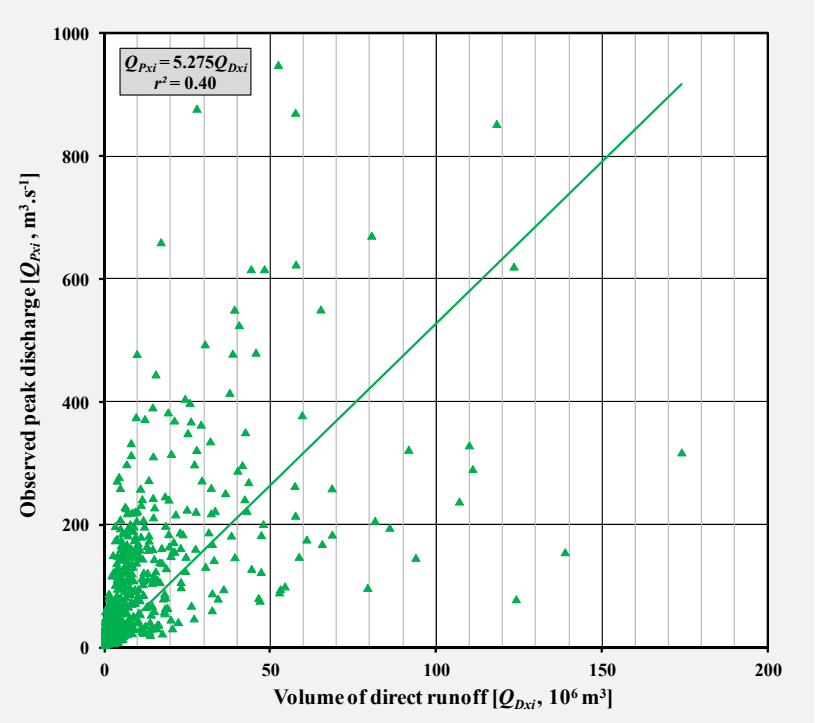

Figure 5.10 Regional Q_{Pxi} versus Q_{Dxi} values in the Northern Interior

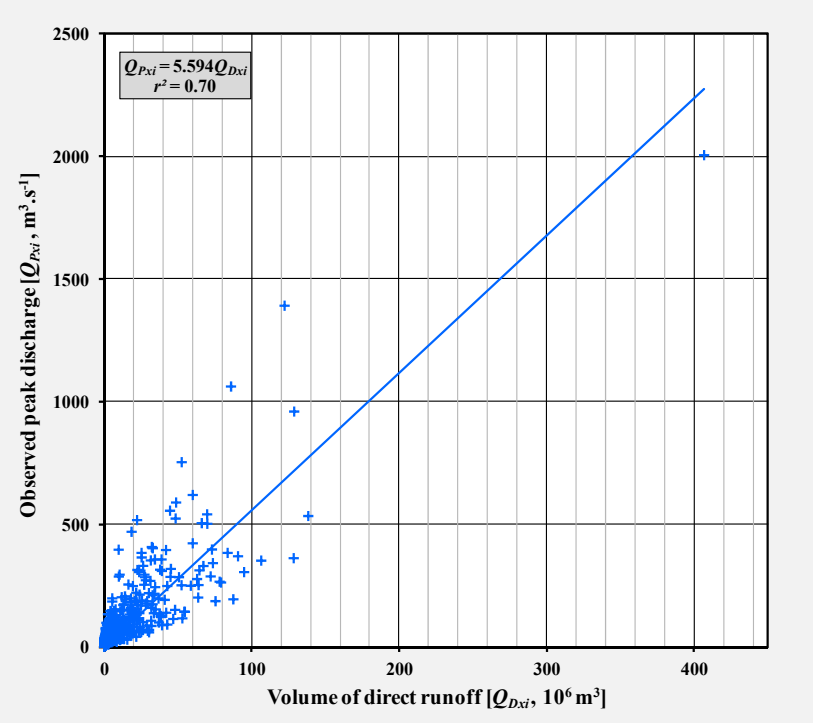

Figure 5.11 Regional Q_{Pxi} versus Q_{Dxi} values in the Central Interior

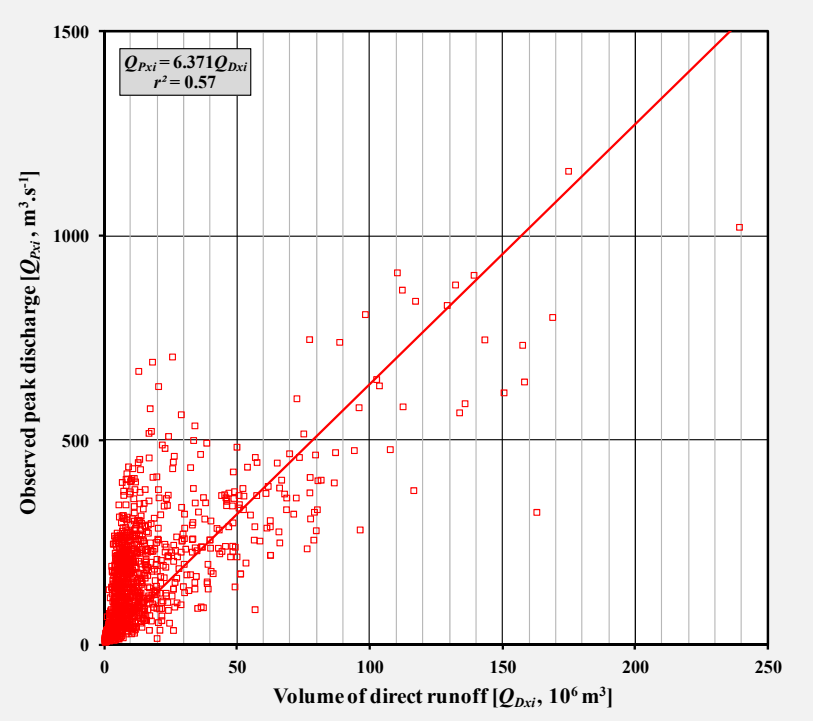

Figure 5.12 Regional Q_{Pxi} versus Q_{Dxi} values in the SWC region

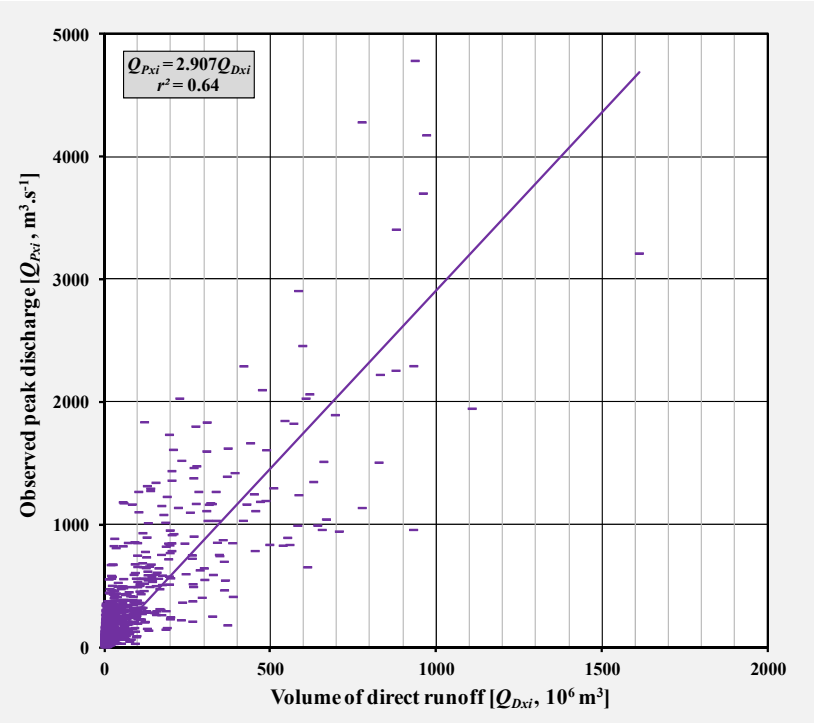

Figure 5.13 Regional Q_{Pxi} versus Q_{Dxi} values in the ESC region

At a regional level (Figures 5.10 to 5.13), the paired Q_{Pxi} and Q_{Dxi} values showed a moderate degree of association with r^2 values between 0.4 and 0.7. However, in using Eq. (5.5) at a catchment level, the overall degree of association between the corresponding Q_{Pxi} and Q_{Dxi} values was much better with r^2 values as high as 0.98 at flow-gauging station C5H053 (Figure 5.14). At a catchment level, the slope of the linear trend-line provides an estimate of the observed catchment T_{Px} value and is computed using Eq. (5.5).

It is also important to note that the catchment T_{Px} values obtained by using Eq. (5.5) showed a high degree of association ($r^2 > 0.97$) when compared to the sample-mean of all the individual responses, *i.e.* $\sum_{i=1}^{N}\left[\frac{Eq.(5.1)}{N}\right]$ and $\sum_{i=1}^{N}\left[\frac{Eq.(5.4)}{N}\right]$. Therefore, Eq. (5.5) is regarded as a useful 'representative value' to ensure that the average of individual T_{Pxi} values is a good reflection of the catchment conditions and sample-mean.

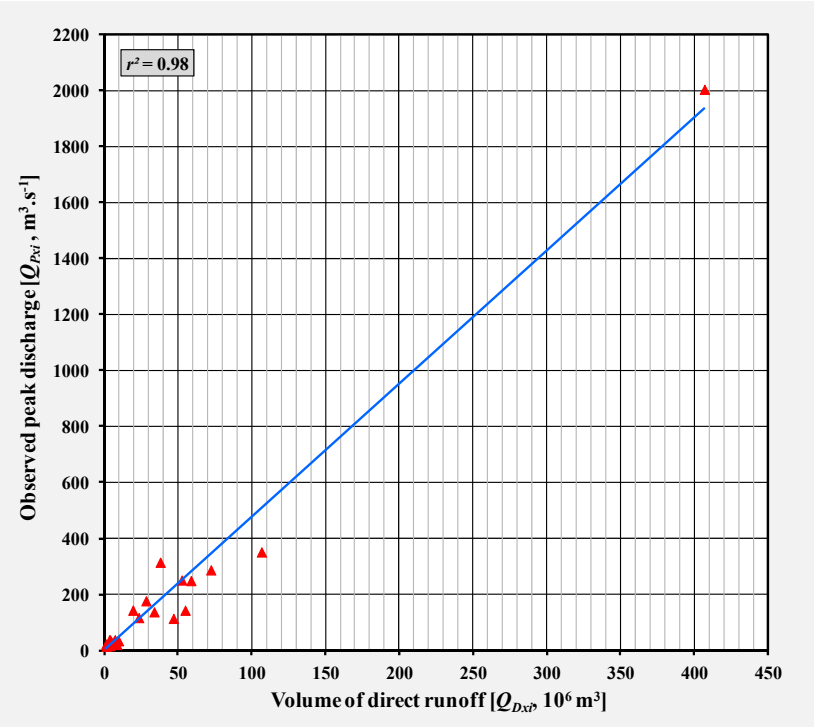

Figure 5.14 Q_{Pxi} versus Q_{Dxi} values at flow-gauging station C5H053 in the Central Interior

The averages of Eqs. (5.1) and (5.4), which showed a high degree of association with Eq. (5.5) [*cf.* Tables 5.2 to 5.5], not only depicted the end of the final screening process, but it also confirmed that catchment response values based on an assumed linear catchment response function could provide results comparable to the sample-mean of all the individual responses times as estimated using Eqs. (5.1) and (5.4).

In Figures 5.15 to 5.18 box plots based on Eq. (5.1) are used to highlight the inherent variability of the T_{Pxi} values estimated directly from the observed streamflow data. In these figures, the whiskers represent the minimum and maximum values computed using Eq. (5.1), the boxes the 25th and 75th percentile values and the change in box colour represent the median value.

The percentage differences between the minimum and maximum T_{Pxi} values range from 45.3 % to 98.9 %. The latter differences are also amplified by the catchment area, and confirm that catchment response at a medium to larger scale is much more variable than in small catchments where a simplified convolution process could apply.

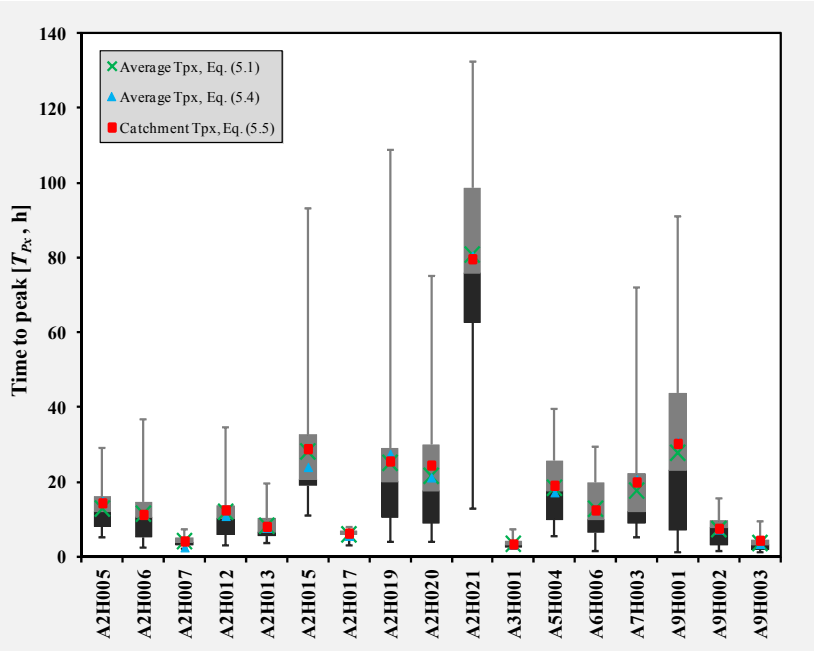

Figure 5.15 Box plots of the T_{Pxi} values obtained directly from observed streamflow data [Eq. (5.1)] and super-imposed data series values of the average T_{Px} [Eqs. (5.1) & (5.4)] and catchment T_{Px} [Eq. (5.5)] estimates for catchments in the Northern Interior

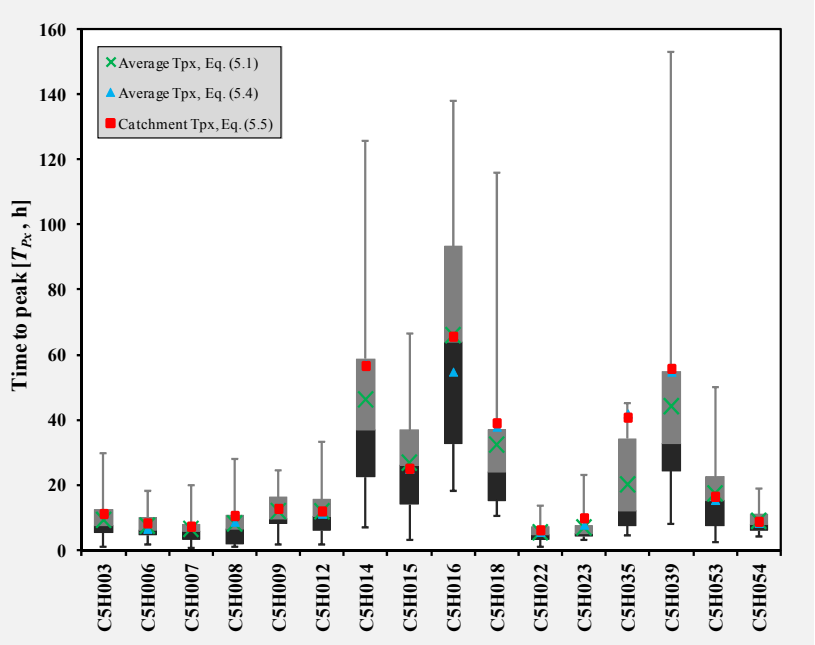

Figure 5.16 Box plots of the T_{Pxi} values obtained directly from observed streamflow data [Eq. (5.1)] and super-imposed data series values of the average T_{Px} [Eqs. (5.1) & (5.4)] and catchment T_{Px} [Eq. (5.5)] estimates for catchments in the Central Interior

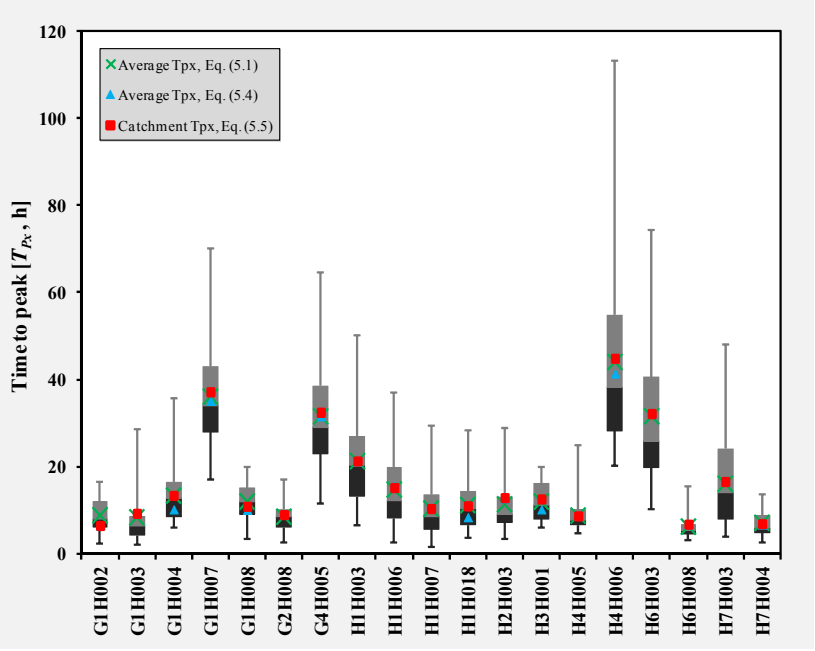

Figure 5.17 Box plots of the T_{Pxi} values obtained directly from observed streamflow data [Eq. (5.1)] and super-imposed data series values of the average T_{Px} [Eqs. (5.1) & (5.4)] and catchment T_{Px} [Eq. (5.5)] estimates for catchments in the SWC region

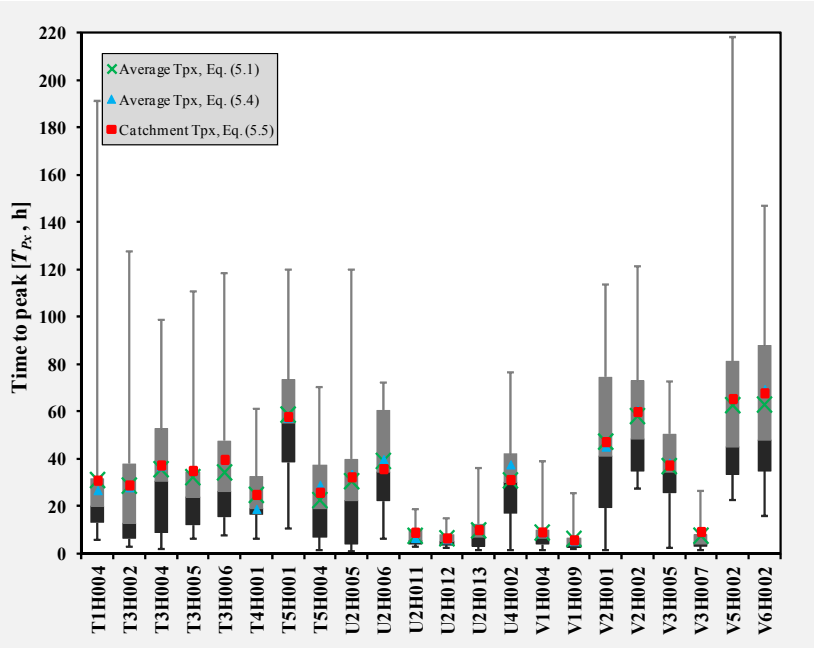

Figure 5.18 Box plots of the T_{Pxi} values obtained directly from observed streamflow data [Eq. (5.1)] and super-imposed data series values of the average T_{Px} [Eqs. (5.1) & (5.4)] and catchment T_{Px} [Eq. (5.5)] estimates for catchments in the ESC region

5.7 Discussion and Conclusions

As highlighted in the Introduction, most of the time parameter estimation methods developed internationally are empirically-based, applicable to small catchments, and based on a simplified convolution process between observed rainfall and runoff data. Similarly, in South Africa, the methodologies of Pullen (1969) and Schmidt and Schulze (1984) were also based on the measured time differences between rainfall and runoff responses and limited to small and/or medium sized catchments.

The limitations of a simplified convolution procedure to estimate catchment response time parameters using time variables measured directly from observed rainfall and runoff data are evident from this research and from the studies conducted by Schmidt and Schulze (1984) and Gericke and Smithers (2014; 2015). In using a simplified convolution process at medium to large catchment scales, the response to rainfall is incorrectly assumed to be uniform, while the spatially non-uniform antecedent soil moisture conditions within the catchment, which are a consequence of both the spatially non-uniform rainfall and the heterogeneous nature of soils and land cover in the catchment, are ignored.

Rainfall and streamflow data are the two primary data sources required when such a simplified convolution process is used to estimate catchment response times. However, the number of rainfall stations internationally has declined steadily over the past few decades. South Africa is no exception, and is now in a similar position with the decline in rainfall station numbers from a high around 1970 to only about half of that in 2004, which is roughly the same number of stations as in 1920 (Pitman, 2011). Furthermore, the rainfall data both in South Africa and internationally, are generally only widely available at more aggregated levels, such as daily and this reflects a paucity of rainfall data at sub-daily timescales, both in the number of rainfall gauges and length of the recorded series. In addition, the paucity of rainfall data and non-uniform distribution, time variables for an individual event cannot always be measured directly from autographic records owing to the difficulties in determining the start time, end time and temporal and spatial distribution of effective rainfall. Problems are further compounded by poorly synchronised rainfall and streamflow recorders which contribute to inaccurate time parameter estimates.

All the above-mentioned limitations, in addition to the difficulty in estimating catchment rainfall for medium to large catchments, emphasise the need for the alternative T_{Px} estimation approach as developed in this chapter. In using the new approach based on the approximation of $T_C \approx T_P$, which is only reliant on observed streamflow data, both the extensive convolution process required to estimate time parameters and the need for rainfall data are eliminated. Furthermore, although streamflow data are internationally less readily available than rainfall data, the data quantity and quality thereof enable the direct estimation of catchment response times at medium to large catchment scales.

In terms of observed streamflow data, the ideal situation is to have flow-gauging stations recording all the flood events at the gauging site, with rating tables that extend to the full range of recorded flood levels. However, the primary purpose of a flow-gauging station is to measure flow volumes and not necessarily extreme flood peak discharges; hence not all observed levels which exceeded the maximum rated levels at a gauging site are available in the DWS database. Therefore, the discharge values extrapolated within the $H_E \leq 1.2\ H$ and $Q_{DE} \leq 0.05\ Q_{Dxi}$ ranges, proved to be sufficiently accurate for the purpose of this research.

The use of the three different methods [Eqs. (5.1), (5.4) and (5.5)] in combination to estimate individual (T_{Pxi}) and catchment (T_{Px}) values proved to be both practical and objective with consistent results. Their combined use also ensured that the high variability of event-based catchment responses is taken into account.

As mentioned in the Methodology, the HAT software did not always process the full range of flood hydrographs when Eq. (5.1) was used and required some user intervention; hence it could be argued that some subjective inconsistencies could have possibly been introduced. Thus, the use of Eq. (5.4) is regarded as being more objective and consistent, while the errors introduced by the triangular approximations are well within the variability associated with the estimation of time parameters. The application of Eqs. (5.4) and (5.9) provided similar results when applied using individual flood events which confirmed that the incorporation of a variable hydrograph shape parameter, as part of a triangular-shaped direct runoff hydrograph approximation, provides a good estimate of catchment response time from observed flood hydrographs. In an unexpected result, the Q_{DRi} volume percentages also proved to be in close agreement with the 37.5 % generally associated with

the conceptual curvilinear unit hydrograph theory which is normally associated with 'small' catchments.

In practical terms, the high variability in individual event-based T_{Pxi} values cannot be easily incorporated into design hydrology practice. Consequently, a reasonable catchment T_{Px} value which can be used for design purposes and in the calibration of empirical equations should be a convergence value based on the similarity of the results obtained when the averages of Eqs. (5.1), (5.4) and Eq. (5.5) are used in combination. Although Eq. (5.1) is regarded as the 'observed T_{Pxi}' of individual flood events, the use of Eq. (5.4) with its triangular-shaped direct runoff hydrograph approximations demonstrated the potential to be used to estimate the catchment response time. This result confirmed that the incorporation of a variable hydrograph shape parameter as part of a triangular-shaped direct runoff hydrograph approximation provides a good estimate of catchment response time estimated from observed flood hydrographs.

Equation (5.5) also ensured that the averages of individual catchment responses using Eqs. (5.1) and/or (5.4) are a good reflection of the catchment conditions and sample-mean. The fact that the catchment T_{Px} values based on Eq. (5.5) provided results comparable to the sample-mean of all the individual response times as estimated using Eqs. (5.1) and (5.4) also confirmed that the catchment response values based on an assumed linear catchment response function [Eq. (5.5)] can provide results comparable to the sample-mean of all the individual response times. The use of the assumed linear catchment response function in combination with the triangular-shaped direct runoff hydrograph approximations of individual storms also provided representative estimates of individual T_{Pxi} values when Eq. (5.9) was used (*cf.* Table 5.7).

Overall, the results obtained, not only displayed the high inherent variability associated with catchment response times, but also confirmed the investigations undertaken. As a consequence, as well as based on the specific results presented in this chapter, it is recommended that for design hydrology and for the calibration of empirical equations to estimate catchment response time, the catchment T_{Px} should be based on a linear catchment response function [Eq. (5.5)]. It is important to note that Eq. (5.5) is only reliant on observed streamflow variables and is therefore not influenced by the limitations and availability of rainfall data in medium to large catchments. Equation (5.5) is also regarded

as an appropriate ‘representative value’ which ensures that the averages of individual event-based catchment responses are a good reflection of the catchment conditions and sample-mean.

Based on the results from this chapter, the current empirical methods used for the estimation of time parameters in medium to large catchments both in South Africa and internationally, should be updated using the catchment response time approaches used in this research. Hence, the objective in the next chapter is therefore to derive empirical T_P equations by using multiple regression analysis to establish the unique relationships between the observed T_{Px} values (estimated in this chapter) and key climatological and geomorphological catchment variables in order to estimate representative catchment T_P values at ungauged catchments.

It is envisaged that the adopted methodologies as included in Chapters 5 and 6 will not only result in both improved and simplified procedures, but ultimately it will result in improved peak discharge estimations at medium to large catchment scales in South Africa.

5.8 Appendix 5.A: Derivation of the Linear Catchment Response Function

Simple linear regression is used as estimation technique to derive the linear catchment response function [Eq. (5.5)] as discussed in Section 5.5.3. The linear regression model determines how the catchment T_{Px} value (dependent variable), on average, is affected by the independent variables, *i.e.* the observed peak discharge [Q_{Pxi}, $m^3.s^{-1}$] and direct runoff volume [Q_{Dxi}, m^3] values as obtained from individual flood hydrographs. In other words, the slope of the assumed linear catchment response function in Eq. (5.5) depicts the rate of change between corresponding Q_{Pxi} and Q_{Dxi} values along the linear regression and equals the average catchment T_{Px} value by considering all the individual Q_{Pxi} and Q_{Dxi} values in a particular catchment. In essence, the best-fit line is fitted through a scatter plot of the Q_{Pxi} and Q_{Dxi} values in such a way that the sum of squared residuals (Z), *i.e.* Z in Q_{Dx}, $\sum\left(Q_{Dxi}-\hat{Q}_{Dxi}\right)^2$ is minimised.

The best-fit line fitted through a scatter plot of the Q_{Pxi} and Q_{Dxi} values is given by:

$$\hat{Q}_{Dxi} = T_{Px}Q_{Pxi}+c \tag{5.A1}$$

By substituting Eq. (5.A1), the sum of squared residuals (Z) is given by:

$$Z = \sum_{i=1}^{N}\left(Q_{Dxi}-T_{Px}Q_{Pxi}-c\right)^2 \tag{5.A2}$$

By minimising Z for the values of c and T_{Px}, then $\partial Z/\partial c = 0$ and $\partial Z/\partial T_{Px} = 0$.

First condition (c = y-intercept = 0):

$$\begin{aligned}\frac{\partial Z}{\partial c} &= \sum_{i=1}^{N}-2\left(Q_{Dxi}-c-T_{Px}Q_{Pxi}\right)\\ &= 2\left(Nc+T_{Px}\sum_{i=1}^{N}Q_{Pxi}-\sum_{i=1}^{N}Q_{Dxi}\right)\\ &= 0\end{aligned} \tag{5.A3}$$

By dividing Eq. (5.A3) with 2 and solve for the y-intercept (c):

$$c = \overline{Q_{Dx}}-T_{Px}\overline{Q_{Px}} \tag{5.A4}$$

Equation (5.A4) indicates that the constant c (y-intercept) is set such that the linear regression line go through the mean of the Q_{Pxi} and Q_{Dxi} values respectively.

Second condition (T_{Px} = slope = 0):

$$\begin{aligned}\frac{\partial Z}{\partial T_{Px}} &= \sum_{i=1}^{N} -2Q_{Pxi}\left(Q_{Dxi} - c - T_{Px}Q_{Pxi}\right) \\ &= \sum_{i=1}^{N} -2\left(Q_{Pxi}Q_{Dxi} - cQ_{Pxi} - T_{Px}{Q_{Pxi}}^{2}\right) \\ &= 0 \end{aligned} \tag{5.A5}$$

By substituting the expression for the *y*-intercept (c) from Eq. (5.A4) into Eq. (5.A5), then:

$$\sum_{i=1}^{N}\left(Q_{Pxi}Q_{Dxi} - Q_{Pxi}\overline{Q_{Dx}} + T_{Px}Q_{Pxi}\overline{Q_{Px}} - T_{Px}{Q_{Pxi}}^{2}\right) = 0 \tag{5.A6}$$

Equation (5.A6) can be separated into two sums:

$$\sum_{i=1}^{N}\left(Q_{Pxi}Q_{Dxi} - Q_{Pxi}\overline{Q_{Dx}}\right) - T_{Px}\sum_{i=1}^{N}\left({Q_{Pxi}}^{2} - Q_{Pxi}\overline{Q_{Px}}\right) = 0 \tag{5.A7}$$

Then, Eq. (5.A7) becomes directly:

$$\begin{aligned} T_{Px} &= \frac{\sum_{i=1}^{N}\left(Q_{Pxi}Q_{Dxi} - Q_{Pxi}\overline{Q_{Dx}}\right)}{\sum_{i=1}^{N}\left({Q_{Pxi}}^{2} - Q_{Pxi}\overline{Q_{Px}}\right)} \\ &= \frac{\sum_{i=1}^{N}\left(Q_{Pxi}Q_{Dxi}\right) - N\overline{Q_{Px}}\,\overline{Q_{Dx}}}{\sum_{i=1}^{N}\left({Q_{Pxi}}^{2}\right) - N\overline{Q_{Px}}^{2}} \end{aligned} \tag{5.A8}$$

Equation (5.A8) can be translated into more intuitively obvious forms, by noting that:

$$\sum_{i=1}^{N}\left(\overline{Q_{Px}}^{2} - Q_{Pxi}\overline{Q_{Px}}\right) = 0 \quad \text{and} \tag{5.A9}$$

$$\sum_{i=1}^{N}\left(\overline{Q_{Px}}\,\overline{Q_{Dx}} - Q_{Dxi}\overline{Q_{Px}}\right) = 0 \tag{5.A10}$$

Therefore, by considering both Eqs. (5.A9) and (5.A10), T_{Px} can be rewritten as the ratio of:

$$\begin{aligned} T_{Px} &= \frac{Cov(Q_{Px}, Q_{Dx})}{Var(Q_{Px})} \\ T_{Px} &= \left[\frac{\sum_{i=1}^{N}\left(Q_{Pxi} - \overline{Q_{Px}}\right)\left(Q_{Dxi} - \overline{Q_{Dx}}\right)}{\sum_{i=1}^{N}\left(Q_{Pxi} - \overline{Q_{Px}}\right)^{2}}\right] \end{aligned} \tag{5.A11}$$

By converting the resulting time units from seconds to hours and incorporating a variable proportionality ratio (default $x = 1$), then Eq. (5.A11) becomes:

$$T_{Px} = \frac{1}{3600x}\left[\frac{\sum_{i=1}^{N}\left(Q_{Pxi} - \overline{Q_{Px}}\right)\left(Q_{Dxi} - \overline{Q_{Dx}}\right)}{\sum_{i=1}^{N}\left(Q_{Pxi} - \overline{Q_{Px}}\right)^2}\right] \tag{5.A12}$$

where T_{Px} = 'average' catchment time to peak based on a linear catchment response function [hours],

Q_{Dxi} = volume of direct runoff for individual flood events [m^3],

$\hat{Q}_{Dxi}$ = predicted value from the least-squares line of Q_{Dxi} on Q_{Pxi} [m^3],

$\overline{Q_{Dx}}$ = mean of Q_{Dxi} [m^3],

Q_{Pxi} = observed peak discharge for individual flood events [$m^3.s^{-1}$],

$\overline{Q_{Px}}$ = mean of Q_{Pxi} [$m^3.s^{-1}$],

c = y-intercept,

N = sample size,

x = variable proportionality ratio (default $x = 1$), which depends on the catchment response time parameter under consideration, and

Z = sum of squared residuals.

It is important to note that Eq. (5.A12) represents Eq. (5.5). As highlighted in Section 5.5.3, the variable proportionality ratio (x) is included in Eq. (5.A12) and/or Eq. (5.5) to increase the flexibility and use thereof, *i.e.* with $x = 1$, either T_{Px} or T_{Cx} could be estimated by acknowledging the approximation of $T_C \approx T_P$ (Gericke and Smithers, 2014) and with $x = 1.667$, T_L could be estimated by assuming that $T_L = 0.6T_C$, which is the time from the centroid of effective rainfall to the time of peak discharge (McCuen, 2009).

6. DERIVATION AND VERIFICATION OF EMPIRICAL CATCHMENT RESPONSE TIME EQUATIONS FOR MEDIUM TO LARGE CATCHMENTS IN SOUTH AFRICA

This chapter is based on the following paper:

Gericke, OJ and Smithers, JC. 2015b. Derivation and verification of empirical catchment response time equations for medium to large catchments in South Africa. *Hydrological Processes* **[Manuscript submitted]**.

6.1 Abstract

Large errors in estimates of peak discharge at a medium to large catchment scale in South Africa can be attributed to the lack of locally derived empirical time parameter estimation methods. The time to peak (T_P), time of concentration (T_C) and lag time (T_L) are internationally the most frequently used catchment response time parameters and are normally estimated using either hydraulic or empirical methods. Almost 95 % of all the time parameter estimation methods developed internationally are empirically-based. This chapter presents the derivation and verification of empirical T_P equations in 74 catchments located in four climatologically different regions of South Africa, with catchment areas ranging from 20 km² to 35 000 km². The objective is to develop unique relationships between observed T_P values and key climatological and geomorphological catchment predictor variables in order to estimate representative catchment T_P values at ungauged catchments. The results showed that the derived empirical T_P equation(s) meet the requirement of consistency and ease of application. Independent verification tests confirmed the consistency, while the statistically significant independent variables included in the regressions provide a good estimation of catchment response times and are also easy to determine by practitioners when required for future applications in ungauged catchments. It is recommended that the methodology used in this research should be expanded to other catchments to enable the development of a regional approach to improve the accuracy of the time parameter estimates, whilst warranting the combination and transfer of information within the identified homogeneous hydrological regions, *i.e.* increase the confidence in using the suggested methodology and equation(s) anywhere in South Africa.

Keywords: *catchment geomorphology; catchment response time; empirical methods; stepwise multiple regression analysis; time parameters*

6.2 Introduction

In Chapter 2 it was highlighted that empirical methods are the most frequently used by practitioners to estimate the catchment response time and almost 95 % of all the methods developed internationally are empirically-based (Gericke and Smithers, 2014). The common practice used in empirical methods to relate time parameters to catchment characteristics using multiple regression analysis necessitate that any derived empirical equation must meet the requirement of statistical significance, consistency and ease of application, *i.e.* inclusion of statistically independent catchment variables that are easy to determine by practitioners in ungauged catchments. However, in order to identify suitable catchment predictor variables, their impact on catchment response time and the resulting runoff must be clearly understood and it is necessary to consider all the catchment processes in a conceptual framework, consisting of three parts: (i) the input (rainfall), (ii) the transfer function (catchment characteristics), and (iii) the output (excess rainfall/direct runoff).

The use of different independent catchment variables in a specific combination to predict the catchment response time could also have a negative impact on estimates. For example, differences in the estimates of the roughness and slope of catchments (overland flow) and main watercourses (channel flow), such as those based on the USBR (1973) equation which considers only the main watercourse characteristics, result in the underestimation of T_C on average by 50 % (McCuen, 2009). Consequently, the resulting peak discharges will be overestimated by between 30 % and 50 % (McCuen, 2009).

Given the sensitivity of design peak discharges to estimated catchment time parameter values as highlighted in the previous chapters, catchment response time at a medium to large catchment scale was also identified as a potential research project to be included as part of the National Flood Studies Programme (NFSP) in South Africa (Smithers *et al.*, 2014). Consequently, this not only served as a motivation for this research, but also emphasised that the continued use of such inappropriate time parameter estimation methods at these catchment scales both in South Africa and internationally, would limit the use of both event-based design flood estimation methods and advanced hydrological models when peak discharges and associated volumes are estimated.

The objectives of this chapter are to (i) derive empirical equations to estimate T_P, (ii) independently assess the performance of the derived equations, (iii) compare the results obtained against the currently used USBR equation, and (iv) assess the impact of different estimates of catchment response time on the estimation of peak discharge. Data from 74 catchments located in four climatological regions of South Africa, with catchment areas ranging from 20 km² to 35 000 km², are used in the research. The focus is on the use of multiple regression analysis to establish the unique relationships between time to peak (T_{Px}) values estimated directly from observed streamflow data (Chapter 5) and key climatological and geomorphological catchment predictor variables in order to estimate representative catchment T_P values at ungauged catchments.

A summary of the study area is contained in the following section, followed by a description of the methodologies adopted and the results obtained. This is then followed by the discussion and conclusions.

6.3 Study Area

South Africa forms the most southern boundary of Africa and is demarcated into 22 primary drainage regions (Midgley *et al*., 1994). The primary drainage regions are further delineated into 148 secondary drainage regions. The 74 study catchments as selected in Chapter 5 are situated in four climatologically different regions, *i.e.* the Northern Interior (NI), Central Interior (CI), Southern Winter Coastal (SWC) and Eastern Summer Coastal (ESC) regions. Please refer to Chapter 5 (*cf.* Table 5.1 and Figure 5.2) for the locality of each region in relation to South Africa and the relevant catchment area ranges.

The layout of each region/catchment, river networks and locality of individual calibration and verification flow-gauging stations are shown in Figures 6.1 to 6.4. The screening criteria as used in Chapter 5 (*cf.* Section 5.5.1, Chapter 5), in conjunction with the location of each flow-gauging station in relation to other stations within a particular secondary drainage region, were used to objectively select the calibration and verification flow-gauging stations respectively. A total of 47 calibration flow-gauging stations were used, while the remaining 27 flow-gauging stations are used in this chapter to independently verify the derived empirical T_P equations.

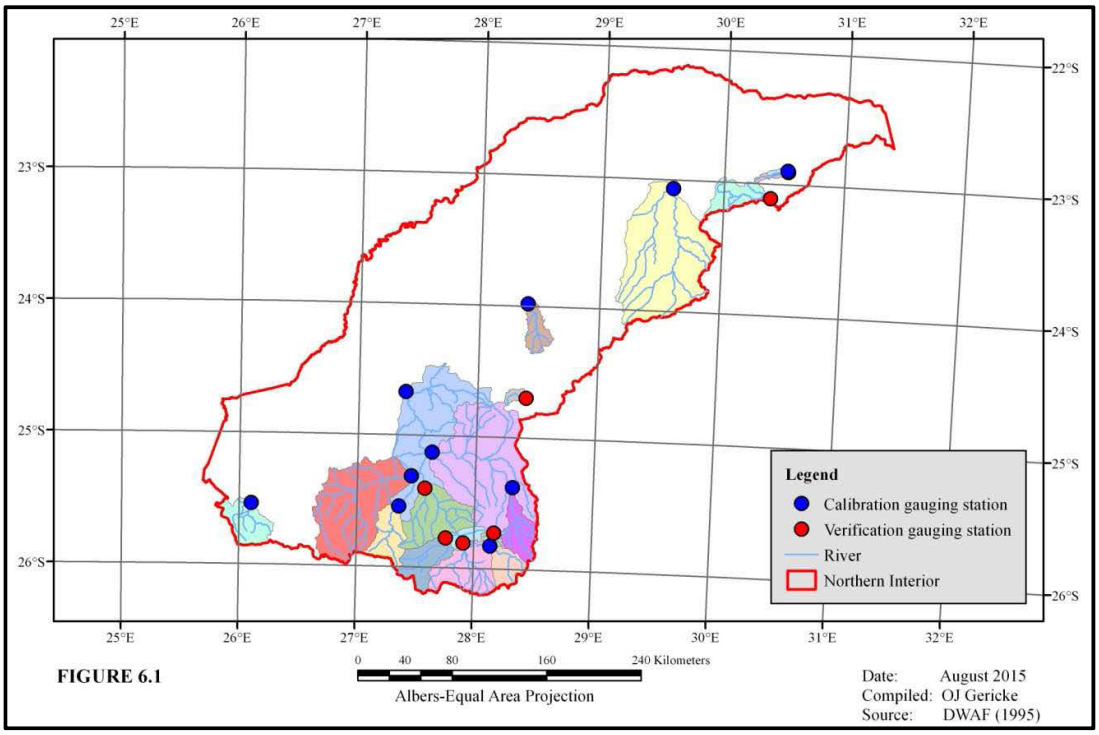

Figure 6.1 Layout and river network of the Northern Interior

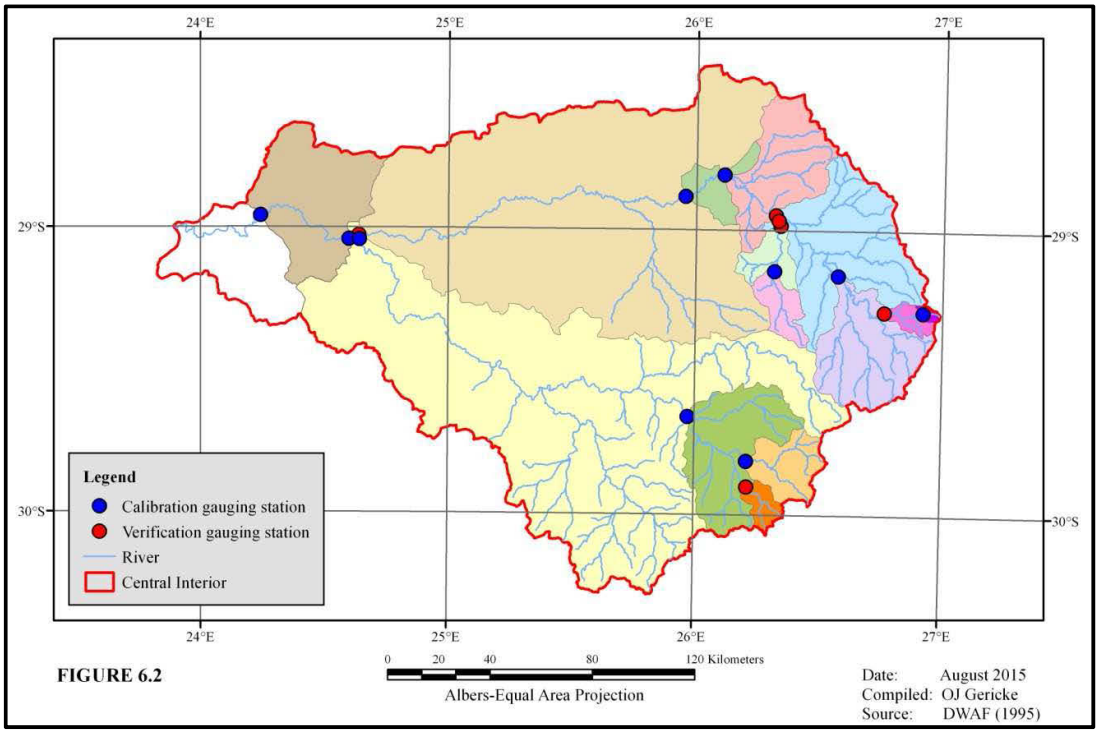

Figure 6.2 Layout and river network of the Central Interior

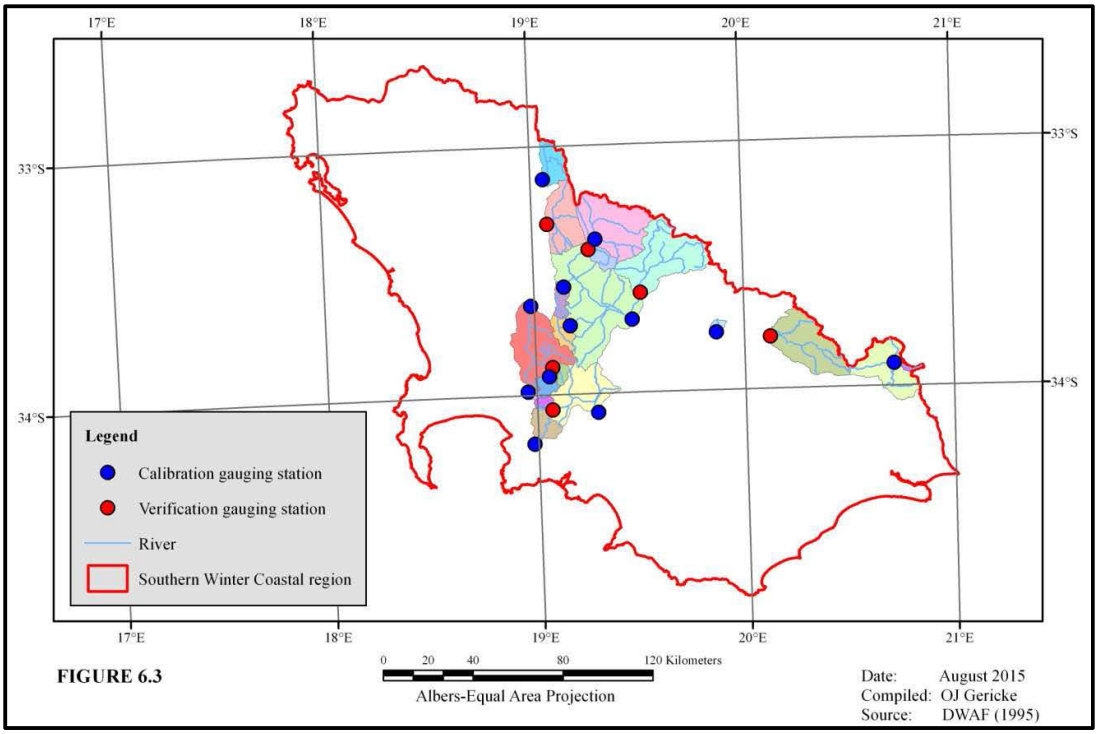

Figure 6.3 Layout and river network of the SWC region

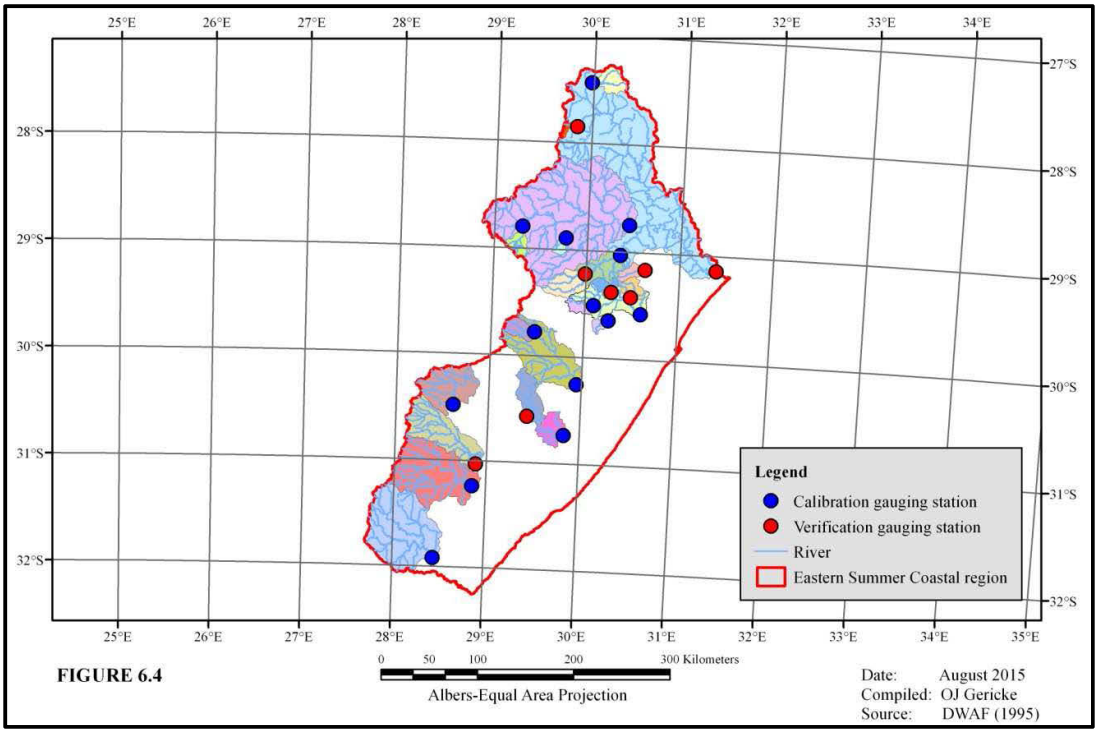

Figure 6.4 Layout and river network of the ESC region

6.4 Methodology

This section provides the detailed methodology applied in the four climatologically different regions. The following procedures were performed: (i) identification and estimation of climatological variables (driving mechanisms), (ii) determination of catchment variables and parameters using appropriate methods and Geographical Information System (GIS) applications, (iii) derivation (calibration) and verification of the derived empirical time to peak (T_{Py}) equations, (iv) independent assessment of the performance of the T_{Py} equations in comparison to the observed catchment T_{Px} values estimated in Chapter 5, (v) comparison of the USBR equation (T_{Cy}) currently used as the 'recommended method' in South Africa with both the T_{Px} values and derived T_{Py} equations, and (vi) translation of the various estimates of catchment response time into peak discharge to highlight the impact of these inconsistent time parameters on estimates of peak discharge.

The station numbers of the Department of Water and Sanitation (DWS) flow-gauging stations located at the outlet of each catchment are used as catchment descriptors for easy reference in all the tables and figures. Subscripts '*x*' and '*y*' are used to distinguish between observed data (*x*) and values estimated (*y*) using either the derived empirical T_{Py} equations (this research) or applying the currently 'recommended' USBR equation as commonly used in South Africa.

6.4.1 Estimation of climatological variables

The Isohyetal method was used to convert the individual *MAP* values (Lynch, 2004) at each rainfall station into average catchment values using the procedures as employed and recommended by Gericke and Du Plessis (2011). The 100-year design rainfall depth (P_{100}) associated with the critical storm duration (T_{Px}) in each catchment was estimated using the rainfall information and procedures as recommended by Alexander (2002).

6.4.2 Estimation of catchment variables

All the relevant GIS and catchment related data were obtained from the DWS (Directorate: Spatial and Land Information Management), which is responsible for the acquisition, processing and digitising of the data. The specific GIS data feature classes (lines, points and polygons) applicable to the four regions were extracted and created from the original

GIS data sets. The data extraction was followed by data projection and transformation, editing of attribute tables and recalculation of catchment geometry (areas, perimeters, widths and hydraulic lengths). These geographical input data sets were transformed to a projected coordinate system using the Africa Albers Equal-Area projected coordinate system with modification (ESRI, 2006a).

All the geomorphological catchment characteristics [*e.g.* area (A), perimeter (P), hydraulic length (L_H), length of longest watercourse/river (L_{CH}), centroid distance (L_C), average catchment slope (S), average slope of main water course/river (S_{CH}) and drainage density (D_D)], were based on and obtained from a projected and transformed version of the Shuttle Radar Topography Mission (SRTM) Digital Elevation Model (DEM) data for Southern Africa at 90-metre resolution (USGS, 2002).

All the above-mentioned geomorphological catchment characteristics were determined using standard procedures available in ArcGIS^{TM} 10.1 (ESRI, 2006b). In using the longitudinal profile of each main river as primary input, the average slope was estimated using the 10-85 method (SANRAL, 2013). Thereafter, all the above-mentioned catchment information was used to estimate the catchment shape parameters, circularity and elongation ratios, all of which may be used as independent predictor variables to estimate catchment response time.

Owing to the high variability associated with the nature and distribution of landcover, vegetation, land-use, geology and soils at a medium to large catchment scale, the use of weighted *CN* values as representative independent variables to estimate time parameters was also considered. The attributes of the National Landcover (NLC) database (CSIR, 2001) were firstly reclassified according to the generalised *CN* categories (*e.g.* agriculture, open space, forest, disturbed land, residential, paved and commercial industry) as proposed by Schulze *et al.* (1992). Thereafter, the generalised *CN* categories and the taxonomical soil forms with associated hydrological soil group information (Schulze, 2012) were combined.

The general catchment attributes (*e.g.* climatological variables, catchment geomorphology, catchment variables and channel geomorphology) of each catchment in the four regions,

are listed in Appendix 6.A, Tables 6.A1 to 6.A4. The influences of each variable or parameter listed in Tables 6.A1 to 6.A4 are highlighted where applicable in the subsequent sections.

6.4.3 Calibration and verification of empirical T_P equations

The XLSTAT^{TM} software (Addinsoft, 2014) was used to perform stepwise multiple regression analyses on the catchment time parameters and geomorphological catchment characteristics to establish calibrated relationships to estimate T_{Px}. The T_{Px} values used as dependent variables were determined in Chapter 5 from observed streamflow data using three different methods in combination, *i.e.* (i) duration of total net rise of a multi-peaked hydrograph [Eq. (5.1)], (ii) triangular-shaped direct runoff hydrograph approximations [Eq. (5.4)], and (iii) linear catchment response functions [Eq. (5.5)]. Equations (5.1) and (5.4) are a measure of the observed time to peak values for individual flood events (T_{Pxi}), while Eq. (5.5) represents the 'average' catchment T_{Px}. Equation (5.5) was used in this chapter, since it proved to be the most consistent approach to estimate the catchment T_{Px} values. The following independent predictor variables were considered for inclusion (Kirpich, 1940; McCuen *et al*., 1984; Schmidt and Schulze, 1984; Simas, 1996; Pegram and Parak, 2004; McCuen, 2005; Gericke and Smithers, 2015): (i) A [km²], (ii) P [km], (iii) L_H [km], (iv) L_{CH} [km], (v) L_C [km], (vi) S [%], (vii) S_{CH} [%], (viii) D_D [km.km^{-2}], (ix) MAP [mm], and (x) weighted CN values.

Linear and Log-linear backward stepwise multiple regression analyses with deletion were used to remove the insignificant potential independent predictor variables (either in a normal and/or transformed format) at each step to minimise the total variation, while the included independent predictor variables were tested for statistical significance at a 95 % confidence level. Hypothesis testing was performed at each step to ensure that only statistically significant independent variables were retained in the model, while insignificant variables were removed. Partial t-tests were used to test the significance of individual independent predictor variables, while total F-tests were used to determine whether T_{Px} as dependent variable is significantly correlated to the independent predictor variables included in the model (McCuen, 2005). A rejected null hypothesis [F-statistic of observed value (F) > critical F-statistic (F_α)] was used to identify the significant contribution of one or more of the independent variables towards the prediction accuracy.

The Goodness-of-Fit (GOF) statistics were assessed using the coefficient of multiple-correlation [Eq. (6.1)] and the standard error of estimate [Eq. (6.2)] (McCuen, 2005). In addition to the assessment of GOF statistics, Eqs. (6.3) and (6.4) were also used as regression diagnostics to identify possible outliers and to estimate standardised residuals (Chatterjee and Simonoff, 2013).

$$R_i^2 = \frac{\sum_{i=1}^{N}\left(y_i - \bar{x}\right)^2}{\sum_{i=1}^{N}\left(x_i - \bar{x}\right)^2} \quad (6.1)$$

$$S_{Ey} = \left[\frac{1}{v}\sum_{i=1}^{N}\left(y_i - x_i\right)^2\right]^{0.5} \quad (6.2)$$

$$h_{ii} = \frac{1}{N} + \frac{\left(x_i - \bar{x}\right)^2}{\sum_{i=1}^{N}\left(x_i - \bar{x}\right)^2} \quad (6.3)$$

$$e_i = \frac{\left(y_i - x_i\right)}{S_{Ey}\sqrt{1-h_{ii}}} \quad (6.4)$$

where R_i = multiple-correlation coefficient for an equation with i independent variables,

S_{Ey} = standard error of estimate,

h_{ii} = the i^{th} leverage value,

e_i = standardised residual,

x_i = observed value (dependent variable),

$\bar{x}$ = mean of observed values (dependent variables),

y_i = estimated value of dependent variable (x_i),

i = number of independent variables,

N = number of observations (sample size), and

v = degrees of freedom (N- i; with intercept = 0).

The performance of the calibrated empirical equation(s) was independently assessed at catchments not used during the calibration process, *i.e.* the observed T_{Px} values (Chapter 5) were compared to the T_{Py} values estimated using the calibrated empirical equation(s).

6.4.4 Comparison of time parameter estimation results

In addition to the calibration and verification testing of the developed empirical equation(s), the 'recommended' USBR (1973) equation [Eq. (6.5)] currently used in South Africa to estimate T_{Cy} was also compared to both the observed (T_{Px}) and empirically estimated (T_{Py}) values respectively. The estimates of T_C and T_P could be compared directly, since the conceptual definition of T_C equals T_P defined as the time interval between the start of effective rainfall and the peak discharge of a single-peaked hydrograph (McCuen *et al.*, 1984; McCuen, 2005; USDA NRCS, 2010), while Gericke and Smithers (2014, 2015) also showed that $T_C \approx T_P$ in medium to large catchments.

$$T_{Cy} = \left(\frac{0.87 L_H^{\,2}}{10 S_{CH}} \right)^{0.385} \tag{6.5}$$

where T_{Cy} = estimated channel flow time of concentration [hours],

L_H = hydraulic length of catchment [km], and

S_{CH} = average main river slope [%].

In order to highlight the impact of inconsistent results when translated into estimates of peak discharge, the 100-year design rainfall depths and catchment areas were substituted into the Standard Design Flood (SDF) method to estimate design peak discharges. The SDF method [Eq. (6.6)] is a regionally calibrated version of the Rational method and is deterministic-probabilistic of nature and applicable to catchment areas up to 40 000 km² (Alexander, 2002; Gericke and Du Plessis, 2012; SANRAL, 2013).

$$Q_{PT} = 0.278 \left[\frac{C_2}{100} + \left(\frac{Y_T}{2.33} \right) \left(\frac{C_{100}}{100} - \frac{C_2}{100} \right) \right] I_T A \tag{6.6}$$

where Q_{PT} = design peak discharge [$m^3.s^{-1}$],

A = catchment area [km²],

C_2 = 2-year return period runoff coefficient,

C_{100} = 100-year return period runoff coefficient,

I_T = average design rainfall intensity [$mm.h^{-1}$], and

Y_T = 100-year return period factor [2.33].

6.5 Results

The results from the application of the methodology are presented in the next sub-sections.

6.5.1 Calibration and verification of empirical T_P equations

The use of backward stepwise multiple linear regression analyses using untransformed data showed promising results, however, negative prediction values were evident in some of the calibration and verification catchments. In the case of transformed data, power-transformed ($y = ax^b$) independent variables, *e.g.* A, P, L_C, L_H, $L_C L_H$ $(0.1S)^{-0.5}$ and $(L_C L_H)^{0.3}$, showed the highest degree of association ($r^2 \geq 0.8$) when individually plotted against the dependent variables (T_{Px} values) in most of the catchments. However, the transformed independent predictor variables performed less satisfactorily when included as part of the multiple regression analyses in most of the catchments. Backward stepwise multiple Log-linear regression analyses with deletion generally resulted in the best prediction model for T_{Py}.

The following independent predictor variables were retained and included in the calibrated equation: (i) MAP, (ii) A, (iii) L_C, (iv) L_H, and (v) S. At a confidence level of 95 %, the independent variables contributed significantly towards the prediction accuracy in most or all of the regions, *i.e.* L_C and S proved to be less significant in one or more region(s). However, the inclusion of these five independent variables proved to be the best combination of 'catchment transfer functions' to estimate the T_{Px} values at a catchment level. Hence, the same equation format, with different regional calibration coefficients was used in each of the four regions. The derived T_{Py} regression is shown in Eq. (6.7) and Eq. (6.8):

$$\ln(T_{Py}) = \ln(x_1)MAP + \ln(x_2)A + \ln(x_3)L_C + \ln(x_4)L_H + \ln(x_5)S \qquad (6.7)$$

In applying some simplification, the final T_{Py} regression is shown in Eq. (6.8):

$$T_{Py} = x_1^{MAP} x_2^{A} x_3^{L_C} x_4^{L_H} x_5^{S} \qquad (6.8)$$

where T_{Py} = estimated time to peak [hours],

A = catchment area [km²],

L_C = centroid distance [km],

L_H = hydraulic length [km],

MAP = Mean Annual Precipitation [mm],

S = average catchment slope [%], and

x_1 to x_5 = regional calibration coefficients as listed in Table 6.1.

Table 6.1 Regional calibration coefficients applicable to Equation (6.8)

Region	Regional calibration coefficients [* 10^{-2}]				
	x_1	x_2	x_3	x_4	x_5
Northern Interior	100.280	99.993	99.865	101.612	91.344
Central Interior	100.313	99.984	106.106	98.608	98.081
SWC region	100.174	99.931	101.805	104.310	99.648
ESC region	100.297	99.991	99.594	101.177	97.529

Scatter plots of the T_{Py} [Eq. (6.8)] and T_{Px} values associated with all the calibration and verification catchments in each region are shown in Figures 6.5 to 6.8 to highlight any regional differences. In Figure 6.9, a frequency distribution histogram of the standardised residuals [Eq. (6.4)] for both the calibration and verification catchments is shown.

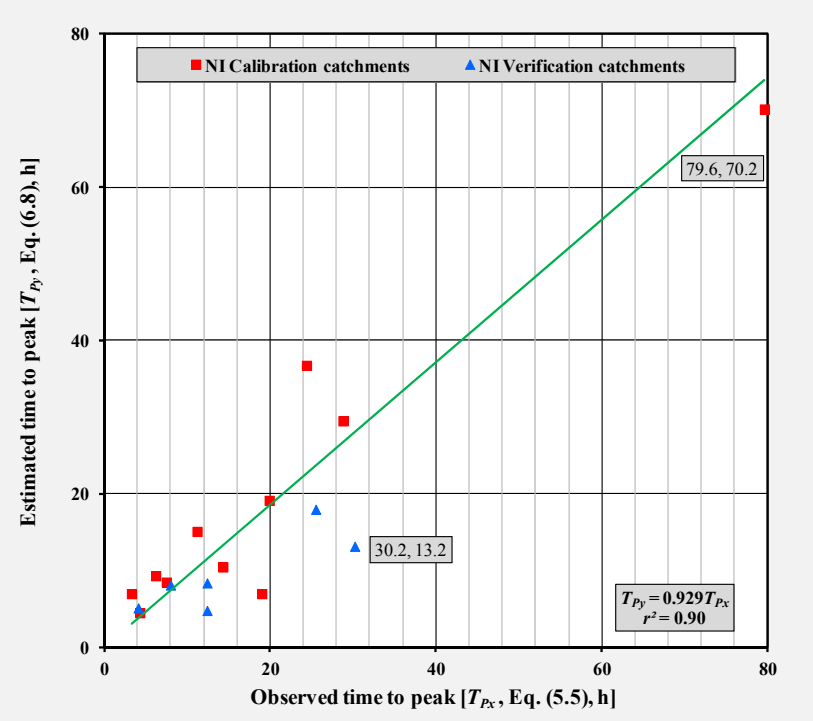

Figure 6.5 Scatter plot of the T_{Py} [Eq. (6.8)] and T_{Px} [Eq. (5.5)] values of the 17 catchments in the Northern Interior

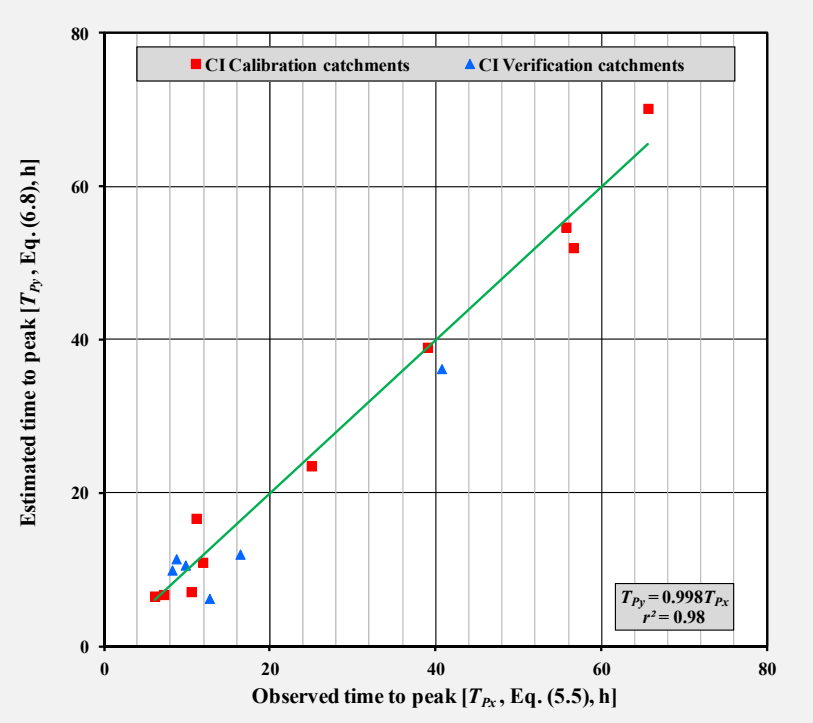

Figure 6.6 Scatter plot of the T_{Py} [Eq. (6.8)] and T_{Px} [Eq. (5.5)] values of the 16 catchments in the Central Interior

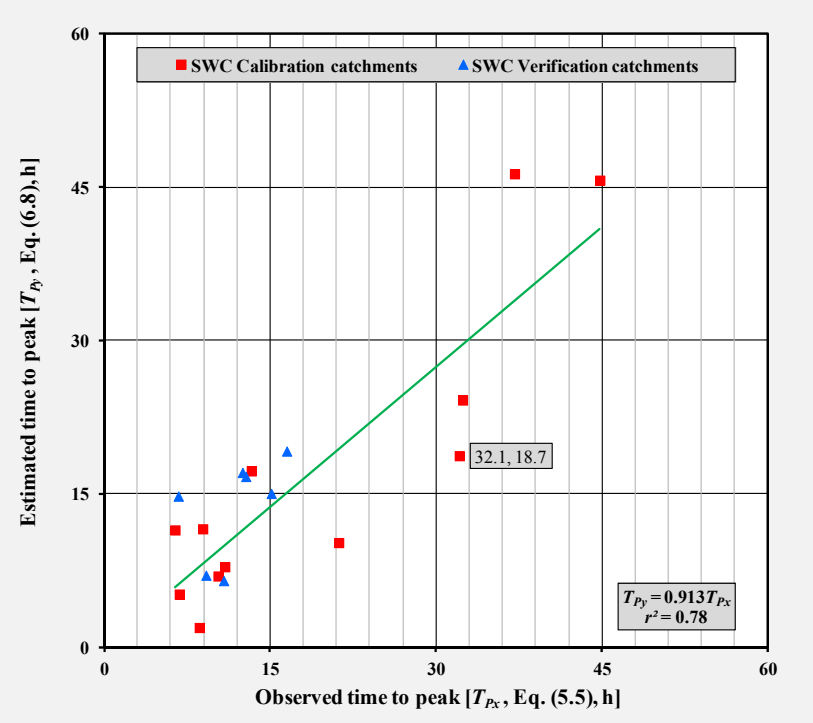

Figure 6.7 Scatter plot of the T_{Py} [Eq. (6.8)] and T_{Px} [Eq. (5.5)] values of the 19 catchments in the SWC region

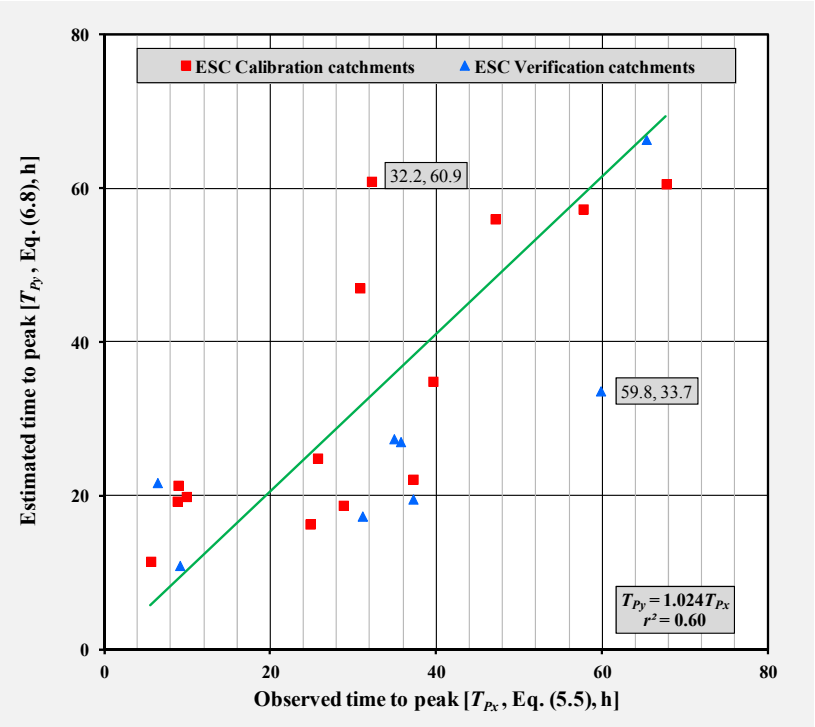

Figure 6.8 Scatter plot of the T_{Py} [Eq. (6.8)] and T_{Px} [Eq. (5.5)] values of the 22 catchments in the ESC region

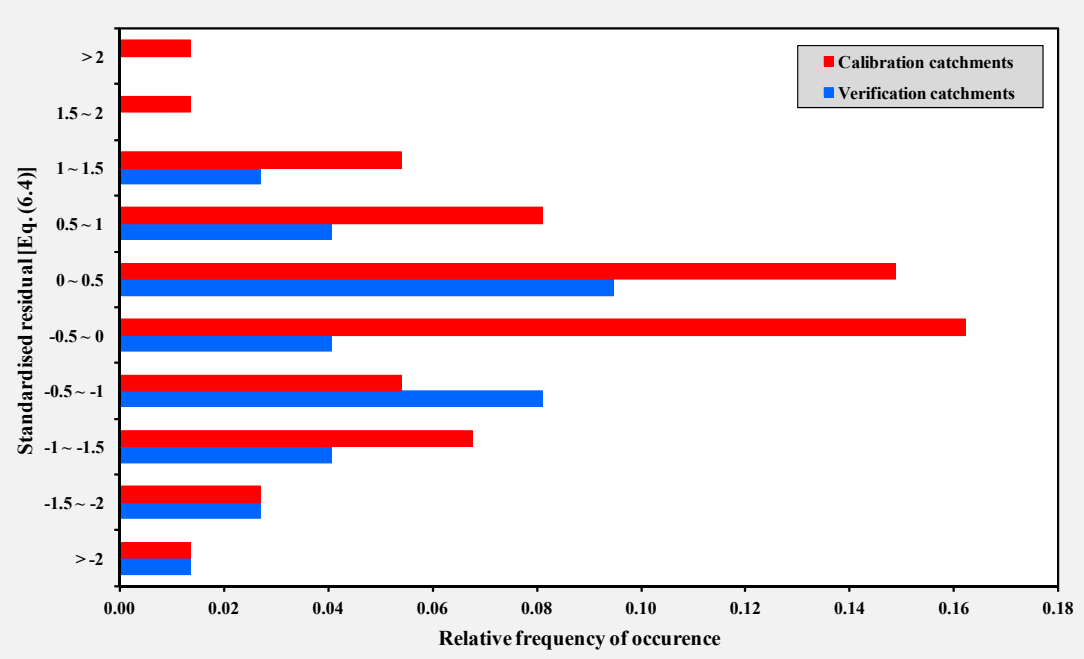

Figure 6.9 Frequency distribution histogram of the standardised residuals [Eq. (6.4)]

In Figures 6.5 to 6.8, the T_{Py} values computed using Eq. (6.8) showed a moderate to high degree of association with the observed T_{Px} values [Eq. (5.5), Chapter 5], with r^2 values ranging between 0.6 and 0.98. In considering the diagnostic plot results in Figure 6.9, it is evident that 96 % of the total sample have standardised residuals within ± 2. According to Chatterjee and Simonoff (2013), it is expected of a reliable regression model to have about 95 % of the standardised residuals between -2 and +2, while standardised residuals > 2 should be investigated as potential outliers. The corresponding T_{Px}-T_{Py} values with standardised residuals ≥ ± 2 are labelled in Figures 6.5 to 6.8. However, it is important to distinguish between 'acceptable' (T_{Py} is consistent with the regression relationship implied by the other T_{Px} values) and 'unacceptable' leverage values, *i.e.* outliers. For example, there are two sets of labelled T_{Px}-T_{Py} values in Figure 6.5. The T_{Px}-T_{Py} (79.6, 70.2) values respresent 'acceptable' leverage points, while the T_{Px}-T_{Py} (30.2, 13.2) values could be regarded as potential outliers, *i.e.* 'unacceptable' leverage values which are inconsistent and which deviate from the regression relationship.

The moderate to high degree of association as depicted in Figures 6.5 to 6.8 and summarised in Figure 6.9, not only confirmed the degree of association between T_{Px} and T_{Py}, but also the usefulness of Eq. (6.8) to estimate the catchment response time in both the calibration and verification catchments. A summary of the GOF statistics and hypothesis testing results are listed in Table 6.2.

Table 6.2 Summary of GOF statistics and hypothesis testing results applicable to both the calibration and verification catchments

Criterion/Region	**T_{Py} [Eq. (6.8)] results**			
	NI	**CI**	**SWC**	**ESC**
Confidence level [(1- α), %]	95	95	95	95
Coefficient of multiple-correlation [Eq. (6.1)]	0.85	0.99	0.90	0.86
Standard error of estimate [Eq. (6.2), h]	8.5	4.1	7.1	14.5
F-Observed value (*F*-statistic)	76.8	297.4	85.3	139.8
Critical *F*-statistic (F_α)	3.1	3.2	3.0	2.8

The best results (Table 6.2) were evident in the CI, with the standard error of the T_{Py} estimate = 4.1 hours and an associated coefficient of multiple-correlation = 0.99. In acknowledging that 75 % of the catchment areas in the CI are larger than 600 km², further emphasis is placed on the actual significance of the latter results, *i.e.* the standard error results in each region must be clearly understood in the context of the actual travel time associated with the size of a particular catchment.

The average T_{Px} values in the NI (18.3 h), CI (24.1 h), SWC (16.7 h) and ESC (32 h) regions could be used to benchmark these standard errors by considering the ratio of S_{Ey}: $\overline{T_{Px}}$ in each region, *e.g.* NI (0.46), CI (0.17), SWC (0.42) and ESC (0.45). Hence the comparable S_{Ey}: $\overline{T_{Px}}$ ratios obtained in the NI and ESC region, in conjunction with their similar R_i^2 values (≈ 0.85), highlight why the estimates in these two regions could be regarded as equivalent. It is also evident from Table 6.2 that, in all the regions, the rejection of the null hypothesis ($F > F_\alpha$) confirmed the significant relationship between T_{Px} and the independent predictor variables included in the regression model [Eq. (6.8)].

As highlighted in Chapter 5, the high T_{Pxi} variability characterising the various flood events in each catchment, are quite difficult to incorporate into design hydrology and it was recommended that an average catchment T_{Px} value based on a linear catchment response function [Eq. (5.5), Chapter 5] should be used to calibrate empirical equations.

Therefore, box plots in Figures 6.10 to 6.13 are used to highlight the variability of the observed T_{Pxi} values expressed as the duration of total net rise of a multi-peaked hydrograph [Eq. (5.1), Chapter 5] compared to the T_{Py} estimations using Eq. (6.8). In the latter figures, the whiskers represent the minimum and maximum values, the boxes the 25th and 75th percentile values and the change in box colour represent the median value. Both the catchment T_{Px} values based on Eq. (5.5) and the T_{Py} predictions [Eq. (6.8)] are super-imposed on Figures 6.10 to 6.13.

By comparing these average catchment T_{Px} values with the T_{Py} values [Eq. (6.8)] in the four regions as shown in Figures 6.10 to 6.13, the catchments in the CI demonstrated the best results with ± 75 % of the catchments showing < 25 % differences between T_{Px} and T_{Py}. However, in the other regions, only ± 40 % of the catchments are characterised by T_{Px}: T_{Py} ratio differences < 25 %.

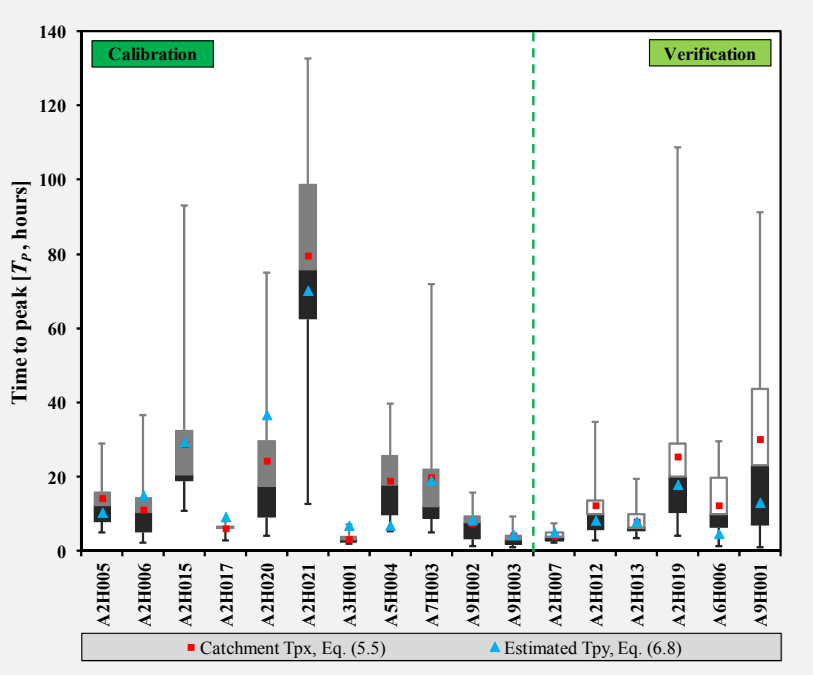

Figure 6.10 Box plots of the T_{Pxi} values [Eq. (5.1)] obtained directly from observed streamflow data and super-imposed data series values of T_{Px} [Eq. (5.5)] and T_{Py} estimations [Eq. (6.8)] for the 17 Northern Interior catchments

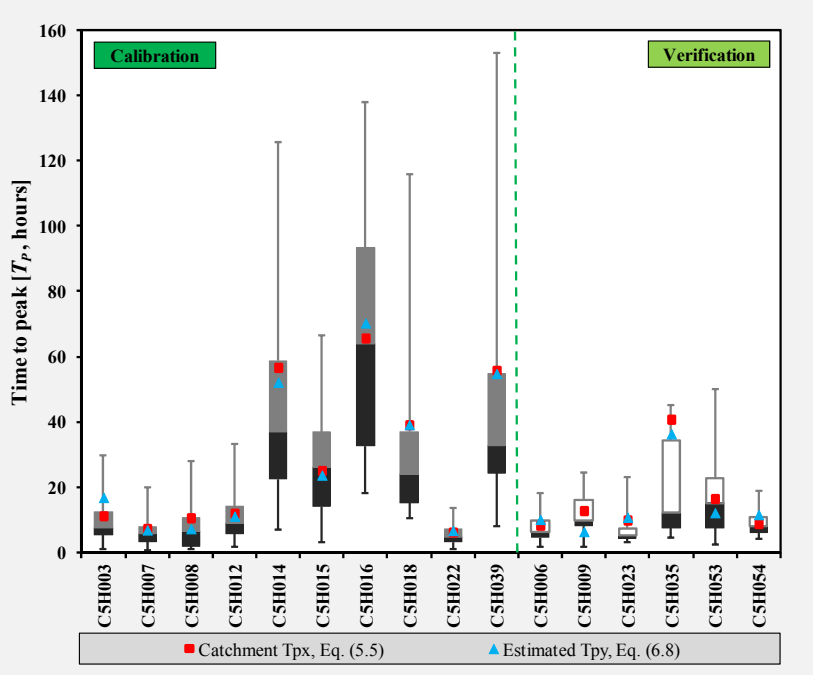

Figure 6.11 Box plots of the T_{Pxi} values [Eq. (5.1)] obtained directly from observed streamflow data and super-imposed data series values of T_{Px} [Eq. (5.5)] and T_{Py} estimations [Eq. (6.8)] for the 16 Central Interior catchments

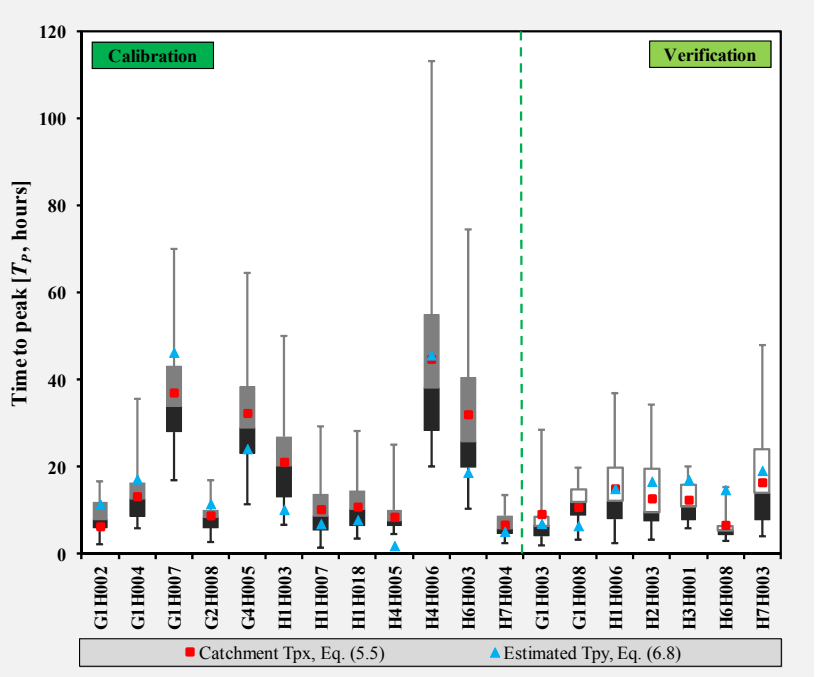

Figure 6.12 Box plots of the T_{Pxi} values [Eq. (5.1)] obtained directly from observed streamflow data and super-imposed data series values of T_{Px} [Eq. (5.5)] and T_{Py} estimations [Eq. (6.8)] for the 19 SWC region catchments

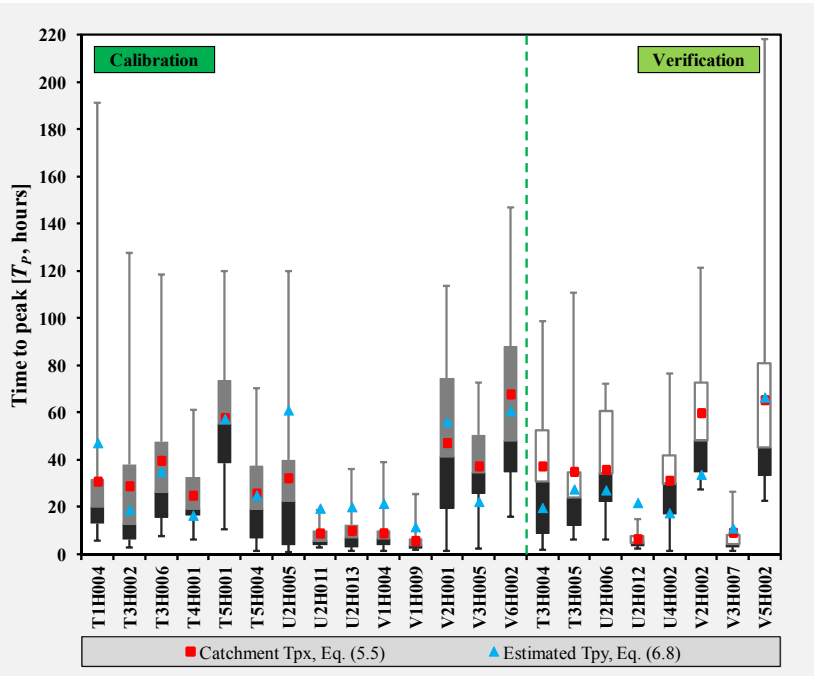

Figure 6.13 Box plots of the T_{Pxi} values [Eq. (5.1)] obtained directly from observed streamflow data and super-imposed data series values of T_{Px} [Eq. (5.5)] and T_{Py} estimations [Eq. (6.8)] for the 22 ESC region catchments

6.5.2 Comparison of time parameter estimation results

The impact of inconsistent or improved T_{Cy} [Eq. (6.5)] and T_{Py} [Eq. (6.8)] estimation results when translated into estimates of peak discharge is highlighted in this section. However, since the underestimation of T_P (conceptual T_C) results in the overestimation of peak discharges and vice versa, *viz.* the overestimation of T_P results in underestimated peak discharges, the time parameter estimation results should be evaluated further before the impact thereof on peak discharge estimates could really be appreciated. The relationship between the estimated (y) and observed (x) time parameter (T_Y/T_X) ratios are summarised by means of a frequency distribution histogram in Figure 6.14.

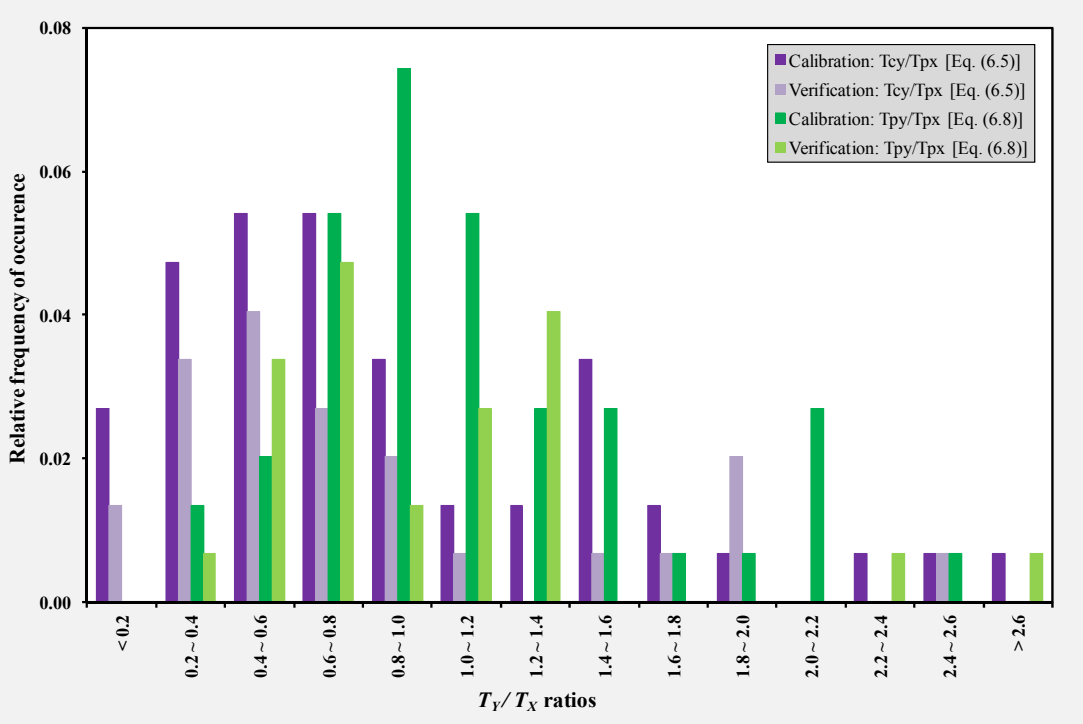

Figure 6.14 Frequency distribution histogram of the time parameter (T_Y/T_X) ratios

The T_{Cy} results illustrated in Figure 6.14 are characterised by several trends. Overall, 70 % of the T_{Cy} values computed using the USBR equation [Eq. (6.5)] underestimated the T_{Px} values and showed a low to moderate degree of association with the observed T_{Px} values in the calibration and verification catchments. The r^2 values ranged from 0.56 to 0.75, while estimates varied between -93 % and +160 %. The poorest results were demonstrated in the SWC and ESC regions, with 90 % of the T_{Cy} values being underestimated in comparison to T_{Px}.

This was to be expected, since the latter two regions are characterised by much higher average $S: S_{CH}$ ratios, which confirm the significant differences between the average catchment and main watercourse slopes in these regions. This is also in agreement with the findings of McCuen (2009), who showed that the USBR (1973) equation which considers only the main watercourse characteristics, tend to underestimate T_{Cy} on average by 50 % in catchments where significant differences in the roughness and slope of catchments and main watercourses are present. It also serves as an additional motivation why S is the preferred slope descriptor in all the catchments under consideration and is included as an independent predictor variable in Eq. (6.8).

The results of estimating T_{Py} [Eq. (6.8)] as shown in Figure 6.14 are also characterised by several trends. The T_{Py} estimations, based on Eq. (6.8), not only demonstrated a higher degree of association with T_{Px} in each region, but the under- and/or overestimations were also less significant when compared to the USBR equation [Eq. (6.5)] in more than 70 % of the catchments under consideration. The 0.8 ~ 1.2 T_Y/T_X ratio range, *i.e.* 20% under- or overestimations, represents ± 35 % of the catchments under consideration, while almost 70 % of the T_{Py} estimates are within the 0.6 ~ 1.4 range. In applying Eq. (6.8) in both the calibration and verification catchments, the degree of association (r^2 values) between the T_{Py} and T_{Px} values and associated under- and/or overestimations were as follows: (i) NI (r^2 = 0.85, -63 % to +112 %), (ii) CI (r^2 = 0.97, -50 % to +50 %), (iii) SWC region (r^2 = 0.74, -77 % to +121 %), and (iv) ESC region (r^2 = 0.60, -47 % to +239 %).

The translation of the different time parameters [T_{Px}, T_{Cy} and T_{Py}] into 100-year design peak discharge values using Eq. (6.6) are shown in Figures 6.15 to 6.18. Both the calibration and verification results are shown.

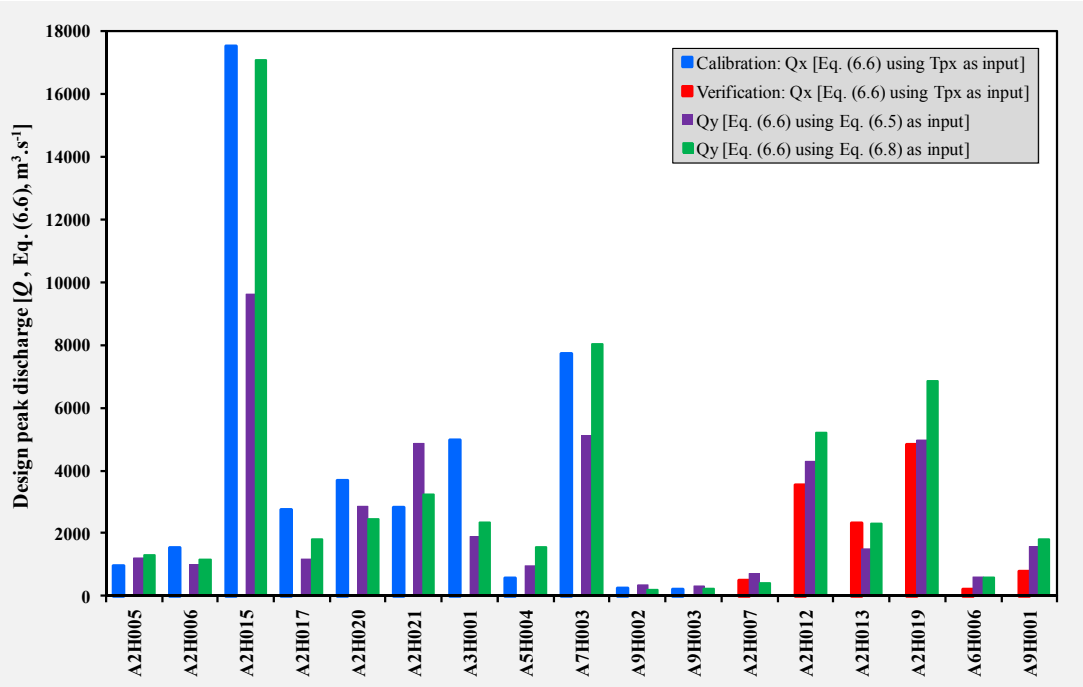

Figure 6.15 Observed (Q_x) versus estimated (Q_y) peak discharge values in the Northern Interior

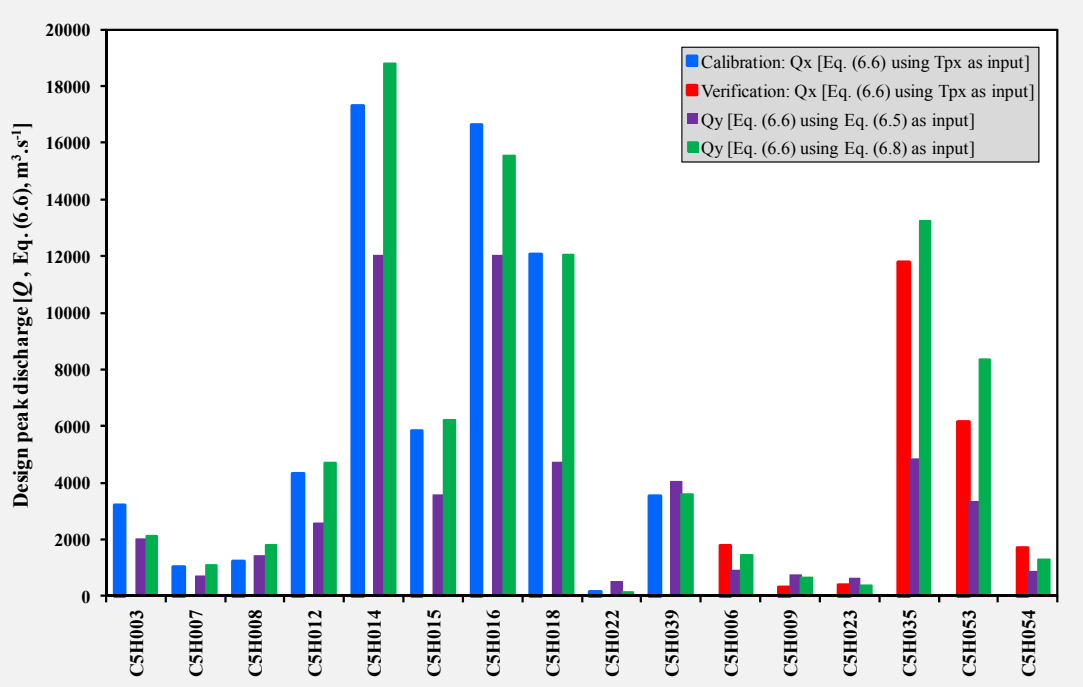

Figure 6.16 Observed (Q_x) versus estimated (Q_y) peak discharge values in the Central Interior

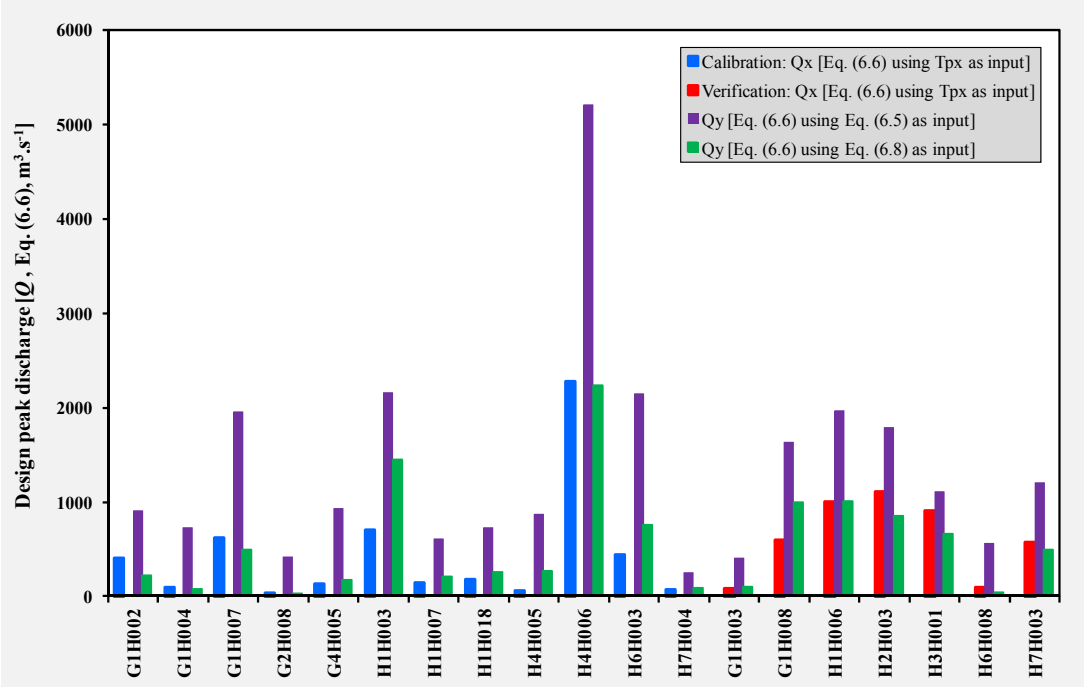

Figure 6.17 Observed (Q_x) versus estimated (Q_y) peak discharge values in the SWC region

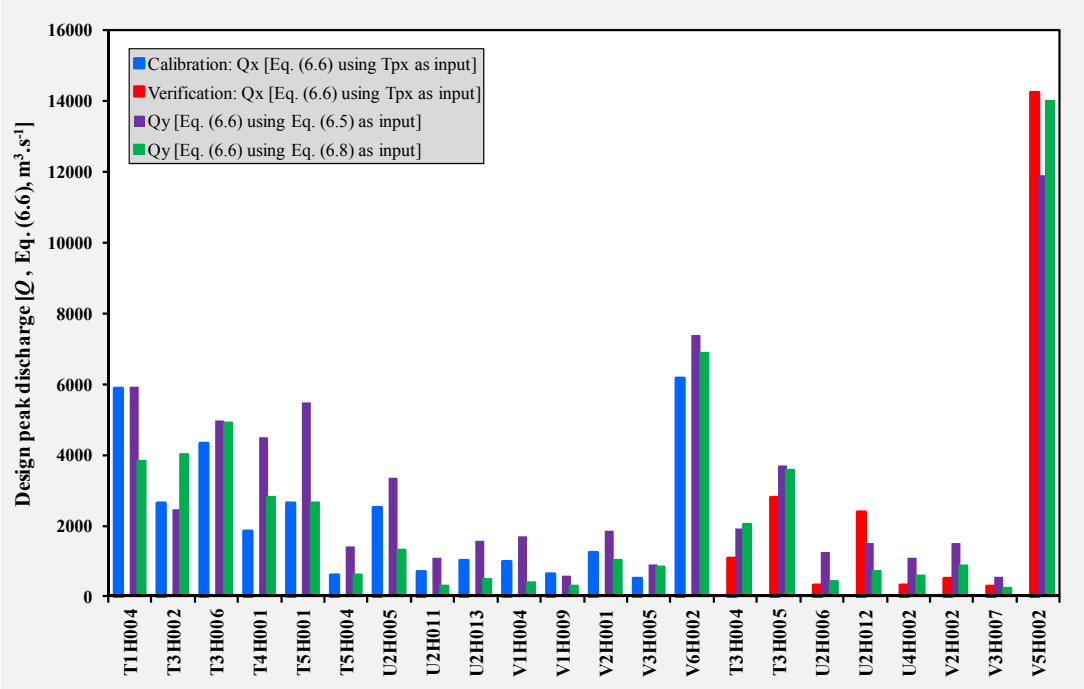

Figure 6.18 Observed (Q_x) versus estimated (Q_y) peak discharge values in the ESC region

The results illustrated in Figures 6.15 to 6.18 demonstrate the inverse relationship between peak discharge and catchment response time. Consequently, due to this inverse relationship and the time parameter results from each catchment, the worst peak discharge estimates are also expected in the catchments characterised by the poorest time parameter estimation results. In Figure 6.19, the relationship between the estimated (y) and observed (x) peak discharge (Q_Y/Q_X) ratios are summarised by means of frequency distribution histogram.

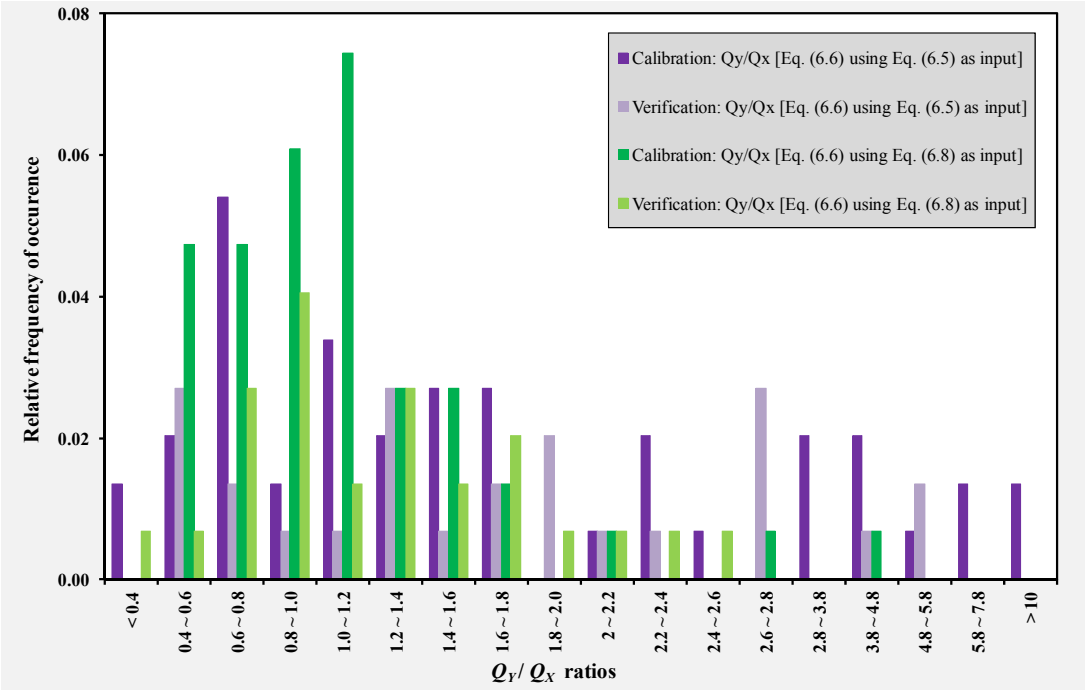

Figure 6.19 Frequency distribution histogram of the peak discharge (Q_Y/Q_X) ratios

Typically, the overestimation of peak discharges by a ratio of 14 or more as evident in Figure 6.19 could be associated with time parameter underestimations of up to -93 %, while peak discharge underestimations of -70 % are likely due to time parameter overestimations of up to +239 %.

The results are discussed and synthesised in the next section.

6.6 Discussion and Conclusions

As highlighted in the Introduction, most of the time parameter estimation methods developed internationally are empirically-based and applicable to small catchments. In South Africa, the T_L estimation methods developed locally by Pullen (1969) and Schmidt and Schulze (1984) are limited to small and/or medium catchments, while none of the recommended methods to estimate T_C were developed using local data. However, according to Gericke and Smithers (2014), the use of empirical time parameter equations applied beyond their original developmental regions and areal range and without the use of any local correction factors is widespread throughout many parts of the world.

The empirical equation(s) derived and verified in this chapter, not only meet the requirement of statistical significance, consistency and ease of application by practitioners in ungauged catchments, but the interaction between the five retained independent predictor variables, improved the estimation of catchment response times and the resulting peak discharge. All the catchment processes are included as part of a conceptual framework, *i.e.* the input (*MAP*), the transfer functions (*A,* L_C*,* L_H and *S*) and the output (*Q*). Internationally, catchment area is often identified as the single most important 'transfer function' as it demonstrates a strong correlation with many flood indices affecting the catchment response time, while the other 'transfer functions' (L_C*,* L_H and *S*) are also regarded as equally important in many studies (Kirpich, 1940; McCuen *et al.*, 1984; Schmidt and Schulze, 1984; Simas, 1996; Pegram and Parak, 2004; McCuen, 2005; Gericke and Smithers, 2015). Furthermore, the inclusion of the average catchment slope is regarded as both conceptually and physically necessary to ensure that the other retained independent variables, *i.e.* the shape (*A*) and distance (L_C and L_H) predictors provide a good indication of catchment storage effects (attenuation and travel time), while the *MAP* incorporates the rainfall variability. In terms of rainfall variability, *MAP* is also preferred to rainfall intensity-related variables at these catchment scales, since the antecedent soil moisture status and the quantity and distribution of rainfall relative to the attenuation of the resulting flood hydrograph as it moves towards the catchment outlet are of more importance than the relationship between rainfall intensity and the infiltration rate of the soil.

As highlighted in Chapter 5, the high variability of T_{Pxi} in most of the catchments is regarded as being directly related and amplified by the catchment area, especially the influence which larger catchment areas have on the spatial distribution of catchment rainfall, as characterised by many rainfall events not covering the entire catchment. Therefore, the inclusion of the catchment area as an independent variable in Eq. (6.8) is not necessarily the obvious reason why some of the corresponding T_{Py} estimations are worse; hence the use of different independent catchment variables in a specific combination to reflect the catchment response time should be critically assessed to quantify whether any unique relationship could have a less desirable impact on estimations. For example, underestimations of T_{Px} by > 25 % at a catchment level in the four regions were associated with L_C: L_H ratios < 0.5, hence the association between the shorter centroid distances and lower T_{Py} estimations. The average catchment shape parameters [$(L_C L_H)^{0.3}$] and circularity ratios [$P/\sqrt{4\pi A}$] associated with the latter catchments were also lower than those parameters and ratios associated with the catchments where T_{Px} was overestimated. The average ratios of the slope descriptors, *i.e.* S: S_{CH} in the NI, CI and SWC regions are comparable and varied between 12 and 20, but in the ESC region, the latter average ratio equals 32. Upon the close examination of the S: S_{CH} ratios in the ESC region, it is evident that the catchments where T_{Px} was underestimated by > 25 %, had higher S: S_{CH} ratios when compared to the other catchments where T_{Px} was overestimated. This is to be expected, since shorter travel times are associated with steeper slopes.

The fact that Eq. (6.8) provided similar results during the calibration and independent verification phases, confirmed the reliability of T_{Py} estimated using Eq. (6.8). Equation (6.8) also highlights the inherent limitations and inconsistencies introduced when the USBR equation, which is currently recommended for general practice in South Africa, is applied outside its bounds without using any local correction factors. The T_{Py} estimations, based on Eq. (6.8), not only demonstrated a higher degree of association with T_{Px} in each region, but the under- and/or overestimations were also less significant. With an improvement in T_{Py} estimates compared to those based on the USBR equation [Eq. (6.5)] in more than 70 % of the catchments, the appropriateness of Eq. (6.8) is even more evident. Typically, Eq. (6.8) resulted in only 20 % under- or overestimations in about 35 % of the catchments under consideration, while almost 70 % of the T_{Py} estimates using Eq. (6.8) were within the 40 % range of under- or overestimations.

The significant impact of inconsistent time parameters on discharge estimates was clearly evident when these time parameters were translated into design peak discharges. Typically, over- and underestimations of time parameters by ratios ranging between 1.4 and 0.1 respectively resulted in the under- and overestimation of peak discharges by ratios ranging between 0.3 and 15. Overall, the use of the derived empirical equation(s) [Eq. (6.8)] as input to the SDF method [Eq. (6.6)] resulted in improved peak discharge estimates in 60 of the 74 catchments under consideration. In ± 40 % of the catchments under consideration, the Q_Y/Q_X ratios using Eq. (6.8) as input were within the 0.8 to 1.2 Q_Y/Q_X range, *i.e.* 20 % under- or over-estimations in peak discharge.

However, Eq. (6.8) also has some potential limitations, especially in terms of its application in ungauged catchments beyond the boundaries of the four climatologically different regions. Therefore, the methodology followed in this chapter, in conjunction with the method to estimate T_{Px} as applied in Chapter 5 should be expanded to other catchments in South Africa and internationally. In addition, adopting a regional approach will improve the accuracy of the time parameter estimates. This could utilise a clustering method (Hosking and Wallis, 1997) based on the geomorphological catchment characteristics and flood statistics to establish the regions and to test the homogeneity respectively.

Therefore, if practitioners continue to use inappropriate time parameter estimation methods such as the USBR equation, then potential improvements for when both event-based design flood estimation methods and advanced hydrological models are used, will not be realised despite the current availability of technologically advanced input parameter estimation methods, *e.g.* GIS-based catchment parameters. In addition, not only will the accuracy of the above-mentioned methods/models be limited, but it will also have an indirect impact on hydraulic designs, *i.e.* underestimated time parameter values would result in over-designed hydraulic structures and the overestimation of time parameters would result in under-designs.

Taking into consideration the significant influence time parameter values have on the resulting hydrograph shape and peak discharge, these newly derived South African empirical time parameter equations will ultimately provide improved peak discharge estimates at ungauged catchments in the four identified climatological regions of

South Africa. Similarly, the method to estimate T_{Px}, as recommended in Chapter 5, should also be applied internationally at medium to large catchment scales to provide consistent observed catchment response times. This will not only enable the derivation of catchment-specific/regional empirical time parameter equations, but would also add new knowledge and enhance the understanding of hydrological processes at these catchment scales.

The catchment descriptors included in Tables 6.A1 to 6.A4 (Appendix 6.A) can be summarised as follows:

(a) Mean Annual Precipitation (*MAP*);
(b) 100-year design rainfall depth (P_{100});
(c) Area (A);
(d) Perimeter (P);
(e) Hydraulic length (L_H);
(f) Centroid distance (L_C);
(g) Average catchment slope (S);
(h) Runoff Curve Number (CN);
(i) SDF runoff coefficients (C_2 and C_{100});
(j) Length of main watercourse (L_{CH});
(k) Average slope of main watercourse (S_{CH}); and
(l) Drainage density (D_D).

The five journal papers as included in Chapters 2 to 6 are discussed and synthesised in the next chapter. The final conclusions and recommendations for future research are also included.

6.7 Appendix 6.A: Summary of the General Catchment Information

Table 6.A1 General information of the catchments situated in the Northern Interior

Catchment descriptor	**A2H005**	**A2H006**	**A2H007**	**A2H012**	**A2H013**	**A2H015**	**A2H017**	**A2H019**	**A2H020**
Climatological variables									
MAP [mm]	673	686	706	682	658	626	652	661	603
P_{100} [mm]	157.5	151.2	131	153.6	144.8	190.2	141.1	181.1	178.1
Catchment geomorphology									
A [km²]	774	1 030	145	2 555	1 161	23 852	1 082	6 120	4 546
P [km]	136	177	64	260	179	808	180	415	347
L_H [km]	51	86	17	57	64	252	76	132	176
L_C [km]	27	51	7	22	37	130	40	73	61
S [%]	2.73	4.76	6.52	5.30	7.03	5.13	7.43	5.78	5.31
Catchment variables									
Weighted *CN* value	74.8	72.4	77.3	69.8	71.6	69.3	71.2	69.6	70.7
SDF C_2 coefficient	10	10	10	10	10	10	10	10	10
SDF C_{100} coefficient	40	40	40	40	40	40	40	40	40
Channel geomorphology									
L_{CH} [km]	48	86	17	57	57	251	76	132	176
S_{CH} [%]	0.44	0.39	1.47	0.69	0.52	0.19	0.49	0.36	0.34
D_D [km.km^{-2}]	0.1	0.2	0.2	0.1	0.1	0.1	0.1	0.1	0.1
Catchment descriptor	**A2H021**	**A3H001**	**A5H004**	**A6H006**	**A7H003**	**A9H001**	**A9H002**	**A9H003**	
Climatological variables									
MAP [mm]	611	566	623	630	433	827	1128	967	
P_{100} [mm]	271.4	125.4	206.3	184.3	206.1	232.6	158	143	
Catchment geomorphology									
A [km²]	7 483	1 175	636	180	6 700	914	103	61	
P [km]	459	174	140	63	396	186	76	44	
L_H [km]	216	47	68	25	162	82	38	16	
L_C [km]	70	17	37	9	79	44	19	11	
S [%]	2.85	3.13	8.73	6.32	2.71	10.17	17.47	15.87	
Catchment variables									
Weighted *CN* value	69.7	68.9	63.6	61.1	61.5	68.4	68.5	70.8	
SDF C_2 & C_{100} coefficients	10 & 40	10 & 40	5 & 30	5 & 30	5 & 40	5 & 40	5 & 40	5 & 40	
Channel geomorphology									
L_{CH} [km]	215	47	68	25	162	82	38	16	
S_{CH} [%]	0.19	0.73	0.71	1.10	0.33	0.50	2.01	1.16	
D_D [km.km^{-2}]	0.1	0.1	0.2	0.1	0.1	0.2	0.4	0.3	

Table 6.A2 General information of the catchments situated in the Central Interior

Catchment descriptor	C5H003	C5H006	C5H007	C5H008	C5H009	C5H012	C5H014	C5H015
Climatological variables								
MAP [mm]	552	515	495	451	464	440	433	519
P_{100} [mm]	130.2	129.1	128.8	130	130.8	130.5	187.6	147.7
Catchment geomorphology								
A [km²]	1 641	676	346	598	189	2 366	31 283	5 939
P [km]	196	145	100	122	71	230	927	384
L_H [km]	71	64	41	41	24	87	326	160
L_C [km]	41	29	17	22	14	45	207	81
S [%]	3.90	2.02	1.75	4.83	3.66	3.28	2.13	2.77
Catchment variables								
Weighted *CN* value	68.0	73.6	73.4	67.3	67.1	67.3	68.8	69.8
SDF C_2 coefficient	15	15	15	15	15	15	15	15
SDF C_{100} coefficient	60	60	60	60	60	60	60	60
Channel geomorphology								
L_{CH} [km]	71	64	40	41	24	87	326	160
S_{CH} [%]	0.26	0.27	0.34	0.49	0.60	0.27	0.10	0.14
D_D [km.km^{-2}]	0.2	0.2	0.2	0.2	0.2	0.2	0.1	0.2
Catchment descriptor	**C5H016**	**C5H018**	**C5H022**	**C5H023**	**C5H035**	**C5H039**	**C5H053**	**C5H054**
Climatological variables								
MAP [mm]	428	459	654	611	459	516	529	515
P_{100} [mm]	196.6	162.5	128.3	129.7	165.6	186.7	132.2	129.3
Catchment geomorphology								
A [km²]	33 278	17 361	39	185	17 359	6 331	4 569	687
P [km]	980	730	28	65	730	411	329	146
L_H [km]	378	375	8	29	373	187	120	68
L_C [km]	230	174	3	17	173	103	56	33
S [%]	2.09	1.73	10.29	7.09	1.73	2.66	3.08	2.07
Catchment variables								
Weighted *CN* value	69.0	70.1	67.8	67.9	70.1	69.8	69.8	73.6
SDF C_2 coefficient	15	15	15	15	15	15	15	15
SDF C_{100} coefficient	60	60	60	60	60	60	60	60
Channel geomorphology								
L_{CH} [km]	378	375	8	29	373	187	119	67
S_{CH} [%]	0.10	0.08	1.70	0.58	0.08	0.13	0.18	0.26
D_D [km.km^{-2}]	0.1	0.1	0.2	0.2	0.1	0.2	0.2	0.2

Table 6.A3 General information of the catchments situated in the SWC region

Catchment descriptor	G1H002	G1H003	G1H004	G1H007	G1H008	G2H008	G4H005	H1H003	H1H006	H1H007
Climatological variables										
MAP [mm]	729	915	1 392	899	586	1 345	1 065	452	455	673
P_{100} [mm]	62.3	69.6	80.2	141.3	73.8	68.8	170.4	135.1	120	108.1
Catchment geomorphology										
A [km²]	186	47	69	724	394	22	146	656	753	80
P [km]	65	32	40	128	93	22	60	130	135	54
L_H [km]	28	10	14	56	26	6	30	39	47	19
L_C [km]	13	5	4	29	6	3	14	22	30	9
S [%]	33.53	28.88	52.31	26.21	18.89	51.76	20.71	16.41	21.20	40.69
Catchment variables										
Weighted *CN* value	59.2	64.5	55.2	61.5	67.9	61.6	64.1	67.4	66.5	60.0
SDF C_2 coefficient	40	40	40	40	40	40	30	30	30	30
SDF C_{100} coefficient	80	80	80	80	80	80	60	60	60	60
Channel geomorphology										
L_{CH} [km]	28	9	14	55	26	5	29	38	46	19
S_{CH} [%]	4.49	1.77	4.06	0.46	1.61	5.53	1.58	0.89	0.96	3.33
D_D [km.km^{-2}]	0.2	0.2	0.3	0.2	0.2	0.5	0.2	0.2	0.2	0.2
Catchment descriptor	**H1H018**	**H2H003**	**H3H001**	**H4H005**	**H4H006**	**H6H003**	**H6H008**	**H7H003**	**H7H004**	
Climatological variables										
MAP [mm]	666	281	413	289	450	859	1 336	524	566	
P_{100} [mm]	109.6	114.3	113.6	103.9	212.2	169.3	99.2	123.5	99.5	
Catchment geomorphology										
A [km²]	109	743	594	29	2 878	500	39	458	28	
P [km]	60	154	123	23	304	135	30	126	36	
L_H [km]	23	62	52	6	110	39	11	48	16	
L_C [km]	9	20	23	3	27	14	5	23	7	
S [%]	41.61	37.06	23.92	43.01	29.21	25.56	40.94	23.13	31.28	
Catchment variables										
Weighted *CN* value	67.1	62.4	70.5	68.0	64.2	61.7	73.0	67.4	72.9	
SDF C_2 coefficient	30	30	30	30	30	30	30	30	30	
SDF C_{100} coefficient	60	60	60	60	60	60	60	60	60	
Channel geomorphology										
L_{CH} [km]	23	60	52	6	102	38	10	47	15	
S_{CH} [%]	3.20	1.54	0.56	14.34	0.47	0.97	6.96	0.94	4.54	
D_D [km.km^{-2}]	0.3	0.2	0.2	0.3	0.2	0.2	0.3	0.2	0.5	

Table 6.A4 General information of the catchments situated in the ESC region

Catchment descriptor	T1H004	T3H002	T3H004	T3H005	T3H006	T4H001	T5H001	T5H004	U2H005	U2H006	U2H011
Climatological variables											
MAP [mm]	897	781	818	866	853	881	960	1 060	979	1 070	1 013
P_{100} [mm]	165.1	161.8	175.5	171.7	179.4	286.1	188.5	130.5	143.7	150.9	155
Catchment geomorphology											
A [km²]	4 923	2 102	1 027	2 565	4 282	723	3 639	537	2 523	338	176
P [km]	333	226	187	299	356	131	329	123	282	108	65
L_H [km]	205	109	103	160	197	68	200	67	175	49	36
L_C [km]	99	23	50	87	113	32	85	24	70	23	18
S [%]	16.10	20.82	16.64	25.52	20.03	21.49	21.48	28.31	15.52	16.36	17.31
Catchment variables											
Weighted *CN* value	70.5	66.5	70.3	69.0	71.7	69.7	70.2	68.5	68.1	75.2	72.6
SDF C_2 coefficient	10	10	10	10	10	15	10	10	10	10	10
SDF C_{100} coefficient	80	80	80	80	80	80	80	80	80	80	80
Channel geomorphology											
L_{CH} [km]	205	109	103	160	197	68	199	67	174	49	35
S_{CH} [%]	0.50	0.14	0.34	0.45	0.34	0.95	0.61	0.77	0.68	0.67	1.28
D_D [km.km^{-2}]	0.2	0.2	0.2	0.3	0.2	0.2	0.2	0.2	0.2	0.3	0.2
Catchment descriptor	**U2H012**	**U2H013**	**U4H002**	**V1H004**	**V1H009**	**V2H001**	**V2H002**	**V3H005**	**V3H007**	**V5H002**	**V6H002**
Climatological variables											
MAP [mm]	954	985	911	1 199	813	901	977	895	869	841	839
P_{100} [mm]	159.5	153	141.5	140	131.6	215.4	226.8	198.1	140.4	231.4	233.4
Catchment geomorphology											
A [km²]	431	296	317	446	195	1 951	945	677	128	28 893	12 854
P [km]	99	91	88	108	62	271	148	134	66	1 098	594
L_H [km]	57	51	48	42	28	188	105	86	25	505	312
L_C [km]	25	29	23	23	15	87	48	50	17	287	118
S [%]	13.33	18.35	13.74	41.39	10.96	15.26	16.15	12.94	20.22	16.24	16.97
Catchment variables											
Weighted *CN* value	68.3	70.0	67.5	72.3	73.6	71.3	72.1	69.7	65.1	70.3	71.6
SDF C_2 coefficient	10	10	10	15	15	15	15	15	15	15	15
SDF C_{100} coefficient	80	80	80	50	50	50	50	50	50	50	50
Channel geomorphology											
L_{CH} [km]	57	50	48	42	28	188	105	86	25	504	312
S_{CH} [%]	0.68	1.78	0.65	2.13	0.58	0.40	0.41	0.25	0.93	0.27	0.24
D_D [km.km^{-2}]	0.2	0.2	0.2	0.3	0.1	0.2	0.2	0.2	0.2	0.2	0.2

7. DISCUSSION, CONCLUSIONS AND RECOMMENDATIONS

This chapter contains a discussion of the five journal papers presented and includes conclusions and recommendations for future research based on the results obtained in each chapter.

7.1 Research Objectives

The primary objective of this research was to develop a new and consistent approach to estimate catchment response times in medium to large catchments, expressed as the time to peak (T_{Px}), and derived using only observed streamflow data. The secondary objective was to derive empirical T_P equations using multiple regression analysis to establish unique relationships between the T_{Px} values estimated directly from observed streamflow data and key climatological and geomorphological catchment predictor variables.

The specific objectives identified in each chapter to achieve the overall objective of this research are discussed in the subsequent sections.

7.2 Review of Time Parameter Estimation Methods

It was evident from the literature review that catchment characteristics, such as climatological variables, catchment geomorphology, catchment variables, and channel geomorphology are highly variable and have a significant influence on the catchment response time. Many researchers have identified catchment area as the single most important geomorphological variable as it demonstrates a strong correlation with many flood indices affecting the catchment response time. Apart from the catchment area, other catchment variables such as hydraulic and main watercourse lengths, centroid distance, average catchment and main watercourse slopes, have been shown to be equally important and worthwhile to be considered as independent predictor variables to estimate the catchment response time at a medium to large catchment scale. In addition to these geomorphological catchment variables, the importance and influence of climatological variables, such as *MAP* values to represent rainfall variability, which arguably also has a large potential influence on any non-linearity present in the catchment response, were also evident.

In summary, the literature review conducted on the time parameter estimation methods used internationally, in conjunction with selected comparisons and applications in medium to large catchments in South Africa, revealed the following aspects:

(a) Catchment response time parameters are one of the primary inputs required to estimate design floods, especially in ungauged catchments.
(b) The time parameters commonly used to express catchment response time are the T_C, T_L and T_P.
(c) The T_C is recognised as the most frequently used time parameter, followed by T_L. In acknowledging this, as well as the basic assumption of the approximation $T_C \approx T_P$, in conjunction with the similarity between the definitions of the T_P and the conceptual T_C, it was evident that the latter two time parameters should be further investigated to develop a new approach to estimate representative response times at these catchment scales.
(d) The use of different conceptual definitions in the literature to define the relationship between two time variables to estimate time parameters such as T_C, T_L and T_P, not only creates confusion, but also resulted in significantly different estimates in most cases.
(e) The use of multiple time parameter definitions, combined with the absence of a 'standard method' to estimate time parameters from observed data, emphasise why the proportionality ratio of T_L: T_C could typically vary between 0.5 and 2 for the same catchment/region.
(f) The generally accepted time parameter proportionality ratios as documented in the literature are only applicable to small catchments. Thus, in addition to the $T_C \approx T_P$ relationship established in this research, the applicability of the T_L proportionality ratio ($x = 1.667$), *i.e.* $T_L = 0.6T_C$, in medium to large catchments should be further investigated.
(g) The two T_C methods recommended for general use in South Africa were both developed and calibrated in the United States of America for catchment areas ≤ 45 ha, while only the T_L methods as proposed by Pullen (1969) and Schmidt and Schulze (1984) were developed locally in South Africa. The methodologies of Schmidt and Schulze (1984) and Pullen (1969) are also limited to small (≤ 30 km²) and medium ($\leq 5\,000$ km²) catchments respectively.

(h) Time parameters are normally estimated using either hydraulic or empirical methods, but almost 95 % of all the time parameter estimation methods developed internationally are empirically-based and the majority of these methods are applicable to and calibrated for small catchments.

(i) The application of empirical time parameter estimation methods must be limited to their original developmental regions, especially if no local correction factors are used, otherwise the use of these estimates could result in considerable errors.

(j) The significant errors in the estimation of the catchment response time, which have a direct impact on estimates of peak discharge, are mainly due to the use of inappropriate time variables, the inadequate use of a simplified convolution process between observed rainfall and runoff time variables, and the lack of locally developed empirical methods.

Given the sensitivity of design peak discharges to estimated catchment time parameter values, the estimation of catchment response time at a medium to large catchment scale was identified as needing to be improved and hence served as a motivation for this research. Despite the many time parameter estimation methods available internationally, the results from the application of these methods proved to be generally inconsistent at these catchment scales. The poor practice and continued use of inappropriate empirical time parameter estimation methods beyond their original developmental regions and areal range in South Africa, in conjunction with the limited availability of only two locally developed T_L equations, emphasise why the use of both event-based design flood estimation methods and advanced hydrological models are limited when peak discharges and associated volumes are estimated at medium to large catchment scales.

In the next section, the inadequacy of the simplified 'small catchment' convolution process between observed rainfall and runoff time variables at a medium to large catchment scale is highlighted and a new approach to estimate catchment response times directly from observed streamflow data is discussed.

7.3 Direct Estimation of Time Parameters from Observed Streamflow Data

The use of a simplified convolution process between a single hyetograph and hydrograph to estimate observed time parameters was regarded as neither practical nor applicable in large heterogeneous catchments where antecedent moisture from previous rainfall events and spatially non-uniform rainfall hyetographs can result in multi-peaked hydrographs. Rainfall and streamflow data are the two primary data sources required when such a simplified convolution process is used to estimate catchment response times. However, the number of rainfall stations in both South Africa and internationally has declined steadily over the past few decades. Furthermore, the rainfall data in both South Africa and internationally, are generally only widely available at more aggregated levels, such as daily and this reflects a paucity of rainfall data at sub-daily timescales, both in the number of rainfall gauges and length of the recorded series. In addition, time variables for an individual event cannot always be measured directly from autographic records owing to the difficulties in determining the start time, end time and temporal and spatial distribution of effective rainfall. Problems are further compounded by poorly synchronised rainfall and streamflow recorders which contribute to inaccurate estimates of time parameters.

All the above-mentioned limitations, in addition to the difficulty in estimating catchment rainfall for medium to large catchments, emphasised the need for the alternative T_{Px} estimation approach as developed in this research. In using the new approach based on the novel approximation of $T_C \approx T_P$, which is only reliant on observed streamflow data, both the extensive convolution process required to estimate time parameters and the need for rainfall data were eliminated. Furthermore, although streamflow data are internationally less readily available than rainfall data, the data quantity and quality thereof enable the direct estimation of catchment response times at medium to large catchment scales.

The catchment T_{Px} values were directly estimated from observed streamflow data using three different methods: (i) duration of total net rise of a multi-peaked hydrograph [Eq. (5.1)], (ii) triangular-shaped direct runoff hydrograph approximation [Eq. (5.4)], and (iii) a linear catchment response function [Eq. (5.5)]. The use of the three different methods in combination to estimate individual event (T_{Pxi}) and catchment (T_{Px}) values proved to be both practical and objective with consistent results. Their combined use also ensured that the high variability of event-based catchment responses is taken into account.

Overall, the results obtained, not only displayed the high inherent variability associated with catchment response times for individual events, but also confirmed the need for the investigations undertaken. Based on the specific results obtained, it is recommended that for design hydrology and for the calibration of empirical equations to estimate catchment response time, the catchment T_{Px} should be estimated based on a linear catchment response function [Eq. (5.5)]. It is important to note that Eq. (5.5) is only reliant on observed streamflow variables and is therefore not influenced by the limitations and availability of rainfall data in medium to large catchments. Equation (5.5) is also regarded as an appropriate 'representative value' which ensures that the averages of individual event-based catchment responses are a good reflection of the catchment conditions and sample-mean.

The derivation and assessment of the performance of empirical time parameter equation(s) to estimate T_{Px} are discussed in the next section.

7.4 Calibration and Verification of Empirical Time Parameter Equations

The observed T_{Px} values [Eq. (5.5)] were used to derive and calibrate new, local empirical equation(s) that meet the requirement of consistency and ease of application, *i.e.* including independent predictor variables (*e.g.* A, L_C, L_H, MAP and S) that are easy to determine by practitioners when required for future applications in ungauged catchments.

The empirical equation(s) [Eq. (6.8)] derived and verified in this research, not only meet the requirement of statistical significance, consistency and ease of application by practitioners in ungauged catchments, but the interaction between the five retained independent predictor variables, improved the estimation of catchment response times and the resulting peak discharge.

The fact that Eq. (6.8) provided similar results during the calibration and independent verification phases, confirmed the reliability of T_{Py} estimated using Eq. (6.8). Equation (6.8) also highlighted the inherent limitations and inconsistencies introduced when the USBR equation, which is currently recommended for general practice in South Africa, is applied outside its bounds without using any local correction factors. The T_{Py} estimations, based on Eq. (6.8), not only demonstrated a higher degree of association

with T_{Px} in each region, but the under- and/or overestimations were also less significant. With an improvement in T_{Py} estimates compared to those based on the USBR equation [Eq. (6.5)] in more than 70 % of the catchments, the appropriateness of Eq. (6.8) is even more evident. Typically, Eq. (6.8) resulted in only 20 % under- or overestimations in about 35 % of the catchments under consideration, while almost 70 % of the T_{Py} estimates using Eq. (6.8) were within the 40 % range of under- or overestimations.

Equation (6.8) also has potential limitations, especially in terms of its application in ungauged catchments beyond the boundaries of the four climatologically different regions where it was developed. Furthermore, some of the independent predictor variables included in Eq. (6.8) proved to be either statistically less significant or demonstrated a high degree of colliniarity. However, from a hydrological perspective at this stage, the inclusion of the five independent predictor variables (*e.g.* A, L_C, L_H, MAP and S) was regarded as both conceptually and physically necessary to ensure that the other retained independent variables provide a good indication of the catchment response time.

Therefore, the methodology followed in this research, should be expanded to other catchments in South Africa. The use of a regional approach based on a clustering method (Hosking and Wallis, 1997) is recommended. Typically, the geomorphological catchment characteristics and flood statistics could be utilised to establish the regions and to test the homogeneity respectively. Thereafter, new empirical equations could be derived for each of the hydrological homogeneous regions.

7.5 Impact on Peak Discharge Estimates

The significant impact of inconsistent time parameters on discharge estimates is clearly evident when these time parameters were translated into design peak discharges. Typically, over- and underestimations of time parameters by ratios ranging between 1.4 and 0.1 respectively resulted in the under- and overestimation of peak discharges by ratios ranging between 0.3 and 15. Overall, the use of the derived empirical equation(s) [Eq. (6.8)] as input to the Standard Design Flood method [Eq. (6.6)] resulted in improved peak discharge estimates in 60 of the 74 catchments under consideration. In ± 40 % of the catchments under consideration, the Q_Y/Q_X ratios using Eq. (6.8) as input were within the 0.8 to 1.2 Q_Y/Q_X range, *i.e.* 20 % under- or over-estimations in peak discharge.

Therefore, if practitioners continue to use inappropriate time parameter estimation methods, such as the USBR equation in South Africa, then potential improvements for when both event-based design flood estimation methods and advanced hydrological models are used will not be realised despite the current availability of technologically advanced input parameter estimation methods. In addition, not only will the accuracy of the methods/models be limited, but it will also have an indirect impact on hydraulic designs, *i.e.* underestimated time parameter values would result in over-designed hydraulic structures and the overestimation of time parameters would result in under-designed structures.

Taking into consideration the significant influence time parameter values have on the resulting hydrograph shape and peak discharge, these newly derived South African empirical time parameter equations will ultimately provide improved peak discharge estimates at ungauged catchments in the four identified climatological regions of South Africa. Similarly, the method to estimate T_{Px}, as recommended in Chapter 5, should also be applied internationally at medium to large catchment scales to provide consistent observed catchment response times. This will not only enable the derivation of catchment-specific/regional empirical time parameter equations, but would also add new knowledge and enhance the understanding of hydrological processes at these catchment scales.

7.6 Achievement of Objectives and Novel Aspects of the Research

The novel approximation of the $T_C \approx T_P$ formed the basis for the new and consistent approach developed in this research to estimate T_{Px} directly from observed streamflow data without the need for rainfall data. Consequently, time parameters can now be estimated directly from streamflow data without applying the required extensive convolution process between observed rainfall and runoff data, which is also regarded as not applicable in medium to large catchments. The empirical T_P equations derived and assessed in this research also demonstrate the unique relationships between the T_{Px} values and key climatological and geomorphological catchment predictor variables.

This research contributes new knowledge for estimating catchment response times, required for design flood estimation, in medium to large catchments in South Africa by solving the 'observed rainfall data problem' and poor synchronisation between rainfall and

runoff data. To date, most of the empirical time parameter estimation methods developed internationally are applicable to small catchments, and are based on a simplified convolution process between observed rainfall and runoff data. Both the studies conducted by Pullen (1969) and Schmidt and Schulze (1984) in South Africa are also based on the measured time differences between rainfall and runoff responses and limited to small and/or medium sized catchments. Therefore, this novel $T_C \approx T_P$ approach not only overcomes the procedural limitations associated with the traditional simplified convolution process at these catchment scales, but catchment response times, as a consequence of both the spatially non-uniform rainfall and the heterogeneous nature of soils and land cover in a catchment, are recognised and incorporated.

In the context of the overarching $T_C \approx T_P$ approach, the focus was primarily on the investigation of the relationship between time parameters and the relevance of conceptualised triangular-shaped direct runoff hydrograph approximations and linear catchment response functions in four climatologically different regions of South Africa. The novel aspects of the research, emanating from achieving the research objectives, not only address the primary focus areas identified, but also contributed to new knowledge for estimating catchment response times in medium to large catchments in South Africa.

The novel aspects of the research could be summarised as follows:

(a) Identification and evaluation of the basic assumptions of the approximation $T_C \approx T_P$ and similarities between the definitions of the T_P and the conceptual T_C.
(b) Implementation of the novel $T_C \approx T_P$ approximation to estimate catchment response time parameters directly from observed streamflow data without the need for both rainfall data and the traditional simplified convolution process using observed rainfall and runoff data.
(c) The use of a proposed method [Eq. (5.1)] to estimate T_{Pxi} values directly from observed streamflow data by recognising that T_{Pxi} could be expressed as the duration of total net rise of a multi-peaked hydrograph in medium to large catchments.
(d) The use of a variable hydrograph shape parameter as part of a triangular-shaped direct runoff hydrograph approximation [Eq. (5.4)] to estimate catchment response

times from observed flood hydrographs by incorporating the actual percentage of direct runoff under the rising limb of each individual hydrograph. Therefore, a variable shape parameter is used instead of the 37.5 % direct runoff volume under the rising limb which is generally associated with the conceptual curvilinear unit hydrograph theory.

(e) The use of a linear catchment response function [Eq. (5.5)] based on the relationship between individual Q_{Pxi} and Q_{Dxi} values of each flood event to provide an independent estimation of the catchment T_{Px}.

(f) The combined use of the averages of Eqs. (5.1) and (5.4) and the independent linear catchment response function [Eq. (5.5)], *i.e.* a convergence value, to overcome the high variability of event-based T_{Pxi} values and to synthesise the individual T_{Pxi} values into a representative catchment T_{Px} value. The use of such a convergence value ensured that the averages of individual event-based catchment responses are a good reflection of the catchment conditions and sample-mean.

(g) The incorporation of independent predictor variables which consider both catchment shape and size (A), distance (L_C and L_H), slope (S), catchment storage effects (A, L_C, L_H and S in combination to simulate attenuation and travel time), and rainfall variability (MAP) in the empirical equation(s) [Eq. (6.8)] derived and verified in this research. The inclusion of climatological (rainfall) variables as suitable predictors of catchment response time in South Africa has, to date, been limited to the research conducted by Schmidt and Schulze (1984). However, in terms of rainfall variability, MAP is preferred to rainfall intensity-related variables at these larger catchment scales, as the antecedent soil moisture status and the quantity and distribution of rainfall relative to the attenuation of the resulting flood hydrograph as it moves towards the catchment outlet, are of more importance than the relationship between rainfall intensity and the infiltration rate of the soil.

Based on the positive results obtained in the four climatologically different regions of South Africa, it is envisaged that the implementation of the approach and methodology developed in this research will contribute fundamentally to both improved time parameter and peak discharge estimations at a medium to large catchment scale in South Africa.

The recommendations for future research are synthesised in the next section.

7.7 Recommendations for Future Research

In view of the results obtained from this research, the methodologies used to estimate observed catchment T_{Px} values and T_{Py} regressions to estimate the T_{Px} values, should be expanded to other catchments in South Africa by taking cognisance of the following recommendations for future research:

(a) **Direct estimation of T_{Px} values from observed streamflow data:** Uncertainty analyses to define the bounds of the high variability in T_{Pxi} estimates should be conducted to confirm the validity of the three methods [Eqs. (5.1), (5.4) and (5.5)] as used in this research, to test the possible use of median T_{Px} values as an alternative option, and to define confidence bands to be considered by the practitioner. The relationship between Q_{Pxi} and Q_{Dxi} values also needs to be further investigated by implementing a classification system, *i.e.* distinguish between the flood events with both high Q_{Pxi} and Q_{Dxi} values, as well as those events characterised by high Q_{Pxi} and low Q_{Dxi} values.

(b) **Time parameter proportionality ratios for medium to large catchments:** The generally accepted time parameter definitions and proportionality ratios for small catchments as documented in the literature should be further investigated to establish the application of these in medium to large catchments. The results from this research and the findings of Gericke and Smithers (2014; 2015) confirmed that $T_C \approx T_P$, but the relevance of the T_L proportionality ratio ($x = 1.667$), *i.e.* $T_L = 0.6T_C$, as suggested for the possible use in Eqs. (5.4) and (5.5), is still not established. Therefore, the suggested T_L proportionality ratio needs to be investigated to either confirm or reject the preliminary findings of Gericke and Smithers (2015), *i.e.* $T_P \approx T_C \approx T_L$ at medium to large catchment scales.

(c) **Regionalisation:** A regionalisation scheme (Hosking and Wallis, 1997) for catchment response time estimation in South Africa should be adopted or developed. Firstly, the relevance of existing homogeneous flood (Kovács, 1988), rainfall (Smithers and Schulze, 2000a; 2000b), geomorphological and veld-type (HRU, 1972; Görgens, 2007) regions in South Africa needs to be established in order to provide guidance as to whether a combination of the above-mentioned regions could be used or alternatively, whether a new regionalisation scheme should be developed.

(d) **Estimation of index catchment response times at ungauged sites:** Once the method of regionalisation has been selected, the procedures to apply the method at ungauged sites need to be developed. This will require the estimation of scaling parameters (*e.g.* index time parameters) at ungauged sites as a function of site characteristics, or the development of a means to transfer the hydrological information from gauged to ungauged sites within a region.

(e) **Assessment of the performance of the developed regional time parameter equations:** In addition to the standard verification processes described and applied in this research, the empirical time parameter equations should also be independently tested in a selection of single-event or continuous simulation design flood estimation methods/models to illustrate the improved translation of runoff volume into hydrographs and associated peak discharge estimates at a medium to large catchment scale. The 'improvement' in the translation of estimated time parameters into design peak discharges should be quantified by comparing the specific design estimates with on-site flood frequency analysis estimates. This will serve as the ultimate test of consistency, robustness and accuracy.

(f) **Development of software interface:** An interface to enable practitioners to apply and use both the developed HAT and regionalised time parameter equations should be developed to enable the implementation of the proposed methodology at a national scale in South Africa.

The recommendations for future research, in conjunction with the methodological approaches developed in this research, could be adopted internationally to improve the estimation of catchment response time parameters at these larger catchment scales.

8. REFERENCES

Addinsoft. 2014. *XLSTAT Software,* Version 2014.6.05 [online]. Addinsoft, New York, USA. Available from: http://www.xlstat.com [7 January 2015].

ADNRW. 2007. *Queensland Urban Drainage Manual.* 2nd ed. Australian Department of Natural Resources and Water, Brisbane, Queensland, Australia.

Alexander, WJR. 2001. *Flood Risk Reduction Measures: Incorporating Flood Hydrology for Southern Africa*. Department of Civil and Biosystems Engineering, University of Pretoria, Pretoria, RSA.

Alexander, WJR. 2002. The standard design flood. *Journal of the South African Institution of Civil Engineering* 44 (1): 26–30.

Arnold, JG, Allen, PM, Muttiah, R, and Bernhardt, G. 1995. Automated baseflow separation and recession analysis techniques. *Ground Water* 33 (6): 1010–1018.

Askew, AJ. 1970. Derivation of formulae for a variable time lag. *Journal of Hydrology* 10: 225–242.

Balme, M, Vischel, T, Level, T, Peugeot, C, and Galle, S. 2006. Assessing the water balance in the Sahel: impact of small scale rainfall variability on runoff. Part 1: Rainfall variability analysis. *Journal of Hydrology* 331 (1–2): 336–348. DOI: 10.1016/j.jhydrol.2006.05.020.

Bell, FC and Kar, SO. 1969. Characteristic response times in design flood estimation. *Journal of Hydrology* 8: 173–196. DOI: 10.1016/0022-1694(69)90120-6.

Bondelid, TR, McCuen, RH, and Jackson, TJ. 1982. Sensitivity of SCS models to curve number variation. *Water Resources Bulletin* 20 (2): 337–349.

Cameron, DS, Beven, KJ, Tawn, J, Blazkova, S, and Naden, P. 1999. Flood frequency estimation by continuous simulation for a gauged upland catchment. *Journal of Hydrology* 219: 169–187.

CCP. 1955. *Culvert Design*. 2nd ed. California Culvert Practice, Department of Public Works, Division of Highways, Sacramento, USA.

Chapman, T. 1999. A comparison of algorithms for streamflow recession and baseflow separation. *Hydrological Processes* 13: 701–714.

Chatterjee, S and Simonoff, JS. 2013. *Handbook of Regression Analysis*. Volume 5, Wiley Handbooks in Applied Statistics. John Wiley and Sons Incorporated, Hoboken, New Jersey, USA. DOI: 10.1002/9781118532843.

Chow, VT. 1964. Runoff. In: ed. Chow, VT, *Handbook of Applied Hydrology,* Ch. 14, 1–54. McGraw-Hill, New York, USA.

Chow, VT, Maidment, DR, and Mays, LW. 1988. *Applied Hydrology.* McGraw-Hill, New York, USA.

Clark, CO. 1945. Storage and the unit hydrograph. *Transactions, American Society of Civil Engineers* 110: 1419–1446.

CSIR. 2001. *GIS Data: Classified Raster Data for National Coverage based on 31 Land Cover Types*. National Land Cover Database, Council for Scientific and Industrial Research, Environmentek, Pretoria, RSA.

DAWS. 1986. Estimation of runoff. In: eds. La G Matthee, JF *et al.*, *National Soil Conservation Manual,* Ch. 5, 5.1–5.5.4. Department of Agriculture and Water Supply, Pretoria, RSA.

Dingman, SL. 2002. *Physical Hydrology*. 2nd ed. Macmillan Press Limited, New York, USA.

Du Plessis, DB. 1984. *Documentation of the March-May 1981 Floods in the Southeastern Cape.* Technical Report No. TR120. Department of Water Affairs and Forestry, Pretoria, RSA.

DWAF. 1995. *GIS Data: Drainage Regions of South Africa.* Department of Water Affairs and Forestry, Pretoria, RSA.

Eagleson, PS. 1962. Unit hydrograph characteristics for sewered areas. *Journal of the Hydraulics Division, ASCE* 88 (HY2): 1–25.

Espey, WH and Altman, DG. 1978. *Urban Runoff Control Planning: Nomographs for 10 minute Unit Hydrographs for Small Watersheds.* Report No. EPA-600/9-78-035. Environmental Protection Agency, Washington, DC, USA.

Espey, WH, Morgan, CW, and Masch, FD. 1966. *A Study of Some Effects of Urbanisation on Storm Runoff from a Small Watershed*. Texas Water Development Board, Austin, Texas, USA.

Espey, WH and Winslow, DE. 1968. *The Effects of Urbanisation on Unit Hydrographs for Small Watersheds, Houston, Texas, 1964–67*. Report No. 68/975U and 1006/U. Tractor Incorporated, Austin, Texas, USA.

ESRI. 2006a. *ArcGIS Desktop Help: Map Projections and Coordinate Systems.* Environmental Systems Research Institute, Redlands, CA, USA.

ESRI. 2006b. *ArcGIS Desktop Help: Geoprocessing.* Environmental Systems Research Institute, Redlands, CA, USA.

FAA. 1970. *Airport Drainage*. Advisory Circular, A/C 150-5320-5B. Federal Aviation Agency, Department of Transport. Washington, DC, USA.

Fang, X, Cleveland, TG, Garcia, CA, Thompson, DB, and Malla, R. 2005. *Estimating Timing Parameters of Direct Runoff and Unit Hydrographs for Texas Watersheds*. Report No. 0/4696/1. Texas Department of Transportation, Department of Civil Engineering, Lamar University, Beaumont, Texas, USA.

Fang, X, Thompson, DB, Cleveland, TG, Pradhan, P, and Malla, R. 2008. Time of concentration estimated using watershed parameters by automated and manual methods. *Journal of Irrigation and Drainage Engineering* 134 (2): 202–211. DOI: 10.1061/(ASCE)0733-9437(2008)134:2(202).

Folmar, ND and Miller, AC. 2008. Development of an empirical lag time equation. *Journal of Irrigation and Drainage Engineering* 134 (4): 501–506. DOI: 10.1061/(ASCE)0733-9437(2008)134:4(501).

Gericke, OJ. 2010. *Evaluation of the SDF Method using a customised Design Flood Estimation Tool*. Unpublished MSc Eng Dissertation, Department of Civil Engineering, University of Stellenbosch, Stellenbosch, RSA.

Gericke, OJ and Du Plessis, JA. 2011. Evaluation of critical storm duration rainfall estimates used in flood hydrology in South Africa. *Water SA* 37 (4): 453–470. DOI: 10.4314/wsa.v37i4.4.

Gericke, OJ and Du Plessis, JA. 2012. Evaluation of the Standard Design Flood method in selected basins in South Africa. *Journal of the South African Institution of Civil Engineering* 54 (2): 2–14.

Gericke, OJ and Du Plessis, JA. 2013. Development of a customised design flood estimation tool to estimate floods in gauged and ungauged catchments. *Water SA* 39 (1): 67–94. DOI: 10.4314/wsa.v39i1.9.

Gericke, OJ and Smithers, JC. 2014. Review of methods used to estimate catchment response time for the purpose of peak discharge estimation. *Hydrological Sciences Journal* 59 (11): 1935–1971. DOI: 10.1080/02626667.2013.866712.

Gericke, OJ and Smithers, JC. 2015. An improved and consistent approach to estimate catchment response time: Case study in the C5 drainage region, South Africa. *Journal of Flood Risk Management*. DOI: 10.1111/jfr3.12206.

Gericke, OJ and Smithers, JC. 2015a. Direct estimation of catchment response time parameters in medium to large catchments using observed streamflow data. *Hydrological Processes* **[Manuscript submitted]**.

Gericke, OJ and Smithers, JC. 2015b. Derivation and verification of empirical catchment response time equations for medium to large catchments in South Africa. *Hydrological Processes* **[Manuscript submitted]**.

Gericke, OJ and Smithers, JC. 2016. Are estimates of catchment response time inconsistent as used in current flood hydrology practice in South Africa? *Journal of the South African Institution of Civil Engineering* 58 (1): 2–15. DOI: 10.17159/2309-8775/2016/v58n1a1.

Görgens, AHM. 2007. *Joint Peak-Volume (JPV) Design Flood Hydrographs for South Africa*. WRC Report No. 1420/3/07. Water Research Commission, Pretoria, RSA.

Görgens, AHM, Lyons, S, Hayes, L, Makhabane, M, and Maluleke, D. 2007. *Modernised South African Design Flood Practice in the Context of Dam Safety*. WRC Report No. 1420/2/07. Water Research Commission, Pretoria, RSA.

Grimaldi, S, Petroselli, A, Tuaro, F, and Porfiri, M. 2012. Time of concentration: a paradox in modern hydrology. *Hydrological Sciences Journal* 57 (2): 217–228. DOI: 10.1080/02626667.2011.644244.

Haan, CT, Barfield, BJ, and Hayes, JC. 1994. *Design Hydrology and Sedimentology for Small Catchments*. Academic Press Incorporated, San Diego, USA.

Haktanir, T and Sezen, N. 1990. Suitability of two-parameter gamma and three-parameter beta distributions as synthetic unit hydrographs in Anatolia. *Hydrological Sciences Journal* 35 (2): 167–184. DOI: 10.1080/02626669009492416.

Hathaway, GA. 1945. Design of drainage facilities. *Transactions of American Society of Civil Engineers* 30: 697–730.

Heggen, R. 2003. Time of concentration, lag time and time to peak. [Internet]. In: eds. Shrestha, B and Rajbhandari, R. *Proceedings of Regional Training Course: Application of Geo-informatics for Water Resources Management*, 3.1-3.23. International Centre for Integrated Mountain Development, Kathmandu, Nepal. Available: http://www.hkh-friend.net.np/rhdc/training/lectures/HEGGEN/Tc3.pdf. [Accessed: 30 September 2010].

Henderson, FM and Wooding, RA. 1964. Overland flow and groundwater flow from a steady rainfall of finite duration. *Journal of Geophysical Research* 69 (8): 129–146. DOI: 10.1029/JZ069i008p01531.

Hickok, RB, Keppel, RV, and Rafferty, BR. 1959. Hydrograph synthesis for small arid-land watersheds. *Journal of Agricultural Engineering ASAE* 40 (10): 608–611.

Hiemstra, LA and Francis, DM. 1979. *The Runhydrograph: Theory and Application for Flood Predictions.* Water Research Commission, Pretoria, RSA.

Hood, MJ, Clausen, JC, and Warner, GS. 2007. Comparison of stormwater lag times for low impact and traditional residential development. *Journal of the American Water Resources Association* 43 (4): 1036–1046. DOI: 10.1111/j.1752-1688.2007.00085.x.

Hosking, JRM and Wallis, JR. 1997. *Regional Frequency Analysis: An Approach Based on L-Moments.* Cambridge University Press, Cambridge, UK.

HRU. 1972. *Design Flood Determination in South Africa*. HRU Report No. 1/72. Hydrological Research Unit, University of the Witwatersrand, Johannesburg, RSA.

Hughes, DA, Hannart, P, and Watkins, D. 2003. Continuous baseflow from time series of daily and monthly streamflow data. *Water SA* 29 (1): 43–48.

IEA. 1977. *Australian Rainfall and Runoff: Flood Analysis and Design*. 2nd ed. Institution of Engineers, Canberra, Australia.

IH. 1999. *Flood Estimation Handbook.* Vol. 4, Institute of Hydrology, Wallingford, Oxfordshire, UK.

James, WP, Winsor, PW, and Williams, JR. 1987. Synthetic unit hydrographs. *Journal of Water Resources Planning and Management* 113 (1): 70–81.

Jena, SK and Tiwari, KN. 2006. Modelling synthetic unit hydrograph parameters with geomorphologic parameters of watersheds. *Journal of Hydrology* 319: 1–14. DOI: 10.1016/j.AQ10 jhydrol.2005.03.025.

Johnstone, D and Cross, WP. 1949. *Elements of Applied Hydrology*. Ronald Press, New York, USA.

Kadoya, M and Fukushima, A. 1979. Concentration time of flood runoff in smaller river basins. In: eds. Morel-Seytoux, HJ, Salas, JD, Sanders, TG, and Smith, RE. *Proceedings of the 3rd International Hydrology Symposium on Theoretical and Applied Hydrology*, 75–88. Water Resources Publication, Colorado State University, Fort Collins, CO, USA.

Kennedy, RJ and Watt, WE. 1967. The relationship between lag time and the physical characteristics of drainage basins in Southern Ontario. *Institute of Advanced Hydrological Studies (IAHS) Publication* 85: 866–874.

Kerby, WS. 1959. Time of concentration for overland flow. *Civil Engineering* 29 (3): 174.

Kirpich, ZP. 1940. Time of concentration of small agricultural watersheds. *Civil Engineering* 10 (6): 362.

Kjeldsen, TR. 2007. *The Revitalised FSR/FEH Rainfall-Runoff Method.* FEH Supplementary Report No. l. Centre for Ecology and Hydrology, Wallingford, Oxfordshire, UK.

Kovács, ZP. 1988. *Regional Maximum Flood Peaks in South Africa*. Technical Report TR137. Department of Water Affairs, Pretoria, RSA.

Larson, CL. 1965. *A Two Phase Approach to the Prediction of Peak Rates and Frequencies of Runoff for Small Ungauged Watersheds.* Technical Report No. 53. Department of Civil Engineering, Stanford University, Stanford, USA.

Li, M and Chibber, P. 2008. Overland flow time on very flat terrains. *Journal of the Transportation Research Board* 2060: 133–140. DOI: 10.3141/2060-15.

Linsley, RK, Kohler, MA, and Paulhus, JLH. 1988. *Hydrology for Engineers*. SI Metric ed. McGraw-Hill, Singapore.

Lorenz, C and Kunstmann, H. 2012. The hydrological cycle in three state-of-the-art reanalyses: intercomparison and performance analysis. *Journal of Hydrometeorology* 13: 1397–1420. DOI: 10.1175/JHM-D-11-088.1.

Loukas, A and Quick, MC. 1996. Physically-based estimation of lag time for forested mountainous watersheds. *Hydrological Sciences Journal* 41 (1): 1–19. DOI: 10.1080/02626669609491475.

Lynch, SD. 2004. *Development of a Raster Database of Annual, Monthly and Daily Rainfall for Southern Africa.* WRC Report No. 1156/1/04. Water Research Commission, Pretoria, RSA.

McCuen, RH. 2005. *Hydrologic Analysis and Design*. 3rd ed. Prentice-Hall, Upper Saddle River, New York, USA.

McCuen, RH. 2009. Uncertainty analyses of watershed time parameters. *Journal of Hydrologic Engineering* 14 (5): 490–498.
DOI: 10.1061/(ASCE)HE.1943-5584.0000011.

McCuen, RH and Spiess, JM. 1995. Assessment of kinematic wave time of concentration. *Journal of Hydraulic Engineering* 121 (3): 256–266.

McCuen, RH, Wong, SL, and Rawls, WJ. 1984. Estimating urban time of concentration. *Journal of Hydraulic Engineering* 110 (7): 887–904.

McEnroe, BM and Zhao, H. 2001. *Lag Times of Urban and Developing Watersheds in Johnson County, Kansas*. Report No. KTRAN: KU-99-5. University of Kansas, Kansas, USA.

Midgley, DC, Pitman, WV, and Middleton, BJ. 1994. *Surface Water Resources of South Africa*. WRC Report No. 298/2/94. Water Research Commission, Pretoria, RSA.

Miller, WC. 1951. Evolving a shortcut for design of storm sewers. *Municipal Utilities* 89 (9): 42–54.

Mimikou, M. 1984. Regional relationships between basin size and runoff characteristics. *Hydrological Sciences Journal* 29 (1, 3): 63–73.
DOI: 10.1080/02626668409490922.

Mockus, V. 1957. *Use of Storm and Watershed Characteristics in Synthetic Hydrograph Analysis and Application.* United States Department of Agriculture, Soil Conservation Service, Washington, DC, USA.

Morgali, JR and Linsley, RK. 1965. Computer simulation of overland flow. *Journal of Hydraulics Division, ASCE* 91 (HY3): 81–100.

Nathan, RJ and McMahon, TA. 1990. Evaluation of automated techniques for baseflow and recession analyses. *Water Resources Research* 26 (7): 1465–1473.

Neitsch, SL, Arnold, JG, Kiniry, JR, and Williams, JR. 2005. *Soil and Water Assessment Tool: Theoretical Documentation*. Agricultural Research Service and Blackland Research Center, Temple, Texas, USA.

NERC. 1975. *Flood Studies Report*. Natural Environment Research Council, London, UK.

Papadakis, KN and Kazan, MN. 1987. Time of concentration in small rural watersheds. In: *Proceedings of the ASCE Engineering Hydrology Symposium,* 633–638. Williamsburg, VA, USA.

Pavlovic, SB and Moglen, GE. 2008. Discretization issues in travel time calculations. *Journal of Hydrologic Engineering* 13 (2): 71–79.
DOI: 10.1061/(ASCE)1084-0699(2008)13:2(71).

Pegram, GGS and Parak, M. 2004. A review of the Regional Maximum Flood and Rational formula using geomorphological information and observed floods. *Water SA* 30 (3): 377–392.

Pilgrim, DH and Cordery, I. 1993. Flood Runoff. In: ed. Maidment, DR, *Handbook of Hydrology*, Ch. 9, 1–42. McGraw-Hill, New York, USA.

Pitman, WV. 2011. Overview of water resource assessment in South Africa: Current state and future challenges. *WaterSA* 37 (5): 659–664. DOI: 10.4314/wsa.v37i5.3.

Pullen, RA. 1969. *Synthetic Unitgraphs for South Africa*. HRU Report No. 3/69. Hydrological Research Unit, University of the Witwatersrand, Johannesburg, RSA.

Putnam, AL. 1972. Rainfall and runoff in urban areas: A case study of flooding in the Piedmont of North Carolina. In: *Proceedings of the Urban Rainfall Management Problems Conference*. University of Kentucky, Lexington, USA.

Ramser, CE. 1927. Runoff from small agricultural areas. *Journal of Agricultural Engineering* 34 (9): 797–823.

Rao, AR and Delleur, JW. 1974. Instantaneous unit hydrograph, peak discharges and time lags in urban areas. *Hydrological Sciences Bulletin* 19 (2): 85–198. DOI: 10.1080/02626667409493898.

Reich, BM. 1962. Soil Conservation Service design hydrographs. *Transactions of South African Institute of Civil Engineers* 4.

Royappen, M, Dye, PJ, Schulze, RE, and Gush, MB. 2002. *An Analysis of Catchment Attributes and Hydrological Response Characteristics in a Range of Small Catchments.* WRC Report No. 1193/01/02. Water Research Commission, Pretoria, RSA.

Sabol, GV. 1993. Lag relations for semi-arid regions and urban areas. In: *Proceedings of the ASCE Engineering Hydrology Symposium,* 168–173. San Francisco, CA, USA.

Sabol, GV. 2008. *Hydrologic Basin Response Parameter Estimation Guidelines*. Dam Safety Report, State of Colorado. Tierra Grande International Incorporated, Scottsdale, AZ, USA.

SANRAL. 2013. *Drainage Manual*. 6th ed. South African National Roads Agency Limited, Pretoria, RSA.

Schmidt, EJ and Schulze, RE. 1984. *Improved Estimation of Peak Flow Rates using Modified SCS Lag Equations*. ACRU Report No. 17. University of Natal, Department of Agricultural Engineering, Pietermaritzburg, RSA.

Schultz, GA. 1964. *Studies in Flood Hydrograph Synthesisation*. Unpublished MSc Dissertation, University of the Witwatersrand, Johannesburg, RSA.

Schulz, EF and Lopez, OG. 1974. *Determination of Urban Watershed Response Time*. Colorado State University, Fort Collins, Colorado, USA.

Schulze, RE. 1995. *Hydrology and Agrohydrology: A Text to Accompany the ACRU 3.00 Agrohydrological Modelling System.* WRC Report No. TT 69/95. Water Research Commission, Pretoria, RSA.

Schulze, RE. 2012. Mapping hydrological soil groups over South Africa for use with the SCS-SA design hydrograph technique: Methodology and results. *Proceedings*, *16th SANCIAHS Hydrology Symposium, 1-3 October 2012*. University of Pretoria, Pretoria, RSA.

Schulze, RE, Schmidt, EJ, and Smithers, JC. 1992. *SCS-SA User Manual: PC-Based SCS Design Flood Estimates for Small Catchments in Southern Africa*. ACRU Report No. 40. Department of Agricultural Engineering, University of Natal, Pietermaritzburg, RSA.

Seybert, TA. 2006. *Stormwater Management for Land Development: Methods and Calculations for Quantity Control.* John Wiley and Sons Incorporated, Hoboken, New Jersey, USA.

Sheridan, JM. 1994. Hydrograph time parameters for flatland watersheds. *Transactions of American Society of Agricultural Engineers* 37 (1): 103–113. DOI: 10.13031/2013.28059.

Simas, MJC. 1996. *Lag Time Characteristics in Small Watersheds in the United States.* Unpublished PhD Thesis, School of Renewable Resources, University of Arizona, Tucson, USA.

Simas, MJC and Hawkins, RH. 2002. Lag time characteristics in small watersheds in the United States. In: *Proceedings of the 2nd Federal Interagency Hydrologic Modelling Conference,* 1–7. Las Vegas, Nevada, USA.

Smakhtin, VU. 2001. Low flow hydrology: A review. *Journal of Hydrology* 240 (2001): 147–186.

Smakhtin, VU and Watkins, DA. 1997. *Low Flow Estimation in South Africa*. WRC Report No. 494/1/97. Water Research Commission, Pretoria, RSA.

Smithers, JC, Chetty, KT, Frezghi, MS, Knoessen, DM, and Tewolde, MH. 2013. Development and assessment of a daily time step continuous simulation modelling approach for design flood estimation at ungauged locations: ACRU model and Thukela Catchment case study. *Water SA* 39 (4): 449–458. DOI: 10.4314/wsa.v39i4.4.

Smithers, JC, Görgens, AHM, Gericke, OJ, Jonker, V, and Roberts P. 2014. *The Initiation of a National Flood Studies Programme for South Africa.* SANCOLD, Pretoria, RSA.

Smithers, JC and Schulze, RE. 2000a. *Development and Evaluation of Techniques for Estimating Short Duration Design Rainfall in South Africa*. WRC Report No. 681/1/00. Water Research Commission, Pretoria, RSA.

Smithers, JC and Schulze, RE. 2000b. *Long Duration Design Rainfall Estimates for South Africa.* WRC Report No. 811/1/00. Water Research Commission, Pretoria, RSA.

Snyder, FF. 1938. Synthetic unit hydrographs. *Transactions of American Geophysical Union* 19: 447.

Su, DH and Fang, X. 2004. Estimating travelling time of flat terrain by 2-dimensional overland flow model. In: eds. Jirka, GH and Uijttewaal, WSJ, *Shallow Flows*, 629–635. Balkema, Rotterdam, Netherland.

Taylor, AB and Schwarz, HE. 1952. Unit hydrograph lag and peak flow related to basin characteristics. *Transactions of the American Geophysics Union* (33): 235–246. DOI: 10.1029/TR033i002p00235.

Thomas, WO, Monde, MC, and Davis, SR. 2000. Estimation of time of concentration for Maryland streams. *Journal of the Transportation Research Board* 1720: 95–99.

UDFCD. 1984. *Urban Storm Drainage Criteria User's Manual*. Revised ed. Urban Drainage and Flood Control District, Denver Regional Council of Governments, Denver, CO, USA.

USACE. 2001. *HEC-HMS Hydrologic Modelling System: User's Manual, Version 2.2.1.* United States Army Corps of Engineers, Vicksburg, Mississippi, USA.

USBR. 1973. *Design of Small Dams*. 2nd ed. United States Bureau of Reclamation, Water Resources Technical Publication, Washington, DC, USA.

USDA NRCS. 2010. Time of concentration. In: eds. Woodward, DE *et al*., *National Engineering Handbook*, Ch. 15 (Section 4, Part 630), 1–18. United States Department of Agriculture Natural Resources Conservation Service, Washington, DC, USA.

USDA SCS. 1985. Hydrology. In: eds. Kent, KM *et al*., *National Engineering Handbook*, Ch. 16 (Section 4, Part 630), 1–23. United States Department of Agriculture Soil Conservation Service, Washington, DC, USA.

USGS. 2002. *SRTM Topography* [online]. United States Geological Survey. Available: http://dds.cr.usgs.gov/srtm/version2_1/Documentation/SRTM_Topo.pdf. [Accessed 2 June 2010].

Van der Spuy, D and Rademeyer, PF. 2010. *Flood Frequency Estimation Methods as applied in the Department of Water Affairs*. Department of Water Affairs, Pretoria, RSA.

Viessman, W, Lewis, GL, and Knapp, JW. 1989. *Introduction to Hydrology*. 3rd ed. Harper and Row Publishers Incorporated, New York, USA.

Viessman, W and Lewis, GL. 1996. *Introduction to Hydrology*. 4th ed. Harper Collins College Publishers Incorporated, New York, USA.

Watt, WE and Chow, KCA. 1985. A general expression for basin lag time. *Canadian Journal of Civil Engineering* 12: 294–300.

Welle, PI and Woodward, D. 1986. *Engineering Hydrology Time of Concentration*. Technical Release, USDA SCS Engineering Division, Pennsylvania, USA.

Williams, GB. 1922. Flood discharges and the dimensions of spillways in India. *Engineering (London)* 134: 321.

Williams, JR and Hann, RWJ. 1973. HYMO: Problem-oriented computer language for building hydrologic models. *Water Resources Research* 8 (1): 79–86.

Wong, TSW and Chen, CN. 1997. Time of concentration formula for sheet flow of varying flow regime. *Journal of Hydrologic Engineering* 2 (3): 136–139. DOI: 10.1061/(ASCE)1084-0699(1997)2:3(136).

Woolhiser, DA and Liggett, JA. 1967. Unsteady one-dimensional flow over a plane: The rising hydrograph. *Water Resources Research* 3 (3): 753–771. DOI: 10.1029/WR003i003p00753.